Contents

Chapter 3

Equalization

The main focus of Chapter 1 was a single use of the channel, signal set, and detector to transmit one of M messages, commonly referred to as "one-shot" transmission. In practice, the transmission system sends a sequence of messages, one after another, in which case the analysis of Chapter 1 applies only if the channel is **memoryless**: that is, for one-shot analysis to apply, these successive transmissions must not interfere with one another. In practice, successive transmissions do often interfere with one another, especially as they are spaced more closely together to increase the data transmission rate. The interference between successive transmissions is called **intersymbol interference (ISI)**. ISI can severely complicate the implementation of an optimum detector.

Figure 3.1 illustrates a receiver for detection of a succession of messages. The matched filter outputs are processed by the receiver, which outputs samples, z_k, that estimate the symbol transmitted at time k, $\hat{x}_k$. Each receiver output sample is the input to the same one-shot detector that would be used on an AWGN channel without ISI. This **symbol-by-symbol (SBS)** detector, while optimum for the AWGN channel, will not be a maximum-likelihood estimator for the sequence of messages. Nonetheless, if the receiver is well-designed, the combination of receiver and detector may work nearly as well as an optimum detector with far less complexity. The objective of the receiver will be to improve the performance of this simple SBS detector. More sophisticated and complex sequence detectors are the topics of Chapters 4, 5 and 9.

Equalization methods are used by communication engineers to mitigate the effects of the intersymbol interference. An equalizer is essentially the content of Figure 3.1's receiver box. This chapter studies both intersymbol interference and several equalization methods, which amount to different structures for the receiver box. The methods presented in this chapter are not optimal for detection, but rather are widely used sub-optimal cost-effective methods that reduce the ISI. These equalization methods try to convert a bandlimited channel with ISI into one that appears memoryless, hopefully synthesizing a new AWGN-like channel at the receiver output. The designer can then analyze the resulting memoryless, equalized channel using the methods of Chapter 1. With an appropriate choice of transmit signals, one of the methods in this chapter - the Decision Feedback Equalizer of Section 3.6 can be generalized into a canonical receiver (effectively achieves the highest possible transmission rate even though not an optimum receiver), which is discussed further in Chapter 5 and occurs only when special conditions are met.

Section 3.1 models linear intersymbol interference between successive transmissions, thereby both illustrating and measuring the problem. In practice, as shown by a simple example, distortion from overlapping symbols can be unacceptable, suggesting that some corrective action must be taken. Section 3.1 also refines the concept of signal-to-noise ratio, which is the method used in this text to quantify receiver performance. The SNR concept will be used consistently throughout the remainder of this text as a quick and accurate means of quantifying transmission performance, as opposed to probability of error, which can be more difficult to compute, especially for suboptimum designs. As Figure 3.1 shows, the objective of the receiver will be to convert the channel into an equivalent AWGN at each time k, independent of all other times k. An AWGN detector may then be applied to the derived channel, and performance computed readily using the gap approximation or other known formulae of Chapters 1 and
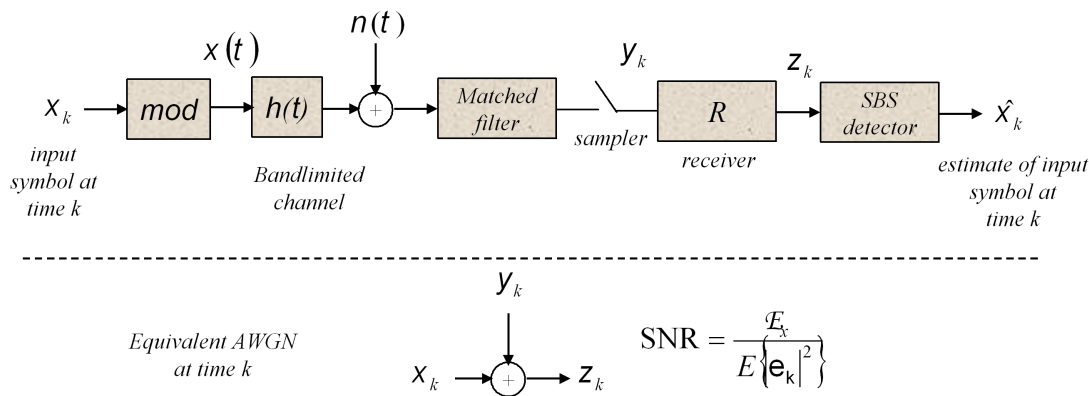
Figure 3.1: The band-limited channel with receiver and SBS detector.

2 with the SNR of the derived AWGN channel. There may be loss of optimality in creating such an equivalent AWGN, which will be measured by the SNR of the equivalent AWGN with respect to the best value that might be expected otherwise for an optimum detector. Section 3.3 discusses some desired types of channel responses that exhibit no intersymbol interference, specifically introducing the Nyquist Criterion for a linear channel (equalized or otherwise) to be free of intersymbol interference. Section 3.4 illustrates the basic concept of equalization through the zero-forcing equalizer (ZFE), which is simple to understand but often of limited effectiveness. The more widely used and higher performance, minimum mean square error linear (MMSE-LE) and decision-feedback equalizers (MMSE-DFE) are discussed in Sections 3.5 and 3.6. Section 3.7 discusses the design of finite-length equalizers. Section 3.8 discusses precoding, a method for eliminating error propagation in decision feedback equalizers and the related concept of partial-response channels and precoding. Section 3.9 generalizes the equalization concepts to systems that have one input, but several outputs, such as wireless transmission systems with multiple receive antennas called "diversity."

The area of transmit optimization for scalar equalization, is yet a higher performance form of equalization for any channel with linear ISI, as discussed in Chapters 4 and 5.

3.1 Intersymbol Interference and Receivers for Successive Message Transmission

Intersymbol interference is a common practical impairment found in many transmission and storage systems, including voiceband modems, digital subscriber loop data transmission, storage disks, digital mobile radio channels, digital microwave channels, and even fiber-optic (where dispersion-limited) cables. This section introduces a model for intersymbol interference. This section then continues and revisits the equivalent AWGN of Figure 3.1 in view of various receiver corrective actions for ISI.

3.1.1 Transmission of Successive Messages

Most communication systems re-use the channel to transmit several messages in succession. From Section 1.1, the message transmissions are separated by T units in time, where T is called the **symbol period**, and $1/T$ is called the **symbol rate**.[1] The **data rate** of Chapter 1 for a communication system that sends one of M possible messages every T time units is

$$R \triangleq \frac{\log_2(M)}{T} = \frac{b}{T} \quad . \tag{3.1}$$

To increase the data rate in a design, either b can be increased (which requires more signal energy to maintain P_e) or T can be decreased. Decreasing T narrows the time between message transmissions and thus increases intersymbol interference on any band-limited channel.

The transmitted signal $x(t)$ corresponding to K successive transmissions is

$$x(t) = \sum_{k=0}^{K-1} x_k(t - kT) \quad . \tag{3.2}$$

Equation (3.2) slightly abuses previous notation in that the subscript k on $x_k(t-kT)$ refers to the index associated with the kth successive transmission. The K successive transmissions could be considered an aggregate or "block" symbol, $x(t)$, conveying one of M^K possible messages. The receiver could attempt to implement MAP or ML detection for this new transmission system with M^K messages. A Gram-Schmidt decomposition on the set of M^K signals would then be performed and an optimum detector designed accordingly. Such an approach has complexity that grows exponentially (in proportion to M^K) with the block message length K. That is, the optimal detector might need M^K matched filters, one for each possible transmitted block symbol. As $K \to \infty$, the complexity can become too large for practical implementation. Chapter 9 addresses such "sequence detectors" in detail, and it may be possible to compute the à posteriori probability function with less than exponentially growing complexity.

An alternative (suboptimal) receiver can detect each of the successive K messages independently. Such detection is called **symbol-by-symbol (SBS)** detection. Figure 3.2 contrasts the SBS detector with the block detector of Chapter 1. The bank of matched filters, presumably found by Gram-Schmitt decomposition of the set of (noiseless) channel output waveforms (of which it can be shown K dimensions are sufficient only if $N = 1$, complex or real), precedes a block detector that determines the K-dimensional vector symbol transmitted. The complexity would become large or infinite as K becomes large or infinite for the block detector. The lower system in Figure 3.2 has a single matched filter to the channel, with output sampled K times, followed by a receiver and an SBS detector. The later system has fixed (and lower) complexity per symbol/sample, but may not be optimum. Interference between successive transmissions, or intersymbol interference (ISI), can degrade the performance of symbol-by-symbol detection. This performance degradation increases as T decreases (or the symbol rate increases) in most communication channels. The designer mathematically analyzes ISI by rewriting (3.2) as

$$x(t) = \sum_{k=0}^{K-1} \sum_{n=1}^{N} x_{kn}\varphi_n(t - kT) \; , \tag{3.3}$$

---

[1] The symbol rate is sometimes also called the "baud rate," although abuse of the term baud (by equating it with data rate even when $M \neq 2$) has rendered the term archaic among communication engineers, and the term "baud" usually now only appears in trade journals and advertisements.
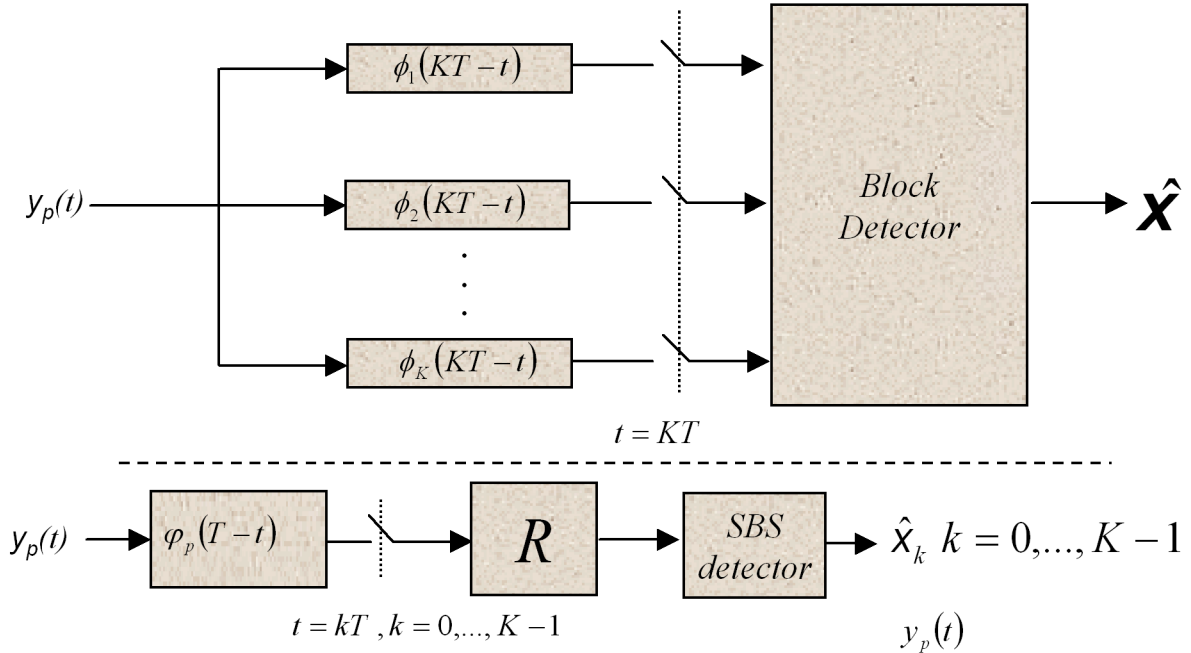
Figure 3.2: Comparison of Block and SBS detectors for successive transmission of K messages.

where the transmissions $x_k(t)$ are decomposed using a common orthonormal basis set $\{\varphi_n(t)\}$. In (3.3), $\varphi_n(t - kT)$ and $\varphi_m(t - lT)$ may be non-orthogonal when $k \neq l$. In some cases, translates of the basis functions are orthogonal. For instance, in QAM, the two bandlimited basis functions

$$\varphi_1(t) = \sqrt{\frac{2}{T}} \cos\left(\frac{m\pi t}{T}\right) \cdot \text{sinc}\left(\frac{t}{T}\right) \tag{3.4}$$

$$\varphi_2(t) = -\sqrt{\frac{2}{T}} \sin\left(\frac{m\pi t}{T}\right) \cdot \text{sinc}\left(\frac{t}{T}\right) \quad , \tag{3.5}$$

or from Chapter 2, the baseband equivalent

$$\varphi(t) = \frac{1}{\sqrt{T}} \text{sinc}\left(\frac{t}{T}\right) \quad . \tag{3.6}$$

(with m a positive integer) are orthogonal for all integer-multiple-of-T time translations. In this case, the successive transmissions, when sampled at time instants kT, are free of ISI, and transmission is equivalent to a succession of "one-shot" uses of the channel. In this case symbol-by-symbol detection is optimal, and the MAP detector for the entire block of messages is the same as a MAP detector used separately for each of the K independent transmissions. Signal sets for data transmission are usually designed to be orthogonal for any translation by an integer multiple of symbol periods. Most linear AWGN channels, however, are more accurately modeled by a filtered AWGN channel as discussed in Section 1.7 and Chapter 2. The filtering of the channel alters the basis functions so that at the channel output the filtered basis functions are no longer orthogonal. The channel thus introduces ISI.

3.1.2 Bandlimited Channels

The bandlimited linear ISI channel, shown in Figure 3.3, is the same as the filtered AWGN channel discussed in Section 1.7. This channel is used, however, for successive transmission of data symbols.
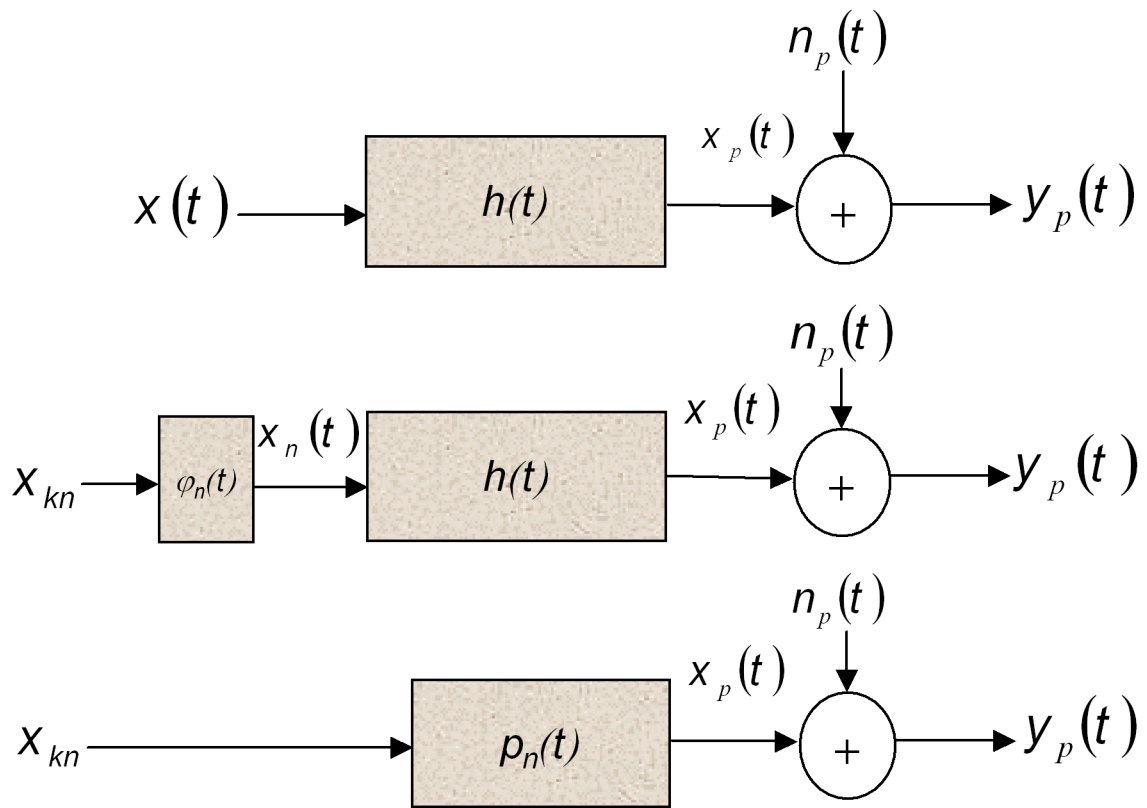
Figure 3.3: The bandlimited channel, and equivalent forms with pulse response.

The (noise-free) channel output, $x_p(t)$, in Figure 3.3 is given by

$$x_p(t) \quad = \quad \sum_{k=0}^{K-1} \sum_{n=1}^{N} x_{kn} \cdot \varphi_n(t - kT) * h(t) \tag{3.7}$$

$$= \quad \sum_{k=0}^{K-1} \sum_{n=1}^{N} x_{kn} \cdot p_n(t - kT) \tag{3.8}$$

where $p_n(t) \triangleq \varphi_n(t) * h(t)$. When $h(t) \neq \delta(t)$, the functions $p_n(t - kT)$ do not necessarily form an orthonormal basis, nor are they even necessarily orthogonal. An optimum (MAP) detector would need to search a signal set of size M^K, which is often too complex for implementation as K gets large. When $N = 1$ (or $N = 2$ with complex signals), there is only one pulse response $p(t)$.

Equalization methods apply a processor, the "equalizer", to the channel output *to try* to convert $\{p_n(t - kT)\}$ to an orthogonal set of functions. Symbol-by-symbol detection can then be used on the equalized channel output. Further discussion of such equalization filters is deferred to Section 3.4. The remainder of this chapter also presumes that the channel-input symbol sequence x_k is independent and identically distributed at each point in time. This presumption will be relaxed in later Chapters.

While a very general theory of ISI could be undertaken for any N, such a theory would unnecessarily complicate the present development.[2] This chapter handles the ISI-equalizer case for $N = 1$. Using the baseband-equivalent systems of Chapter 2, this chapter's (Chapter 3's) analysis will also apply to quadrature modulated systems modeled as complex (equivalent to two-dimensional real) channels. In this way, the developed theory of ISI and equalization will apply equally well to any one-dimensional (e.g. PAM) or two-dimensional (e.g. QAM or hexagonal) constellation. This was the main motivation for the introduction of bandpass analysis in Chapter 2.

The **pulse response** for the transmitter/channel fundamentally quantifies ISI:

> **Definition 3.1.1 (Pulse Response)** *The **pulse response** of a bandlimited channel is defined by*
>
> $$p(t) = \varphi(t) * h(t) \quad . \tag{3.9}$$
>
> *For the complex QAM case, $p(t)$, $\varphi(t)$, and $h(t)$ can be complex time functions.*

The one-dimensional noiseless channel output $x_p(t)$ is

$$x_p(t) \quad = \quad \sum_{k=0}^{K-1} x_k \cdot \varphi(t - kT) * h(t) \tag{3.10}$$

$$= \quad \sum_{k=0}^{K-1} x_k \cdot p(t - kT) \quad . \tag{3.11}$$

The signal in (3.11) is real for a one-dimensional system and complex for a baseband equivalent quadrature modulated system. The pulse response energy $\|p\|^2$ is not necessarily equal to 1, and this text introduces the **normalized pulse response**:

$$\varphi_p(t) \triangleq \frac{p(t)}{\|p\|} \quad , \tag{3.12}$$

where

$$\|p\|^2 = \int_{-\infty}^{\infty} p(t) p^*(t) dt = \langle p(t), p(t) \rangle \quad . \tag{3.13}$$

The subscript p on $\varphi_p(t)$ indicates that $\varphi_p(t)$ is a normalized version of $p(t)$. Using (3.12), Equation (3.11) becomes

$$x_p(t) = \sum_{k=0}^{K-1} x_{p,k} \cdot \varphi_p(t - kT) \quad , \tag{3.14}$$

---

[2]Chapter 4 considers multidimensional signals and intersymbol interference, while Section 3.7 considers diversity receivers that may have several observations a single or multiple channel output(s).
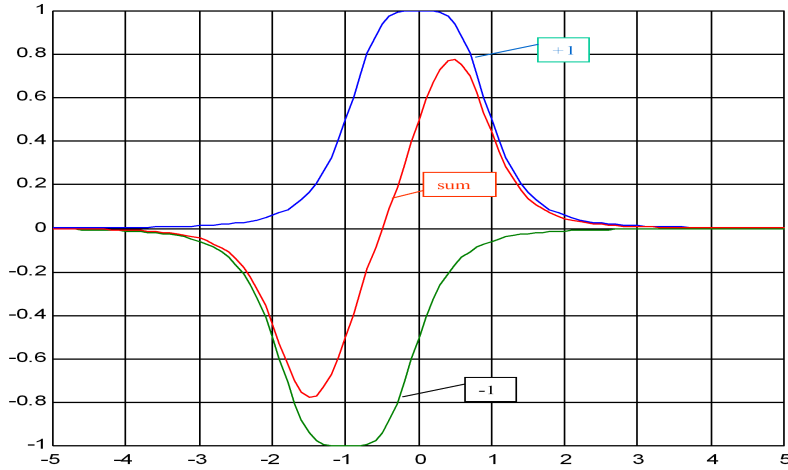
Figure 3.4: Illustration of intersymbol interference for $p(t) = \frac{1}{1+t^4}$ with $T = 1$.

where

$$x_{p,k} \overset{\Delta}{=} x_k \cdot \|p\| \quad . \tag{3.15}$$

$x_{p,k}$ absorbs the channel gain/attenuation $\|p\|$ into the definition of the input symbol, and thus has energy $\mathcal{E}_p = E\left[|x_{p,k}|^2\right] = \mathcal{E}_{\boldsymbol{x}} \cdot \|p\|^2$. While the functions $\varphi_p(t - kT)$ are normalized, they are not necessarily orthogonal, so symbol-by-symbol detection is not necessarily optimal for the signal in (3.14).

EXAMPLE 3.1.1 (Intersymbol interference and the pulse response) As an example of intersymbol interference, consider the pulse response $p(t) = \frac{1}{1+t^4}$ and two successive transmissions of opposite polarity (-1 followed by $+1$) through the corresponding channel. Figure 3.4 illustrates the two isolated pulses with correct polarity and also the waveform corresponding to the two transmissions separated by 1 unit in time. Clearly the peaks of the pulses have been displaced in time and also significantly reduced in amplitude. Higher transmission rates would force successive transmissions to be closer and closer together. Figure 3.5 illustrates the resultant sum of the two waveforms for spacings of 1 unit in time, .5 units in time, and .1 units in time. Clearly, ISI has the effect of severely reducing pulse strength, thereby reducing immunity to noise.

EXAMPLE 3.1.2 (Pulse Response Orthogonality - Modified Duobinary) A PAM modulated signal using rectangular pulses is

$$\varphi(t) = \frac{1}{\sqrt{T}}(u(t) - u(t - T)) \quad . \tag{3.16}$$

The channel introduces ISI, for example, according to

$$h(t) = \delta(t) + \delta(t - T). \tag{3.17}$$
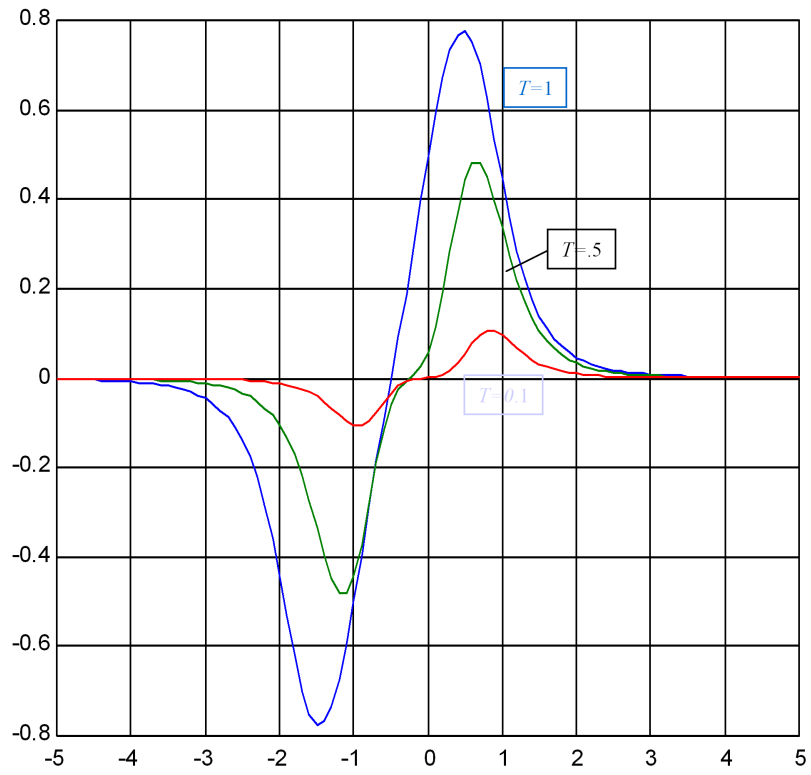
Figure 3.5: ISI with increasing symbol rate.

The resulting pulse response is

$$p(t) = \frac{1}{\sqrt{T}}(u(t) - u(t - 2T)) \tag{3.18}$$

and the normalized pulse response is

$$\varphi_p(t) = \frac{1}{\sqrt{2T}}(u(t) - u(t - 2T)). \tag{3.19}$$

The pulse-response translates $\varphi_p(t)$ and $\varphi_p(t - T)$ are not orthogonal, even though $\varphi(t)$ and $\varphi(t - T)$ were originally orthonormal.

Noise Equivalent Pulse Response

Figure 3.6 models a channel with additive Gaussian noise that is not white, which often occurs in practice. The power spectral density of the noise is $\frac{N_0}{2} \cdot S_n(f)$. When $S_n(f) \neq 0$ (noise is never exactly zero at any frequency in practice), the noise psd has an invertible square root as in Section 1.7. The invertible square-root can be realized as a filter in the beginning of a receiver. Since this filter is invertible, by the reversibility theorem of Chapter 1, no information is lost. The designer can then construe this filter as being pushed back into, and thus a part of, the channel as shown in the lower part of Figure 3.6. The noise equivalent pulse response then has Fourier Transform $P(f)/S_n^{1/2}(f)$ for an equivalent filtered-AWGN channel. The concept of noise equivalence allows an analysis for AWGN to be valid (using the equivalent pulse response instead of the original pulse response). Then also "colored noise" is equivalent in its effect to ISI, and furthermore the compensating equalizers that are developed later in this chapter can also be very useful on channels that originally have no ISI, but that do have "colored noise." An AWGN channel with a notch in $H(f)$ at some frequency is thus equivalent to a "flat channel" with $H(f) = 1$, but with narrow-band Gaussian noise at the same frequency as the notch.

3.1.3 The ISI-Channel Model

A model for linear ISI channels is shown in Figure 3.7. In this model, x_k is scaled by $\|p\|$ to form $x_{p,k}$ so that $\mathcal{E}_{\boldsymbol{x}_p} = \mathcal{E}_{\boldsymbol{x}} \cdot \|p\|^2$. The additive noise is white Gaussian, although correlated Gaussian noise can be included by transforming the correlated-Gaussian-noise channel into an equivalent white Gaussian noise channel using the methods in the previous subsection and illustrated in Figure 3.6. The channel output $y_p(t)$ is passed through a matched filter $\varphi_p^*(-t)$ to generate $y(t)$. Then, $y(t)$ is sampled at the symbol rate and subsequently processed by a discrete time receiver. The following theorem illustrates that there is no loss in performance that is incurred via the matched-filter/sampler combination.

> **Theorem 3.1.1 (ISI-Channel Model Sufficiency)** *The discrete-time signal samples $y_k = y(kT)$ in Figure 3.7 are sufficient to represent the continuous-time ISI-model channel output $y(t)$, if $0 < \|p\| < \infty$. (i.e., a receiver with minimum P_e can be designed that uses only the samples y_k).*
>
> **Sketch of Proof:**
> Define
> $$\varphi_{p,k}(t) \stackrel{\Delta}{=} \varphi_p(t - kT) \quad , \tag{3.20}$$
> where $\{\varphi_{p,k}(t)\}_{k \in (-\infty, \infty)}$ is a linearly independent set of functions. The set $\{\varphi_{p,k}(t)\}_{k \in (-\infty, \infty)}$ is related to a set of orthogonal basis functions $\{\phi_{p,k}(t)\}_{k \in (-\infty, \infty)}$ by an invertible transformation Γ (use Gram-Schmidt an infinite number of times). The transformation and its inverse are written
> $$\{\phi_{p,k}(t)\}_{k \in (-\infty, \infty)} = \Gamma(\{\varphi_{p,k}(t)\}_{k \in (-\infty, \infty)}) \tag{3.21}$$
> $$\{\varphi_{p,k}(t)\}_{k \in (-\infty, \infty)} = \Gamma^{-1}(\{\phi_{p,k}(t)\}_{k \in (-\infty, \infty)}) \quad , \tag{3.22}$$
> where Γ is the invertible transformation. In Figure 3.8, the transformation outputs are the filter samples $y(kT)$. The infinite set of filters $\{\phi_{p,k}^*(-t)\}_{k \in (-\infty, \infty)}$ followed by Γ^{-1} is

$\sigma^2 \cdot S_n(f)$

(AGN)

x_k → $P(f)$ → + → $S_n^{-\frac{1}{2}}(f)$ →

reversible filter
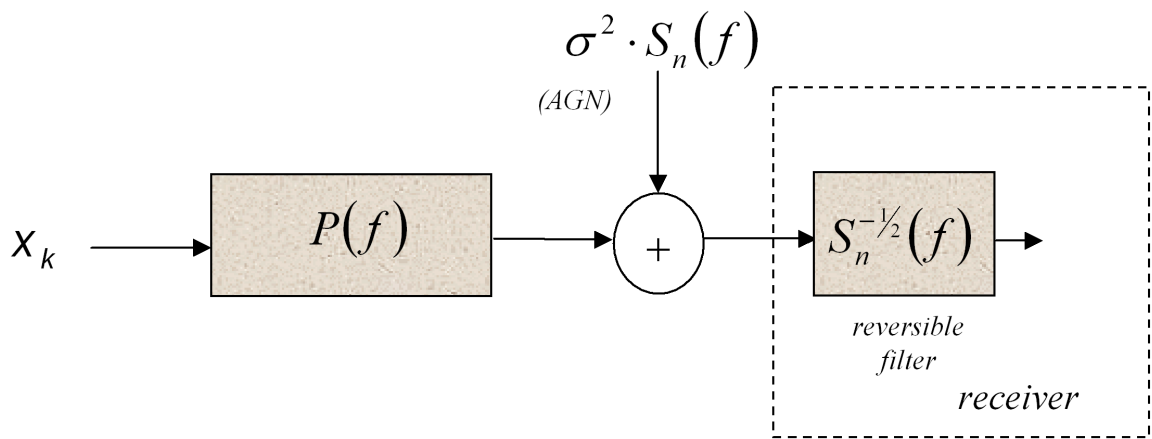
receiver

White-noise equiv channel (with reversible receiver "noise-whitening" filter as part of pulse response)

σ^2

(AWGN)

x_k → $P(f) \big/ S_n^{\frac{1}{2}}(f)$ → + → To matched filter ...

equivalent pulse response
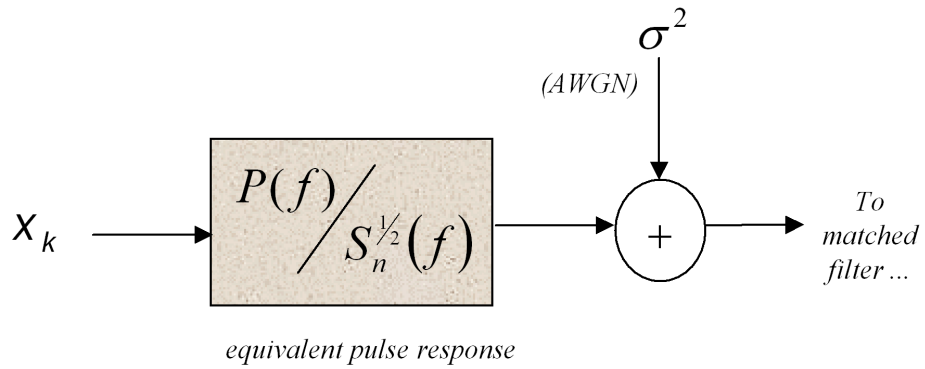
Figure 3.6: White Noise Equivalent Channel.

pulse response p(t)

$n_p(t)$

x_k → $\|p\|$ → $x_{p,k}$ → $\varphi_p(t)$ → $x_p(t)$ → Σ → $y_p(t)$ → $\varphi_p^*(-t)$ → $y(t)$ → y_k → discrete time receiver → $\hat{x}_k$

sample at times kT

$q(t) = \varphi_p(t) * \varphi_p^*(-t)$
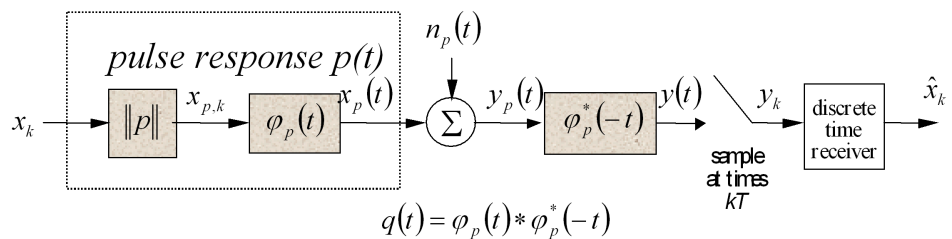
Figure 3.7: The ISI-Channel model.

158
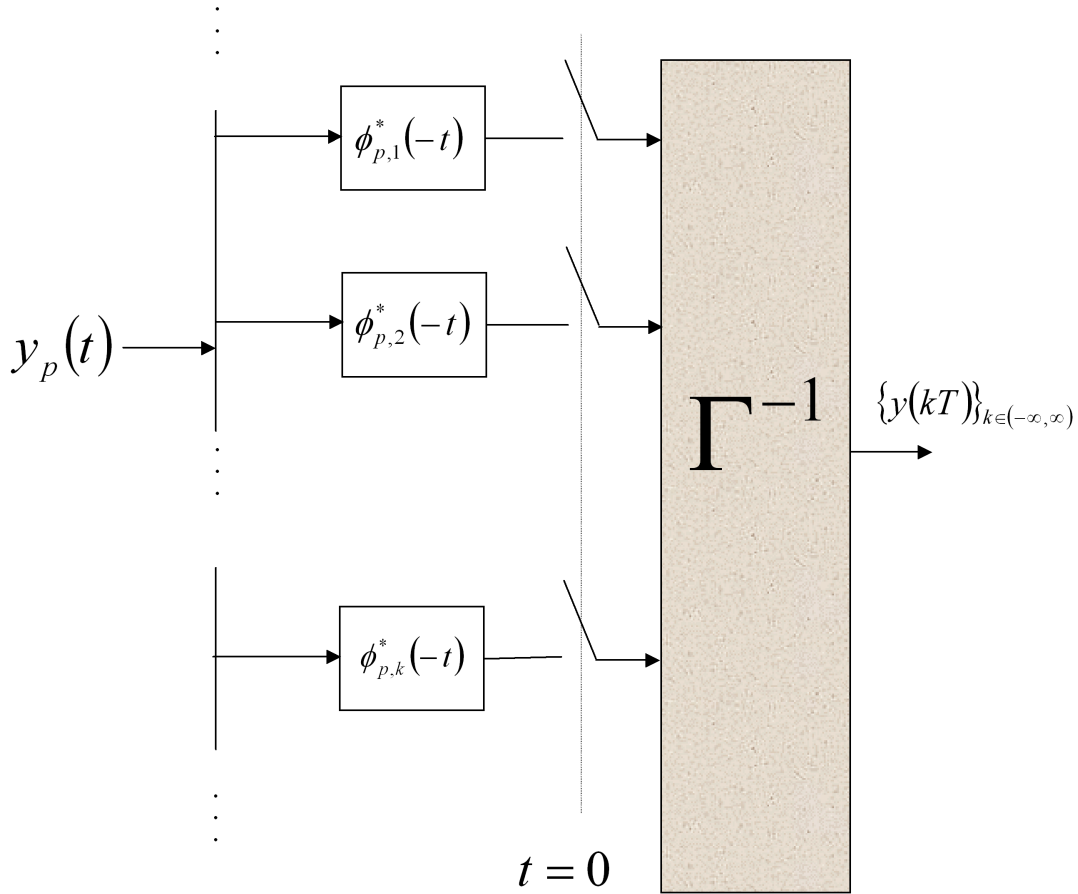
Figure 3.8: Equivalent diagram of ISI-channel model matched-filter/sampler

equivalent to an infinite set of matched filters to $\left\{\varphi_{p,k}^*(-t)\right\}_{k\in(-\infty,\infty)}$. By (3.20) this last set is equivalent to a single matched filter $\varphi_p^*(-t)$, whose output is sampled at $t = kT$ to produce $y(kT)$. Since the set $\{\phi_{p,k}(t)\}_{k\in(-\infty,\infty)}$ is orthonormal, the set of sampled filter outputs in Figure 3.8 are sufficient to represent $y_p(t)$. Since Γ^{-1} is invertible (inverse is Γ), then by the theorem of reversibility in Chapter 1, the sampled matched filter output $y(kT)$ is a sufficient representation of the ISI-channel output $y_p(t)$. **QED.**

Referring to Figure 3.7,

$$y(t) = \sum_k \|p\| \cdot x_k q(t - kT) + n_p(t) * \varphi_p^*(-t) \quad , \tag{3.23}$$

where

$$q(t) \stackrel{\Delta}{=} \varphi_p(t) * \varphi_p^*(-t) = \frac{p(t) * p^*(-t)}{\|p\|^2} \quad . \tag{3.24}$$

The deterministic autocorrelation function $q(t)$ is Hermitian ($q^*(-t) = q(t)$). Also, $q(0) = 1$, so the symbol x_k passes at time kT to the output with amplitude scaling $\|p\|$. The function $q(t)$ can also exhibit ISI, as illustrated in Figure 3.9. The plotted $q(t)$ corresponds to $q_k = [-.1159\ .2029\ 1\ .2029\ -.1159]$ or, equivalently, to the channel $p(t) = \sqrt{\frac{1}{T}} \cdot (\text{sinc}(t/T) + .25 \cdot \text{sinc}((t-T)/T) - .125 \cdot \text{sinc}((t-2T)/T))$, or

159
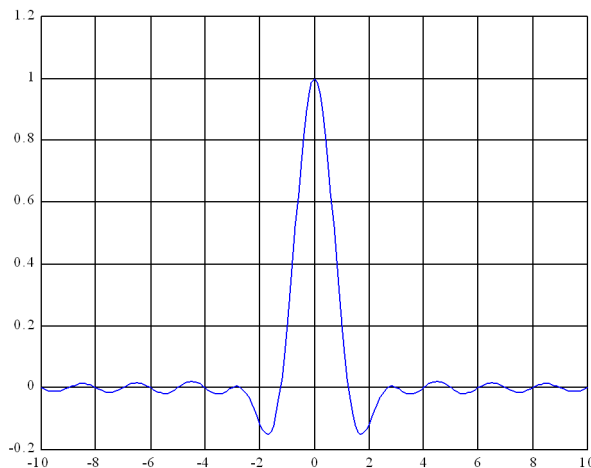
Figure 3.9: ISI in q(t)

$P(D) = \frac{1}{\sqrt{T}} \cdot (1 + .5D)(1 - .25D)$ (the notation $P(D)$ is defined in Appendix A.2). (The values for q_k can be confirmed by convolving $p(t)$ with its time reverse, normalizing, and sampling.) For notational brevity, let $y_k \triangleq y(kT)$, $q_k \triangleq q(kT)$, $n_k \triangleq n(kT)$ where $n(t) \triangleq n_p(t) * \varphi_p^*(-t)$. Thus

$$y_k = \underbrace{\|p\| \cdot x_k}_{\text{scaled input (desired)}} + \underbrace{n_k}_{\text{noise}} + \underbrace{\|p\| \cdot \sum_{m \neq k} x_m q_{k-m}}_{\text{ISI}} \quad . \tag{3.25}$$

The output y_k consists of the scaled input, noise and ISI. The scaled input is the desired information-bearing signal. The ISI and noise are unwanted signals that act to distort the information being transmitted. The ISI represents a new distortion component not previously considered in the analysis of Chapters 1 and 2 for a suboptimum SBS detector. This SBS detector is the same detector as in Chapters 1 and 2, except used under the (false) assumption that the ISI is just additional AWGN. Such a receiver can be decidedly suboptimum when the ISI is nonzero.

Using D-transform notation, (3.25) becomes

$$Y(D) = X(D) \cdot \|p\| \cdot Q(D) + N(D) \tag{3.26}$$

where $Y(D) \triangleq \sum_{k=-\infty}^{\infty} y_k \cdot D^k$. If the receiver uses symbol-by-symbol detection on the sampled output y_k, then the noise sample n_k of (one-dimensional) variance $\frac{N_0}{2}$ at the matched-filter output combines with ISI from the sample times mT ($m \neq k$) in corrupting $\|p\| \cdot x_k$.

There are two common measures of ISI distortion. The first is **Peak Distortion**, which only has meaning for real-valued $q(t)$: [3]

Definition 3.1.2 (Peak Distortion Criterion) *If $|x_{max}|$ is the maximum value for $|x_k|$, then the peak distortion is:*

$$\mathcal{D}_p \triangleq |x|_{max} \cdot \|p\| \cdot \sum_{m \neq 0} |q_m| \quad . \tag{3.27}$$

---

[3]In the real case, the magnitudes correspond to actual values. However, for complex-valued terms, the ISI is characterized by both its magnitude and phase. So, addition of the magnitudes of the symbols ignores the phase components, which may significantly change the ISI term.

For $q(t)$ in Figure 3.9 with $x_{max} = 3$, $\mathcal{D}_p = 3 \cdot \|p\|(.1159 + .2029 + .2029 + .1159) \approx 3 \cdot \sqrt{1.078} \cdot .6376 \approx 1.99$.

The peak distortion represents a worst-case loss in minimum distance between signal points in the signal constellation for x_k, or equivalently

$$P_e \leq N_e Q \left[\frac{\|p\| \frac{d_{\min}}{2} - \mathcal{D}_p}{\sigma} \right] \quad , \tag{3.28}$$

for symbol-by-symbol detection. Consider two matched filter outputs y_k and y'_k that the receiver attempts to distinguish by suboptimally using symbol-by-symbol detection. These outputs are generated by two different sequences $\{x_k\}$ and $\{x'_k\}$. Without loss of generality, assume $y_k > y'_k$, and consider the difference

$$y_k - y'_k = \|p\| \left[(x_k - x'_k) + \sum_{m \neq k} (x_m - x'_m) q_{k-m} \right] + \tilde{n} \tag{3.29}$$

The summation term inside the brackets in (3.29) represents the change in distance between y_k and y'_k caused by ISI. Without ISI the distance is

$$y_k - y'_k \geq \|p\| \cdot d_{min} \quad , \tag{3.30}$$

while with ISI the distance can decrease to

$$y_k - y'_k \geq \|p\| \left[d_{min} - 2|x|_{max} \sum_{m \neq 0} |q_m| \right] \quad . \tag{3.31}$$

Implicitly, the distance interpretation in (3.31) assumes $2\mathcal{D}_p \leq \|p\|d_{\min}$.[4]

While peak distortion represents the worst-case ISI, this worst case might not occur very often in practice. For instance, with an input alphabet size $M = 4$ and a $q(t)$ that spans 15 symbol periods, the probability of occurrence of the worst-case value (worst level occurring in all 14 ISI contributors) is $4^{-14} = 3.7 \times 10^{-9}$, well below typical channel P_e's in data transmission. Nevertheless, there may be other ISI patterns of nearly just as bad interference that can also occur. Rather than separately compute each possible combination's reduction of minimum distance, its probability of occurrence, and the resulting error probability, data transmission engineers more often use a measure of ISI called **Mean-Square Distortion** (valid for 1 or 2 dimensions):

Definition 3.1.3 (Mean-Square Distortion) *The* **Mean-Square Distortion** *is defined by:*

$$\mathcal{D}_{ms} \quad \triangleq \quad E \left\{ | \sum_{m \neq k} x_{p,m} \cdot q_{k-m}|^2 \right\} \tag{3.32}$$

$$= \quad \mathcal{E}_{\boldsymbol{x}} \cdot \|p\|^2 \cdot \sum_{m \neq 0} |q_m|^2 \quad , \tag{3.33}$$

where (3.33) is valid when the successive data symbols are independent and identically distributed with zero mean.

In the example of Figure 3.9, the mean-square distortion (with $\mathcal{E}_{\boldsymbol{x}} = 5$) is $\mathcal{D}_{ms} = 5\|p\|^2(.1159^2 + .2029^2 + .2029^2 + .1159^2) \approx 5(1.078).109 \approx .588$. The fact $\sqrt{.588} = .767 < 1.99$ illustrates that $\mathcal{D}_{ms} \leq \mathcal{D}_p^2$. (The proof of this fact is left as an exercise to the reader.)

The mean-square distortion criterion assumes (erroneously[5]) that $\mathcal{D}_{ms}$ is the variance of an uncorrelated Gaussian noise that is added to n_k. With this assumption, P_e is approximated by

$$P_e \approx N_e \cdot Q \left[\frac{\|p\|d_{\min}}{2\sqrt{\sigma^2 + \bar{\mathcal{D}}_{ms}}} \right] \quad . \tag{3.34}$$

---

[4]On channels for which $2\mathcal{D}_p \geq \|p\|d_{\min}$, the worst-case ISI occurs when $|2\mathcal{D}_p - \|p\|d_{\min}|$ is maximum.

[5]This assumption is only true when x_k is Gaussian. In very well-designed data transmission systems, x_k is approximately i.i.d. and Gaussian, see Chapter 6, so that this approximation of Gaussian ISI becomes accurate.

One way to visualize ISI is through the "eye diagram", some examples of which are shown in Figures 3.10 and 3.11. The eye diagram is similar to what would be observed on an oscilloscope, when the trigger is synchronized to the symbol rate. The eye diagram is produced by overlaying several successive symbol intervals of the modulated and filtered continuous-time waveform (except Figures 3.10 and 3.11 do not include noise). The Lorentzian pulse response $p(t) = 1/(1 + (3t/T)^2)$ is used in both plots. For binary transmission on this channel, there is a significant opening in the eye in the center of the plot in Figure 3.10. With 4-level PAM transmission, the openings are much smaller, leading to less noise immunity. The ISI causes the spread among the path traces; more ISI results in a narrower eye opening. Clearly increasing M reduces the eye opening.
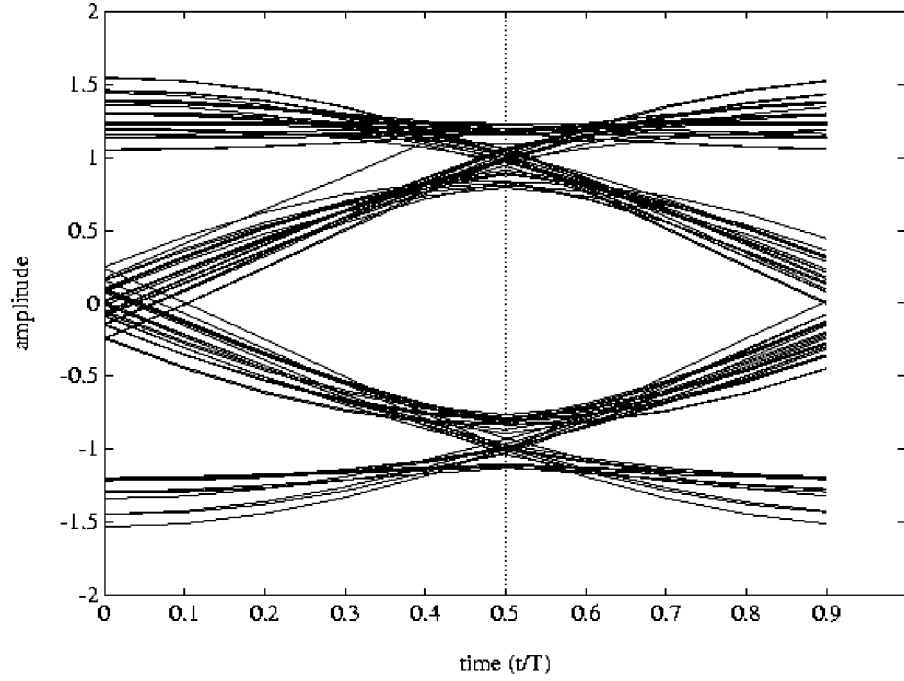
Figure 3.10: Binary eye diagram for a Lorentzian pulse response.
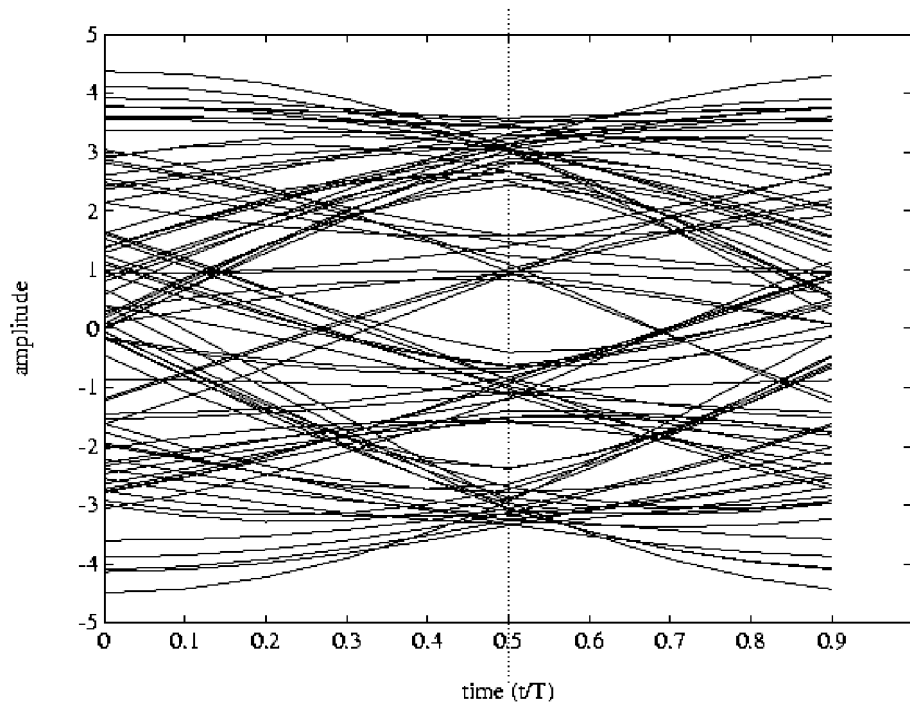
Figure 3.11: 4-Level eye diagram for a Lorentzian pulse response.
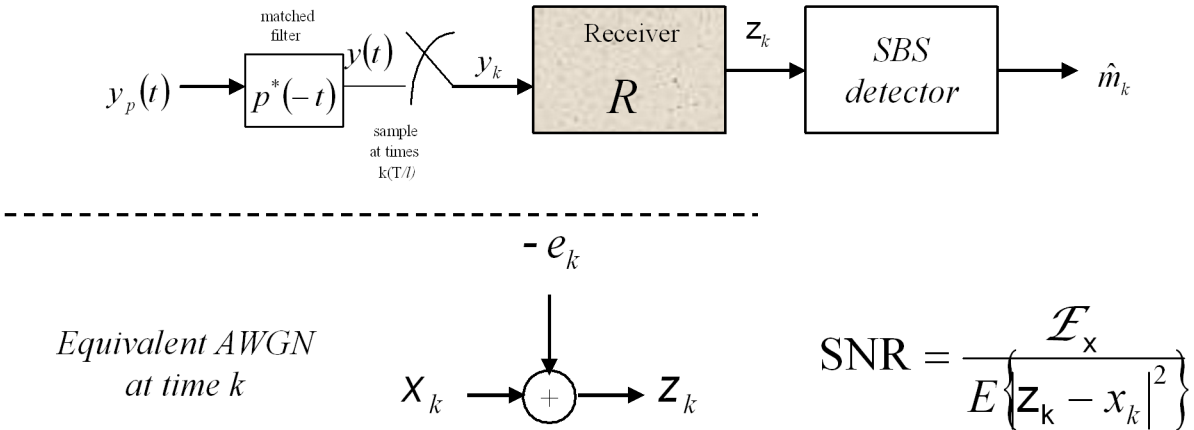
Figure 3.12: Use of possibly suboptimal receiver to approximate/create an equivalent AWGN.

3.2   Basics of the Receiver-generated Equivalent AWGN

Figure 3.12 focuses upon the receiver and specifically the device shown generally as R. When channels have ISI, such a receiving device is inserted at the sampler output. The purpose of the receiver is to attempt to convert the channel into an equivalent AWGN that is also shown below the dashed line. Such an AWGN is not always exactly achieved, but nonetheless any deviation between the receiver output z_k and the channel input symbol x_k is viewed as additive white Gaussian noise. An SNR, as in Subsection 3.2.1 can be used then to analyze the performance of the symbol-by-symbol detector that follows the receiver R. Usually, smaller deviation from the transmitted symbol means better performance, although not exactly so as Subsection 3.2.2 discusses. Subsection 3.2.3 finishes this section with a discussion of the highest possible SNR that a designer could expect for any filtered AWGN channel, the so-called "matched-filter-bound" SNR, SNR_{MFB}. This section shall not be specific as to the content of the box shown as R, but later sections will allow both linear and slightly nonlinear structures that may often be good choices because their performance can be close to SNR_{MFB}.

3.2.1   Receiver Signal-to-Noise Ratio

Definition 3.2.1 (Receiver SNR) *The* **receiver SNR***, SNR_R for any receiver R with (pre-decision) output z_k, and decision regions based on x_k (see Figure 3.12) is*

$$SNR_R \triangleq \frac{\mathcal{E}_{\boldsymbol{x}}}{E|e_k|^2} \quad , \tag{3.35}$$

where $e_k \overset{\Delta}{=} x_k - z_k$ is the **receiver error***. The denominator of (3.35) is the* **mean-square error** *$MSE = E|e_k|^2$. When $E[z_k|x_k] = x_k$, the receiver is* **unbiased** *(otherwise* **biased***) with respect to the decision regions for x_k.*

The concept of a receiver SNR facilitates evaluation of the performance of data transmission systems with various compensation methods (i.e. equalizers) for ISI. Use of SNR as a performance measure builds upon the simplifications of considering mean-square distortion, that is both noise and ISI are jointly considered in a single measure. The two right-most terms in (3.25) have normalized mean-square value $\sigma^2 + \bar{\mathcal{D}}_{ms}$. The SNR for the matched filter output y_k in Figure 3.12 is the ratio of channel output sample energy $\bar{\mathcal{E}}_{\boldsymbol{x}}\|p\|^2$ to the mean-square distortion $\sigma^2 + \bar{\mathcal{D}}_{ms}$. This SNR is often directly related to probability of error and is a function of both the receiver and the decision regions for the SBS detector. This text uses SNR consistently, replacing probability of error as a measure of comparative performance. SNR is easier to compute than P_e, independent of M at constant $\bar{\mathcal{E}}_{\boldsymbol{x}}$, and a generally good measure
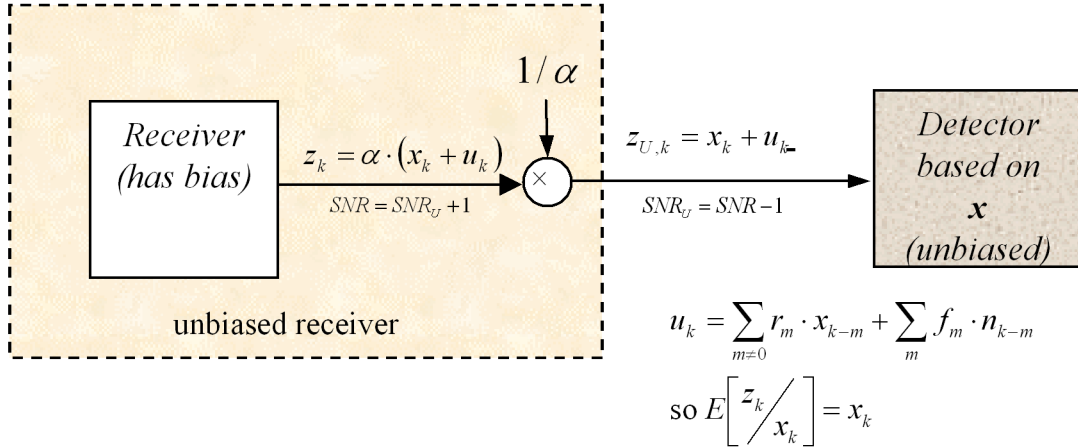
Figure 3.13: Receiver SNR concept.

of performance: higher SNR means lower probability of error. The probability of error is difficult to compute exactly because the distribution of the ISI-plus-noise is not known or is difficult to compute. The SNR is easier to compute and this text assumes that the insertion of the appropriately scaled SNR (see Chapter 1 - Sections 1.4 - 1.6)) into the argument of the Q-function approximates the probability of error for the suboptimum SBS detector. Even when this insertion into the Q-function is not sufficiently accurate, comparison of SNR's for different receivers usually relates which receiver is better.

3.2.2   Receiver Biases

Figure 3.13 illustrates a receiver that somehow has tried to reduce the combination of ISI and noise. Any time-invariant receiver's output samples, z_k, satisfy

$$z_k = \alpha \cdot (x_k + u_k) \tag{3.36}$$

where α is some positive scale factor that may have been introduced by the receiver and u_k is an uncorrelated distortion

$$u_k = \sum_{m \neq 0} r_m \cdot x_{k-m} + \sum_m f_m \cdot n_{k-m} \quad . \tag{3.37}$$

The coefficients for residual intersymbol interference r_m and the coefficients of the filtered noise f_k will depend on the receiver and generally determine the level of mean-square distortion. The uncorrelated distortion has no remnant of the current symbol being decided by the SBS detector, so that $E[u_k/x_k] = 0$. However, the receiver may have found that by scaling (reducing) the x_k component in z_k by α that the SNR improves (small signal loss in exchange for larger uncorrelated distortion reduction). When $E[z_k/x_k] = \alpha \cdot x_k \neq x_k$, the decision regions in the SBS detector are "biased." Removal of the bias is easily achieved by scaling by $1/\alpha$ as also in Figure 3.13. If the distortion is assumed to be Gaussian noise, as is the assumption with the SBS detector, then removal of bias by scaling by $1/\alpha$ improves the probability of error of such a detector as in Chapter 1. (Even when the noise is not Gaussian as is the case with the ISI component, scaling the signal correctly improves the probability of error on the average if the input constellation has zero mean.)

The following theorem relates the SNR's of the unbiased and biased decision rules for any receiver R:

Theorem 3.2.1 (Unconstrained and Unbiased Receivers) *Given an unbiased receiver R for a decision rule based on a signal constellation corresponding to x_k, the maximum unconstrained SNR corresponding to that same receiver with any biased decision rule is*

$$SNR_R = SNR_{R,U} + 1 \quad , \tag{3.38}$$

where $SNR_{R,U}$ is the SNR using the unbiased decision rule.

Proof: From Figure 3.13, the SNR after scaling is easily

$$\text{SNR}_{R,U} = \frac{\bar{\mathcal{E}}_{\boldsymbol{x}}}{\bar{\sigma}_u^2} \quad . \tag{3.39}$$

The maximum SNR for the biased signal z_k prior to the scaling occurs when α is chosen to maximize the unconstrained SNR

$$\text{SNR}_R = \frac{\mathcal{E}_{\boldsymbol{x}}}{|\alpha|^2 \sigma_u^2 + |1 - \alpha|^2 \mathcal{E}_{\boldsymbol{x}}} \quad . \tag{3.40}$$

Allowing for complex α with phase θ and magnitude $|\alpha|$, the SNR maximization over alpha is equivalent to minimizing

$$1 - 2|\alpha|cos(\theta) + |\alpha|^2(1 + \frac{1}{\text{SNR}_{R,U}}) \quad . \tag{3.41}$$

Clearly $\theta = 0$ for a minimum and differentiating with respect to $|\alpha|$ yields $-2 + 2|\alpha|(1 + \frac{1}{\text{SNR}_{R,U}}) = 0$ or $\alpha_{opt} = 1/(1 + (\text{SNR}_{R,U})^{-1})$. Substitution of this value into the expression for SNR_R finds

$$\text{SNR}_R = \text{SNR}_{R,U} + 1 \quad . \tag{3.42}$$

Thus, a receiver R and a corresponding SBS detector that have zero bias will not correspond to a maximum SNR – the SNR can be improved by scaling (reducing) the receiver output by α_{opt}. Conversely, a receiver designed for maximum SNR can be altered slightly through simple output scaling by $1/\alpha_{opt}$ to a related receiver that has no bias and has SNR thereby reduced to $\text{SNR}_{R,U} = \text{SNR}_R - 1$. **QED**.

To illustrate the relationship of unbiased and biased receiver SNRs, suppose an ISI-free AWGN channel has an SNR=10 with $\mathcal{E}_{\boldsymbol{x}} = 1$ and $\sigma_u^2 = \frac{N_0}{2} = .1$. Then, a receiver could scale the channel output by $\alpha = 10/11$. The resultant new error signal is $e_k = x_k(1 - \frac{10}{11}) - \frac{10}{11}n_k$, which has MSE=$E[|e_k|^2] = \frac{1}{121} + \frac{100}{121}(.1) = \frac{1}{11}$, and SNR=11. Clearly, the biased SNR is equal to the unbiased SNR plus 1. The scaling has done nothing to improve the system, and the appearance of an improved SNR is an artifact of the SNR definition, which allows noise to be scaled down without taking into account the fact that actual signal power after scaling has also been reduced. Removing the bias corresponds to using the actual signal power, and the corresponding performance-characterizing SNR can always be found by subtracting 1 from the biased SNR. A natural question is then "Why compute the biased SNR?" The answer is that the biased receiver corresponds directly to minimizing the mean-square distortion, and the SNR for the "MMSE" case will often be easier to compute. Figure 3.27 in Section 3.5 illustrates the usual situation of removing a bias (and consequently reducing SNR, but not improving P_e since the SBS detector works best when there is no bias) from a receiver that minimizes mean-square distortion (or error) to get an unbiased decision. The bias from a receiver that maximizes SNR by equivalently minimizing mean-square error can then be removed by simple scaling and the resultant more accurate SNR is thus found for the unbiased receiver by subtracting 1 from the more easily computed biased receiver. This concept will be very useful in evaluating equalizer performance in later sections of this chapter, and is formalized in Theorem 3.2.2 below.

Theorem 3.2.2 (Unbiased MMSE Receiver Theorem) *Let $\mathcal{R}$ be any allowed class of receivers R producing outputs z_k, and let R_{opt} be the receiver that achieves the maximum signal-to-noise ratio $SNR(R_{opt})$ over all $R \in \mathcal{R}$ with an unconstrained decision rule. Then the receiver that achieves the maximum SNR with an unbiased decision rule is also R_{opt}, and*

$$\max_{R \in \mathcal{R}} SNR_{R,U} = SNR(R_{opt}) - 1. \tag{3.43}$$

Proof. From Theorem 3.2.1, for any $R \in \mathcal{R}$, the relation between the signal-to-noise ratios of unbiased and unconstrained decision rules is $\text{SNR}_{R,U} = \text{SNR}_R - 1$, so

$$\max_{R \in \mathcal{R}}[\text{SNR}_{R,U}] = \max_{R \in \mathcal{R}}[\text{SNR}_R] - 1 = \text{SNR}_{R_{opt}} - 1 \quad . \tag{3.44}$$

QED.

This theorem implies that the optimum unbiased receiver and the optimum biased receiver settings are identical except for any scaling to remove bias; only the SNR measures are different. For any SBS detector, $SNR_{R,U}$ is the SNR that corresponds to best P_e. The quantity $SNR_{R,U} + 1$ is artificially high because of the bias inherent in the general SNR definition.

3.2.3 The Matched-Filter Bound

The **Matched-Filter Bound (MFB)**, also called the "one-shot" bound, specifies an upper SNR limit on the performance of data transmission systems with ISI.

> **Lemma 3.2.1 (Matched-Filter Bound SNR)** *The SNR_{MFB} is the SNR that characterizes the best achievable performance for a given pulse response $p(t)$ and signal constellation (on an AWGN channel) if the channel is used to transmit only one message. This SNR is*
>
> $$SNR_{MFB} = \frac{\bar{\mathcal{E}}_{\boldsymbol{x}} \|p\|^2}{\frac{N_0}{2}} \tag{3.45}$$
>
> MFB *denotes the square of the argument to the Q-function that arises in the equivalent "one-shot" analysis of the channel.*

Proof: Given a channel with pulse response $p(t)$ and isolated input x_0, the maximum output sample of the matched filter is $\|p\| \cdot x_0$. The normalized average energy of this sample is $\|p\|^2 \bar{\mathcal{E}}_{\boldsymbol{x}}$, while the corresponding noise sample energy is $\frac{N_0}{2}$, $SNR_{MFB} = \frac{\bar{\mathcal{E}}_{\boldsymbol{x}} \|p\|^2}{\frac{N_0}{2}}$. **QED**.

The probability of error, measured after the matched filter and prior to the symbol-by-symbol detector, satisfies $P_e \geq N_e \cdot Q(\sqrt{MFB})$. When $\bar{\mathcal{E}}_{\boldsymbol{x}}$ equals $(d_{min}^2/4)/\kappa$, then MFB equals $SNR_{MFB} \cdot \kappa$. In effect the MFB forces no ISI by disallowing preceding or successive transmitted symbols. An optimum detector is used for this "one-shot" case. The performance is tacitly a function of the transmitter basis functions, implying performance is also a function of the symbol rate $1/T$. No other (for the same input constellation) receiver for continuous transmission could have better performance, if x_k is an i.i.d. sequence, since the sequence must incur some level of ISI. The possibility of correlating the input sequence $\{x_k\}$ to take advantage of the channel correlation will be considered in Chapters 4 and 5.

The following example illustrates computation of the MFB for several cases of practical interest:

> **EXAMPLE 3.2.1 (Binary PAM)** For binary PAM,
>
> $$x_p(t) = \sum_k x_k \cdot p(t - kT) \quad, \tag{3.46}$$
>
> where $x_k = \pm\sqrt{\mathcal{E}_{\boldsymbol{x}}}$. The minimum distance at the matched-filter output is $\|p\| \cdot d_{\min} = \|p\| \cdot d = 2 \cdot \|p\| \cdot \sqrt{\mathcal{E}_{\boldsymbol{x}}}$, so $\mathcal{E}_{\boldsymbol{x}} = \frac{d_{\min}^2}{4}$ and $\kappa = 1$. Then,
>
> $$MFB = SNR_{MFB} \quad. \tag{3.47}$$
>
> Thus for a binary PAM channel, the MFB (in dB) is just the "channel-output" SNR, SNR_{MFB}. If the transmitter symbols x_k are equal to ± 1 ($\mathcal{E}_{\boldsymbol{x}} = 1$), then
>
> $$MFB = \frac{\|p\|^2}{\sigma^2} \quad, \tag{3.48}$$
>
> where, again, $\sigma^2 = \frac{N_0}{2}$. The binary-PAM P_e is then bounded by
>
> $$P_e \geq Q(\sqrt{SNR_{MFB}}) \quad. \tag{3.49}$$

EXAMPLE 3.2.2 (M-ary PAM) For M-ary PAM, $x_k = \pm\frac{d}{2}, \pm\frac{3d}{2}, ..., \pm\frac{(M-1)d}{2}$ and

$$\frac{d}{2} = \sqrt{\frac{3\mathcal{E}_{\boldsymbol{x}}}{M^2 - 1}} \quad , \tag{3.50}$$

so $\kappa = 3/(M^2 - 1)$. Thus,

$$\text{MFB} = \frac{3}{M^2 - 1}\text{SNR}_{MFB} \quad , \tag{3.51}$$

for $M \geq 2$. If the transmitter symbols x_k are equal to $\pm 1, \pm 3, , ..., \pm(M-1)$, then

$$\text{MFB} = \frac{\|p\|^2}{\sigma^2} \quad . \tag{3.52}$$

Equation (3.52) is the same result as (3.48), which should be expected since the minimum distance is the same at the transmitter, and thus also at the channel output, for both (3.48) and (3.52). The M'ary-PAM P_e is then bounded by

$$P_e \geq 2(1 - 1/M) \cdot Q(\sqrt{\frac{3 \cdot \text{SNR}_{MFB}}{M^2 - 1}}) \quad . \tag{3.53}$$

EXAMPLE 3.2.3 (QPSK) For QPSK, $x_k = \pm\frac{d}{2} \pm \jmath\frac{d}{2}$, and $d = 2\sqrt{\mathcal{E}_{\boldsymbol{x}}}$, so $\kappa = 1$. Thus

$$\text{MFB} = \text{SNR}_{MFB} \quad . \tag{3.54}$$

Thus, for a QPSK (or 4SQ QAM) channel, MFB (in dB) equals the channel output SNR. If the transmitter symbols x_k are $\pm 1 \pm \jmath$, then

$$\text{MFB} = \frac{\|p\|^2}{\sigma^2} \quad . \tag{3.55}$$

The best QPSK P_e is then approximated by

$$\bar{P}_e \approx Q(\sqrt{\text{SNR}_{MFB}}) \quad . \tag{3.56}$$

EXAMPLE 3.2.4 (M-ary QAM Square) For M-ary QAM, $\Re\{x_k\} = \pm\frac{d}{2}, \pm\frac{3d}{2}, ..., \pm\frac{(\sqrt{M}-1)d}{2}$, $\Im\{x_k\} = \pm\frac{d}{2}, \pm\frac{3d}{2}, ..., \pm\frac{(\sqrt{M}-1)d}{2}$, (recall that $\Re$ and $\Im$ denote real and imaginary parts, respectively) and

$$\frac{d}{2} = \sqrt{\frac{3\bar{\mathcal{E}}_{\boldsymbol{x}}}{M - 1}} \quad , \tag{3.57}$$

so $\kappa = 3/(M - 1)$. Thus

$$\text{MFB} = \frac{3}{M - 1}\text{SNR}_{MFB} \quad , \tag{3.58}$$

for $M \geq 4$. If the real and imaginary components of the transmitter symbols x_k equal $\pm 1, \pm 3, , ..., \pm(\sqrt{M} - 1)$, then

$$\text{MFB} = \frac{\|p\|^2}{\sigma^2} \quad . \tag{3.59}$$

The best M'ary QAM P_e is then approximated by

$$\bar{P}_e \approx 2(1 - 1/\sqrt{M}) \cdot Q(\sqrt{\frac{3 \cdot \text{SNR}_{MFB}}{M - 1}}) \quad . \tag{3.60}$$

In general for square QAM constellations,

$$\text{MFB} = \frac{3}{4^{\bar{b}} - 1} \text{SNR}_{MFB} \quad . \tag{3.61}$$

For the QAM Cross constellations,

$$\text{MFB} = \frac{\frac{2\bar{\mathcal{E}}_{\boldsymbol{x}}\|p\|^2}{\frac{31}{48}M - \frac{2}{3}}}{\sigma^2} = \frac{96}{31 \cdot 4^{\bar{b}} - 32} \text{SNR}_{MFB} \quad . \tag{3.62}$$

For the suboptimum receivers to come in later sections, $\text{SNR}_U \leq \text{SNR}_{MFB}$. As $\text{SNR}_U \to \text{SNR}_{MFB}$, then the receiver is approaching the bound on performance. It is not always possible to design a receiver that attains SNR_{MFB}, even with infinite complexity, unless one allows co-design of the input symbols x_k in a channel-dependent way (see Chapters 4 and 5). The loss with respect to matched filter bound will be determined for any receiver by $\text{SNR}_u/\text{SNR}_{MFB} \leq 1$, in effect determining a loss in signal power because successive transmissions interfere with one another – it may well be that the loss in signal power is an acceptable exchange for a higher rate of transmission.

3.3 Nyquist's Criterion

Nyquist's Criterion specifies the conditions on $q(t) = \varphi_p(t) * \varphi_p^*(-t)$ for an ISI-free channel on which a symbol-by-symbol detector is optimal. This section first reviews some fundamental relationships between $q(t)$ and its samples $q_k = q(kT)$ in the frequency domain.

$$
q(kT) \;=\; \frac{1}{2\pi} \int_{-\infty}^{\infty} Q(\omega) e^{\jmath \omega kT} d\omega \tag{3.63}
$$

$$
=\; \frac{1}{2\pi} \sum_{n=-\infty}^{\infty} \int_{\frac{(2n-1)\pi}{T}}^{\frac{(2n+1)\pi}{T}} Q(\omega) e^{\jmath \omega kT} d\omega \tag{3.64}
$$

$$
=\; \frac{1}{2\pi} \sum_{n=-\infty}^{\infty} \int_{-\frac{\pi}{T}}^{\frac{\pi}{T}} Q(\omega + \frac{2\pi n}{T}) e^{\jmath(\omega + \frac{2\pi n}{T})kT} d\omega \tag{3.65}
$$

$$
=\; \frac{1}{2\pi} \int_{-\frac{\pi}{T}}^{\frac{\pi}{T}} Q_{eq}(\omega) e^{\jmath \omega kT} d\omega \quad , \tag{3.66}
$$

where $Q_{eq}(\omega)$, the **equivalent frequency response** becomes

$$
Q_{eq}(\omega) \triangleq \sum_{n=-\infty}^{\infty} Q(\omega + \frac{2\pi n}{T}) \quad . \tag{3.67}
$$

The function $Q_{eq}(\omega)$ is periodic in ω with period $\frac{2\pi}{T}$. This function is also known as the *folded* or *aliased* spectrum of $Q(\omega)$ because the sampling process causes the frequency response outside of the fundamental interval $(-\frac{\pi}{T}, \frac{\pi}{T})$ to be added (i.e. "folded in"). Writing the Fourier Transform of the sequence q_k as $Q(e^{-\jmath \omega T}) = \sum_{k=-\infty}^{\infty} q_k e^{-\jmath \omega kT}$ leads to

$$
\frac{1}{T} \cdot Q_{eq}(\omega) = Q(e^{-\jmath \omega T}) \triangleq \sum_{k=-\infty}^{\infty} q_k e^{-\jmath \omega kT} \quad , \tag{3.68}
$$

a well-known relation between the discrete-time and continuous-time representations of any waveform in digital signal processing.

It is now straightforward to specify Nyquist's Criterion:

> **Theorem 3.3.1 (Nyquist's Criterion)** *A channel specified by pulse response $p(t)$ (and resulting in $q(t) = \frac{p(t) * p^*(-t)}{\|p\|^2}$) is ISI-free if and only if*
>
> $$
> Q(e^{-\jmath \omega T}) = \frac{1}{T} \sum_{n=-\infty}^{\infty} Q(\omega + \frac{2\pi n}{T}) = 1 \quad . \tag{3.69}
> $$
>
> **Proof:**
> By definition the channel is ISI-free if and only if $q_k = 0$ for all $k \neq 0$ (recall $q_0 = 1$ by definition). The proof follows directly by substitution of $q_k = \delta_k$ into (3.68). **QED.**

Functions that satisfy (3.69) are called "Nyquist pulses." One function that satisfies Nyquist's Criterion is

$$
q(t) = \text{sinc}\left(\frac{t}{T}\right) \quad , \tag{3.70}
$$

which corresponds to normalized pulse response

$$
\varphi_p(t) = \frac{1}{\sqrt{T}} \text{sinc}\left(\frac{t}{T}\right) \quad . \tag{3.71}
$$

The function $q(kT) = \text{sinc}(k) = \delta_k$ satisfies the ISI-free condition. One feature of $\text{sinc}(t/T)$ is that it has minimum bandwidth for no ISI. No other function has this same minimum bandwidth and also satisfies
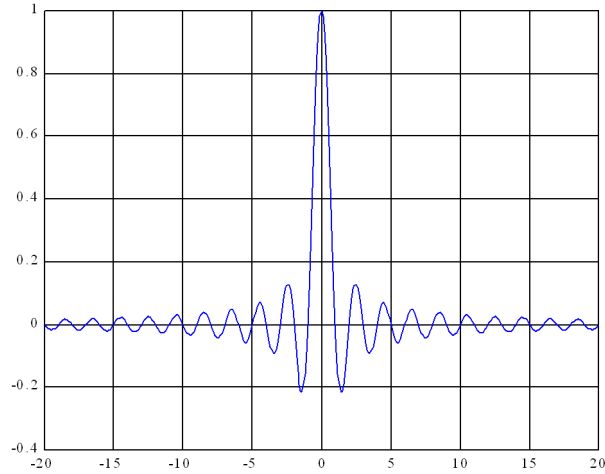
Figure 3.14: The sinc(t/T) function.

the Nyquist Criterion. (Proof is left as an exercise to the reader.) The $\text{sinc}(t/T)$ function is plotted in Figure 3.14 for $-20T \leq t \leq 20T$.

The frequency $\frac{1}{2T}$ (1/2 the symbol rate) is often construed as the maximum frequency of a sampled signal that can be represented by samples at the sampling rate. In terms of positive-frequencies, $1/2T$ represents a minimum bandwidth necessary to satisfy the Nyquist Criterion, and thus has a special name in data transmission:

> **Definition 3.3.1 (Nyquist Frequency)** *The frequency* $\omega = \frac{\pi}{T}$ *or* $f = \frac{1}{2T}$ *is called the* **Nyquist frequency**.[6]

3.3.1 Vestigial Symmetry

In addition to the $\text{sinc}(t/T)$ Nyquist pulse, data-transmission engineers use responses with up to twice the minimum bandwidth. For all these pulses, $Q(\omega) = 0$ for $|\omega| > \frac{2\pi}{T}$. These wider bandwidth responses will provide more immunity to timing errors in sampling as follows: The $\text{sinc}(t/T)$ function decays in amplitude only linearly with time. Thus, any sampling-phase error in the sampling process of Figure 3.7 introduces residual ISI with amplitude that only decays linearly with time. In fact for $q(t) = \text{sinc}(t/T)$, the ISI term $\sum_{k \neq 0} q(\tau + kT)$ with a sampling timing error of $\tau \neq 0$ is not absolutely summable, resulting in infinite peak distortion. The envelope of the time domain response decays more rapidly if the frequency response is smooth (i.e. continuously differentiable). To meet this smoothness condition and also satisfy Nyquist's Criterion, the response must occupy a larger than minimum bandwidth that is between $1/2T$ and $1/T$. A $q(t)$ with higher bandwidth can exhibit significantly faster decay as $|t|$ increases, thus reducing sensitivity to timing phase errors. Of course, any increase in bandwidth should be as small as possible, while still meeting other system requirements. The **percent excess bandwidth**[7], or **percent roll-off**, is a measure of the extra bandwidth.

> **Definition 3.3.2 (Percent Excess Bandwidth)** *The* **percent excess bandwidth** α *is determined from a strictly bandlimited* $Q(\omega)$ *by finding the highest frequency in* $Q(\omega)$ *for*

---

[6]This text distinguishes the Nyquist Frequency from the Nyquist Rate in sampling theory, where the latter is twice the highest frequency of a signal to be sampled and is not the same as the Nyquist Frequency here.

[7]The quantity *alpha* used here is not a bias factor, and similarly $Q(\cdot)$ is a measure of ISI and not the integral of a unit-variance Gaussian function – uses should be clear to reasonable readers who'll understand that sometimes symbols are re-used in obviously differenct contexts.
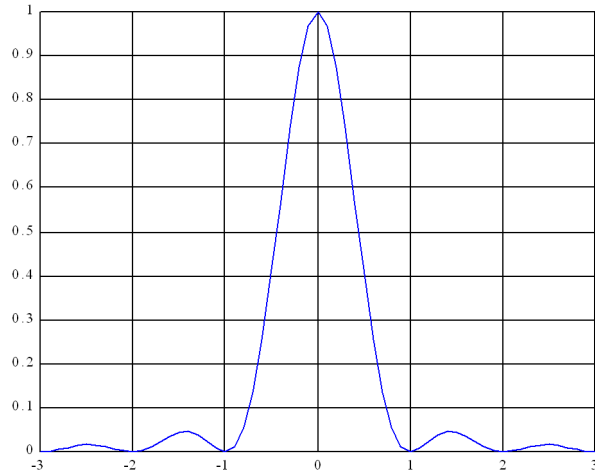
Figure 3.15: The $sinc^2(t/T)$ Function – time-domain

which there is nonzero energy transfer. That is

$$Q(\omega) = \left\{ \begin{array}{cc} nonzero & |\omega| \leq (1+\alpha)\frac{\pi}{T} \\ 0 & |\omega| > (1+\alpha)\frac{\pi}{T} \end{array} \right. \qquad . \tag{3.72}$$

Thus, if $\alpha = .15$ (a typical value), the pulse $q(t)$ is said to have "15% excess bandwidth." Usually, data transmission systems have $0 \leq \alpha \leq 1$. In this case in equation (3.69), only the terms $n = -1, 0, +1$ contribute to the folded spectrum and the Nyquist Criterion becomes

$$1 = Q(e^{-\jmath\omega T}) \tag{3.73}$$

$$= \frac{1}{T}\left\{ Q\left(\omega + \frac{2\pi}{T}\right) + Q\left(\omega\right) + Q\left(\omega - \frac{2\pi}{T}\right) \right\} \quad -\frac{\pi}{T} \leq \omega \leq \frac{\pi}{T} \quad . \tag{3.74}$$

Further, recalling that $q(t) = \varphi_p(t) * \varphi_p^*(-t)$ is Hermitian and has the properties of an autocorrelation function, then $Q(\omega)$ is real and $Q(\omega) \geq 0$. For the region $0 \leq \omega \leq \frac{\pi}{T}$ (for real signals), (3.74) reduces to

$$1 = Q(e^{-\jmath\omega T}) \tag{3.75}$$

$$= \frac{1}{T}\left\{ Q\left(\omega\right) + Q\left(\omega - \frac{2\pi}{T}\right) \right\} \quad . \tag{3.76}$$

For complex signals, the negative frequency region $(-\frac{\pi}{T} \leq \omega \leq 0)$ should also have

$$1 = Q(e^{-\jmath\omega T}) \tag{3.77}$$

$$= \frac{1}{T}\left\{ Q\left(\omega\right) + Q\left(\omega + \frac{2\pi}{T}\right) \right\} \quad . \tag{3.78}$$

Any $Q(\omega)$ satisfying (3.76) (and (3.78) in the complex case) is said to be **vestigially symmetric** with respect to the Nyquist Frequency. An example of a vestigially symmetric response with 100% excess bandwidth is $q(t) = \text{sinc}^2(t/T)$, which is shown in Figures 3.15 and 3.16.

3.3.2 Raised Cosine Pulses

The most widely used set of functions that satisfy the Nyquist Criterion are the **raised-cosine** pulse shapes:
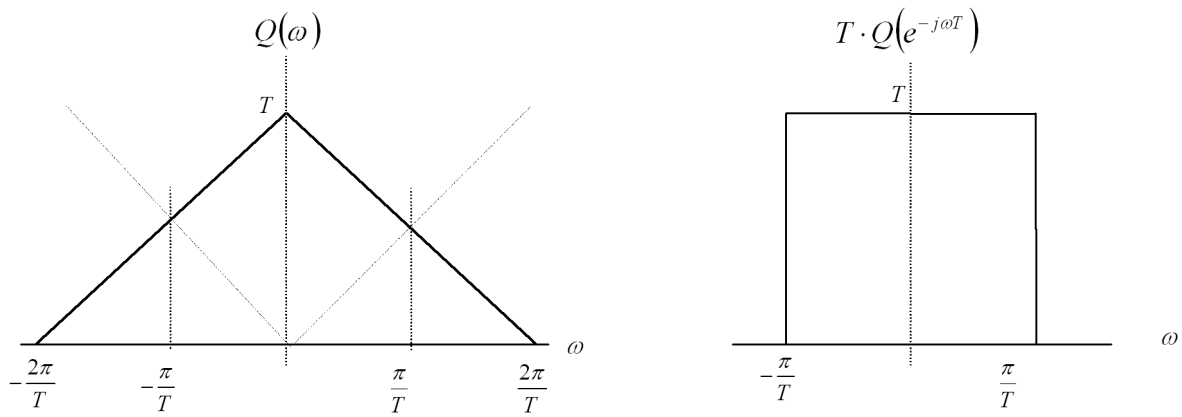
Figure 3.16: The $sinc^2(t/T)$ function – frequency-domain
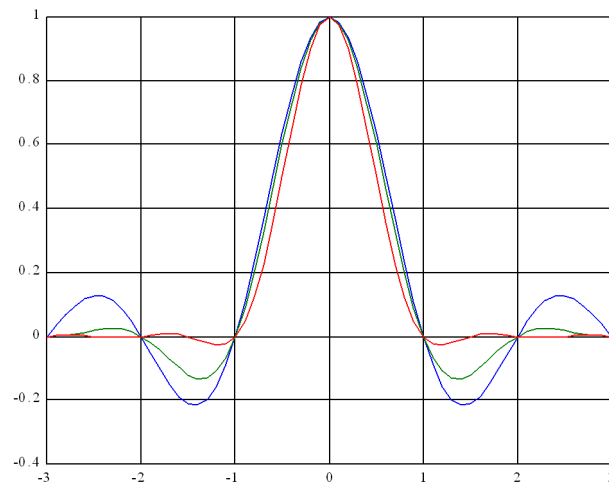
Figure 3.17: Raised cosine pulse shapes – time-domain

173
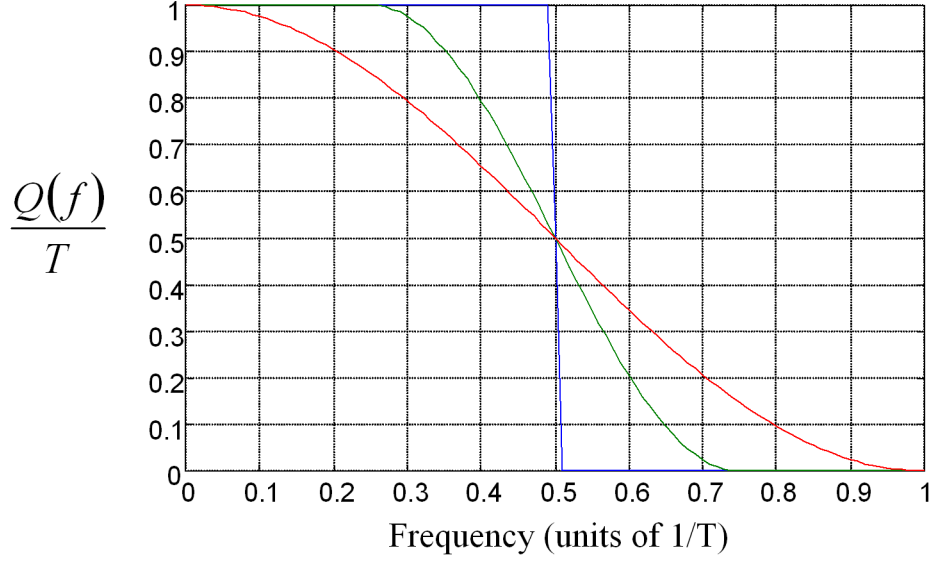
Figure 3.18: Raised Cosine Pulse Shapes – frequency-domain

Definition 3.3.3 (Raised-Cosine Pulse Shapes) *The raised cosine family of pulse shapes (indexed by $0 \leq \alpha \leq 1$) is given by*

$$q(t) = sinc\left(\frac{t}{T}\right) \cdot \left[\frac{\cos\left(\frac{\alpha \pi t}{T}\right)}{1 - \left(\frac{2\alpha t}{T}\right)^2}\right] \quad , \tag{3.79}$$

and have Fourier Transforms

$$Q(\omega) = \begin{cases} T & |\omega| \leq \frac{\pi}{T}(1-\alpha) \\ \frac{T}{2}\left[1 - \sin\left(\frac{T}{2\alpha}(|\omega| - \frac{\pi}{T})\right)\right] & \frac{\pi}{T}(1-\alpha) \leq |\omega| \leq \frac{\pi}{T}(1+\alpha) \\ 0 & \frac{\pi}{T}(1+\alpha) \leq |\omega| \end{cases} \quad . \tag{3.80}$$

The raised cosine pulse shapes are shown in Figure 3.17 (time-domain) and Figure 3.18 (frequency-domain) for $\alpha = 0, .5$, and 1. When $\alpha = 0$, the raised cosine reduces to a sinc function, which decays asymptotically as $\frac{1}{t}$ for $t \to \infty$, while for $\alpha \neq 0$, the function decays as $\frac{1}{t^3}$ for $t \to \infty$.

3.3.3 Square-Root Splitting of the Nyquist Pulse

The optimum ISI-free transmission system that this section has described has transmit-and-channel filtering $\varphi_p(t)$ and receiver matched filter $\varphi_p^*(-t)$ such that $q(t) = \varphi_p(t) * \varphi_p^*(-t)$ or equivalently

$$\Phi_p(\omega) = Q^{1/2}(\omega) \tag{3.81}$$

so that the matched filter and transmit/channel filters are "square-roots" of the Nyquist pulse. When $h(t) = \delta(t)$ or equivalently $\varphi_p(t) = \varphi(t)$, the transmit filter (and the receiver matched filters) are square-roots of a Nyquist pulse shape. Such square-root transmit filtering is often used even when $\varphi_p(t) \neq \varphi(t)$ and the pulse response is the convolution of $h(t)$ with the square-root filter.

The raised-cosine pulse shapes are then often used in square-root form, which is

$$\sqrt{Q(\omega)} = \begin{cases} \sqrt{T} & |\omega| \leq \frac{\pi}{T}(1-\alpha) \\ \sqrt{\frac{T}{2}}\left[1 - \sin\left(\frac{T}{2\alpha}(|\omega| - \frac{\pi}{T})\right)\right]^{1/2} & \frac{\pi}{T}(1-\alpha) \leq |\omega| \leq \frac{\pi}{T}(1+\alpha) \\ 0 & \frac{\pi}{T}(1+\alpha) \leq |\omega| \end{cases} \quad . \tag{3.82}$$

This expression can be inverted to the time-domain via use of the identity $sin^2(\theta) = .5(1 - \cos(2\theta))$, as in the exercises, to obtain

$$\varphi_p(t) = \frac{4\alpha}{\pi\sqrt{T}} \cdot \frac{\cos\left([1+\alpha]\frac{\pi t}{T}\right) + \frac{T \cdot \sin\left([1-\alpha]\frac{\pi t}{T}\right)}{4\alpha t}}{1 - \left(\frac{4\alpha t}{T}\right)^2} \quad . \tag{3.83}$$

3.4 Linear Zero-Forcing Equalization

This section examines the **Zero-Forcing Equalizer** (ZFE), which is the easiest type of equalizer to analyze and understand, but has inferior performance to some other equalizers to be introduced in later sections. The ISI model in Figure 3.7 is used to describe the zero-forcing version of the discrete-time receiver. The ZFE is often a first non-trivial attempt at a receiver R in Figure 3.12 of Section 3.2.

The ZFE sets R equal to a linear time-invariant filter with discrete impulse response w_k that acts on y_k to produce z_k, which is an estimate of x_k. Ideally, for symbol-by-symbol detection to be optimal, $q_k = \delta_k$ by Nyquist's Criterion. The equalizer tries to restore this Nyquist Pulse character to the channel. In so doing, the ZFE ignores the noise and shapes the signal y_k so that it is free of ISI. From the ISI-channel model of Section 3.1 and Figure 3.7,

$$y_k = \|p\| \cdot x_k * q_k + n_k \quad . \tag{3.84}$$

In the ZFE case, n_k is initially viewed as being zero. The D-transform of y_k is (See Appendix A.2)

$$Y(D) = \|p\| \cdot X(D) \cdot Q(D) \quad . \tag{3.85}$$

The ZFE output, z_k, has Transform

$$Z(D) = W(D) \cdot Y(D) = W(D) \cdot Q(D) \cdot \|p\| \cdot X(D) \quad , \tag{3.86}$$

and will be free of ISI if $Z(D) = X(D)$, leaving the ZFE filter characteristic:

Definition 3.4.1 (Zero-Forcing Equalizer) *The ZFE transfer characteristic is*

$$W(D) = \frac{1}{Q(D) \cdot \|p\|} \quad . \tag{3.87}$$

This discrete-time filter processes the discrete-time sequence corresponding to the matched-filter output. The ZFE is so named because ISI is "forced to zero" at all sampling instants kT except $k = 0$. The receiver uses symbol-by-symbol detection, based on decision regions for the constellation defined by x_k, on the output of the ZFE.

3.4.1 Performance Analysis of the ZFE

The variance of the noise, which is not zero in practice, at the output of the ZFE is important in determining performance, even if ignored in the ZFE design of Equation (3.87). As this noise is produced by a linear filter acting on the discrete Gaussian noise process n_k, it is also Gaussian. The designer can compute the discrete autocorrelation function (the bar denotes normalized to one dimension, so $N = 2$ for the complex QAM case) for the noise n_k as

$$\bar{r}_{nn,k} = E\left[n_l n_{l-k}^*\right] / N \tag{3.88}$$

$$= \int_{-\infty}^{\infty} \int_{-\infty}^{\infty} \overline{E\left[n_p(t) n_p^*(s)\right]} \varphi_p^*(t - lT) \varphi_p(s - (l-k)T) dt ds \tag{3.89}$$

$$= \int_{-\infty}^{\infty} \int_{-\infty}^{\infty} \frac{\mathcal{N}_0}{2} \delta(t - s) \varphi_p^*(t - lT) \varphi_p(s - (l-k)T) dt ds \tag{3.90}$$

$$= \frac{\mathcal{N}_0}{2} \int_{-\infty}^{\infty} \varphi_p^*(t - lT) \varphi_p(t - (l-k)T) dt \tag{3.91}$$

$$= \frac{\mathcal{N}_0}{2} \int_{-\infty}^{\infty} \varphi_p^*(u) \varphi_p(u + kT) du \quad \text{(letting } u = t - lT) \tag{3.92}$$

$$= \frac{\mathcal{N}_0}{2} q_{-k}^* = \frac{\mathcal{N}_0}{2} q_k \quad , \tag{3.93}$$

or more simply

$$\bar{R}_{nn}(D) = \frac{\mathcal{N}_0}{2} Q(D) \quad , \tag{3.94}$$

where the analysis uses the substitution $u = t - lT$ in going from (3.91) to (3.92), and assumes baseband equivalent signals for the complex case. The complex baseband-equivalent noise, has (one-dimensional) sample variance $\frac{\mathcal{N}_0}{2}$ at the normalized matched filter output. The noise at the output of the ZFE, $n_{ZFE,k}$, has autocorrelation function

$$\bar{r}_{ZFE,k} = \bar{r}_{nn,k} * w_k * w_{-k}^* \quad . \tag{3.95}$$

The D-Transform of $\bar{r}_{ZFE,k}$ is then

$$\bar{R}_{ZFE}(D) = \frac{\mathcal{N}_0}{2} \frac{Q(D)}{\|p\|^2 \cdot Q^2(D)} = \frac{\frac{\mathcal{N}_0}{2}}{\|p\|^2 \cdot Q(D)} \quad . \tag{3.96}$$

The power spectral density of the noise samples $n_{ZFE,k}$ is then $\bar{R}_{ZFE}(e^{-j\omega T})$. The (per-dimensional) variance of the noise samples at the output of the ZFE is the (per-dimensional) mean-square error between the desired x_k and the ZFE output z_k. Since

$$z_k = x_k + n_{ZFE,k} \quad , \tag{3.97}$$

then σ_{ZFE}^2 is computed as

$$\sigma_{ZFE}^2 = \frac{T}{2\pi} \int_{-\frac{\pi}{T}}^{\frac{\pi}{T}} \bar{R}_{ZFE}(e^{-j\omega T}) d\omega = \frac{T}{2\pi} \int_{-\frac{\pi}{T}}^{\frac{\pi}{T}} \frac{\frac{\mathcal{N}_0}{2}}{\|p\|^2 \cdot Q(e^{-j\omega T})} d\omega = \frac{\frac{\mathcal{N}_0}{2}}{\|p\|^2} \gamma_{ZFE} = \frac{\frac{\mathcal{N}_0}{2}}{\|p\|} \cdot w_0 \quad , \tag{3.98}$$

where

$$\gamma_{ZFE} = \frac{T}{2\pi} \int_{-\frac{\pi}{T}}^{\frac{\pi}{T}} \frac{1}{Q(e^{-j\omega T})} d\omega = w_0 \cdot \|p\| \quad . \tag{3.99}$$

The **center tap** of a linear equalizer is w_0, or if the ZFE is explicity used, then $w_{ZFE,0}$. This tap is easily shown to always have the largest magnitude for a ZFE and thus spotted readily when plotting the impulse response of any linear equalizer. From (3.97) and the fact that $E[n_{ZFE,k}] = 0$, $E[z_k/x_k] = x_k$, so that the ZFE is unbiased for a detection rule based on x_k. The SNR at the output of the ZFE is

$$\text{SNR}_{ZFE} = \frac{\bar{\mathcal{E}}_{\boldsymbol{x}}}{\sigma_{ZFE}^2} = \text{SNR}_{MFB} \cdot \frac{1}{\gamma_{ZFE}} \quad . \tag{3.100}$$

Computation of $d_{\min}$ over the signal set corresponding to x_k leads to a relation between $\bar{\mathcal{E}}_{\boldsymbol{x}}$, $d_{\min}$, and M, and the NNUB on error probability for a symbol-by-symbol detector at the ZFE output is (please, do not confuse the Q function with the channel autocorrelation $Q(D)$)

$$P_{ZFE,e} \approx N_e \cdot Q\left(\frac{d_{\min}}{2\sigma_{ZFE}}\right) \quad . \tag{3.101}$$

Since symbol-by-symbol detection can never have performance that exceeds the MFB,

$$\sigma^2 \leq \sigma_{ZFE}^2 \|p\|^2 = \sigma^2 \frac{T}{2\pi} \int_{-\frac{\pi}{T}}^{\frac{\pi}{T}} \frac{d\omega}{Q(e^{-j\omega T})} = \sigma^2 \cdot \gamma_{ZFE} \tag{3.102}$$

$$\text{SNR}_{MFB} \geq \text{SNR}_{ZFE} \tag{3.103}$$

$$\gamma_{ZFE} \geq 1 \quad , \tag{3.104}$$

with equality if and only if $Q(D) = 1$.

Finally, the ZFE equalization loss, $1/\gamma_{ZFE}$, defines the SNR reduction from the MFB:

Definition 3.4.2 (ZFE Equalization Loss) *The **ZFE Equalization Loss**, γ_{ZFE} in decibels is*

$$\gamma_{ZFE} \triangleq 10 \cdot \log_{10}\left(\frac{SNR_{MFB}}{SNR_{ZFE}}\right) = 10 \log_{10} \frac{\|p\|^2 \cdot \sigma_{ZFE}^2}{\sigma^2} = 10 \log_{10} \|p\| \cdot w_{ZFE,0} \quad , \tag{3.105}$$

and is a measure of the loss (in dB) with respect to the MFB for the ZFE. The sign of the loss is often ignored since it is always a negative (or 0) number and only its magnitude is of concern.

Equation (3.105) always thus provides a non-negative number.
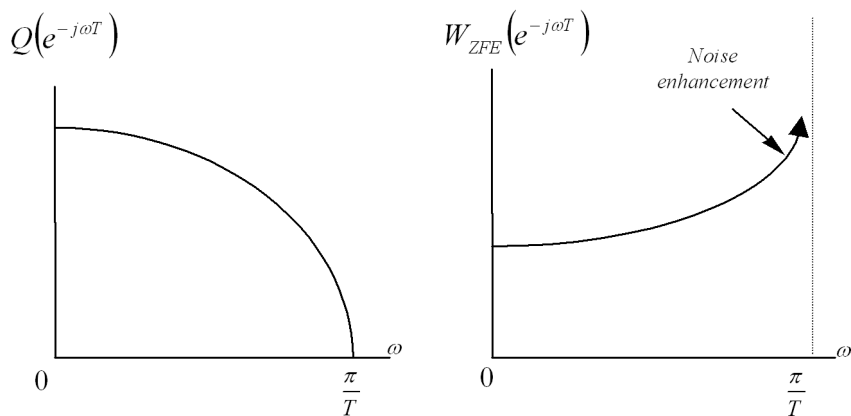
Figure 3.19: Noise Enhancement

3.4.2 Noise Enhancement

The design of $W(D)$ for the ZFE ignored the effects of noise. This oversight can lead to **noise enhancement**, a σ^2_{ZFE} that is unacceptably large, and the consequent poor performance.

Figure 3.19 hypothetically illustrates an example of a lowpass channel with a notch at the Nyquist Frequency, that is, $Q(e^{-\jmath\omega T})$ is zero at $\omega = \frac{\pi}{T}$. Since $W(e^{-\jmath\omega T}) = 1/(\|p\| \cdot Q(e^{-\jmath\omega T}))$, then any noise energy near the Nyquist Frequency is enhanced (increased in power or energy), in this case so much that $\sigma^2_{ZFE} \to \infty$. Even when there is no channel notch at any frequency, σ^2_{ZFE} can be finite, but large, leading to unacceptable performance degradation.

In actual computation of examples, the author has found that the table in Table 3.1 is useful in recalling basic digital signal processing equivalences related to scale factors between continuous time convolution and discrete-time convolution.

The following example clearly illustrates the noise-enhancement effect:

EXAMPLE 3.4.1 $(1 + .9D^{-1}$ - ZFE) Suppose the pulse response of a (strictly bandlimited) channel used with binary PAM is

$$P(\omega) = \begin{cases} \sqrt{T}\left(1 + .9e^{\jmath\omega T}\right) & |\omega| \le \frac{\pi}{T} \\ 0 & |\omega| > \frac{\pi}{T} \end{cases} . \tag{3.106}$$

Then $\|p\|^2$ is computed as

$$\|p\|^2 = \frac{1}{2\pi} \int_{-\frac{\pi}{T}}^{\frac{\pi}{T}} |P(\omega)|^2 d\omega \tag{3.107}$$

$$= \frac{1}{2\pi} \int_{-\frac{\pi}{T}}^{\frac{\pi}{T}} T\left[1.81 + 1.8\cos(\omega T)\right] d\omega \tag{3.108}$$

$$= \frac{T}{2\pi}1.81\frac{2\pi}{T} = 1.81 = 1^2 + .9^2 . \tag{3.109}$$

The magnitude of the Fourier transform of the pulse response appears in Figure 3.20. Thus, with $\Phi_p(\omega)$ as the Fourier transform of $\{\varphi_p(t)\}$,

$$\Phi_p(\omega) = \begin{cases} \sqrt{\frac{T}{1.81}}\left(1 + .9e^{\jmath\omega T}\right) & |\omega| \le \frac{\pi}{T} \\ 0 & |\omega| > \frac{\pi}{T} \end{cases} . \tag{3.110}$$

178

time	frequency	
$p(t) \leftrightarrow P(\omega)$		continuous-time
$p_k = p(kT) \leftrightarrow P\left(e^{-j\omega T}\right) = \dfrac{1}{T} \displaystyle\sum_{n=-\infty}^{\infty} P\left(\omega + \dfrac{2\pi n}{T}\right)$		discrete-time
$y(t) = x(t) * p(t) \leftrightarrow Y(\omega) = X(\omega) \cdot P(\omega)$		continuous-time
$y(kT) = T \cdot x_k * p_k \leftrightarrow Y\left(e^{-j\omega T}\right) = T \cdot X\left(e^{-j\omega T}\right) \cdot P\left(e^{-j\omega T}\right)$		discrete-time
$Y\left(e^{-j\omega T}\right) = \dfrac{1}{T} \cdot X(\omega) \cdot P(\omega)$		sampling theorem satisfied
$\|p\|^2 = \displaystyle\int_{-\infty}^{\infty} |p(t)|^2 \, dt = \dfrac{1}{2\pi} \displaystyle\int_{-\infty}^{\infty} |P(\omega)|^2 \, d\omega$		continuous-time
$\|p\|^2 = T \displaystyle\sum_{k=-\infty}^{\infty} |p_k|^2 = \dfrac{T^2}{2\pi} \displaystyle\int_{-\frac{\pi}{T}}^{\frac{\pi}{T}} \left|P\left(e^{-j\omega T}\right)\right|^2 \, d\omega$		discrete-time (sampling thm satisfied)

Table 3.1: Conversion factors of T.
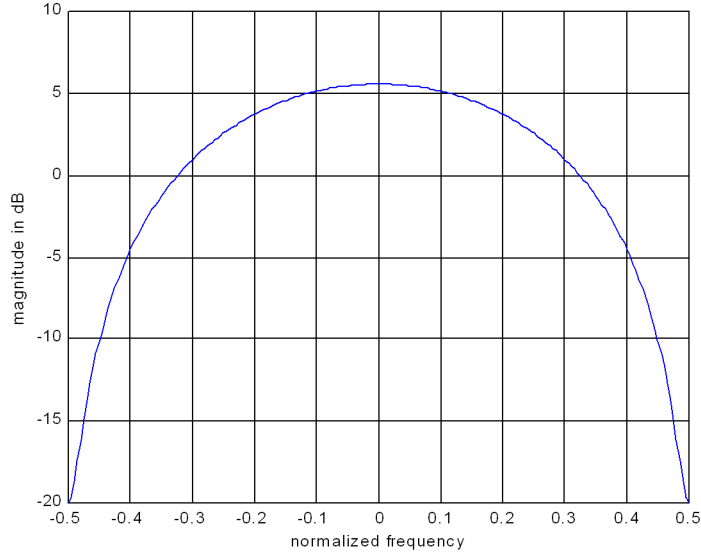
Figure 3.20: Magnitude of Fourier transform of (sampled) pulse response.

Then, (using the bandlimited property of $P(\omega)$ in this example)

$$Q(e^{-\jmath\omega T}) \quad = \quad \frac{1}{T}|\Phi_p(\omega)|^2 \tag{3.111}$$

$$= \quad \frac{1}{1.81}|1 + .9e^{\jmath\omega T}|^2 \tag{3.112}$$

$$= \quad \frac{1.81 + 1.8\cos(\omega T)}{1.81} \tag{3.113}$$

$$Q(D) \quad = \quad \frac{.9D^{-1} + 1.81 + .9D}{1.81} \quad . \tag{3.114}$$

Then

$$W(D) = \frac{\sqrt{1.81}D}{.9 + 1.81D + .9D^2} \quad . \tag{3.115}$$

The magnitude of the Fourier transform of the ZFE response appears in Figure 3.21. The time-domain sample response of the equalizer is shown in Figure 3.22.

Computation of σ^2_{ZFE} allows performance evaluation, [8]

$$\sigma^2_{ZFE} \quad = \quad \frac{T}{2\pi}\int_{-\frac{\pi}{T}}^{\frac{\pi}{T}} \frac{\frac{\mathcal{N}_0}{2}}{Q(e^{-\jmath\omega T}) \cdot \|p\|^2} d\omega \tag{3.116}$$

$$= \quad \frac{T}{2\pi}\int_{-\frac{\pi}{T}}^{\frac{\pi}{T}} \frac{(1.81/1.81) \cdot \frac{\mathcal{N}_0}{2}}{1.81 + 1.8\cos(\omega T)} d\omega \tag{3.117}$$

$$= \quad \frac{\mathcal{N}_0}{2}\frac{1}{2\pi}\int_{-\pi}^{\pi} \frac{1}{1.81 + 1.8\cos u} du \tag{3.118}$$

---

[8]From a table of integrals
$\int \frac{1}{a+b\cos u}du = \frac{2}{\sqrt{a^2-b^2}}\mathrm{Tan}^{-1}\left(\frac{\sqrt{a^2-b^2}\tan(\frac{u}{2})}{a+b}\right).$
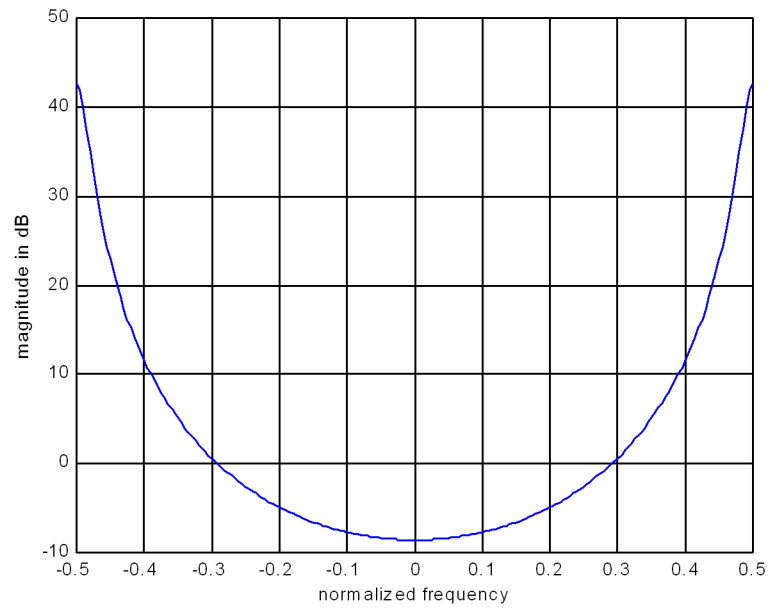
Figure 3.21: ZFE magnitude for example.
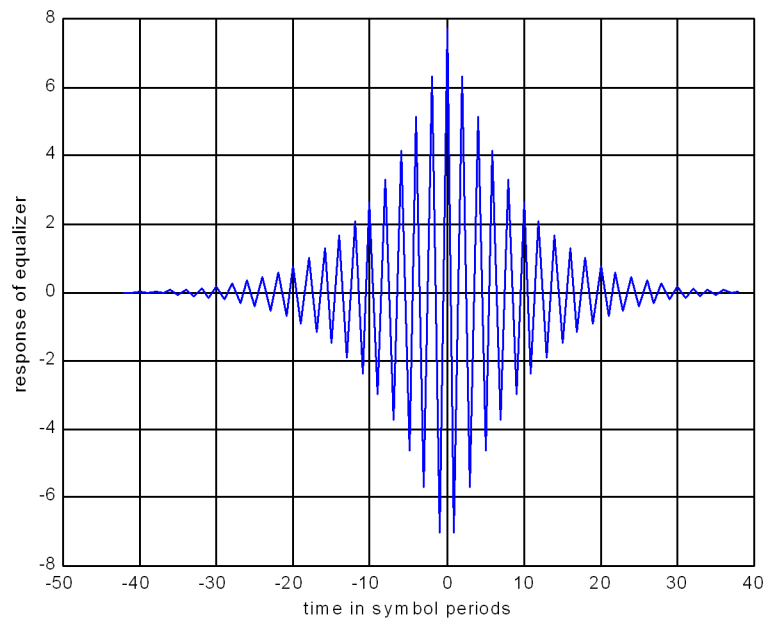
Figure 3.22: ZFE time-domain response.

$$= \quad (\frac{\mathcal{N}_0}{2})\frac{2}{2\pi}\left[\frac{2}{\sqrt{1.81^2-1.8^2}}\text{Tan}^{-1}\frac{\sqrt{1.81^2-1.8^2}\tan\frac{u}{2}}{1.81+1.8}\right]_0^\pi \qquad (3.119)$$

$$= \quad (\frac{\mathcal{N}_0}{2})\frac{4}{2\pi\sqrt{1.81^2-1.8^2}}\cdot\frac{\pi}{2} \qquad (3.120)$$

$$= \quad (\frac{\mathcal{N}_0}{2})\frac{1}{\sqrt{1.81^2-1.8^2}} \qquad (3.121)$$

$$= \quad \frac{\mathcal{N}_0}{2}(5.26) \quad . \qquad (3.122)$$

The ZFE-output SNR is

$$\text{SNR}_{ZFE} = \frac{\bar{\mathcal{E}}\boldsymbol{x}}{5.26\frac{\mathcal{N}_0}{2}} \quad . \qquad (3.123)$$

This SNR_{ZFE} is also the argument of the Q-function for a binary detector at the ZFE output. Assuming the two transmitted levels are $x_k = \pm1$, then we get

$$\text{MFB} = \frac{\|p\|^2}{\sigma^2} = \frac{1.81}{\sigma^2} \quad , \qquad (3.124)$$

leaving

$$\gamma_{ZFE} = 10\log_{10}(1.81\cdot5.26) \approx 9.8\text{dB} \qquad (3.125)$$

for any value of the noise variance. This is very poor performance on this channel. No matter what b is used, the loss is almost 10 dB from best performance. Thus, noise enhancement can be a serious problem. Chapter 9 demonstrates a means by which to ensure that there is no loss with respect to the matched filter bound for this channel. With alteration of the signal constellation, Chapter 10 describes a means that ensures an error rate of 10^{-5} on this channel, with no information rate loss, which is far below the error rate achievable even when the MFB is attained. thus, there are good solutions, but the simple concept of a ZFE is not a good solution.

Another example illustrates the generalization of the above procedure when the pulse response is complex (corresponding to a QAM channel):

EXAMPLE 3.4.2 (QAM: $-.5D^{-1}+(1+.25\jmath)-.5\jmath D$ Channel) Given a baseband equivalent channel

$$p(t) = \frac{1}{\sqrt{T}}\left\{-\frac{1}{2}\text{sinc}\left(\frac{t+T}{T}\right)+\left(1+\frac{\jmath}{4}\right)\text{sinc}\left(\frac{t}{T}\right)-\frac{\jmath}{2}\text{sinc}\left(\frac{t-T}{T}\right)\right\} \quad , \qquad (3.126)$$

the discrete-time channel samples are

$$p_k = \frac{1}{\sqrt{T}}\left[-\frac{1}{2}, \left(1+\frac{\jmath}{4}\right), -\frac{\jmath}{2}\right] \quad . \qquad (3.127)$$

This channel has the transfer function of Figure 3.23. The pulse response norm (squared) is

$$\|p\|^2 = \frac{T}{T}(.25+1+.0625+.25) = 1.5625 \quad . \qquad (3.128)$$

Then q_k is given by

$$q_k = q(kT) = T\left(\varphi_{p,k}*\varphi_{p,-k}^*\right) = \frac{1}{1.5625}\left[-\frac{\jmath}{4}, \frac{5}{8}(-1+\jmath), 1.5625, -\frac{5}{8}(1+\jmath), \frac{\jmath}{4}\right] \qquad (3.129)$$

or

$$Q(D) = \frac{1}{1.5625}\left[-\frac{\jmath}{4}D^{-2}+\frac{5}{8}(-1+\jmath)D^{-1}+1.5625-\frac{5}{8}(1+\jmath)D+\frac{\jmath}{4}D^2\right] \qquad (3.130)$$

182

complex baseband channel pulse response magnitude
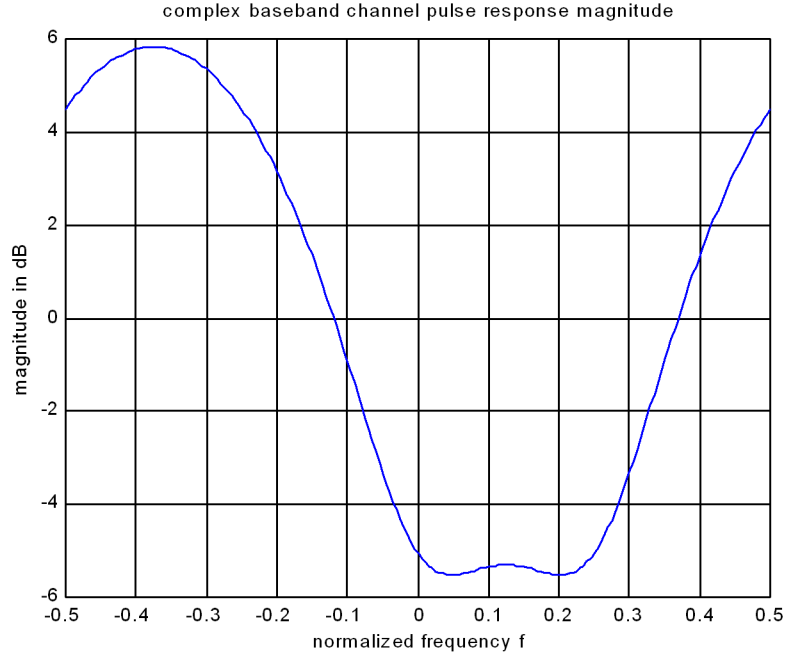
Figure 3.23: Fourier transform magnitude for pulse response for complex channel example.

Then, $Q(D)$ factors into

$$Q(D) = \frac{1}{1.5625} \left\{ (1 - .5\jmath D)\left(1 - .5D^{-1}\right)\left(1 + .5\jmath D^{-1}\right)(1 - .5D) \right\} \quad , \qquad (3.131)$$

and

$$W_{ZFE}(D) = \frac{1}{Q(D)\|p\|} \qquad (3.132)$$

or

$$W_{ZFE}(D) = \frac{\sqrt{1.5625}}{(-.25\jmath D^{-2} + .625(-1 + \jmath)D^{-1} + 1.5625 - .625(1 + \jmath)D + .25\jmath D^2)} \quad . \quad (3.133)$$

The Fourier transform of the ZFE is in Figure 3.24. The real and imaginary parts of the equalizer response in the time domain are shown in Figure 3.25 Then

$$\sigma^2_{ZFE} = \frac{T}{2\pi} \int_{-\frac{\pi}{T}}^{\frac{\pi}{T}} \frac{\frac{\mathcal{N}_0}{2}}{\|p\|^2 Q(e^{-\jmath\omega T})} d\omega \quad , \qquad (3.134)$$

or

$$\sigma^2_{ZFE} = \frac{\mathcal{N}_0}{2} \frac{w_0}{\|p\|} \quad , \qquad (3.135)$$

where w_0 is the zero (center) coefficient of the ZFE. This coefficient can be extracted from

$$\begin{aligned} W_{ZFE}(D) &= \sqrt{1.5625} \left[\frac{D^2(-4\jmath)}{\{(D + 2\jmath)(D - 2)(D - .5)(D + .5\jmath)\}} \right] \\ &= \sqrt{1.5625} \left[\frac{A}{D - 2} + \frac{B}{D + 2\jmath} + \text{terms not contributing to } w_0 \right] \quad , \end{aligned}$$

where A and B are coefficients in the partial-fraction expansion (the residuez and residue commands in Matlab can be very useful here):

$$A = \frac{4(-4\jmath)}{(2 + 2\jmath)(2 + .5\jmath)(1.5)} = -1.5686 - \jmath.9412 = 1.8293\angle - 2.601 \qquad (3.136)$$

183
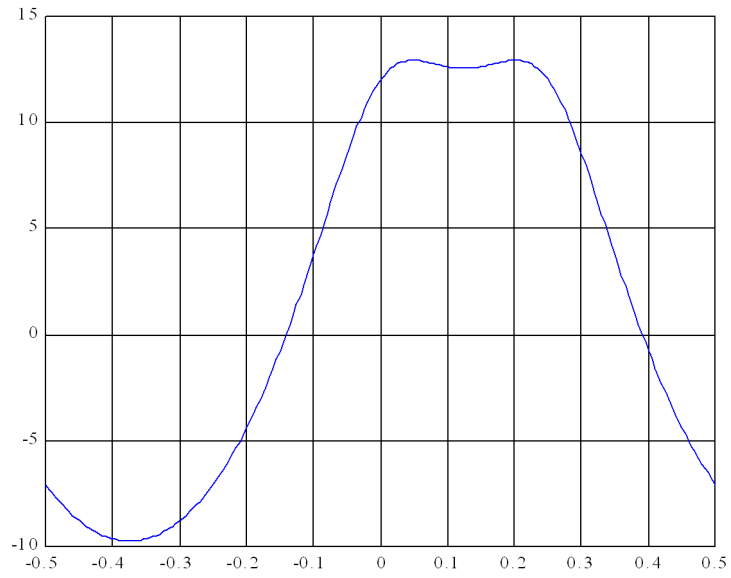
Figure 3.24: Fourier transform magnitude of the ZFE for the complex baseband channel example.
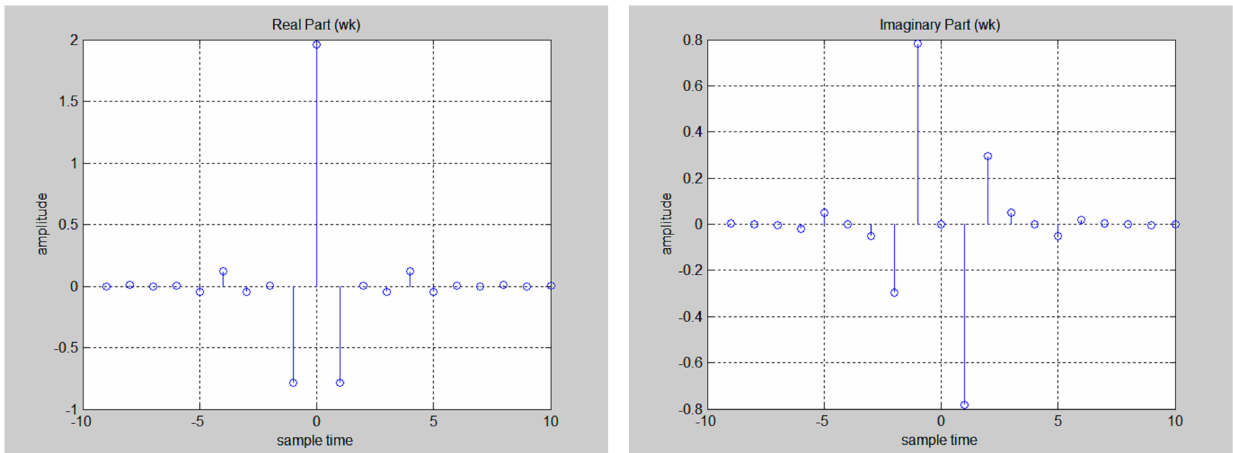
Figure 3.25: Time-domain equalizer coefficients for complex channel.

$$B = \frac{-4(-4j)}{(-2j-.5)(-2j-2)(-1.5j)} = .9412 + j1.5685 = 1.8293\angle 1.030 \quad . \quad (3.137)$$

Finally

$$W_{ZFE}(D) = \sqrt{1.5625}\left[\frac{A(-.5)}{1-.5D} + \frac{B(-.5j)}{(1-.5jD)} + \text{terms}\right] \quad , \quad (3.138)$$

and

$$w_0 = \sqrt{1.5625}\left[(-.5)(-1.5686 - j.9412) - .5j(.9412 + j1.5686)\right] \quad (3.139)$$

$$= \sqrt{1.5625}(1.57) = 1.96 \quad (3.140)$$

The ZFE loss can be shown to be

$$\gamma_{ZFE} = 10 \cdot \log_{10}(w_0 \cdot \|p\|) = 3.9 \text{ dB} \quad , \quad (3.141)$$

which is better than the last channel because the frequency spectrum is not as near zero in this complex example as it was earlier on the PAM example. Nevertheless, considerably better performance is also possible on this complex channel, but not with the ZFE.

To compute P_e for 4QAM, the designer calculates

$$\bar{P}_e \approx Q\left(\sqrt{\text{SNR}_{MFB} - 3.9 \text{ dB}}\right) \quad . \quad (3.142)$$

If $\text{SNR}_{MFB} = 10$dB, then $\bar{P}_e \approx 2.2 \times 10^{-2}$. If $\text{SNR}_{MFB} = 17.4$dB, then $\bar{P}_e \approx 1.0 \times 10^{-6}$. If $\text{SNR}_{MFB} = 23.4$dB for 16QAM, then $\bar{P}_e \approx 2.0 \times 10^{-5}$.

3.5 Minimum Mean-Square Error Linear Equalization

The **Minimum Mean-Square Error Linear Equalizer** (MMSE-LE) balances a reduction in ISI with noise enhancement. The MMSE-LE always performs as well as, or better than, the ZFE and is of the same complexity of implementation. Nevertheless, it is slightly more complicated to describe and analyze than is the ZFE. The MMSE-LE uses a linear time-invariant filter w_k for R, but the choice of filter impulse response w_k is different than the ZFE.

The MMSE-LE is a linear filter w_k that acts on y_k to form an output sequence z_k that is the best MMSE estimate of x_k. That is, the filter w_k minimizes the Mean Square Error (MSE):

Definition 3.5.1 (Mean Square Error (for the LE)) *The* **LE error** *signal is given by*

$$e_k = x_k - w_k * y_k = x_k - z_k \quad . \tag{3.143}$$

The **Minimum Mean Square Error** *(MMSE) for the linear equalizer is defined by*

$$\sigma^2_{MMSE-LE} \triangleq \min_{w_k} E\left[|x_k - z_k|^2\right] \quad . \tag{3.144}$$

The MSE criteria for filter design does not ignore noise enhancement because the optimization of this filter compromises between eliminating ISI and increasing noise power. Instead, the filter output is as close as possible, in the Minimum MSE sense, to the data symbol x_k.

3.5.1 Optimization of the Linear Equalizer

Using D-transforms,

$$E(D) = X(D) - W(D)Y(D) \tag{3.145}$$

By the orthogonality principle in Appendix A, at any time k, the error sample e_k must be uncorrelated with any equalizer input signal y_m. Succinctly,

$$E\left[E(D)Y^*(D^{-*})\right] = 0 \quad . \tag{3.146}$$

Evaluating (3.146), using (3.145), yields

$$0 = \bar{R}_{xy}(D) - W(D)\bar{R}_{yy}(D) \quad , \tag{3.147}$$

where ($N = 1$ for PAM, $N = 2$ for Quadrature Modulation)[9]

$$\begin{aligned}
\bar{R}_{xy}(D) &= E\left[X(D)Y^*(D^{-*})\right]/N = \|p\|Q(D)\bar{\mathcal{E}}_{\boldsymbol{x}} \\
\bar{R}_{yy}(D) &= E\left[Y(D)Y^*(D^{-*})\right]/N = \|p\|^2 Q^2(D)\bar{\mathcal{E}}_{\boldsymbol{x}} + \frac{\mathcal{N}_0}{2}Q(D) = Q(D)\left(\|p\|^2 Q(D)\bar{\mathcal{E}}_{\boldsymbol{x}} + \frac{\mathcal{N}_0}{2}\right) \quad .
\end{aligned}$$

Then the MMSE-LE becomes

$$W(D) = \frac{\bar{R}_{xy}(D)}{\bar{R}_{yy}(D)} = \frac{1}{\|p\|\left(Q(D) + 1/\text{SNR}_{MFB}\right)} \quad . \tag{3.148}$$

The MMSE-LE differs from the ZFE only in the additive positive term in the denominator of (3.148). The transfer function for the equalizer $W(e^{-\jmath\omega T})$ is also real and positive for all finite signal-to-noise ratios. This small positive term prevents the denominator from ever becoming zero, and thus makes the MMSE-LE well defined even when the channel (or pulse response) is zero for some frequencies or frequency bands. Also $W(D) = W^*(D^{-*})$. Figure 3.26 repeats Figure 3.19 with addition of the MMSE-LE transfer characteristic. The MMSE-LE transfer function has magnitude $\bar{\mathcal{E}}_{\boldsymbol{x}}/\sigma^2$ at $\omega = \frac{\pi}{T}$, while the ZFE becomes infinite at this same frequency. This MMSE-LE leads to better performance, as the next subsection computes.

---

[9]The expression $R_{xx}(D) \triangleq E\left[X(D)X^*(D^{-*})\right]$ is used in a symbolic sense, since the terms of $X(D)X^*(D^{-*})$ are of the form $\sum_k x_k x^*_{k-j}$, so that we are implying the additional operation $\lim_{K\to\infty}[1/(2K+1)]\sum_{-K\leq k\leq K}$ on the sum in such terms. This is permissable for stationary (and ergodic) discrete-time sequences.
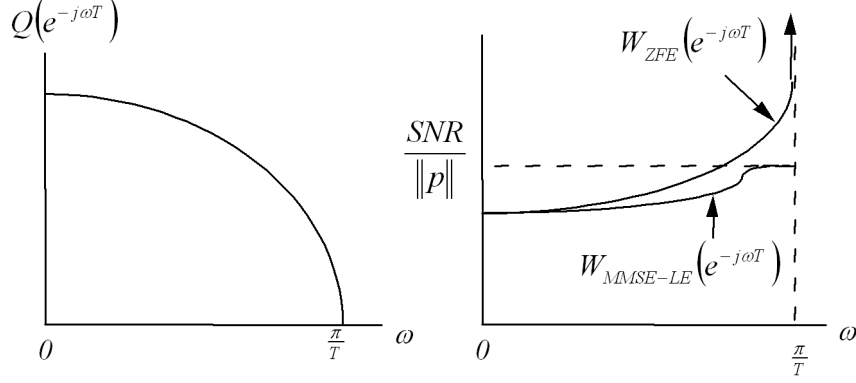
Figure 3.26: Example of MMSE-LE versus ZFE.

3.5.2 Performance of the MMSE-LE

The MMSE is the time-0 coefficient of the error autocorrelation sequence

$$
\begin{align}
\bar{R}_{ee}(D) &= E\left[E(D)E^*(D^{-*})\right]/N \tag{3.149} \\
&= \bar{\mathcal{E}}_{\boldsymbol{x}} - W^*(D^{-*})\bar{R}_{xy}(D) - W(D)\bar{R}^*_{xy}(D^{-*}) + W(D)\bar{R}_{yy}(D)W^*(D^{-*}) \tag{3.150} \\
&= \bar{\mathcal{E}}_{\boldsymbol{x}} - W(D)\bar{R}_{yy}(D)W^*(D^{-*}) \tag{3.151} \\
&= \bar{\mathcal{E}}_{\boldsymbol{x}} - \frac{Q(D)\left(\|p\|^2 \cdot Q(D)\bar{\mathcal{E}}_{\boldsymbol{x}} + \frac{\mathcal{N}_0}{2}\right)}{\|p\|^2\left(Q(D) + 1/\mathrm{SNR}_{MFB}\right)^2} \tag{3.152} \\
&= \bar{\mathcal{E}}_{\boldsymbol{x}} - \frac{\bar{\mathcal{E}}_{\boldsymbol{x}}Q(D)}{\left(Q(D) + 1/\mathrm{SNR}_{MFB}\right)} \tag{3.153} \\
&= \frac{\frac{\mathcal{N}_0}{2}}{\|p\|^2\left(Q(D) + 1/\mathrm{SNR}_{MFB}\right)} \tag{3.154}
\end{align}
$$

The third equality follows from

$$
\begin{align}
W(D)\bar{R}_{yy}(D)W^*(D^{-*}) &= W(D)\bar{R}_{yy}(D)\bar{R}_{yy}(D)^{-1}\bar{R}^*_{xy}(D^{-*}) \\
&= W(D)\bar{R}^*_{xy}(D^{-*}) \quad,
\end{align}
$$

and that $\left(W(D)\bar{R}_{yy}(D)W^*(D^{-*})\right)^* = W(D)\bar{R}_{yy}(D)W^*(D^{-*})$. The MMSE then becomes

$$
\sigma^2_{MMSE-LE} = \frac{T}{2\pi}\int_{-\frac{\pi}{T}}^{\frac{\pi}{T}} \bar{R}_{ee}(e^{-\jmath\omega T})d\omega = \frac{T}{2\pi}\int_{-\frac{\pi}{T}}^{\frac{\pi}{T}} \frac{\frac{\mathcal{N}_0}{2}d\omega}{\|p\|^2\left(Q(e^{-\jmath\omega T}) + 1/\mathrm{SNR}_{MFB}\right)} \quad. \tag{3.155}
$$

By recognizing that $W(e^{-\jmath\omega T})$ is multiplied by the constant $\frac{\mathcal{N}_0}{2}/\|p\|$ in (3.155), then

$$
\sigma^2_{MMSE-LE} = w_0 \frac{\frac{\mathcal{N}_0}{2}}{\|p\|} \quad. \tag{3.156}
$$

From comparison of (3.155) and (3.98), that

$$
\sigma^2_{MMSE-LE} \leq \sigma^2_{ZFE} \quad, \tag{3.157}
$$

with equality if and only if $\mathrm{SNR}_{MFB} \to \infty$. Furthermore, since the ZFE is unbiased, and $\mathrm{SNR}_{MMSE-LE} = \mathrm{SNR}_{MMSE-LE,U} + 1$ and $\mathrm{SNR}_{MMSE-LE,U}$ are the maximum-SNR corresponding to unconstrained and unbiased linear equalizers, respectively,

$$
\mathrm{SNR}_{ZFE} \leq \mathrm{SNR}_{MMSE-LE,U} = \frac{\bar{\mathcal{E}}_{\boldsymbol{x}}}{\sigma^2_{MMSE-LE}} - 1 \leq \mathrm{SNR}_{MFB} \quad. \tag{3.158}
$$

One confirms that the MMSE-LE is a biased receiver by writing the following expression for the equalizer output

$$Z(D) = W(D)Y(D) \tag{3.159}$$

$$= \frac{1}{\|p\|\left(Q(D)+1/\text{SNR}_{MFB}\right)}\left(Q(D)\|p\|X(D)+N(D)\right) \tag{3.160}$$

$$= X(D) - \frac{1/\text{SNR}_{MFB}}{Q(D)+1/\text{SNR}_{MFB}}X(D) + \frac{N(D)}{\|p\|\left(Q(D)+1/\text{SNR}_{MFB}\right)} \quad, \tag{3.161}$$

for which the x_k-dependent residual ISI term contains a component

$$\text{signal-basis term} = -1/\text{SNR}_{MFB}w_0 \cdot \|p\| \cdot x_k \tag{3.162}$$

$$= -1/\text{SNR}_{MFB} \cdot \frac{\sigma^2_{MMSE-LE}\|p\|^2}{\frac{N_0}{2}}x_k \tag{3.163}$$

$$= -\frac{\sigma^2_{MMSE-LE}}{\bar{\mathcal{E}}_{\boldsymbol{x}}} \cdot x_k \tag{3.164}$$

$$= -\frac{1}{\text{SNR}_{MMSE-LE}} \cdot x_k \quad. \tag{3.165}$$

$$\tag{3.166}$$

So $z_k = \left(1 - \frac{1}{\text{SNR}_{MMSE-LE}}\right)x_k - e'_k$ where e'_k is the error for unbiased detection and R. The optimum unbiased receiver with decision regions scaled by $1 - \frac{1}{\text{SNR}_{MMSE-LE}}$ (see Section 3.2.1) has the signal energy given by

$$\left(1 - \frac{1}{\text{SNR}_{MMSE-LE}}\right)^2 \bar{\mathcal{E}}_{\boldsymbol{x}} \quad. \tag{3.167}$$

A new error for the scaled decision regions is $e'_k = (1 - 1/\text{SNR}_{MMSE-LE})x_k - z_k = e_k - \frac{1}{\text{SNR}_{MMSE-LE}}x_k$, which is also the old error with the x_k dependent term removed. Since e'_k and x_k are then independent, then

$$\sigma^2_e = \sigma^2_{MMSE-LE} = \sigma^2_{e'} + \left(\frac{1}{\text{SNR}_{MMSE-LE}}\right)^2 \bar{\mathcal{E}}_{\boldsymbol{x}} \quad, \tag{3.168}$$

leaving

$$\sigma^2_{e'} = \sigma^2_{MMSE-LE} - \left(\frac{1}{\text{SNR}_{MMSE-LE}}\right)^2 \bar{\mathcal{E}}_{\boldsymbol{x}} = \frac{\text{SNR}^2_{MMSE-LE}\sigma^2_{MMSE-LE} - \bar{\mathcal{E}}_{\boldsymbol{x}}}{\text{SNR}^2_{MMSE-LE}} = \frac{\bar{\mathcal{E}}_{\boldsymbol{x}}\left(\text{SNR}_{MMSE-LE}-1\right)}{\text{SNR}^2_{MMSE-LE}} \quad. \tag{3.169}$$

The SNR for the unbiased MMSE-LE then becomes (taking the ratio of (3.167) to $\sigma^2_{e'}$)

$$\text{SNR}_{MMSE-LE,U} = \frac{\frac{(\text{SNR}_{MMSE-LE}-1)^2}{\text{SNR}^2_{MMSE-LE}}\bar{\mathcal{E}}_{\boldsymbol{x}}}{\bar{\mathcal{E}}_{\boldsymbol{x}}\frac{(\text{SNR}_{MMSE-LE}-1)}{\text{SNR}^2_{MMSE-LE}}} = \text{SNR}_{MMSE-LE} - 1 \quad, \tag{3.170}$$

which corroborates the earlier result on the relation of the optimum biased and unbiased SNR's for any particular receiver structure (at least for the LE structure). The unbiased SNR is

$$\text{SNR}_{MMSE-LE,U} = \frac{\bar{\mathcal{E}}_{\boldsymbol{x}}}{\sigma^2_{MMSE-LE}} - 1 \quad, \tag{3.171}$$

which is the performance level that this text always uses because it corresponds to the best error probability for an SBS detector, as was discussed earlier in Section 3.1. Figure 3.27 illustrates the concept with the effect of scaling on a 4QAM signal shown explicitly. Again, MMSE receivers (of which the MMSE-LE is one) reduce noise power at the expense of introducing a bias, the scaling up removes
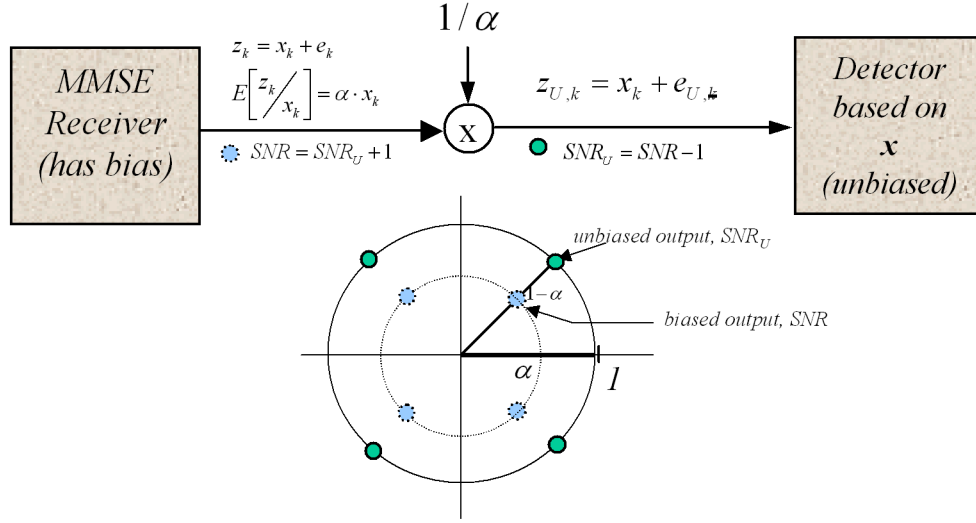
Figure 3.27: Illustration of bias and its removal.

the bias, and ensures the detector achieves the best P_e it can. Since the ZFE is also an unbiased receiver, (3.158) must hold. The first inequality in (3.158) tends to equality if the ratio $\frac{\bar{\mathcal{E}}_{\boldsymbol{x}}}{\sigma^2} \to \infty$ or if the channel is free of ISI ($Q(D) = 1$). The second inequality tends to equality if $\frac{\bar{\mathcal{E}}_{\boldsymbol{x}}}{\sigma^2} \to 0$ or if the channel is free of ISI ($Q(D) = 1$).

The unbiased MMSE-LE loss with respect to the MFB is

$$\gamma_{MMSE-LE} = \frac{\text{SNR}_{MFB}}{\text{SNR}_{MMSE-LE,U}} = \left(\frac{\|p\|^2 \sigma^2_{MMSE-LE}}{\sigma^2} \right) \left(\frac{\bar{\mathcal{E}}_{\boldsymbol{x}}}{\bar{\mathcal{E}}_{\boldsymbol{x}} - \sigma^2_{MMSE-LE}} \right) \quad . \tag{3.172}$$

The $\frac{\|p\|^2 \sigma^2_{MMSE-LE}}{\sigma^2}$ in (3.172) is the increase in noise variance of the MMSE-LE, while the term $\frac{\bar{\mathcal{E}}_{\boldsymbol{x}}}{\bar{\mathcal{E}}_{\boldsymbol{x}} - \sigma^2_{MMSE-LE}}$ term represents the loss in signal power at the equalizer output that accrues to lower noise enhancement.

The MMSE-LE also requires no additional complexity to implement and should always be used in place of the ZFE when the receiver uses symbol-by-symbol detection on the equalizer output.

The error is not necessarily Gaussian in distribution. Nevertheless, engineers commonly make this assumption in practice, with a good degree of accuracy, despite the potential non-Gaussian residual ISI component in $\sigma^2_{MMSE-LE}$. This text also follows this practice. Thus,

$$P_e \approx N_e Q \left(\sqrt{\kappa \text{SNR}_{MMSE-LE,U}} \right) \quad , \tag{3.173}$$

where κ depends on the relation of $\bar{\mathcal{E}}_{\boldsymbol{x}}$ to $d_{\min}$ for the particular constellation of interest, for instance $\kappa = 3/(M-1)$ for Square QAM. The reader may recall that the symbol Q is used in two separate ways in these notes, for the Q-function, and for the transform of the matched-filter-pulse-response cascade. The actual meaning should always be obvious in context.)

3.5.3 Examples Revisited

This section returns to the earlier ZFE examples to compute the improvement of the MMSE-LE on these same channels.

EXAMPLE 3.5.1 (PAM - MMSE-LE) The pulse response of a channel used with binary PAM is again given by

$$P(\omega) = \begin{cases} \sqrt{T} \left(1 + .9 e^{j\omega T} \right) & |\omega| \le \frac{\pi}{T} \\ 0 & |\omega| > \frac{\pi}{T} \end{cases} \quad . \tag{3.174}$$

189
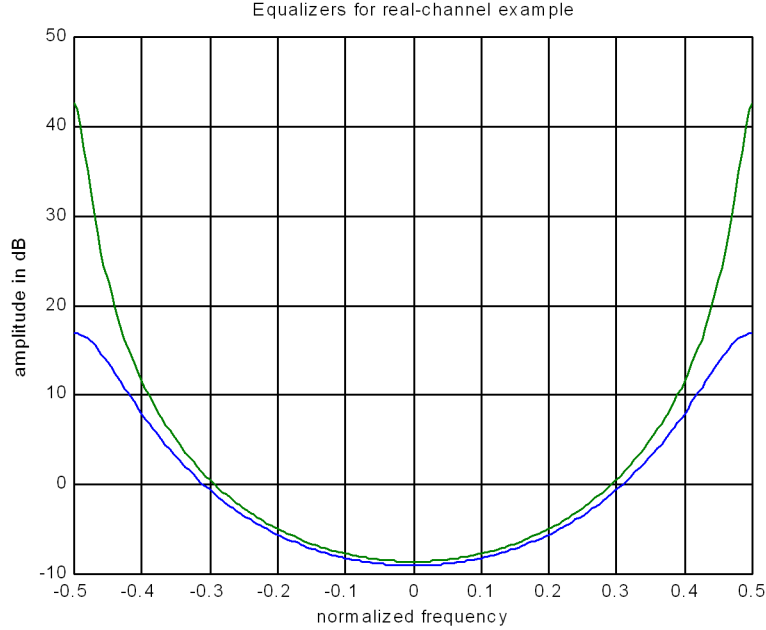
Figure 3.28: Comparison of equalizer frequency-domain responses for MMSE-LE and ZFE on baseband example.

Let us suppose $\text{SNR}_{MFB} = 10\text{dB}$ $(= \bar{\mathcal{E}}_{\boldsymbol{x}}\|p\|^2/\frac{\mathcal{N}_0}{2})$ and that $\mathcal{E}_{\boldsymbol{x}} = 1$.

The equalizer is

$$W(D) = \frac{1}{\|p\| \cdot \left(\frac{.9}{1.81}D^{-1} + 1.1 + \frac{.9}{1.81}D\right)} \quad . \tag{3.175}$$

Figure 3.28 shows the frequency response of the equalizer for both the ZFE and MMSE-LE. Clearly the MMSE-LE has a lower magnitude in its response.

The $\sigma^2_{MMSE-LE}$ is computed as

$$\sigma^2_{MMSE-LE} = \frac{T}{2\pi}\int_{-\frac{\pi}{T}}^{\frac{\pi}{T}} \frac{\frac{\mathcal{N}_0}{2}}{1.81 + 1.8\cos(\omega T) + 1.81/10}d\omega \tag{3.176}$$

$$= \frac{\mathcal{N}_0}{2}\frac{1}{\sqrt{1.991^2 - 1.8^2}} \tag{3.177}$$

$$= \frac{\mathcal{N}_0}{2}(1.175) \quad , \tag{3.178}$$

which is considerably smaller than σ^2_{ZFE}. The SNR for the MMSE-LE is

$$\text{SNR}_{MMSE-LE,U} = \frac{1 - 1.175(.181)}{1.175(.181)} = 3.7 \ (5.7\text{dB}) \quad . \tag{3.179}$$

The loss with respect to the MFB is 10dB - 5.7dB = 4.3dB. This is 5.5dB better than the ZFE (9.8dB - 4.3dB = 5.5dB), but still not good for this channel.

Figure 3.29 compares the frequency-domain responses of the equalized channel. Figure 3.30 compares the time-domain responses of the equalized channel. The MMSE-LE clearly does not have an ISI-free response, but mean-square error/distortion is minimized and the MMSE-LE has better performance than the ZFE.

The relatively small energy near the Nyquist Frequency in this example is the reason for the poor performance of both linear equalizers (ZFE and MMSE-LE) in this example. To
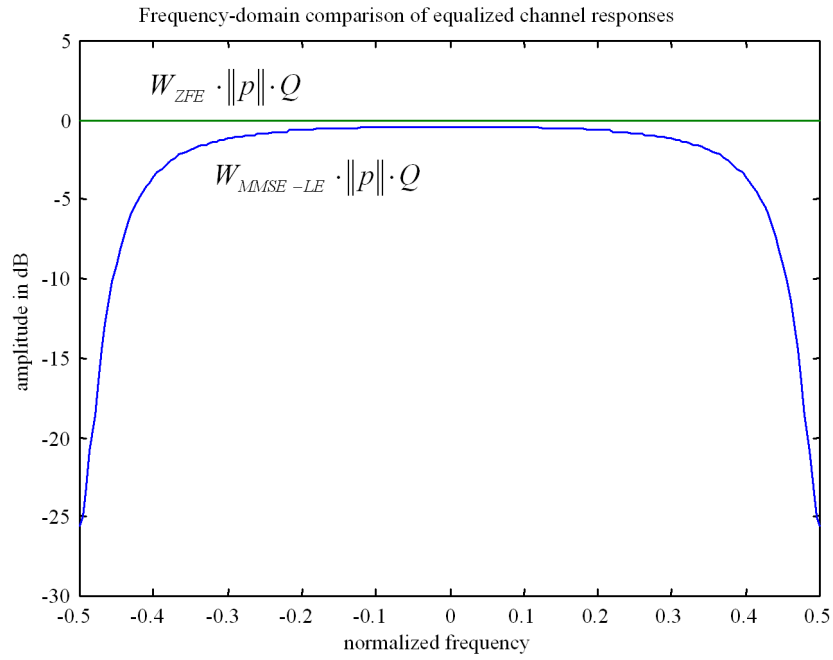
Figure 3.29: Comparison of equalized frequency-domain responses for MMSE-LE and ZFE on baseband example.
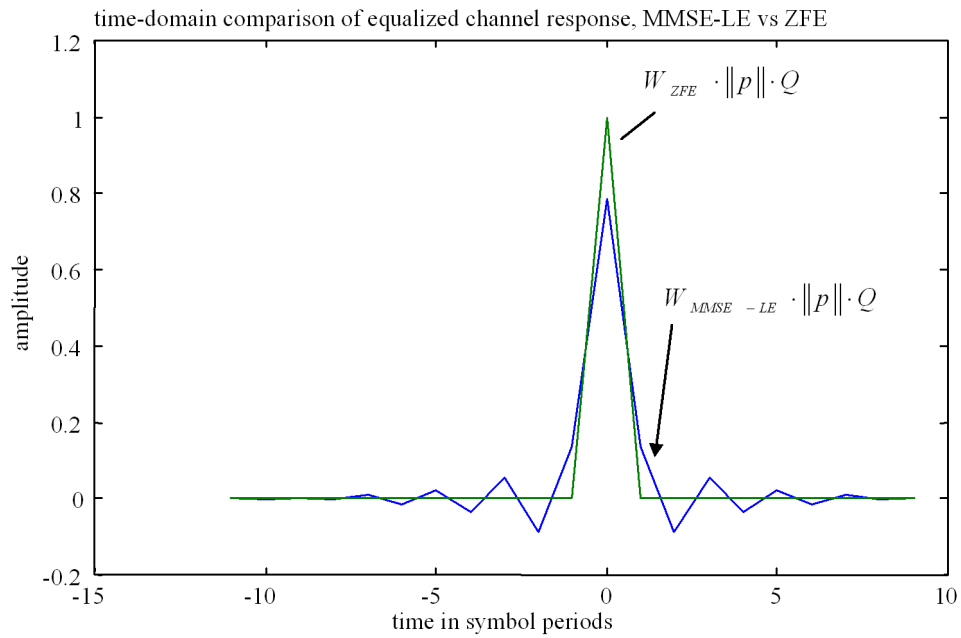
Figure 3.30: Comparison of equalized time-domain responses for MMSE-LE and ZFE on baseband example.
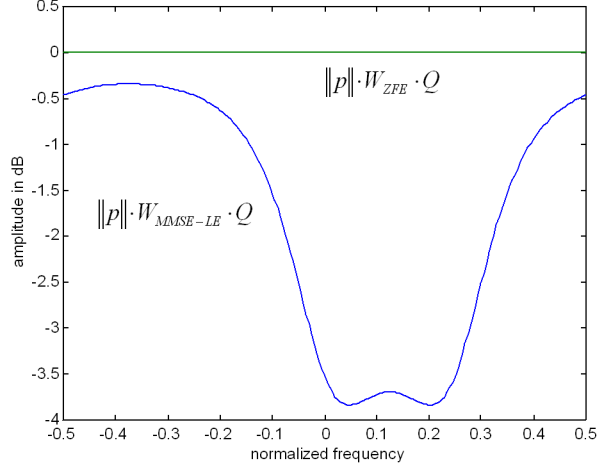
Figure 3.31: Comparison of MMSE-LE and ZFE for complex channel example.

improve performance further, decision-assisted equalization is examined in Section 3.6 and in Chapter 5 (or codes combined with equalization, as discussed in Chapters 10 and 11). Another yet better method appears in Chapter 4.

The complex example also follows in a straightforward manner.

EXAMPLE 3.5.2 (QAM - MMSE-LE) Recall that the equivalent baseband pulse response samples were given by

$$p_k = \frac{1}{\sqrt{T}} \left[-\frac{1}{2} , \left(1 + \frac{\jmath}{4} \right) , -\frac{\jmath}{2} \right] \quad . \tag{3.180}$$

Again, $\text{SNR}_{MFB} = 10\text{dB}$ $(= \bar{\mathcal{E}}_{\boldsymbol{x}} \|p\|^2 / \frac{\mathcal{N}_0}{2})$, $\bar{\mathcal{E}}_{\boldsymbol{x}} = 1$, and thus

$$\sigma^2_{MMSE-LE} = w_0 \frac{\mathcal{N}_0}{2} \|p\|^{-1} \quad . \tag{3.181}$$

The equalizer is, noting that $\frac{\mathcal{N}_0}{2} = \frac{\bar{\mathcal{E}}_{\boldsymbol{x}} \|p\|^2}{\text{SNR}_{MFB}} = 1.5625/10 = .15625$,

$$W(D) = \frac{1}{(Q(D) + 1/\text{SNR}_{MFB}) \|p\|} \tag{3.182}$$

or

$$= \frac{\sqrt{1.5625}}{-.25\jmath D^{-2} + .625(-1 + \jmath)D^{-1} + 1.5625(1 + .1) - .625(1 + \jmath)D^1 + .25\jmath D^2} \quad . \tag{3.183}$$

Figure 3.31 compares the MMSE-LE and ZFE equalizer responses for this same channel. The MMSE-LE high response values are considerably more limited than the ZFE values. The roots of $Q(D) + 1/\text{SNR}_{MFB}$, or of the denominator in (3.183), are

$$D = 2.217\angle^{-1.632} = -.1356 - \jmath2.213 \tag{3.184}$$

$$D = 2.217\angle^{.0612} = 2.213 + \jmath.1356 \tag{3.185}$$

$$D = .451\angle^{-1.632} = -.0276 - \jmath.4502 \tag{3.186}$$

$$D = .451\angle^{.0612} = .4502 + \jmath.0276 \quad , \tag{3.187}$$

and (3.183) becomes

$$W(D) = \frac{\left[\sqrt{1.5625}D^2/(.25\jmath)\right]}{(D - 2.22\angle^{-1.632})(D - 2.22\angle^{.0612})(D - .451\angle^{-1.632})(D - .451\angle^{.0612})} \quad (3.188)$$

or

$$W(D) = \frac{A}{D - 2.22\angle^{-1.632}} + \frac{B}{D - 2.22\angle^{.0612}} + \dots \quad , \quad (3.189)$$

where the second expression (3.189) has ignored any terms in the partial fraction expansion that will not contribute to w_0. Then,

$$\begin{aligned} A &= \frac{\sqrt{1.5625}(-4\jmath)(2.22\angle^{-1.632})^2}{(2.22\angle^{-1.632} - 2.22\angle^{.0612})(2.22\angle^{-1.632} - .451\angle^{-1.632})(2.22\angle^{-1.632} - .451\angle^{.0612})} \\ &= \sqrt{1.5625}(-\jmath.805 + 1.20)\jmath = 1.0079 + \jmath1.5025 \quad (3.190) \\ B &= \frac{\sqrt{1.5625}(-4\jmath)(2.22\angle^{.0612})^2}{(2.22\angle^{.0612} - 2.22\angle^{-1.632})(2.22\angle^{.0612} - .451\angle^{-1.632})(2.22\angle^{.0612} - .451\angle^{.0612})} \\ &= \sqrt{1.5625}(\jmath1.20 - .805)\jmath = -1.5025 - 1.0079\jmath \quad . \quad (3.191) \end{aligned}$$

Then, from (3.189),

$$w_0 = A(-.451\angle^{1.632}) + B(-.451\angle^{-.0612}) = \sqrt{1.5625}(1.125) \quad . \quad (3.192)$$

Then

$$\sigma^2_{MMSE-LE} = 1.125\frac{\mathcal{N}_0}{2} = 1.125(.15625) = .1758 \quad , \quad (3.193)$$

$$\mathrm{SNR}_{MMSE-LE,U} = \frac{[1 - 1.125(.15625)]}{1.125(.15625)} = 4.69 \ (\ 6.7 \text{ dB} \ ) \quad , \quad (3.194)$$

which is 3.3 dB below the matched filter bound SNR of 10dB, or equivalently,

$$\gamma_{MMSE-LE} = 10\log_{10}(10/4.69) = 10\log_{10}(2.13) = 3.3 \text{ dB} \quad , \quad (3.195)$$

but .6 dB better than the ZFE. It is also possible to do considerably better on this channel, but structures not yet introduced will be required. Nevertheless, the MMSE-LE is one of the most commonly used equalization structures in practice.

Figure 3.31 compares the equalized channel responses for both the MMSE-LE and ZFE. While the MMSE-LE performs better, there is a significant deviation from the ideal flat response. This deviation is good and gains .6 dB improvement. Also, because of biasing, the MMSE-LE output is everywhere slightly lower than the ZFE output (which is unbiased). This bias can be removed by scaling by 5.69/4.69.

3.5.4 Fractionally Spaced Equalization

To this point in the study of the discrete time equalizer, a matched filter $\varphi_p^*(-t)$ precedes the sampler, as was shown in Figure 3.7. While this may be simple from an analytical viewpoint, there are several practical problems with the use of the matched filter. First, $\varphi_p^*(-t)$ is a continuous time filter and may be much more difficult to design accurately than an equivalent digital filter. Secondly, the precise sampling frequency and especially its phase, must be known so that the signal can be sampled when it is at maximum strength. Third, the channel pulse response may not be accurately known at the receiver, and an adaptive equalizer (see Chapter 7), is instead used. It may be difficult to design an adaptive, analog, matched filter.

For these reasons, sophisticated data transmission systems often replace the matched-filter/sampler/equalizer system of Figure 3.7 with the Fractionally Spaced Equalizer (FSE) of Figure 3.32. Basically, the sampler and the matched filter have been interchanged with respect to Figure 3.7. Also the sampling rate has been increased by some rational number l $(l > 1)$. The new sampling rate is chosen sufficiently high so
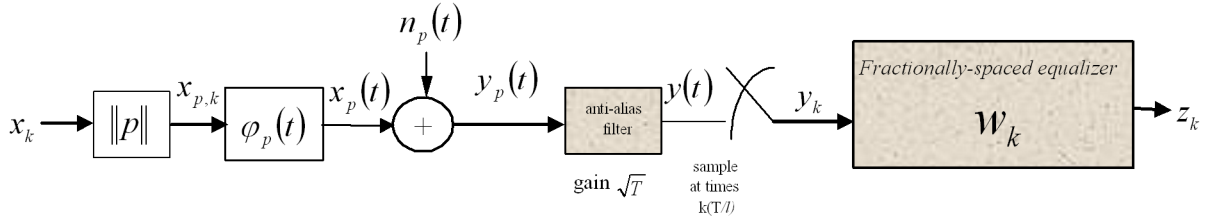
Figure 3.32: Fractionally spaced equalization.

as to be greater than twice the highest frequency of $x_p(t)$. Then, the matched filtering operation and the equalization filtering are performed at rate l/T, and the cascade of the two filters is realized as a single filter in practice. An anti-alias or noise-rejection filter always precedes the sampling device (usually an analog-to-digital converter). This text assumes this filter is an ideal lowpass filter with gain $\sqrt{T}$ transfer over the frequency range $-l\frac{\pi}{T} \leq \omega \leq l\frac{\pi}{T}$. The variance of the noise samples at the filter output will then be $\frac{N_0}{2}l$ per dimension.

In practical systems, the four most commonly found values for l are $\frac{4}{3}$, 2, 3, and 4. The major drawback of the FSE is that to span the same interval in time (when implemented as an FIR filter, as is typical in practice), it requires a factor of l more coefficients, leading to an increase in memory by a factor of l. The FSE outputs may also appear to be computed l times more often in real time. However, only $\left(\frac{1}{l}\right)^{th}$ of the output samples need be computed (that is, those at the symbol rate, as that is when we need them to make a decision), so computation is approximately l times that of symbol-spaced equalization, corresponding to l times as many coefficients to span the same time interval, or equivalently, to l times as many input samples per symbol.

The FSE will digitally realize the cascade of the matched filter and the equalizer, eliminating the need for an analog matched filter. (The entire filter for the FSE can also be easily implemented adaptively, see Chapter 7.) The FSE can also exhibit a significant improvement in sensitivity to sampling-phase errors. To investigate this improvement briefly, in the original symbol-spaced equalizers (ZFE or MMSE-LE) may have the sampling-phase on the sampler in error by some small offset t_0. Then, the sampler will sample the matched filter output at times $kT + t_0$, instead of times kT. Then,

$$y(kT + t_0) = \sum_m x_m \cdot \|p\| \cdot q(kT - mT + t_0) + n_k \quad , \tag{3.196}$$

which corresponds to $q(t) \to q(t + t_0)$ or $Q(\omega) \to Q(\omega)e^{-\jmath\omega t_0}$. For the system with sampling offset,

$$Q(e^{-\jmath\omega T}) \to \frac{1}{T}\sum_n Q(\omega - \frac{2\pi n}{T})e^{-\jmath(\omega - \frac{2\pi n}{T})t_0} \quad , \tag{3.197}$$

which is no longer nonnegative real across the entire frequency band. In fact, it is now possible (for certain nonzero timing offsets t_0, and at frequencies just below the Nyquist Frequency) that the two aliased frequency characteristics $Q(\omega)e^{-\jmath\omega t_0}$ and $Q(\omega - \frac{2\pi}{T})e^{-\jmath(\omega - \frac{2\pi}{T})t_0}$ add to approximately zero, thus producing a notch within the critical frequency range $(-\frac{\pi}{T}, \frac{\pi}{T})$. Then, the best performance of the ensuing symbol-spaced ZFE and/or MMSE-LE can be significantly reduced, because of noise enhancement. The resulting noise enhancement can be a major problem in practice, and the loss in performance can be several dB for reasonable timing offsets. When the anti-alias filter output is sampled at greater than twice the highest frequency in $x_p(t)$, then information about the entire signal waveform is retained. Equivalently, the FSE can synthesize, via its transfer characteristic, a phase adjustment (effectively interpolating to the correct phase) so as to correct the timing offset, t_0, in the sampling device. The symbol-spaced equalizer cannot interpolate to the correct phase, because no interpolation is correctly performed at the symbol rate. Equivalently, information has been lost about the signal by sampling at a speed that is too low in the symbol-spaced equalizer without matched filter. This possible notch is an

example of information loss at some frequency; this loss cannot be recovered in a symbol-spaced equalizer without a matched filter. In effect, the FSE equalizes before it aliases (aliasing does occur at the output of the equalizer where it decimates by l for symbol-by-symbol detection), whereas the symbol-spaced equalizer aliases before it equalizes; the former alternative is often the one of choice in practical system implementation, if the extra memory and computation can be accommodated. Effectively, with an FSE, the sampling device need only be locked to the symbol rate, but can otherwise provide any sampling phase. The phase is tacitly corrected to the optimum phase inside the linear filter implementing the FSE.

The sensitivity to sampling phase is channel dependent: In particular, there is usually significant channel energy near the Nyquist Frequency in applications that exhibit a significant improvement of the FSE with respect to the symbol-spaced equalizer. In channels with little energy near the Nyquist Frequency, the FSE is avoided, because it provides little performance gain, and is significantly more complex to implement (more parameters and higher sampling rate).

Infinite-Length FSE Settings   To derive the settings for the FSE, this section assumes that l, the oversampling factor, is an integer. The sampled output of the anti-alias filter can be decomposed into l sampled-at-rate-$1/T$ interleaved sequences with D-transforms $Y_0(D)$, $Y_2(D)$, ..., $Y_{l-1}(D)$, where $Y_l(D)$ corresponds to the sample sequence $y[kT - iT/l]$. Then,

$$Y_i(D) = P_i(D) \cdot X(D) + N_i(D) \tag{3.198}$$

where $P_i(D)$ is the transform of the symbol-rate-spaced-i^{th}-phase-of-$p(t)$ sequence $p[kT - (i-1)T/l]$, and similarly $N_i(D)$ is the transform of a symbol-rate sampled white noise sequence with autocorrelation function $R_{nn}(D) = l \cdot \frac{\mathcal{N}_0}{2}$ per dimension, and these noise sequences are also independent of one another. A column vector transform is

$$\boldsymbol{Y}(D) = \begin{bmatrix} Y_0(D) \\ \vdots \\ Y_{l-1}(D) \end{bmatrix} = \boldsymbol{P}(D)X(D) + \boldsymbol{N}(D) \quad . \tag{3.199}$$

Also

$$\boldsymbol{P}(D) \triangleq \begin{bmatrix} P_0(D) \\ \vdots \\ P_{l-1}(D) \end{bmatrix} \text{ and } \boldsymbol{N}(D) = \begin{bmatrix} N_0(D) \\ \vdots \\ N_{l-1}(D) \end{bmatrix} \quad . \tag{3.200}$$

By considering the FSE output at sampling rate $1/T$, the interleaved coefficients of the FSE can also be written in a row vector $\boldsymbol{W}(D) = [W_1(D), ..., W_l(D)]$. Thus the FSE output is

$$Z(D) = \boldsymbol{W}(D)\boldsymbol{Y}(D) \quad . \tag{3.201}$$

Again, the orthogonality condition says that $E(D) = X(D) - Z(D)$ should be orthogonal to $Y(D)$, which can be written in vector form as

$$E\left[E(D)\boldsymbol{Y}^*(D^{-*})\right] = \boldsymbol{R}_{x\boldsymbol{Y}}(D) - \boldsymbol{W}(D)\boldsymbol{R}_{\boldsymbol{Y}\boldsymbol{Y}}(D) = 0 \quad , \tag{3.202}$$

where

$$\boldsymbol{R}_{x\boldsymbol{Y}}(D) \quad \triangleq \quad E\left[X(D)\boldsymbol{Y}^*(D^{-*})\right] = \bar{\mathcal{E}}_{\boldsymbol{x}}\boldsymbol{P}^*(D^{-*}) \tag{3.203}$$

$$\boldsymbol{R}_{\boldsymbol{Y}\boldsymbol{Y}}(D) \quad \triangleq \quad E\left[\boldsymbol{Y}(D)\boldsymbol{Y}^*(D^{-*})\right] = \bar{\mathcal{E}}_{\boldsymbol{x}}\boldsymbol{P}(D)\boldsymbol{P}^*(D^{-*}) + l \cdot \frac{\mathcal{N}_0}{2}I \quad . \tag{3.204}$$

MMSE-FSE filter setting is then

$$W(D) = \boldsymbol{R}_{x\boldsymbol{Y}}(D)\boldsymbol{R}_{\boldsymbol{Y}\boldsymbol{Y}}^{-1}(D) = \boldsymbol{P}^*(D^{-*})\left[\boldsymbol{P}(D)\boldsymbol{P}^*(D^{-*}) + l/\text{SNR}\right]^{-1} \quad . \tag{3.205}$$

The corresponding error sequence has autocorrelation function

$$\bar{R}_{ee}(D) = \bar{\mathcal{E}}_{\boldsymbol{x}} - \boldsymbol{R}_{x\boldsymbol{Y}}(D)\boldsymbol{R}_{\boldsymbol{Y}\boldsymbol{Y}}^{-1}(D)\boldsymbol{R}_{\boldsymbol{Y}x}(D) = \frac{l \cdot \frac{\mathcal{N}_0}{2}}{\boldsymbol{P}^*(D^{-*})\boldsymbol{P}(D) + l/\text{SNR}} \quad . \tag{3.206}$$
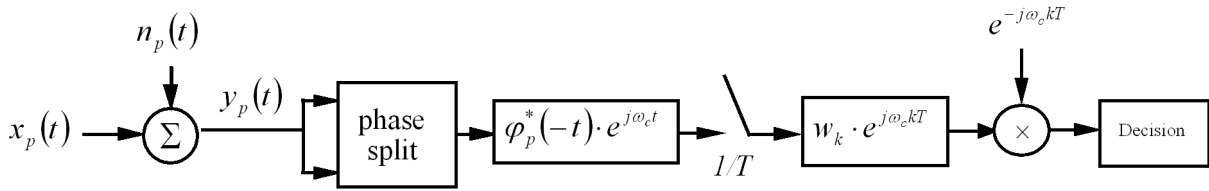
Figure 3.33: Passband equalization, direct synthesis of analytic-equivalent equalizer.

The MMSE is then computed as

$$\text{MMSE}_{MMSE-FSE} = \frac{T}{2\pi} \int_{-\frac{\pi}{T}}^{\frac{\pi}{T}} \frac{l \cdot \frac{N_0}{2} d\omega}{\|\boldsymbol{P}(e^{-\jmath\omega T})\|^2 + l/\text{SNR}} = \text{MMSE}_{MMSE-LE} \quad , \tag{3.207}$$

where $\|\boldsymbol{P}(e^{-\jmath\omega T})\|^2 = \sum_{i=1}^{l} |P_i(e^{-\jmath\omega T})|^2$. The SNR's, biased and unbiased, are also then exactly the same as given for the MMSE-LE, as long as the sampling rate exceeds twice the highest frequency of $P(f)$.

The reader is cautioned against letting $\frac{N_0}{2} \to 0$ to get the ZF-FSE. This is because the matrix $\boldsymbol{R_{YY}}(D)$ will often be singular when this occurs. To avoid problems with singularity, an appropriate pseudoinverse, which zeros the FSE characteristic when $P(\omega) = 0$ is recommended.

Passband Equalization

This chapter so far assumed for the complex baseband equalizer that the passband signal has been demodulated according to the methods described in Chapter 2 before filtering and sampling. An alternative method, sometimes used in practice when ω_c is not too high (or intermediate-frequency up/down conversion is used), is to commute the demodulation and filtering functions. Sometimes this type of system is also called "direct conversion," meaning that no carrier demodulation occurs prior to sampling. This commuting can be done with either symbol-spaced or fractionally spaced equalizers. The main reason for the interchange of filtering and demodulation is the recovery of the carrier frequency in practice. Postponing the carrier demodulation to the equalizer output can lead to significant improvement in the tolerance of the system to any error in estimating the carrier frequency, as Chapter 6 investigates. In the present (perfect carrier phase lock) development, passband equalization and baseband equalization are exactly equivalent and the settings for the passband equalizer are identical to those of the corresponding baseband equalizer, other than a translation in frequency by ω_c radians/sec.

Passband equalization is best suited to CAP implementations (See Section 4 of Chapter 2) where the complex channel is the analytic equivalent. The complex equalizer then acts on the analytic equivalent channel and signals to eliminate ISI in a MMSE sense. When used with CAP, the final rotation shown in Figure 3.33 is not necessary – such a rotation is only necessary with a QAM transmit signal.

The passband equalizer is illustrated in Figure 3.33. The phase splitting is the forming of the analytic equivalent with the use of the Hilbert Transform, as discussed in Chapter 2. The matched filtering and equalization are then performed on the passband signal with digital demodulation to baseband deferred to the filter output. The filter w_k can be a ZFE, a MMSE-LE, or any other desired setting (see Chapter 4 and Sections 3.5 and 3.6). In practice, the equalizer can again be realized as a fractionally spaced equalizer by interchanging the positions of the matched filter and sampler, increasing the sampling rate, and absorbing the matched filtering operation into the filter w_k, which would then be identical to the (modulated) baseband-equivalent FSE with output sample rate decimated appropriately to produce outputs only at the symbol sampling instants.

Often in practice, the cross-coupled nature of the complex equalizer $W(D)$ is avoided by sampling the FSE at a rate that exceeds twice the highest frequency of the passband signal $y(t)$ prior to demodulation. (If intermediate frequency (IF) demodulation is used, then twice the highest frequency after the IF.) In

196

this case the phase splitter (contains Hilbert transform in parallel with a unit gain) is also absorbed into the equalizer, and the same sampled sequence is applied independently to two equalizers, one of which estimates the real part, and one the imaginary part, of the analytic representation of the data sequence $x_k e^{\jmath \omega_c kT}$. The two filters can sometimes (depending on the sampling rate) be more cost effective to implement than the single complex filter, especially when one considers that the Hilbert transform is incorporated into the equalizer. This approach is often taken with adaptive implementations of the FSE, as the Hilbert transform is then implemented more exactly adaptively than is possible with fixed design.[10] This is often called **Nyquist Inband Equalization**. A particularly common variant of this type of equalization is to sample at rate $2/T$ both of the outputs of a continuous-time phase splitter, one stream of samples staggered by $T/4$ with respect to the other. The corresponding $T/2$ complex equalizer can then be implemented adaptively with four independent adaptive equalizers (rather than the two filters, real and imaginary part, that nominally characterize complex convolution). The adaptive filters will then correct for any imperfections in the phase-splitting process, whereas the two filters with fixed conjugate symmetry could not.

---

[10]However, this structure also slows convergence of many adaptive implementations.
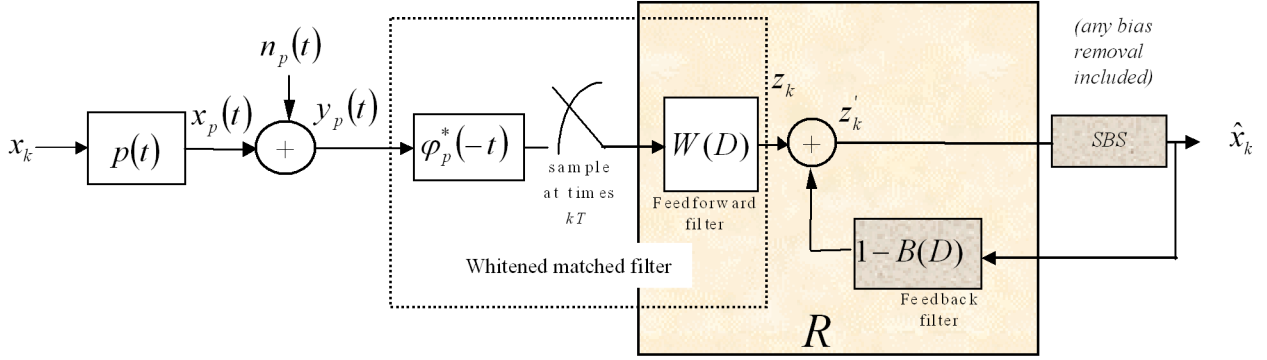
Figure 3.34: Decision feedback equalization.

3.6 Decision Feedback Equalization

Decision Feedback Equalization makes use of previous decisions in attempting to estimate the current symbol (with an SBS detector). Any "trailing" intersymbol interference caused by previous symbols is reconstructed and then subtracted. The DFE is inherently a nonlinear receiver. However, it can be analyzed using linear techniques, if one assumes all previous decisions are correct. There is both a MMSE and a zero-forcing version of decision feedback, and as was true with linear equalization in Sections 3.4 and 3.5, the zero-forcing solution will be a special case of the least-squares solution with the SNR→ ∞. Thus, this section derives the MMSE solution, which subsumes the zero-forcing case when SNR → ∞.

The Decision Feedback Equalizer (DFE) is shown in Figure 3.34. The configuration contains a linear feedforward equalizer, $W(D)$, (the settings for this linear equalizer are not necessarily the same as those for the ZFE or MMSE-LE), augmented by a linear, causal, feedback filter, $1 - B(D)$, where $b_0 = 1$. The feedback filter accepts as input the decision from the previous symbol period; thus, the name "decision feedback." The output of the feedforward filter is denoted $Z(D)$, and the input to the decision element $Z'(D)$. The feedforward filter will try to shape the channel output signal so that it is a causal signal. The feedback section will then subtract (without noise enhancement) any trailing ISI. Any bias removal in Figure 3.34 is absorbed into the SBS.

This section assumes that previous decisions are correct. In practice, this may not be true, and can be a significant weakness of decision-feedback that cannot be overlooked. Nevertheless, the analysis becomes intractable if it includes errors in the decision feedback section. To date, the most efficient way to specify the effect of feedback errors has often been via measurement. Section 3.7 provides an exact error-propagation analysis for finite-length DFE's that can (unfortunately) require enormous computation on a digital computer. Section 3.8.1 shows how to eliminate error propagation with precoders.

3.6.1 Minimum-Mean-Square-Error Decision Feedback Equalizer (MMSE-DFE)

The **Minimum-Mean-Square Error Decision Feedback Equalizer** (MMSE-DFE) jointly optimizes the settings of both the feedforward filter w_k and the feedback filter $\delta_k - b_k$ to minimize the MSE:

Definition 3.6.1 (Mean Square Error (for DFE)) *The* **MMSE-DFE error** *signal is*

$$e_k = x_k - z'_k \quad . \tag{3.208}$$

The MMSE *for the* MMSE-DFE *is*

$$\sigma^2_{MMSE-DFE} \overset{\Delta}{=} \min_{w_k, b_k} E\left[|x_k - z'_k|^2\right] \quad . \tag{3.209}$$

The error sequence can be written as

$$E(D) = X(D) - W(D) \cdot Y(D) - [1 - B(D)]X(D) = B(D) \cdot X(D) - W(D) \cdot Y(D) \quad . \tag{3.210}$$

For any fixed $B(D)$, $E[E(D)Y^*(D^{-*})] = 0$ to minimize MSE, which leads us to the relation

$$B(D) \cdot \bar{R}_{xy}(D) - W(D) \cdot \bar{R}_{yy}(D) = 0 \quad . \tag{3.211}$$

Thus,

$$W(D) = \frac{B(D)}{\|p\| \left(Q(D) + \frac{1}{\text{SNR}_{MFB}} \right)} = B(D) \cdot W_{\text{MMSE-LE}}(D) \quad , \tag{3.212}$$

for any $B(D)$ with $b_0 = 1$. (Also, $W(D) = W_{\text{MMSE-LE}}(D) \cdot B(D)$, a consequence of the linearity of the MMSE estimate, so that $E(D) = B(D) \cdot E_{\text{MMSE-LE}}(D)$)

The autocorrelation function for the error sequence with arbitrary monic $B(D)$ is

$$
\begin{aligned}
\bar{R}_{ee}(D) &= B(D)\bar{\mathcal{E}}_{\boldsymbol{x}}B^*(D^{-*}) - 2\Re\left\{ B(D)\bar{R}_{xy}(D)W^*(D^{-*}) \right\} + W(D)\bar{R}_{yy}(D)W^*(D^{-*}) && (3.213) \\
&= B(D)\bar{\mathcal{E}}_{\boldsymbol{x}}B^*(D^{-*}) - W(D)\bar{R}_{yy}(D)W^*(D^{-*}) && (3.214) \\
&= B(D)\bar{\mathcal{E}}_{\boldsymbol{x}}B^*(D^{-*}) - B(D)\frac{\bar{R}_{xy}(D)}{\|p\| \left(Q(D) + \frac{1}{\text{SNR}_{MFB}} \right)}B^*(D^{-*}) && (3.215) \\
&= B(D)R_{MMSE-LE}(D)B^*(D^{-*}) && (3.216)
\end{aligned}
$$

where $R_{MMSE-LE}(D) = \frac{\frac{\mathcal{N}_0}{2}}{\|p\|^2}1/(Q(D) + 1/\text{SNR}_{MFB})$ is the autocorrelation function for the error sequence of a MMSE linear equalizer. The solution for $B(D)$ is then the forward prediction filter associated with this error sequence as discussed in the Appendix. The linear prediction approach is developed more in what is called the "linear prediction DFE," in an exercise where the MMSE-DFE is the concatenation of a MMSE-LE and a linear-predictor that whitens the error sequence.

In more detail on $B(D)$, the (scaled) inverse autocorrelation has spectral factorization:

$$Q(D) + \frac{1}{\text{SNR}_{MFB}} = \gamma_0 \cdot G(D) \cdot G^*(D^{-*}), \tag{3.217}$$

where γ_0 is a positive real number and $G(D)$ is a canonical filter response. A filter response $G(D)$ is called **canonical** if it is **causal** ($g_k = 0$ for $k < 0$), **monic** ($g_0 = 1$), and **minimum-phase** (all its poles are outside the unit circle, and all its zeroes are on or outside the unit circle). If $G(D)$ is canonical, then $G^*(D^{-*})$ is **anti-canonical** i.e., anti-causal, monic, and "maximum-phase" (all poles inside the unit circle, and all zeros in or on the unit circle). Using this factorization,

$$
\begin{aligned}
\bar{R}_{ee}(D) &= \frac{B(D) \cdot B^*(D^{-*})}{Q(D) + 1/\text{SNR}_{MFB}} \cdot \frac{\frac{\mathcal{N}_0}{2}}{\|p\|^2} && (3.218) \\
&= \frac{B(D)}{G(D)} \cdot \frac{B^*(D^{-*})}{G^*(D^{-*})} \cdot \frac{\frac{\mathcal{N}_0}{2}}{\gamma_0\|p\|^2} && (3.219) \\
r_{ee,0} &\geq \frac{\frac{\mathcal{N}_0}{2}}{\gamma_0\|p\|^2} \quad , && (3.220)
\end{aligned}
$$

with equality if and only if $B(D) = G(D)$. Thus, the MMSE will then be $\sigma^2_{MMSE-DFE} = \frac{\frac{\mathcal{N}_0}{2}}{\gamma_0\|p\|^2}$. The feedforward filter then becomes

$$W(D) = \frac{G(D)}{\|p\| \cdot \gamma_0 \cdot G(D) \cdot G^*(D^{-*})} = \frac{1}{\|p\| \cdot \gamma_0 \cdot G^*(D^{-*})} \quad . \tag{3.221}$$

The last step in (3.220) follows from the observations that

$$r_{ee,0} = \|\frac{B}{G}\|^2 \frac{\frac{\mathcal{N}_0}{2}}{\gamma_0 \cdot \|p\|^2} \quad , \tag{3.222}$$

the fractional polynomial inside the squared norm is necessary monic and causal, and therefore the squared norm has a minimum value of 1. $B(D)$ and $W(D)$ specify the MMSE-DFE:

Lemma 3.6.1 (MMSE-DFE) *The MMSE-DFE has* **feedforward section**

$$W(D) = \frac{1}{\|p\| \cdot \gamma_0 \cdot G^*(D^{-*})} \tag{3.223}$$

(realized with delay, as it is strictly noncausal) and **feedback section**

$$B(D) = G(D) \tag{3.224}$$

where $G(D)$ is the unique canonical factor of the following equation:

$$Q(D) + \frac{1}{SNR_{MFB}} = \gamma_0 \cdot G(D) \cdot G^*(D^{-*}) \quad . \tag{3.225}$$

*This text also calls the joint matched-filter/sampler/$W(D)$ combination in the forward path of the DFE the "*__Mean-Square Whitened Matched Filter (MS-WMF)__*". These settings for the MMSE-DFE minimize the MSE as was shown above.*

3.6.2 Performance Analysis of the MMSE-DFE

Again, the autocorrelation function for the error sequence is

$$\bar{R}_{ee}(D) = \frac{\frac{\mathcal{N}_0}{2}}{\gamma_0 \cdot \|p\|^2} \quad . \tag{3.226}$$

This last result states that the error sequence for the MMSE-DFE is "white" when minimized (since $\bar{R}_{ee}(D)$ is a constant) and has MMSE or average energy (per real dimension) $\frac{\mathcal{N}_0}{\|p\|^2}\gamma_0^{-1}$. Also,

$$\frac{T}{2\pi} \int_{-\frac{\pi}{T}}^{\frac{\pi}{T}} \ln\left(Q(e^{-\jmath\omega T}) + \frac{1}{SNR_{MFB}}\right) d\omega = \ln(\gamma_0) + \frac{T}{2\pi} \int_{-\frac{\pi}{T}}^{\frac{\pi}{T}} \ln\left(G(e^{-\jmath\omega T})G^*(e^{-\jmath\omega T})\right) d\omega \tag{3.227}$$

$$= \ln(\gamma_0) \quad . \tag{3.228}$$

This last result leads to a famous expression for $\sigma^2_{MMSE-DFE}$, which was first derived by Salz in 1973,

$$\sigma^2_{MMSE-DFE} = \frac{\frac{\mathcal{N}_0}{2}}{\|p\|^2} \cdot e^{-\frac{T}{2\pi} \int_{-\frac{\pi}{T}}^{\frac{\pi}{T}} \ln\left(Q(e^{-\jmath\omega T}) + \frac{1}{SNR_{MFB}}\right) d\omega} \quad . \tag{3.229}$$

The SNR for the MMSE-DFE can now be easily computed as

$$SNR_{MMSE-DFE} = \frac{\bar{\mathcal{E}}_{\boldsymbol{x}}}{\sigma^2_{MMSE-DFE}} = \gamma_0 \cdot SNR_{MFB} \tag{3.230}$$

$$= SNR_{MFB} e^{\frac{T}{2\pi} \int_{-\frac{\pi}{T}}^{\frac{\pi}{T}} \ln\left(Q(e^{-\jmath\omega T}) + \frac{1}{SNR_{MFB}}\right) d\omega} \quad . \tag{3.231}$$

From the $k = 0$ term in the defining spectral factorization, γ_0 can also be written

$$\gamma_0 = \frac{1 + 1/SNR_{MFB}}{\|g\|^2} = \frac{1 + 1/SNR_{MFB}}{1 + \sum_{i=1}^{\infty} |g_i|^2} \quad . \tag{3.232}$$

From this expression, if $G(D) = 1$ (no ISI), then $SNR_{MMSE-DFE} = SNR_{MFB} + 1$, so that the SNR would be higher than the matched filter bound. The reason for this apparent anomaly is the artificial signal power introduced by biased decision regions. This bias is noted by writing

$$Z'(D) = X(D) - E(D) \tag{3.233}$$

$$= X(D) - G(D) \cdot X(D) + \frac{1}{\|p\| \cdot \gamma_0 \cdot G^*(D^{-*})} Y(D) \tag{3.234}$$

$$= X(D) - G(D)X(D) + \frac{Q(D)}{\gamma_0 G^*(D^{-*})} X(D) + N(D)\frac{1}{\|p\|\gamma_0 G^*(D^{-*})} \tag{3.235}$$

$$= X(D) - \frac{1/SNR_{MFB}}{\gamma_0 \cdot G^*(D^{-*})} X(D) + N(D)\frac{1}{\|p\| \cdot \gamma_0 \cdot G^*(D^{-*})} \quad . \tag{3.236}$$

The current sample, x_k, corresponds to the time zero sample of $1 - \frac{1/\text{SNR}_{MFB}}{\gamma_0 \cdot G^*(D^{-*})}$, and is equal to $(1 - \frac{1}{\text{SNR}_{MMSE-DFE}})x_k$. Thus z'_k contains a signal component of x_k that is reduced in magnitude. Thus, again using the result from Section 3.2.1, the SNR corresponding to the lowest probability of error corresponds to the same MMSE-DFE receiver with output scaled to remove the bias. This leads to the more informative SNR

$$\text{SNR}_{MMSE-DFE,U} = \text{SNR}_{MMSE-DFE} - 1 = \gamma_0 \cdot \text{SNR}_{MFB} - 1 \quad . \tag{3.237}$$

If $G(D) = 1$, then $\text{SNR}_{MMSE-DFE,U} = \text{SNR}_{MFB}$. Also,

$$\gamma_{MMSE-DFE} = \frac{\text{SNR}_{MFB}}{\text{SNR}_{MMSE-DFE,U}} = \frac{\text{SNR}_{MFB}}{\gamma_0 \cdot \text{SNR}_{MFB} - 1} = \frac{1}{\gamma_0 - 1/\text{SNR}_{MFB}} \quad . \tag{3.238}$$

Rather than scale the decision input, the receiver can scale (up) the feedforward output by $\frac{1}{1 - \frac{1}{\text{SNR}_{MMSE-DFE}}}$. This will remove the bias, but also increase MSE by the square of the same factor. The SNR will then be $\text{SNR}_{MMSE-DFE,U}$. This result is verified by writing the MS-WMF output

$$Z(D) = [X(D) \cdot \|p\| \cdot Q(D) + N(D)] \frac{1}{\|p\| \cdot \gamma_0 \cdot G^*(D^{-*})} \tag{3.239}$$

where $N(D)$, again, has autocorrelation $\bar{R}_{nn}(D) = \frac{N_0}{2}Q(D)$. $Z(D)$ expands to

$$Z(D) = [X(D) \cdot \|p\| \cdot Q(D) + N(D)] \frac{1}{\|p\| \cdot \gamma_0 \cdot G^*(D^{-*})} \tag{3.240}$$

$$= X(D)\frac{\gamma_0 \cdot G(D) \cdot G^*(D^{-*}) - 1/\text{SNR}_{MFB}}{\gamma_0 \cdot G^*(D^{-*})} + N(D)\frac{1}{\|p\| \cdot \gamma_0 \cdot G^*(D^{-*})} \tag{3.241}$$

$$= X(D) \cdot G(D) - \frac{X(D)}{\text{SNR}_{MFB} \cdot \gamma_0 \cdot G^*(D^{-*})} + N'(D) \tag{3.242}$$

$$= X(D)\left[G(D) - \frac{1}{\text{SNR}_{MMSE-DFE}}\right] + \frac{1}{\text{SNR}_{MMSE-DFE}}\left[1 - \frac{1}{G^*(D^{-*})}\right]X(D) + N'(D) \tag{3.243}$$

$$= X(D)\left[G(D) - \frac{1}{\text{SNR}_{MMSE-DFE}}\right] + E'(D) \quad , \tag{3.244}$$

where $N'(D)$ is the filtered noise at the MS-WMF output, and has autocorrelation function

$$\bar{R}_{n'n'}(D) = \frac{\frac{N_0}{2}Q(D)}{\|p\|^2 \cdot \gamma_0^2 \cdot G(D) \cdot G^*(D^{-*})} = \frac{\bar{\mathcal{E}}_{\boldsymbol{x}}}{\text{SNR}_{MMSE-DFE}}\left[1 - \frac{1/\text{SNR}_{MFB}}{Q(D) + 1/\text{SNR}_{MFB}}\right] \quad , \tag{3.245}$$

and

$$e'_k = -e_k + \frac{1}{\text{SNR}_{MMSE-DFE}}x_k \quad . \tag{3.246}$$

The error e'_k is not a white sequence in general. Since x_k and e'_k are uncorrelated, $\sigma_e^2 = \sigma_{MMSE-DFE}^2 = \sigma_{e'}^2 + \frac{\bar{\mathcal{E}}_{\boldsymbol{x}}}{\text{SNR}_{MMSE-DFE}^2}$. If one defines an "unbiased" monic, causal polynomial

$$G_U(D) = \frac{\text{SNR}_{MMSE-DFE}}{\text{SNR}_{MMSE-DFE,U}}\left[G(D) - \frac{1}{\text{SNR}_{MMSE-DFE}}\right] \quad , \tag{3.247}$$

then the MMSE-DFE output is

$$Z(D) = \frac{\text{SNR}_{MMSE-DFE,U}}{\text{SNR}_{MMSE-DFE}}X(D)G_U(D) + E'(D) \quad . \tag{3.248}$$

$Z_U(D)$ removes the scaling

$$Z_U(D) = Z(D)\frac{\text{SNR}_{MMSE-DFE}}{\text{SNR}_{MMSE-DFE,U}} = X(D)G_U(D) + E_U(D) \quad , \tag{3.249}$$
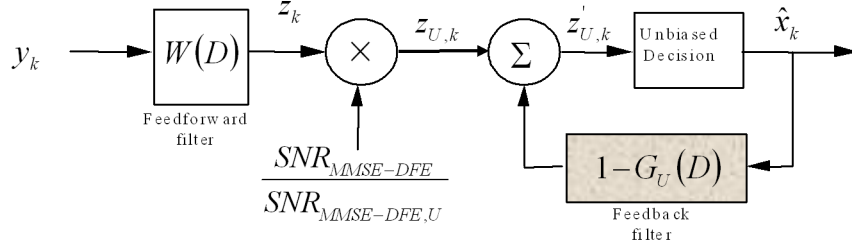
Figure 3.35: Decision feedback equalization with unbiased feedback filter.

where $E_U(D) = \frac{\text{SNR}_{MMSE-DFE}}{\text{SNR}_{MMSE-DFE,U}} E'(D)$ and has power

$$\sigma_{e_U}^2 = \left(\sigma_{MMSE-DFE}^2 - \frac{\bar{\mathcal{E}}_{\boldsymbol{x}}}{\text{SNR}_{MMSE-DFE}^2} \right) \left(\frac{\text{SNR}_{MMSE-DFE}}{\text{SNR}_{MMSE-DFE,U}} \right)^2 \tag{3.250}$$

$$= \frac{\text{SNR}_{MMSE-DFE}^2 \sigma_{MMSE-DFE}^2 - \bar{\mathcal{E}}_{\boldsymbol{x}}}{\text{SNR}_{MMSE-DFE}^2} \frac{\text{SNR}_{MMSE-DFE}^2}{\text{SNR}_{MMSE-DFE,U}^2} \tag{3.251}$$

$$= \frac{\bar{\mathcal{E}}_{\boldsymbol{x}}[(\text{SNR}_{MMSE-DFE}/\bar{\mathcal{E}}_{\boldsymbol{x}})\text{SNR}_{MMSE-DFE}\sigma_{MMSE-DFE}^2 - 1]}{\text{SNR}_{MMSE-DFE,U}^2} \tag{3.252}$$

$$= \frac{\bar{\mathcal{E}}_{\boldsymbol{x}}[\text{SNR}_{MMSE-DFE} - 1]}{\text{SNR}_{MMSE-DFE,U}^2} \tag{3.253}$$

$$= \frac{\bar{\mathcal{E}}_{\boldsymbol{x}}}{\text{SNR}_{MMSE-DFE,U}} \quad . \tag{3.254}$$

SNR for this scaled and unbiased MMSE-DFE is thus verified to be $\frac{\bar{\mathcal{E}}_{\boldsymbol{x}}}{\bar{\mathcal{E}}_{\boldsymbol{x}}/\text{SNR}_{MMSE-DFE,U}} = \text{SNR}_{MMSE-DFE,U}$.
The feedback section of this new unbiased MMSE-DFE becomes the polynomial $1 - G_U(D)$, if the scaling is performed before the summing junction, but is $1 - G(D)$ if scaling is performed after the summing junction. The alternative unbiased MMSE-DFE is shown in Figure 3.35.

All the results on fractional spacing for the LE still apply to the feedforward section of the DFE – thus this text does not reconsider them for the DFE, other than to state that the characteristic of the feedforward section is different than the LE characteristic in all but trivial channels. Again, the realization of any characteristic can be done with a matched filter and symbol-spaced sampling or with an anti-alias filter and fractionally spaced sampling, as in Section 3.5.4.

3.6.3 Zero-Forcing DFE

The ZF-DFE feedforward and feedback filters are found by setting $\text{SNR}_{MFB} \to \infty$ in the expressions for the MMSE-DFE. The spectral factorization (assuming $\ln(Q(e^{j\omega T})$ is integrable over $(-\frac{\pi}{T}, \frac{\pi}{T})$, see Appendix A)

$$Q(D) = \eta_0 \cdot P_c(D) \cdot P_c^*(D^{-*}) \tag{3.255}$$

then determines the ZF-DFE filters as

$$B(D) = P_c(D) \quad , \tag{3.256}$$

$$W(D) = \frac{1}{\eta_0 \cdot \|p\| \cdot P_c^*(D^{-*})} \quad . \tag{3.257}$$

P_c is sometimes called a **canonical pulse response** for the channel. Since $q_0 = 1 = \eta_0 \cdot \|P_c\|^2$, then

$$\eta_0 = \frac{1}{1 + \sum_{i=1}^{\infty} |p_{c,i}|^2} \quad . \tag{3.258}$$

Equation (3.258) shows that there is a signal power loss of the ratio of the squared first tap magnitude in the canonical pulse response to the squared norm of all the taps. This loss ratio is minimized for a minimum phase polynomial, and $P_c(D)$ is the minimum-phase equivalent of the channel pulse response. The noise at the output of the feedforward filter has (white) autocorrelation function $\frac{N_0}{2}/(\|p\|^2 \cdot \eta_0)$, so that

$$\sigma^2_{ZFDFE} = \frac{\frac{N_0}{2}}{\|p\|^2}\frac{1}{\eta_0} = \frac{\frac{N_0}{2}}{\|p\|^2}e^{-\frac{T}{2\pi}\int_{-\frac{\pi}{T}}^{\frac{\pi}{T}}\ln\left(Q(e^{j\omega T})\right)d\omega} \qquad . \tag{3.259}$$

The corresponding SNR is then

$$\mathrm{SNR}_{ZF-DFE} = \eta_0 \cdot \mathrm{SNR}_{MFB} = \frac{1}{1 + \sum_{i=1}^{\infty} p_{c,i}^2} \cdot \mathrm{SNR}_{MFB} \qquad . \tag{3.260}$$

3.6.4 Examples Revisited

EXAMPLE 3.6.1 (PAM - DFE) The pulse response of a channel used with binary PAM is again given by

$$P(\omega) = \left\{ \begin{array}{ll} \sqrt{T}\left(1 + .9e^{j\omega T}\right) & |\omega| \leq \frac{\pi}{T} \\ 0 & |\omega| > \frac{\pi}{T} \end{array} \right. \qquad . \tag{3.261}$$

Again, the SNR_{MFB} is 10dB and $\mathcal{E}_{\boldsymbol{x}} = 1$.

Then $\tilde{Q}(D) \triangleq Q(D) + 1/\mathrm{SNR}_{MFB}$ is computed as

$$\tilde{Q}(e^{-j\omega T}) = \frac{1.81 + 1.8\cos(\omega T) + 1.81/10}{1.81} \tag{3.262}$$

$$\tilde{Q}(D) = \frac{1}{1.81}(1 + .9D)(1 + .9D^{-1}) + .1 \tag{3.263}$$

$$= \frac{1}{1.81}\left(.9D + 1.991 + .9D^{-1}\right) \qquad . \tag{3.264}$$

The roots of $\tilde{Q}(D)$ are $-.633$ and -1.58. The function $\tilde{Q}(D)$ has canonical factorization

$$\tilde{Q}(D) = .785(1 + .633D)(1 + .633D^{-1}) \qquad . \tag{3.265}$$

Then, $\gamma_0 = .785$. The feedforward section is

$$W(D) = \frac{1}{\sqrt{1.81}(.785)(1 + .633D^{-1})} = \frac{.9469}{1 + .633D^{-1}} \qquad , \tag{3.266}$$

and the feedforward filter transfer function appears in Figure 3.36. The feedback section is

$$B(D) = G(D) = 1 + .633D \qquad , \tag{3.267}$$

with magnitude in Figure 3.37. The MS-WMF filter transfer function appears in Figure 3.38, illustrating the near all-pass character of this filter.

The MMSE is

$$\sigma^2_{MMSE-DFE} = \frac{N_0}{2}\frac{1}{\|p\|^2\gamma_0} = .\frac{.181}{1.81 \cdot .785} = .1274 \tag{3.268}$$

and

$$\mathrm{SNR}_{MMSE-DFE,U} = \frac{1 - .1274}{.1274} = 6.85 \ (8.4\mathrm{dB}) \qquad . \tag{3.269}$$

Thus, the MMSE-DFE is only 1.6dB below the MFB on this channel. However, the ZF-DFE for this same channel would produce $\eta_0 = 1/\|p_c\|^2 = .5525$. In this case $\sigma^2_{ZFDFE} = .181/(.5525)1.81 = .181$ and the loss with respect to the MFB would be $\eta_0 = 2.6$ dB, 1 dB lower than the MMSE-DFE for this channel.

It will in fact be possible to do yet better on this channel, using sequence detection, as discussed in Chapter 9, and/or by codes (Chapters 10 and 11). However, what originally appeared as a a stunning loss of 9.8 dB with the ZFE has now been reduced to a much smaller 1.6 dB.
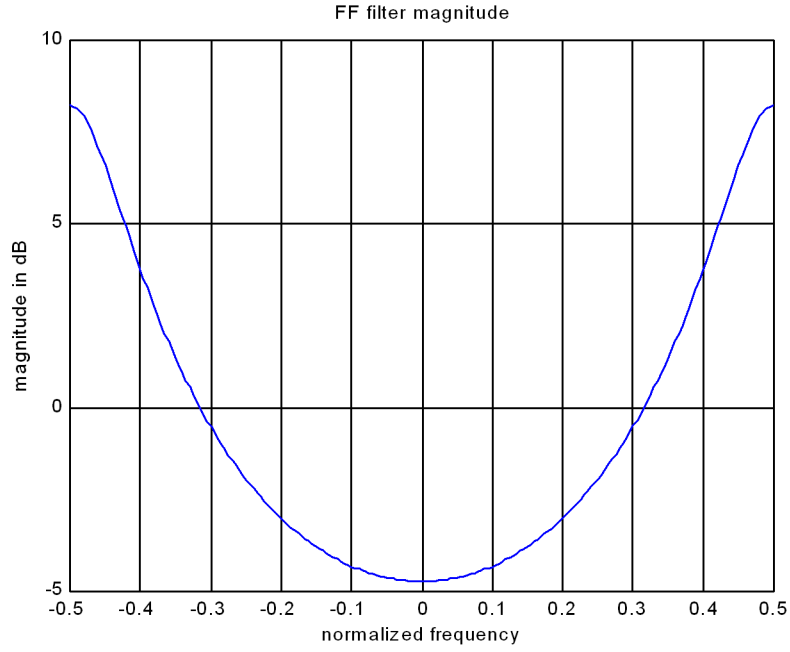
Figure 3.36: Feedforward filter transfer function for real-channel example.
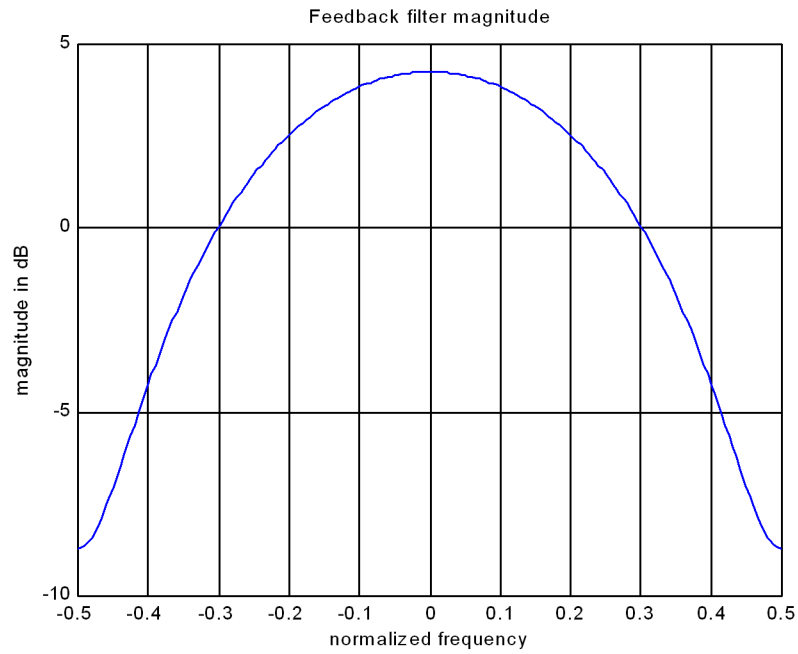
Figure 3.37: Feedback filter transfer function for real-channel example.
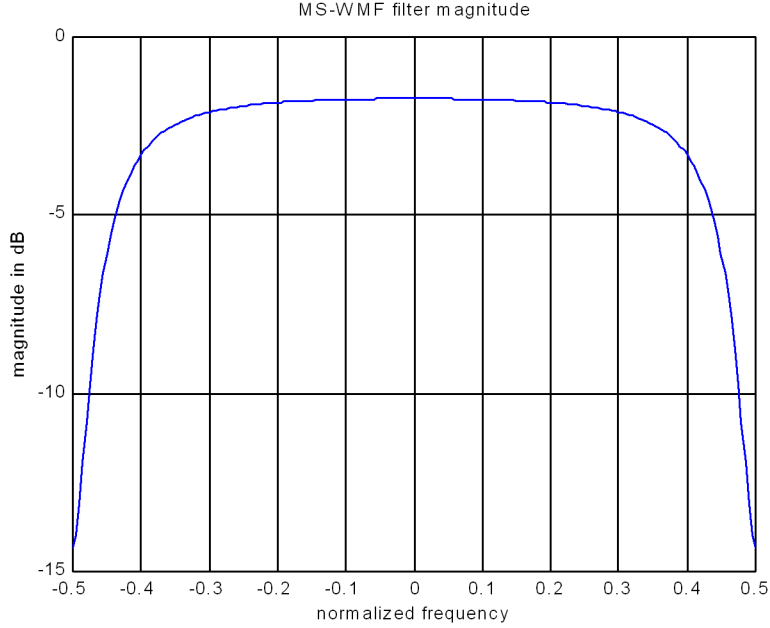
Figure 3.38: MS-WMF transfer function for real-channel example.

The QAM example is also revisited here:

EXAMPLE 3.6.2 (QAM - DFE) Recall that the equivalent baseband pulse response samples were given by

$$p_k = \frac{1}{\sqrt{T}} \left[-\frac{1}{2} \quad \left(1 + \frac{\jmath}{4}\right) \quad -\frac{\jmath}{2} \right] \quad . \tag{3.270}$$

The SNR_{MFB} is again 10 dB. Then,

$$\tilde{Q} = \frac{-.25\jmath D^{-2} + .625(-1+\jmath)D^{-1} + 1.5625(1+.1) - .625(1+\jmath)D + .25\jmath D^2}{1.5625} \quad . \tag{3.271}$$

or

$$\tilde{Q} = (1 - .451\angle^{1.632}D)(1 - .451\angle^{-.0612}D)(1 - .451\angle^{-1.632}D^{-1})(1 - .451\angle^{.0612}D^{-1}) \cdot$$
$$\cdot \frac{-\jmath}{1.5625 \cdot 4 \cdot (.451\angle^{-1.632})(.451\angle^{.0612})} \tag{3.272}$$

from which one extracts $\gamma_0 = .7866$ and $G(D) = 1 - .4226(1+\jmath)D + .2034\jmath D^2$. The feedforward and feedback sections can be computed in a straightforward manner, as

$$B(D) = G(D) = 1 - .4226(1+\jmath)D + .2034\jmath D^2 \tag{3.273}$$

and

$$W(D) = \frac{1.017}{1 - .4226(1-\jmath)D^{-1} - .2034\jmath D^{-2}} \quad . \tag{3.274}$$

The MSE is

$$\sigma^2_{MMSE-DFE} = (.15625)\frac{1}{.7866(1.5625)} = .1271 \quad . \tag{3.275}$$

and the corresponding SNR is

$$\text{SNR}_{MMSE-DFE,U} = \frac{1}{.1271} - 1 = 8.4\text{dB} \quad . \tag{3.276}$$

205

The loss is (also coincidentally) 1.6 dB with respect to the MFB and is 1.7 dB better than the MMSE-LE on this channel.

For the ZF-DFE,

$$Q(D) = (1 - .5\angle^{\pi/2}D)(1 - .5D)(1 - .5\angle^{-\pi/2}D^{-1})(1 - .5D^{-1}) \cdot \qquad (3.277)$$

$$\cdot \frac{-\jmath}{1.5625 \cdot 4 \cdot (.5\angle^{-\pi/2})(.5)} \qquad (3.278)$$

and thus $\eta_0 = .6400$ and $P_c(D) = 1 - .5(1 + \jmath)D + .25\jmath D^2$. The feedforward and feedback sections can be computed in a straightforward manner, as

$$B(D) = P_c(D) = 1 - .5(1 + \jmath)D + .25\jmath D^2 \qquad (3.279)$$

and

$$W(D) = \frac{1.25}{1 - .5(1 - \jmath)D^{-1} - .25\jmath D^{-2}} \quad . \qquad (3.280)$$

The output noise variance is

$$\sigma^2_{ZFDFE} = (.15625)\frac{1}{.6400(1.5625)} = .1563 \quad . \qquad (3.281)$$

and the corresponding SNR is

$$\text{SNR}_{ZFDFE} = \frac{1}{.1563} = 6.4 = 8.0\text{dB} \quad . \qquad (3.282)$$

The loss is 2.0 dB with respect to the MFB and is .4 dB worse than the MMSE-DFE.
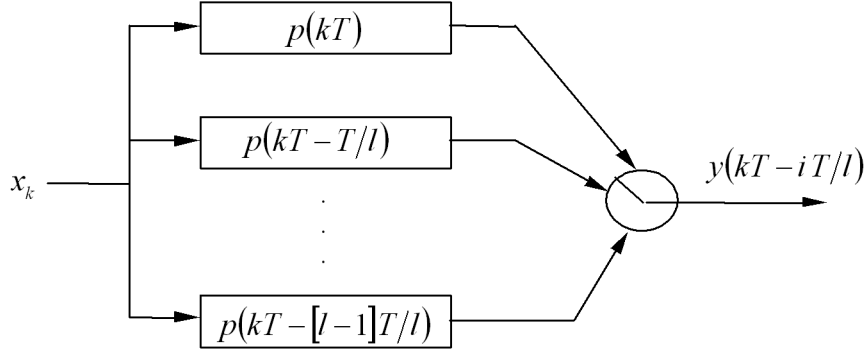
Figure 3.39: Polyphase subchannel representation of the channel pulse response.

3.7 Finite Length Equalizers

The previous developments of discrete-time equalization structures presumed that the equalizer could exist over an infinite interval in time. Equalization filters, w_k, are almost exclusively realized as finite-impulse-response (FIR) filters in practice. Usually these structures have better numerical properties than IIR structures. Even more importantly, adaptive equalizers (see Section 3.8 and Chapter 13) are often implemented with FIR structures for w_k (and also for b_k, in the case of the adaptive DFE). This section studies the design of and the performance analysis of FIR equalizers.

Both the LE and the DFE cases are examined for both zero-forcing and least-squares criteria. This section describes design for the MMSE situation and then lets SNR$\to \infty$ to get the zero-forcing special case. Because of the finite length, the FIR zero-forcing equalizer cannot completely eliminate ISI in general.

3.7.1 FIR MMSE-LE

Returning to the FSE in Figure 3.32, the matched filtering operation will be performed digitally (at sampling rate l/T) and the FIR MMSE-LE will then incorporate both matched filtering and equalization. Perfect anti-alias filtering with gain $\sqrt{T}$ precedes the sampler and the combined pulse-response/anti-alias filter is $\tilde{p}(t)$. The assumption that l is an integer simplifies the specification of matrices.

One way to view the oversampled channel output is as a set of l parallel T-spaced subchannels whose pulse responses are offset by T/l from each other as in Figure 3.39. Each subchannel produces one of the l phases per symbol period of the output set of samples at sampling rate l/T. Mathematically, it is convenient to represent such a system with vectors as shown below.

The channel output $y(t)$ is

$$y(t) = \sum_m x_m \cdot \tilde{p}(t - mT) + n(t) \quad , \tag{3.283}$$

which, if sampled at time instants $t = kT - \frac{iT}{l}$, $i = 0, ..., l-1$, becomes

$$y(kT - \frac{iT}{l}) = \sum_{m=-\infty}^{\infty} x_m \cdot \tilde{p}(kT - \frac{iT}{l} - mT) + n(kT - \frac{iT}{l}) \quad . \tag{3.284}$$

The (per-dimensional) variance of the noise samples is $\frac{N_0}{2} \cdot l$ because the gain of the anti-alias filter, $\sqrt{T}$, is absorbed into $p(t)$. The l phases per symbol period of the oversampled $y(t)$ are contained in

$$\boldsymbol{y}_k = \begin{bmatrix} y(kT) \\ y(kT - \frac{T}{l}) \\ \vdots \\ y(kT - \frac{l-1}{l}T) \end{bmatrix} \quad . \tag{3.285}$$

The vector $\boldsymbol{y}_k$ can be written as

$$\boldsymbol{y}_k = \sum_{m=-\infty}^{\infty} x_m \cdot \boldsymbol{p}_{k-m} + \boldsymbol{n}_k = \sum_{m=-\infty}^{\infty} x_{k-m} \cdot \boldsymbol{p}_m + \boldsymbol{n}_k \quad , \tag{3.286}$$

where

$$\boldsymbol{p}_k = \begin{bmatrix} \tilde{p}(kT) \\ \tilde{p}(kT - \frac{T}{l}) \\ \vdots \\ \tilde{p}(kT - \frac{l-1}{l}T) \end{bmatrix} \quad \text{and} \quad \boldsymbol{n}_k = \begin{bmatrix} n(kT) \\ n(kT - \frac{T}{l}) \\ \vdots \\ n(kT - \frac{l-1}{l}T) \end{bmatrix} \tag{3.287}$$

The response $\tilde{p}(t)$ is assumed to extend only over a finite time interval. In practice, this assumption requires any nonzero component of $p(t)$ outside of this time interval to be negligible. This time interval is $0 \le t \le \nu T$. Thus, $\boldsymbol{p}_k = 0$ for $k < 0$, and for $k > \nu$. The sum in (3.284) becomes

$$\boldsymbol{y}_k = [\, \boldsymbol{p}_0 \ \boldsymbol{p}_1 \,, ..., \boldsymbol{p}_\nu \,] \begin{bmatrix} x_k \\ x_{k-1} \\ \vdots \\ \vdots \\ x_{k-\nu} \end{bmatrix} + \boldsymbol{n}_k \quad . \tag{3.288}$$

Each row in (3.288) corresponds to a sample at the output of one of the filters in Figure 3.39. More generally, for N_f successive l-tuples of samples of $y(t)$,

$$\boldsymbol{Y}_k \triangleq \begin{bmatrix} \boldsymbol{y}_k \\ \boldsymbol{y}_{k-1} \\ \vdots \\ \boldsymbol{y}_{k-N_f+1} \end{bmatrix} \tag{3.289}$$

$$= \begin{bmatrix} \boldsymbol{p}_0 & \boldsymbol{p}_1 & \cdots & \boldsymbol{p}_\nu & 0 & 0 & \cdots & 0 \\ 0 & \boldsymbol{p}_0 & \boldsymbol{p}_1 & \cdots & \cdots & \boldsymbol{p}_\nu & \cdots & 0 \\ \vdots & \vdots & \ddots & \ddots & \ddots & \ddots & \vdots \\ 0 & \cdots & 0 & 0 & \boldsymbol{p}_0 & \boldsymbol{p}_1 & \cdots & \boldsymbol{p}_\nu \end{bmatrix} \begin{bmatrix} x_k \\ x_{k-1} \\ \vdots \\ \vdots \\ x_{k-N_f-\nu+1} \end{bmatrix}$$

$$+ \begin{bmatrix} \boldsymbol{n}_k \\ \boldsymbol{n}_{k-1} \\ \vdots \\ \boldsymbol{n}_{k-N_f+1} \end{bmatrix} \quad . \tag{3.290}$$

This text uses $\boldsymbol{P}$ to denote the large $(N_f \cdot l) \times (N_f + \nu)$ matrix in (3.290), while $\boldsymbol{X}_k$ denotes the data vector, and $\boldsymbol{N}$ denotes the noise vector. Then, the oversampled vector representation of the channel is

$$\boldsymbol{Y}_k = \boldsymbol{P}\boldsymbol{X}_k + \boldsymbol{N}_k \quad . \tag{3.291}$$

When $l = n/m$ (a rational fraction), then (3.291) still holds with $\boldsymbol{P}$ an $[N_f \cdot \frac{n}{m}] \times (N_f + \nu)$ matrix that does not follow the form in (3.290), with each row possibly having a set of coefficients unrelated to the other rows.[11]

An equalizer is applied to the sampled channel output vector $\boldsymbol{Y}_k$ by taking the inner product of an $N_f l$-dimensional row vector of equalizer coefficients, $\boldsymbol{w}$, and $\boldsymbol{Y}_k$, so $Z(D) = W(D)Y(D)$ can be written

$$z_k = \boldsymbol{w}\boldsymbol{Y}_k \quad . \tag{3.292}$$

---

[11]In this case, (3.283) is used to compute each row at the appropriate sampling instants. $N_f \cdot \frac{n}{m}$ should also be an integer so that $\boldsymbol{P}$ is constant. Otherwise, $\boldsymbol{P}$ becomes a "time-varying" matrix $\boldsymbol{P}_k$.

For causality, the designer picks a channel-equalizer system delay $\Delta \cdot T$ symbol periods,

$$\Delta \approx \frac{\nu + N_f}{2} \quad , \tag{3.293}$$

with the exact value being of little consequence unless the equalizer length N_f is very short. The delay is important in finite-length design because a non-causal filter cannot be implemented, and the delay allows time for the transmit data symbol to reach the receiver. With infinite-length filters, the need for such a delay does not enter the mathematics because the infinite-length filters are not realizable in any case, so that infinite-length analysis simply provides best bounds on performance. Δ is approximately the sum of the channel and equalizer delays in symbol periods. The equalizer output error is then

$$e_k = x_{k-\Delta} - z_k \quad , \tag{3.294}$$

and the corresponding MSE is

$$\sigma^2_{MMSE-LE} = E\left\{|e_k|^2\right\} = E\left\{e_k e_k^*\right\} = E\left\{(x_{k-\Delta} - z_k)(x_{k-\Delta} - z_k)^*\right\} \quad . \tag{3.295}$$

Using the Orthogonality Principle of Appendix A, the MSE in (3.295) is minimized when

$$E\left\{e_k \boldsymbol{Y}_k^*\right\} = 0 \quad . \tag{3.296}$$

In other words, the equalizer error signal will be minimized (in the mean square sense) when this error is uncorrelated with any channel output sample in the delay line of the FIR MMSE-LE. Thus

$$E\left\{x_{k-\Delta}\,\boldsymbol{Y}_k^*\right\} - \boldsymbol{w}E\left\{\boldsymbol{Y}_k\boldsymbol{Y}_k^*\right\} = 0 \quad . \tag{3.297}$$

The two statistical correlation quantities in (3.297) have a very special significance (both $y(t)$ and x_k are stationary):

Definition 3.7.1 (Autocorrelation and Cross-Correlation Matrices) *The* **FIR MMSE autocorrelation matrix** *is defined as*

$$\boldsymbol{R_{YY}} \triangleq E\left\{\boldsymbol{Y}_k\boldsymbol{Y}_k^*\right\}/N \quad , \tag{3.298}$$

while the **FIR MMSE-LE cross-correlation vector** *is defined by*

$$\boldsymbol{R_{Y}}_x \triangleq E\left\{\boldsymbol{Y}_k x_{k-\Delta}^*\right\}/N \quad , \tag{3.299}$$

where $N = 1$ for real and $N = 2$ for complex. Note $\boldsymbol{R}_{x\boldsymbol{Y}} = \boldsymbol{R}_{\boldsymbol{Y}x}^*$, and $\boldsymbol{R_{YY}}$ is not a function of Δ.

With the above definitions in (3.297), the designer obtains the MMSE-LE:

Definition 3.7.2 (FIR MMSE-LE) *The FIR MMSE-LE for sampling rate l/T, delay Δ, and of length N_f symbol periods has coefficients*

$$\boldsymbol{w} = \boldsymbol{R}_{\boldsymbol{Y}x}^* \boldsymbol{R_{YY}}^{-1} = \boldsymbol{R}_{x\boldsymbol{Y}} \boldsymbol{R_{YY}}^{-1} \quad , \tag{3.300}$$

or equivalently,

$$\boldsymbol{w}^* = \boldsymbol{R_{YY}}^{-1} \boldsymbol{R}_{\boldsymbol{Y}x} \quad . \tag{3.301}$$

In general, it may be of interest to derive more specific expressions for $\boldsymbol{R_{YY}}$ and $\boldsymbol{R}_{x\boldsymbol{Y}}$.

$$
\begin{aligned}
\boldsymbol{R}_{x\boldsymbol{Y}} &= \overline{E\left\{x_{k-\Delta}\boldsymbol{Y}_k^*\right\}} = \overline{E\left\{x_{k-\Delta}\boldsymbol{X}_k^*\right\}}\boldsymbol{P}^* + \overline{E\left\{x_{k-\Delta}\boldsymbol{N}_k^*\right\}} & \tag{3.302}\\
&= \left[\,0\,...\,0\,\bar{\mathcal{E}}_{\boldsymbol{x}}\,0\,...\,0\,\right]\boldsymbol{P}^* + 0 & \tag{3.303}\\
&= \bar{\mathcal{E}}_{\boldsymbol{x}}\left[\,0\,...\,0\,\boldsymbol{p}_\nu^*\,...\,\boldsymbol{p}_0^*\,0\,...\,0\,\right] & \tag{3.304}
\end{aligned}
$$

$$\boldsymbol{R_{YY}} \quad = \quad \overline{E\left\{\boldsymbol{Y}_k\boldsymbol{Y}_k^*\right\}} = \boldsymbol{P}\overline{E\left\{\boldsymbol{X}_k\boldsymbol{X}_k^*\right\}}\boldsymbol{P}^* + \overline{E\left\{\boldsymbol{N}_k\boldsymbol{N}_k^*\right\}} \tag{3.305}$$

$$= \quad \bar{\mathcal{E}}_{\boldsymbol{x}}\boldsymbol{P}\boldsymbol{P}^* + l \cdot \frac{\mathcal{N}_0}{2} \cdot \boldsymbol{R_{nn}} \quad , \tag{3.306}$$

where the ($l \cdot \frac{\mathcal{N}_0}{2}$-normalized) noise autocorrelation matrix $\boldsymbol{R_{nn}}$ is equal to I when the noise is white. A convenient expression is

$$[0...0\ \boldsymbol{p}_\nu^*...\boldsymbol{p}_0^*\ 0...0] = \boldsymbol{1}_\Delta^*\boldsymbol{P}^* \quad , \tag{3.307}$$

so that $\boldsymbol{1}_\Delta$ is an $N_f + \nu$-vector of 0's and a 1 in the $(\Delta+1)^{th}$ position. Then the FIR MMSE-LE becomes (in terms of $\boldsymbol{P}$, SNR and Δ)

$$\boldsymbol{w} = \boldsymbol{1}_\Delta^*\boldsymbol{P}^*\left[\boldsymbol{P}\boldsymbol{P}^* + \frac{1}{\text{SNR}}\boldsymbol{R_{nn}}\right]^{-1} = \boldsymbol{1}_\Delta^*\left[\boldsymbol{P}^*\boldsymbol{R_{nn}^{-1}}\boldsymbol{P} + \frac{l}{\text{SNR}}\cdot I\right]^{-1}\boldsymbol{P}^*\boldsymbol{R_{nn}^{-1}} \quad . \tag{3.308}$$

The matrix inversion lemma of Appendix B is used in deriving the above equation.

The position of the nonzero elements in (3.304) depend on the choice of Δ. The MMSE, $\sigma^2_{MMSE-LE}$, can be found by evaluating (3.295) with (3.300):

$$\sigma^2_{MMSE-LE} \quad = \quad \overline{E\left\{x_{k-\Delta}x_{k-\Delta}^* - x_{k-\Delta}\boldsymbol{Y}_k^*\boldsymbol{w}^* - \boldsymbol{w}\boldsymbol{Y}_kx_{k-\Delta}^* + \boldsymbol{w}\boldsymbol{Y}_k\boldsymbol{Y}_k^*\boldsymbol{w}^*\right\}} \tag{3.309}$$

$$= \quad \bar{\mathcal{E}}_{\boldsymbol{x}} - \boldsymbol{R}_{x\boldsymbol{Y}}\boldsymbol{w}^* - \boldsymbol{w}\boldsymbol{R}_{\boldsymbol{Y}x} + \boldsymbol{w}\boldsymbol{R_{YY}}\boldsymbol{w}^* \tag{3.310}$$

$$= \quad \bar{\mathcal{E}}_{\boldsymbol{x}} - \boldsymbol{w}\boldsymbol{R_{YY}}\boldsymbol{w}^* \tag{3.311}$$

$$= \quad \bar{\mathcal{E}}_{\boldsymbol{x}} - \boldsymbol{R}_{x\boldsymbol{Y}}\boldsymbol{R_{YY}^{-1}}\boldsymbol{R}_{\boldsymbol{Y}x} \tag{3.312}$$

$$= \quad \bar{\mathcal{E}}_{\boldsymbol{x}} - \boldsymbol{w}\boldsymbol{R}_{\boldsymbol{Y}x} \quad , \tag{3.313}$$

With algebra, (3.313) is the same as

$$\sigma^2_{MMSE-LE} = \overline{\frac{l \cdot \frac{\mathcal{N}_0}{2}}{\|p\|^2}\boldsymbol{1}_\Delta^*\left(\frac{\boldsymbol{P}^*\boldsymbol{R_{nn}^{-1}}\boldsymbol{P}}{\|p\|^2} + \frac{l}{\text{SNR}_{MFB}}I\right)^{-1}\boldsymbol{1}_\Delta} = \frac{l \cdot \frac{\mathcal{N}_0}{2}}{\|p\|^2}\boldsymbol{1}_\Delta^*\bar{Q}^{-1}\boldsymbol{1}_\Delta \quad , \tag{3.314}$$

so that the best value of Δ (the position of the 1 in the vectors above) corresponds to the smallest diagonal element of the inverted ("Q-tilde") matrix in (3.314) – this means that only one matrix need be inverted to obtain the correct Δ value as well as compute the equalizer settings. A homework problem develops some interesting relationships for $\boldsymbol{w}$ in terms of $\boldsymbol{P}$ and SNR. Thus, the SNR for the FIR MMSE-LE is

$$\text{SNR}_{MMSE-LE} = \frac{\bar{\mathcal{E}}_{\boldsymbol{x}}}{\sigma^2_{MMSE-LE}} \quad , \tag{3.315}$$

and the corresponding unbiased SNR is

$$\text{SNR}_{MMSE-LE,U} = \text{SNR}_{MMSE-LE} - 1 \quad . \tag{3.316}$$

The loss with respect to the MFB is, again,

$$\gamma_{MMSE-LE} = \frac{\text{SNR}_{MFB}}{\text{SNR}_{MMSE-LE,U}} \quad . \tag{3.317}$$

3.7.2 FIR ZFE

One obtains the FIR ZFE by letting the SNR$\to \infty$ in the FIR MMSE, which alters $\boldsymbol{R_{YY}}$ to

$$\boldsymbol{R_{YY}} = \boldsymbol{P}\boldsymbol{P}^*\bar{\mathcal{E}}_{\boldsymbol{x}} \tag{3.318}$$

and then $\boldsymbol{w}$ remains as

$$\boldsymbol{w} = \boldsymbol{R}_{x\boldsymbol{Y}}\boldsymbol{R_{YY}^{-1}} \quad . \tag{3.319}$$

Because the FIR equalizer may not be sufficiently long to cancel all ISI, the FIR ZFE may still have nonzero residual ISI. This ISI power is given by

$$\sigma^2_{MMSE-ZFE} = \bar{\mathcal{E}}_{\boldsymbol{x}} - \boldsymbol{w}\boldsymbol{R}_{\boldsymbol{Y}_x} \quad . \tag{3.320}$$

However, (3.320) still ignores the enhanced noise at the FIR ZFE output.[12] The power of this noise is easily found to be

$$\text{FIR ZFE noise power} = \frac{\mathcal{N}_0}{2} \cdot l \cdot \|\boldsymbol{w}\|^2_{\boldsymbol{R_{nn}}} \quad , \tag{3.321}$$

making the SNR at the ZFE output

$$\text{SNR}_{ZFE} = \frac{\bar{\mathcal{E}}_{\boldsymbol{x}}}{\bar{\mathcal{E}}_{\boldsymbol{x}} - \boldsymbol{w}\boldsymbol{R}_{\boldsymbol{Y}_x} + \frac{\mathcal{N}_0}{2}l\|\boldsymbol{w}\|^2_{\boldsymbol{R_{nn}}}} \quad . \tag{3.322}$$

The ZFE is still unbiased in the finite-length case:[13]

$$\begin{aligned}
E\left[\boldsymbol{w}\boldsymbol{Y}_k/x_{k-\Delta}\right] &= \boldsymbol{R}_{\boldsymbol{x}\boldsymbol{Y}}\boldsymbol{R}^{-1}_{\boldsymbol{Y}\boldsymbol{Y}}\left\{\boldsymbol{P}E\left[\boldsymbol{X}_k/x_{k-\Delta}\right] + E[\boldsymbol{N}_k]\right\} \tag{3.323}\\
&= [0\,0\,...1\,0]E\left\{\boldsymbol{P}^*(\boldsymbol{P}\boldsymbol{P}^*)^{-1}\boldsymbol{P}\boldsymbol{X}_k/x_{k-\Delta}\right\} \tag{3.324}\\
&= [0\,0\,...1\,0]\boldsymbol{P}^*(\boldsymbol{P}\boldsymbol{P}^*)^{-1}\boldsymbol{P}E\left\{\begin{bmatrix} x_k \\ x_{k-1} \\ \vdots \\ x_{k-N_f} \\ \text{don't care} \end{bmatrix}/x_{k-\Delta}\right\} \tag{3.325}\\
&= x_{k-\Delta} \quad . \tag{3.326}
\end{aligned}$$

Equation (3.326) is true if Δ is a practical value and the finite-length ZFE has enough taps. The loss is the ratio of the SNR to SNR_{ZFE},

$$\gamma\text{ZFE} = \frac{\text{SNR}_{MFB}}{\text{SNR}_{ZFE}} \quad . \tag{3.327}$$

3.7.3 example

For the earlier PAM example, one notes that sampling with $l = 1$ is sufficient to represent all signals. First, choose $N_f = 3$ and note that $\nu=1$. Then

$$\boldsymbol{P} = \begin{bmatrix} .9 & 1 & 0 & 0 \\ 0 & .9 & 1 & 0 \\ 0 & 0 & .9 & 1 \end{bmatrix} \quad . \tag{3.328}$$

With a choice of $\Delta = 2$, then

$$\boldsymbol{R}_{\boldsymbol{Y}_x} = \bar{\mathcal{E}}_{\boldsymbol{x}}\boldsymbol{P}\begin{bmatrix} 0 \\ 0 \\ 1 \\ 0 \end{bmatrix} \tag{3.329}$$

$$= \begin{bmatrix} 0 \\ 1 \\ .9 \end{bmatrix} \quad , \tag{3.330}$$

---

[12]The notation $\|\boldsymbol{w}\|^2_{\boldsymbol{R_{nn}}}$ means $\boldsymbol{w}\boldsymbol{R_{nn}}\boldsymbol{w}^*$.

[13]The matrix $P^*(PP^*)^{-1}P$ is a "projection matrix" and PP^* is full rank; therefore the entry of $x_{k-\Delta}$ passes directly (or is zeored, in which case Δ needs to be changed).
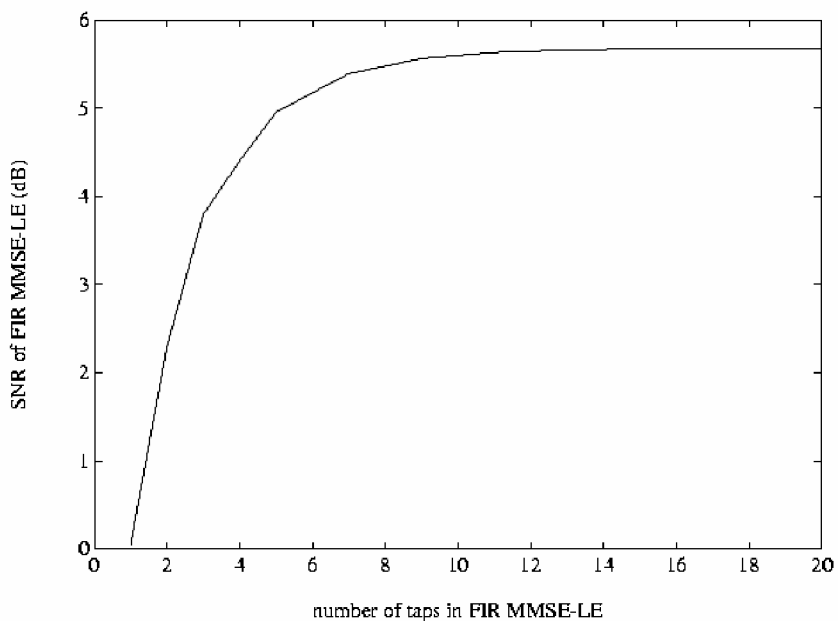
Figure 3.40: FIR equalizer performance for $1 + .9D^{-1}$ versus number of equalizer taps.

and

$$
\boldsymbol{R_{YY}} \;\; = \;\; \bar{\mathcal{E}}_{\boldsymbol{x}} \left(\boldsymbol{PP^*} + \frac{1}{\text{SNR}} I \right) \tag{3.331}
$$

$$
= \;\; \begin{bmatrix} 1.991 & .9 & 0 \\ .9 & 1.991 & .9 \\ 0 & .9 & 1.991 \end{bmatrix} \;\;, \tag{3.332}
$$

The FIR MMSE is

$$
\boldsymbol{w}^* = \boldsymbol{R_{YY}^{-1} R_{Y}}_x = \begin{bmatrix} .676 & -.384 & .174 \\ -.384 & .849 & -.384 \\ .174 & -.384 & .676 \end{bmatrix} \begin{bmatrix} 0 \\ 1 \\ .9 \end{bmatrix} = \begin{bmatrix} -.23 \\ .51 \\ .22 \end{bmatrix} \tag{3.333}
$$

Then

$$
\sigma^2_{MMSE-LE} = \left(1 - [-.23\ .51\ .22] \begin{bmatrix} 0 \\ 1 \\ .9 \end{bmatrix} \right) = .294 \tag{3.334}
$$

The SNR is computed to be

$$
\text{SNR}_{MMSE-LE,U} = \frac{1}{.294} - 1 = 2.4\ (3.8\text{ dB}) \;\;. \tag{3.335}
$$

which is 6.2dB below MFB performance and 1.9dB worse than the infinite length MMSE-LE for this channel.

With sufficiently large number of taps for this channel, the infinite length performance level can be attained. This performance is plotted as versus the number of equalizer taps in Figure 3.40. Clearly, 15 taps are sufficient for infinite-length performance.

EXAMPLE 3.7.1 For the earlier complex QAM example, sampling with $l = 1$ is sufficient

212

to represent all signals. First, choose $N_f = 4$ and note that $\nu = 2$. Then

$$
\boldsymbol{P} = \begin{bmatrix}
-.5 & 1 + \jmath/4 & -\jmath/2 & 0 & 0 & 0 \\
0 & -.5 & 1 + \jmath/4 & -\jmath/2 & 0 & 0 \\
0 & 0 & -.5 & 1 + \jmath/4 & -\jmath/2 & 0 \\
0 & 0 & 0 & -.5 & 1 + \jmath/4 & -\jmath/2
\end{bmatrix} \quad .
\tag{3.336}
$$

The matrix $(\boldsymbol{P}^* \boldsymbol{P} + .15625 \cdot \boldsymbol{I})^{-1}$ has the same smallest element 1.3578 for both $\Delta = 2, 3$, so choosing $\Delta = 2$ will not unnecessarily increase system delay. With a choice of $\Delta = 2$, then

$$
\boldsymbol{R_{Y}}_x \;=\; \bar{\mathcal{E}}_x \boldsymbol{P} \begin{bmatrix} 0 \\ 0 \\ 1 \\ 0 \\ 0 \\ 0 \end{bmatrix}
\tag{3.337}
$$

$$
= \begin{bmatrix} -.5\jmath \\ 1 + \jmath/4 \\ -.5 \\ 0 \end{bmatrix} \quad,
\tag{3.338}
$$

and

$$
\boldsymbol{R_{YY}} \;=\; \bar{\mathcal{E}}_x \left(\boldsymbol{P}\boldsymbol{P}^* + \frac{1}{\text{SNR}} \boldsymbol{I} \right)
\tag{3.339}
$$

$$
= \begin{bmatrix}
1.7188 & -0.6250 - 0.6250\jmath & \jmath/4 & 0 \\
-0.6250 + 0.6250\jmath & 1.7188 & -0.6250 - 0.6250\jmath & \jmath/4 \\
-\jmath/4 & -0.6250 + 0.6250\jmath & 1.7188 & -0.6250 - 0.6250\jmath \\
0 & -\jmath/4 & -0.6250 + 0.6250\jmath & 1.7188
\end{bmatrix} \quad .
$$

The FIR MMSE is

$$
\boldsymbol{w}^* = \boldsymbol{R_{YY}^{-1}} \boldsymbol{R_{Y}}_x = \begin{bmatrix} 0.2570 - 0.0422\jmath \\ 0.7313 - 0.0948\jmath \\ -0.1182 - 0.2982\jmath \\ -0.1376 + 0.0409\jmath \end{bmatrix} \quad .
\tag{3.340}
$$

Then

$$
\sigma^2_{MMSE-LE} \;=\; (1 - \boldsymbol{w}\boldsymbol{R_{Y}}_x)
\tag{3.341}
$$

$$
= \;.2121 \quad .
\tag{3.342}
$$

The SNR is computed to be

$$
\text{SNR}_{MMSE-LE,U} = \frac{1}{.2121} - 1 = 3.714 \; (5.7 \text{ dB}) \quad,
\tag{3.343}
$$

which is 4.3 dB below MFB performance and 2.1 dB worse than the infinite-length MMSE-LE for this channel. With sufficiently large number of taps for this channel, the infinite-length performance level can be attained.

3.7.4   FIR MMSE-DFE

The FIR DFE case is similar to the feed-forward equalizers just discussed, except that we now augment the fractionally spaced feed-forward section with a symbol-spaced feedback section. The MSE for the DFE case, as long as $\boldsymbol{w}$ and $\boldsymbol{b}$ are sufficiently long, is

$$
MSE = E\left\{ |x_{k-\Delta} - \boldsymbol{w}\boldsymbol{Y}_k + \boldsymbol{b}x_{k-\Delta-1}|^2 \right\} \quad,
\tag{3.344}
$$

where $\boldsymbol{b}$ is the vector of coefficients for the feedback FIR filter

$$\boldsymbol{b} \triangleq [\, b_1 \; b_2 \; ... \; b_{N_b}] \quad , \tag{3.345}$$

and $\boldsymbol{x}_{k-\Delta-1}$ is the vector of data symbols in the feedback path. It is mathematically convenient to define an augmented response vector for the DFE as

$$\tilde{\boldsymbol{w}} \triangleq \left[\boldsymbol{w} \,\vdots\, -\boldsymbol{b} \right] \quad , \tag{3.346}$$

and a corresponding augmented DFE input vector as

$$\tilde{\boldsymbol{Y}}_k \triangleq \left[\begin{array}{c} \boldsymbol{Y}_k \\ \boldsymbol{x}_{k-\Delta-1} \end{array} \right] \quad . \tag{3.347}$$

Then, (3.344) becomes

$$MSE = E\left\{ |x_{k-\Delta} - \tilde{\boldsymbol{w}}\tilde{\boldsymbol{Y}}_k|^2 \right\} \quad . \tag{3.348}$$

The solution, paralleling (3.299) - (3.301), is determined using the following two definitions:

Definition 3.7.3 (FIR MMSE-DFE Autocorrelation and Cross-Correlation Matrices)
The **FIR MMSE-DFE autocorrelation matrix** *is defined as*

$$\boldsymbol{R}_{\tilde{\boldsymbol{Y}}\tilde{\boldsymbol{Y}}} \quad \triangleq \quad E\left\{ \tilde{\boldsymbol{Y}}_k \tilde{\boldsymbol{Y}}_k^* \right\} / N \tag{3.349}$$

$$= \quad \left[\begin{array}{cc} \boldsymbol{R}_{\boldsymbol{Y}\boldsymbol{Y}} & E[\boldsymbol{Y}_k \boldsymbol{x}_{k-\Delta-1}^*] \\ E[\boldsymbol{x}_{k-\Delta-1}\boldsymbol{Y}_k^*] & \bar{\mathcal{E}}_{\boldsymbol{x}} I_{N_b} \end{array} \right] \tag{3.350}$$

$$= \quad \left[\begin{array}{cc} \bar{\mathcal{E}}_{\boldsymbol{x}}\left(\boldsymbol{P}\boldsymbol{P}^* + \frac{l \cdot \boldsymbol{R_{nn}}}{SNR} \right) & \bar{\mathcal{E}}_{\boldsymbol{x}}\boldsymbol{P}J_\Delta] \\ \bar{\mathcal{E}}_{\boldsymbol{x}}J_\Delta^* \boldsymbol{P}^* & \bar{\mathcal{E}}_{\boldsymbol{x}} I_{N_b} \end{array} \right] \quad , \tag{3.351}$$

where J_Δ is an $(N_f + \nu) \times N_b$ matrix of 0's and 1's, which has the upper $\Delta + 1$ rows zeroed and an identity matrix of dimension $min(N_b, N_f + \nu - \Delta - 1)$ with zeros to the right (when $N_f + \nu - \Delta - 1 < N_b$), zeros below (when $N_f + \nu - \Delta - 1 > N_b$), or no zeros to the right or below exactly fitting in the bottom of J_Δ (when $N_f + \nu - \Delta - 1 = N_b$).

The corresponding **FIR MMSE-DFE cross-correlation vector** *is*

$$\boldsymbol{R}_{\tilde{\boldsymbol{Y}}x} \quad \triangleq \quad E\left\{ \tilde{\boldsymbol{Y}}_k x_{k-\Delta}^* \right\} / N \tag{3.352}$$

$$= \quad \left[\begin{array}{c} \boldsymbol{R}_{\boldsymbol{Y}x} \\ 0 \end{array} \right] \tag{3.353}$$

$$= \quad \left[\begin{array}{c} \bar{\mathcal{E}}_{\boldsymbol{x}}\boldsymbol{P}\mathbf{1}_\Delta \\ 0 \end{array} \right] \quad , \tag{3.354}$$

where, again, $N = 1$ for real signals and $N = 2$ for complex signals.

The FIR MMSE-DFE for sampling rate l/T, delay Δ, and of length N_f and N_b has coefficients

$$\tilde{\boldsymbol{w}} = \boldsymbol{R}_{x\tilde{\boldsymbol{Y}}} \boldsymbol{R}_{\tilde{\boldsymbol{Y}}\tilde{\boldsymbol{Y}}}^{-1} \quad . \tag{3.355}$$

Equation (3.355) can be rewritten in detail as

$$\left[\boldsymbol{w}\,\vdots\, -\boldsymbol{b} \right] \cdot \bar{\mathcal{E}}_{\boldsymbol{x}} \cdot \left[\begin{array}{cc} \boldsymbol{P}\boldsymbol{P}^* + \frac{l}{SNR}\boldsymbol{R_{nn}} & \boldsymbol{P}J_\Delta \\ J_\Delta^* \boldsymbol{P}^* & I_{N_b} \end{array} \right] = \left[\bar{\mathcal{E}}_{\boldsymbol{x}} \cdot \mathbf{1}_\Delta^* \boldsymbol{P}^* \,\vdots\, 0 \right] \quad , \tag{3.356}$$

which reduces to the pair of equations

$$\boldsymbol{w}\left(\boldsymbol{P}\boldsymbol{P}^* + \frac{l}{SNR}\boldsymbol{R_{nn}} \right) - \boldsymbol{b}J_\Delta^* \boldsymbol{P}^* \quad = \quad \mathbf{1}_\Delta^* \boldsymbol{P}^* \tag{3.357}$$

$$\boldsymbol{w}\boldsymbol{P}J_\Delta - \boldsymbol{b} \quad = \quad 0 \quad . \tag{3.358}$$

Then
$$b = wPJ_\Delta \ , \qquad (3.359)$$

and thus
$$w\left(PP^* - PJ_\Delta J_\Delta^* P^* + \frac{l}{\text{SNR}} Rnn\right) = 1_\Delta^* P^* \qquad (3.360)$$

or
$$w = 1_\Delta^* P^* \left(PP^* - PJ_\Delta J_\Delta^* P^* + \frac{l}{\text{SNR}} Rnn\right)^{-1} \ . \qquad (3.361)$$

Then
$$b = 1_\Delta^* P^* \left(PP^* - PJ_\Delta J_\Delta^* P^* + \frac{l}{\text{SNR}} Rnn\right)^{-1} PJ_\Delta \ . \qquad (3.362)$$

The MMSE is then
$$
\begin{aligned}
\sigma^2_{MMSE-DFE} &= \bar{\mathcal{E}}_x - \tilde{w} R_{\tilde{Y}_x} & (3.363) \\
&= \bar{\mathcal{E}}_x - w R_{Y_x} & (3.364) \\
&= \bar{\mathcal{E}}_x \left(1 - 1_\Delta^* P^* \left(PP^* - PJ_\Delta J_\Delta^* P^* + \frac{l}{\text{SNR}} Rnn\right)^{-1} P 1_\Delta \right) \ , & (3.365)
\end{aligned}
$$

which is a function to be minimized over Δ. Thus, the SNR for the unbiased FIR MMSE-DFE is
$$\text{SNR}_{MMSE-DFE,U} = \frac{\bar{\mathcal{E}}_x}{\sigma^2_{MMSE-DFE}} - 1 = \frac{\tilde{w} R_{\tilde{Y}_x}}{\bar{\mathcal{E}}_x - \tilde{w} R_{\tilde{Y}_x}} \ , \qquad (3.366)$$

and the loss is again
$$\gamma_{MMSE-DFE} = \frac{\text{SNR}_{MFB}}{\text{SNR}_{MMSE-DFE,U}} \ . \qquad (3.367)$$

EXAMPLE 3.7.2 (MMSE-DFEs, PAM and QAM) For the earlier example with $l = 1$, $N_f = 2$, and $N_b = 1$ and $\nu = 1$, we will also choose $\Delta = 1$. Then

$$P = \begin{bmatrix} .9 & 1 & 0 \\ 0 & .9 & 1 \end{bmatrix} \ , \qquad (3.368)$$

$$J_\Delta = \begin{bmatrix} 0 \\ 0 \\ 1 \end{bmatrix} \ , \qquad (3.369)$$

$$1_\Delta = \begin{bmatrix} 0 \\ 1 \\ 0 \end{bmatrix} \ , \qquad (3.370)$$

and

$$R_{YY} = \begin{bmatrix} 1.991 & .9 \\ .9 & 1.991 \end{bmatrix} \ . \qquad (3.371)$$

Then

$$
\begin{aligned}
w &= [0\ 1\ 0] \begin{bmatrix} .9 & 0 \\ 1 & .9 \\ 0 & 1 \end{bmatrix} \left\{ \begin{bmatrix} 1.991 & .9 \\ .9 & 1.991 \end{bmatrix} - \begin{bmatrix} 0 \\ 1 \end{bmatrix} [0\ 1] \right\}^{-1} & (3.372) \\
&= [1\ .9] \begin{bmatrix} 1.991 & .9 \\ .9 & 0.991 \end{bmatrix}^{-1} & (3.373) \\
&= [.1556\ .7668] & (3.374) \\
b &= wPJ_\Delta & (3.375) \\
&= [.1556\ .7668] \begin{bmatrix} .9 & 1 & 0 \\ 0 & .9 & 1 \end{bmatrix} \begin{bmatrix} 0 \\ 0 \\ 1 \end{bmatrix} & (3.376) \\
&= .7668 \ . & (3.377)
\end{aligned}
$$
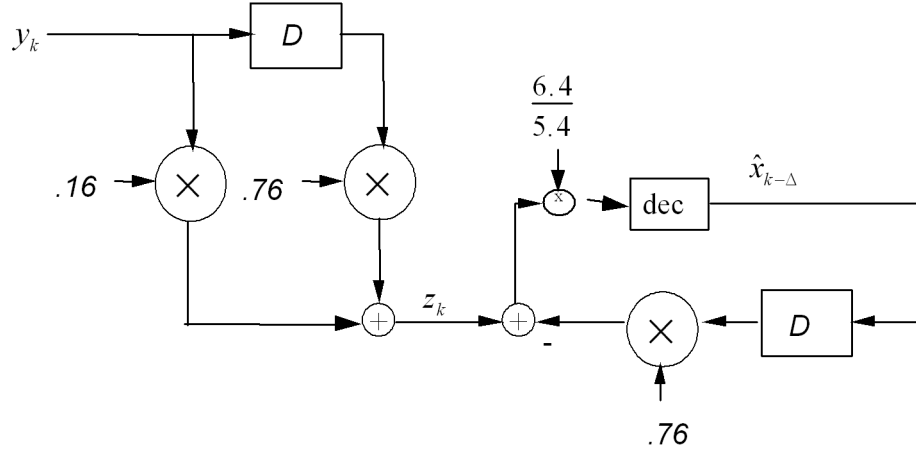
Figure 3.41: FIR MMSE-DFE Example.

Then

$$\sigma^2_{MMSE-DFE} = \left(1 - [.16\ .76]\begin{bmatrix} 1 \\ .9 \end{bmatrix}\right) = .157 \ . \tag{3.378}$$

The SNR is computed to be

$$\text{SNR}_{MMSE-DFE,U} = \frac{1 - .157}{.157} = 5.4\ (7.3\text{dB}) \quad , \tag{3.379}$$

which is 2.7 dB below MFB performance, but 2.8 dB better than the **infinite-length** MMSE-LE for this channel! The loss with respect to the infinite-length MMSE-DFE is 1.1 dB. A picture of the FIR MMSE-DFE is shown in Figure 3.41. With sufficiently large number of taps for this channel, the infinite-length performance level can be attained. This performance is plotted versus the number of feed-forward taps (only one feedback tap is necessary for infinite-length performance) in Figure 3.42. In this case, 7 feed-forward and 1 feedback taps are necessary for infinite-length performance. Thus, the finite-length DFE not only outperforms the finite or infinite-length LE, it uses less taps (less complexity) also. For the QAM example $l = 1$, $N_f = 2$, $N_b = 2$, and $\nu = 2$, we also choose $\Delta = 1$. Actually this channel will need more taps to do well with the DFE structure, but we can still choose these values and proceed. Then

$$\boldsymbol{P} = \begin{bmatrix} -.5 & 1 + \jmath/4 & -\jmath/2 & 0 \\ 0 & -.5 & 1 + \jmath/4 & -\jmath/2 \end{bmatrix} \quad , \tag{3.380}$$

$$J_\Delta = \begin{bmatrix} 0 & 0 \\ 0 & 0 \\ 1 & 0 \\ 0 & 1 \end{bmatrix} \quad , \tag{3.381}$$

$$\boldsymbol{1}_\Delta = \begin{bmatrix} 0 \\ 1 \\ 0 \\ 0 \end{bmatrix} \quad , \tag{3.382}$$

and

$$\boldsymbol{R_{YY}} = \begin{bmatrix} 1.7188 & -0.6250 - 0.6250\jmath \\ -0.6250 - 0.6250\jmath & 1.7188 \end{bmatrix} \quad . \tag{3.383}$$

Then

$$\boldsymbol{w} \;=\; [0\ 1\ 0\ 0]\begin{bmatrix} -.5 & 0 \\ 1 - \jmath/4 & -.5 \\ \jmath/2 & 1 - \jmath/4 \\ 0 & \jmath/2 \end{bmatrix} \cdot \tag{3.384}$$

$$\left\{ \begin{bmatrix} 1.7188 & -0.6250 - 0.6250\jmath \\ -0.6250 - 0.6250\jmath & 1.7188 \end{bmatrix} - \begin{bmatrix} 1/4 & -1/8 - \jmath/2 \\ -1/8 + \jmath/2 & 1.3125 \end{bmatrix} \right\}^{-1}$$

$$=\; [1 - \jmath/2 \ \ -.5]\begin{bmatrix} 1.2277 & 1.5103 + \jmath.3776 \\ 1.5103 - \jmath.3776 & 4.4366 \end{bmatrix} \tag{3.385}$$

$$=\; [.4720 - \jmath.1180 \ \ -.6136] \tag{3.386}$$

$$\boldsymbol{b} \;=\; \boldsymbol{w}\boldsymbol{P}J_\Delta \tag{3.387}$$

$$=\; [.4720 - \jmath.1180 \ \ .6136]\begin{bmatrix} -.5 & 1 + \jmath/4 & -\jmath/2 & 0 \\ 0 & -.5 & 1 + \jmath/4 & -\jmath/2 \end{bmatrix}\begin{bmatrix} 0 & 0 \\ 0 & 0 \\ 1 & 0 \\ 0 & 1 \end{bmatrix} \tag{3.388}$$

$$=\; [-.6726 - \jmath.3894 \ \ .3608\jmath] \quad . \tag{3.389}$$

Then

$$\sigma^2_{MMSE-DFE} = .1917 \ . \tag{3.390}$$

The SNR is computed to be

$$\mathrm{SNR}_{MMSE-DFE,U} = \frac{1 - .1917}{.1917} = 6.23\mathrm{dB} \quad , \tag{3.391}$$

which is 3.77 dB below MFB performance, and not very good on this channel! The reader may evaluate various filter lengths and delays to find a best use of 3, 4, 5, and 6 parameters on this channel.

FIR ZF-DFE One obtains the FIR ZF-DFE by letting the SNR$\to \infty$ in the FIR MMSE-DFE, which alters $\boldsymbol{R}_{\tilde{Y}\tilde{Y}}$ to

$$\boldsymbol{R}_{\tilde{Y}\tilde{Y}} = \begin{bmatrix} \bar{\mathcal{E}}_{\boldsymbol{x}}\tilde{\boldsymbol{P}}\tilde{\boldsymbol{P}}^* & \bar{\mathcal{E}}_{\boldsymbol{x}}\boldsymbol{P}J_\Delta \\ \bar{\mathcal{E}}_{\boldsymbol{x}}J_\Delta^*\boldsymbol{P}^* & \bar{\mathcal{E}}_{\boldsymbol{x}} \cdot I_{N_b} \end{bmatrix} \tag{3.392}$$

and then $\tilde{\boldsymbol{w}}$ remains as

$$\tilde{\boldsymbol{w}} = \boldsymbol{R}_{x\tilde{Y}}\boldsymbol{R}_{\tilde{Y}\tilde{Y}}^{-1} \quad . \tag{3.393}$$

Because the FIR equalizer may not be sufficiently long to cancel all ISI, the FIR ZF-DFE may still have nonzero residual ISI. This ISI power is given by

$$\sigma^2_{MMSE-DFE} = \bar{\mathcal{E}}_{\boldsymbol{x}} - \tilde{\boldsymbol{w}}\boldsymbol{R}_{\tilde{Y}_x} \quad . \tag{3.394}$$

However, (3.394) still ignores the enhanced noise at the $\tilde{\boldsymbol{w}}_k$ filter output. The power of this noise is easily found to be

$$\mathrm{FIR\ ZFDFE\ noise\ variance} = \frac{\mathcal{N}_0}{2} \cdot l \cdot \|\boldsymbol{w}\|^2 \quad , \tag{3.395}$$

making the SNR at the FIR ZF-DFE output

$$\mathrm{SNR}_{ZF-DFE} = \frac{\bar{\mathcal{E}}_{\boldsymbol{x}}}{\bar{\mathcal{E}}_{\boldsymbol{x}} - \tilde{\boldsymbol{w}}\boldsymbol{R}_{\tilde{Y}_x} + \frac{\bar{\mathcal{E}}_{\boldsymbol{x}}}{\mathrm{SNR}}l\|\boldsymbol{w}\|^2} \quad . \tag{3.396}$$

The filter is $\boldsymbol{w}$ in (3.395) and (3.396), not $\tilde{\boldsymbol{w}}$ because only the feed-forward section filters noise. The loss is:

$$\gamma_{\mathrm{ZF\text{-}DFE}} = \frac{\mathrm{SNR}_{MFB}}{\mathrm{SNR}_{ZF-DFE}} \quad . \tag{3.397}$$
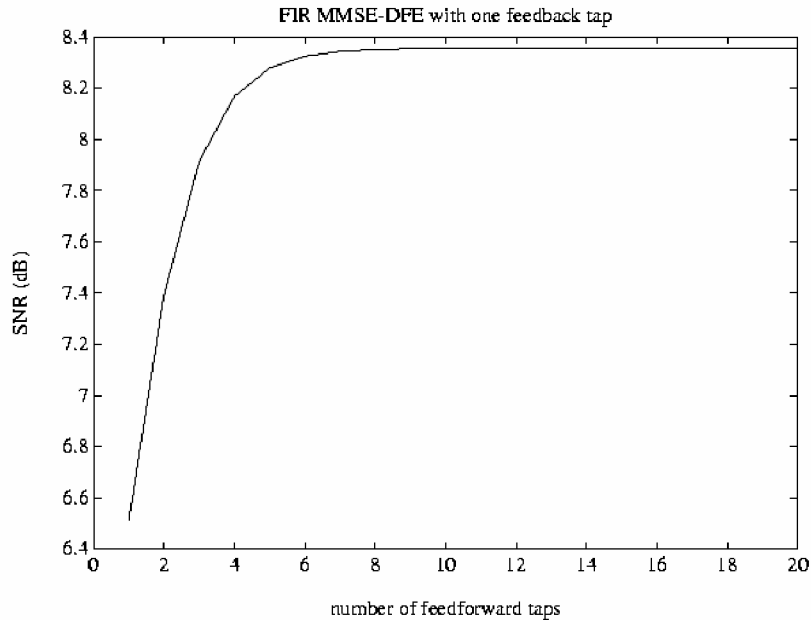
Figure 3.42: FIR MMSE-DFE performance for $1 + .9D^{-1}$ versus number of feed-forward equalizer taps.

3.7.5   An Alternative Approach to the DFE

While the above approach directly computes the settings for the FIR DFE, it yields less insight into the internal structure of the DFE than did the infinite-length structures investigated in Section 3.6, particularly the spectral (canonical) factorization into causal and anti-causal ISI components is not explicit. This subsection provides such an alternative caused by the finite-length filters. This is because finite-length filters inherently correspond to non-stationary processing.[14]

The vector of inputs at time k to the feed-forward filter is again $\boldsymbol{Y}_k$, and the corresponding vector of filter coefficients is $\boldsymbol{w}$, so the feed-forward filter output is $z_k = \boldsymbol{w}\boldsymbol{Y}_k$. Continuing in the same fashion, the DFE error signal is then described by

$$e_k = \boldsymbol{b}\boldsymbol{X}_k(\Delta) - \boldsymbol{w}\boldsymbol{Y}_k \quad , \tag{3.398}$$

where $\boldsymbol{x}^*_{k:k-N_b} = \begin{bmatrix} x^*_k \ ... \ x^*_{k-N_b} \end{bmatrix}$, and $\boldsymbol{b}$ is now slightly altered to be monic and causal

$$\boldsymbol{b} \triangleq \begin{bmatrix} 1 \ b_1 \ b_2 \ ... \ b_{N_b} \end{bmatrix} \quad . \tag{3.399}$$

The mean-square of this error is to be minimized over $\boldsymbol{b}$ and $\boldsymbol{w}$. Signals will again be presumed to be complex, but all developments here simplify to the one-dimensional real case directly, although it is important to remember to divide any complex signal's variance by 2 to get the energy per real dimension. The SNR equals $\bar{\mathcal{E}}_{\boldsymbol{x}}/\frac{N_0}{2} = \mathcal{E}_{\boldsymbol{x}}/\mathcal{N}_0$ in either case.

Optimizing the feed-forward and feedback filters   For any fixed $\boldsymbol{b}$ in (3.398), the cross-correlation between the error and the vector of channel outputs $\boldsymbol{Y}_k$ should be zero to minimize MSE,

$$E\left[e_k \boldsymbol{Y}^*_k\right] = 0 \quad . \tag{3.400}$$

So,

$$\boldsymbol{w}\boldsymbol{R}_{\boldsymbol{Y}\boldsymbol{Y}} = \boldsymbol{b}\boldsymbol{R}_{\boldsymbol{X}\boldsymbol{Y}}(\Delta) \quad , \tag{3.401}$$

---

[14] A more perfect analogy between finite-length and infinite-length DFE's occurs in Chapter 5, where the best finite-length DFE's are actually periodic over a packet period corresponding to the length of the feed-forward filter.

and

$$\boldsymbol{R_{XY}}(\Delta) \;=\; E\left\{\boldsymbol{X}_k(\Delta)\left[x_k^*\; x_{k-1}^* \;...\; x_{k-N_f-\nu+1}^*\right]\boldsymbol{P}^*\right\} \tag{3.402}$$

$$=\; \bar{\mathcal{E}}_{\boldsymbol{x}}\tilde{J}_\Delta^*\boldsymbol{P}^* \;\;, \tag{3.403}$$

where the matrix $\tilde{J}_\Delta^*$ has the first Δ columns all zeros, then an (up to) $N_b \times N_b$ identity matrix at the top of the up to N_b columns, and zeros in any row entries below that identity, and possibly zeroed columns following the identity if $N_f + \nu - 1 > N_b$. The following matlab commands produce $\tilde{J}_\Delta^*$, using for instance $N_f = 8$, $N_b = 5$, $\Delta = 3$, and $\nu = 5$,

```
>> size=min(Delta,Nb);
>> Jdelta=[ zeros(size,size) eye(size) zeros(size, max(Nf+nu-2*size,0))
zeros(max(Nb-Delta,0),Nf+nu)]

Jdelta =

    0    0    0    1    0    0    0    0    0    0    0    0    0
    0    0    0    0    1    0    0    0    0    0    0    0    0
    0    0    0    0    0    1    0    0    0    0    0    0    0
    0    0    0    0    0    0    0    0    0    0    0    0    0
    0    0    0    0    0    0    0    0    0    0    0    0    0
```

or for $N_f = 8$, $N_b = 2$, $\Delta = 3$, and $\nu = 5$,

```
>> >> size=min(Delta,Nb)
size = 2
>> Jdelta=[ zeros(size,size) eye(size) zeros(size, max(Nf+nu-2*size,0)),
zeros(max(Nb-Delta,0),Nf+nu)]

Jdelta =

    0    0    1    0    0    0    0    0    0    0    0    0    0
    0    0    0    1    0    0    0    0    0    0    0    0    0
```

The MSE for this fixed value of $\boldsymbol{b}$ then becomes

$$\sigma_\epsilon^2(\Delta) \;=\; \boldsymbol{b}^*\left(\bar{\mathcal{E}}_{\boldsymbol{x}}I - \boldsymbol{R_{XY}}(\Delta)\boldsymbol{R_{YY}^{-1}}\boldsymbol{R_{YX}}(\Delta)\right)\boldsymbol{b} \tag{3.404}$$

$$=\; \boldsymbol{b}^*\boldsymbol{R_{X/Y}^\perp}(\Delta)\boldsymbol{b} \tag{3.405}$$

$$=\; \boldsymbol{b}^*\left(\bar{\mathcal{E}}_{\boldsymbol{x}}I_{N_b} - \tilde{J}_\Delta^*\boldsymbol{P}^*\left(\boldsymbol{P}\boldsymbol{P}^* + \frac{l}{\text{SNR}}\boldsymbol{R_{nn}}\right)^{-1}\boldsymbol{P}\tilde{J}_\Delta(\Delta)\right)\boldsymbol{b} \tag{3.406}$$

$$=\; l\cdot\frac{\mathcal{N}_0}{2}\left\{\boldsymbol{b}^*\tilde{J}_\Delta^*\left(\boldsymbol{P}^*\boldsymbol{R_{nn}^{-1}}\boldsymbol{P} + \frac{l}{\text{SNR}}I\right)^{-1}\boldsymbol{P}\tilde{J}_\Delta(\Delta)\tilde{J}_\Delta\boldsymbol{b}\right\} \;\;, \tag{3.407}$$

and $\boldsymbol{R_{X/Y}^\perp}(\Delta) \overset{\Delta}{=} \bar{\mathcal{E}}_{\boldsymbol{x}}I - \boldsymbol{R_{XY}}(\Delta)\boldsymbol{R_{YY}^{-1}}\boldsymbol{R_{YX}}(\Delta)$, the autocorrelation matrix corresponding to the MMSE vector in estimating $\boldsymbol{X}(\Delta)$ from $\boldsymbol{Y}_k$. This expression is the equivalent of (3.216). That is $\boldsymbol{R_{X/Y}^\perp}(\Delta)$ is the autocorrelation matrix for the error sequence of length $N - b$ that is associated with a "matrix" MMSE-LE. The solution then requires factorization of the inner matrix into canonical factors, which is executed with Cholesky factorization for finite matrices.

By defining

$$\tilde{\boldsymbol{Q}}(\Delta) = \left\{\tilde{J}_\Delta^*\left(\boldsymbol{P}^*\boldsymbol{P} + \frac{l}{\text{SNR}}I\right)^{-1}\tilde{J}_\Delta\right\}^{-1} \;\;, \tag{3.408}$$

this matrix is equivalent to (3.217), except for the "annoying" $\tilde{J}_\Delta$ matrices that become identities as N_f and N_b become infinite, then leaving $\tilde{\boldsymbol{Q}}$ as essentially the autocorrelation of the channel output. The

$\tilde{J}_\Delta$ factors, however, cannot be ignored in the finite-length case. Canonical factorization of $\tilde{Q}$ proceeds according to

$$\sigma_\epsilon^2(\Delta) = \boldsymbol{b} G_\Delta^{-1} S_\Delta G_\Delta^{-*} \boldsymbol{b}^* \ , \tag{3.409}$$

which is minimized when

$$\boldsymbol{b} = \boldsymbol{g}(\Delta) \ , \tag{3.410}$$

the top row of the upper-triangular matrix G_Δ. The MMSE is thus obtained by computing Cholesky factorizations of $\tilde{Q}$ for all reasonable values of Δ and then setting $\boldsymbol{b} = \boldsymbol{g}(\Delta)$. Then

$$\sigma_\epsilon^2(\Delta) = S_o(\Delta) \ . \tag{3.411}$$

From previous developments, as the lengths of filters go to infinity, any value of Δ works and also $S_0 \to \gamma_0 \frac{N_0}{2}/\bar{\mathcal{E}}_{\boldsymbol{x}}$ to ensure the infinite-length MMSE-DFE solution of Section 3.6.

The feed-forward filter then becomes

$$\boldsymbol{w} = \boldsymbol{b} R_{\boldsymbol{XY}}(\Delta) R_{\boldsymbol{YY}}^{-1} \tag{3.412}$$

$$= \boldsymbol{g}(\Delta) \tilde{J}_\Delta \boldsymbol{P}^* \left(\boldsymbol{P}\boldsymbol{P}^* + \frac{l}{\text{SNR}} I \right)^{-1} \tag{3.413}$$

$$= \underbrace{\boldsymbol{g}(\Delta) \tilde{J}_\Delta \left(\boldsymbol{P}^* \boldsymbol{P} + \frac{l}{\text{SNR}} I \right)^{-1}}_{\text{feedforward filter}} \underbrace{\boldsymbol{P}^*}_{\text{matched filter}} \ , \tag{3.414}$$

which can be interpreted as a matched filter followed by a feed-forward filter that becomes $1/G^*(D^{-*})$ as its length goes to infinity. However, the result that the feed-forward filter is an anti-causal factor of the canonical factorization does not follow for finite length. Chapter 5 will find a situation that is an exact match and for which the feed-forward filter is an inverse of a canonical factor, but this requires the DFE filters to become periodic in a period equal to the number of taps of the feed-forward filter (plus an excess bandwidth factor).

The SNR is as always

$$\text{SNR}_{MMSE-DFE,U} = \frac{\bar{\mathcal{E}}_{\boldsymbol{x}}}{S_0(\Delta)} - 1 \ . \tag{3.415}$$

Bias can be removed by scaling the decision-element input by the ratio of $\text{SNR}_{MMSE-DFE}/\text{SNR}_{MMSE-DFE,U}$, thus increasing its variance by $(\text{SNR}_{MMSE-DFE}/\text{SNR}_{MMSE-DFE,U})^2$.

Finite-length Noise-Predictive DFE

Problem 3.8 introduces the "noise-predictive" form of the DFE, which is repeated here in Figure 3.43. In this figure, the error sequence is feedback instead of decisions. The filter essentially tries to predict the noise in the feedforward filter output and then cancel this noise, whence the name "noise-predictive" DFE. Correct solution to the infinite-length MMSE filter problem 3.8 will produce that the filter $B(D)$ remains equal to the same $G(D)$ found for the infinite-length MMSE-DFE. The filter $U(D)$ becomes the MMSE-LE so that $Z(D)$ has no ISI, but a strongly correlated (and enhanced) noise. The preditor then reduces the noise to a white error sequence. If $W(D) = \frac{1}{\gamma_0 \cdot \|p\| \cdot G^{-*}(D^{-*})}$ of the normal MMSE-DFE, then it can be shown also (see Problem 3.8) that

$$U(D) = \frac{W(D)}{G(D)} \ . \tag{3.416}$$

The MMSE, all SNR's, and biasing/unbiasing remain the same.

An analogous situation occurs for the finite-length case, and it will be convenient notationally to say that the number of taps in the feedforward filter $\boldsymbol{u}$ is $(N_f - \nu)l$. Clearly if ν is fixed as always, then any number of taps (greater than ν can be investigated without loss of generality with this early notational abuse. Clearly by abusing N_f (which is not the number of taps), ANY positive number of taps in $\boldsymbol{u}$ can
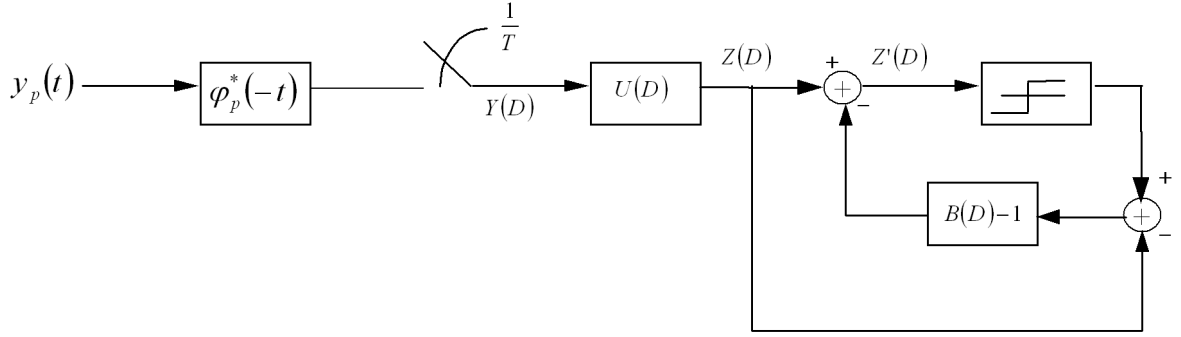
Figure 3.43: Noise-Predictive DFE

be constructed without loss of generality for any value of $\nu \geq 0$. In this case, the error signal can be written as

$$e_k = \boldsymbol{b}_k \boldsymbol{X}_k(\Delta) - \boldsymbol{bZ} \tag{3.417}$$

where

$$\boldsymbol{Z}_k = \begin{bmatrix} z_k \\ \vdots \\ z_{k-\nu} \end{bmatrix} \quad . \tag{3.418}$$

Then,

$$\boldsymbol{Z}_k = U\boldsymbol{Y}_k \tag{3.419}$$

where

$$U = \begin{bmatrix} \boldsymbol{u} & 0 & \dots & 0 \\ 0 & \boldsymbol{u} & \dots & 0 \\ \vdots & \ddots & \ddots & \vdots \\ 0 & \dots & 0 & \boldsymbol{u} \end{bmatrix} \tag{3.420}$$

and

$$\boldsymbol{Y}_k = \begin{bmatrix} y_k \\ \vdots \\ y_{k-N_f+1} \end{bmatrix} \quad . \tag{3.421}$$

By defining the $(N_f)l$-tap filter

$$\boldsymbol{w} \stackrel{\Delta}{=} \boldsymbol{b}U \quad , \tag{3.422}$$

then the error becomes

$$e_k = \boldsymbol{b}_k \boldsymbol{X}_k(\Delta) - \boldsymbol{wY} \quad , \tag{3.423}$$

which is the same error as in the alternate viewpoint of the finite-length DFE earlier in this section. Thus, solving for the $\boldsymbol{b}$ and $\boldsymbol{w}$ of the conventional finite-length MMSE-DFE can be followed by the step of solving Equation (3.422) for U when $\boldsymbol{b}$ and $\boldsymbol{w}$ are known. However, it follows directly then from Equation (3.401) that

$$\boldsymbol{u} = \boldsymbol{R}_{\boldsymbol{XY}}(\Delta)\boldsymbol{R}_{\boldsymbol{YY}}^{-1} \quad , \tag{3.424}$$

so following the infinite-case form, $\boldsymbol{u}$ is the finite-length MMSE-LE with $(N_f - \nu)l$ taps. The only difference from the infinite-length case is the change in length.

3.7.6 The Stanford DFE Program

A matlab program has been created, used, and refined by the students of EE379A over a period of many years. The program has the following call command:

function (SNR, wt) = **dfe** (l,p,nff, nbb, delay, Ex, noise);
where the inputs and outputs are listed as

- l = oversampling factor
- p = pulse response, oversampled at l (size)
- nff = number of feed-forward taps
- nbb = number of feedback taps
- delay $\approx$ delay of system Nff + length of p - nbb ; if delay = -1, then choose the best delay
- Ex = average energy of signals
- noise = autocorrelation vector (size l*nff) (NOTE: noise is assumed to be stationary). For white noise, this vector is simply $[\sigma^2\ 0...0]$.
- SNR = equalizer SNR, unbiased and in dB
- wt = equalizer coefficients

The student may use this program to a substantial advantage in avoiding tedious matrix calculations. The program has come to be used throughout the industry to compute/project equalizer performance (setting nbb=0 also provides a linear equalizer). The reader is cautioned against the use of a number of rules of thumb (like "DFE SNR is the SNR(f) at the middle of the band") used by various who call themselves experts and often over-estimate the DFE performance using such formulas. Difficult transmission channels may require large numbers of taps and considerable experimentation to find the best settings.

```
function [dfseSNR,w_t,opt_delay]=dfsecolorsnr(l,p,nff,nbb,delay,Ex,noise);
% ------------------------------------------------------------
% [dfseSNR,w_t] = dfecolor(l,p,nff,nbb,delay,Ex,noise);
% l     = oversampling factor
% p     = pulse response, oversampled at l (size)
% nff   = number of feed-forward taps
% nbb   = number of feedback taps
% delay = delay of system <= nff+length of p - 2 - nbb
%         if delay = -1, then choose best delay
% Ex    = average energy of signals
% noise = noise autocorrelation vector (size l*nff)
% NOTE: noise is assumed to be stationary
%
% outputs:
% dfseSNR = equalizer SNR, unbiased in dB
% w_t = equalizer coefficients [w -b]
% opt_delay = optimal delay found if delay =-1 option used.
%             otherwise, returns delay value passed to function
% created 4/96;
% ------------------------------------------------------------

size = length(p);
nu = ceil(size/l)-1;
p = [p zeros(1,(nu+1)*l-size)];
```

```
% error check
if nff<=0
  error('number of feed-forward taps > 0');
end
if delay > (nff+nu-1-nbb)
  error('delay must be <=  (nff+(length of p)-2-nbb)');
elseif delay < -1
  error('delay must be >= -1');
elseif delay == -1
    delay = 0:1:nff+nu-1-nbb;
end

%form ptmp = [p_0 p_1 ... p_nu] where p_i=[p(i*l) p(i*l-1)... p((i-1)*l+1)
ptmp(1:l,1) = [p(1); zeros(l-1,1)];
for i=1:nu
  ptmp(1:l,i+1) = conj((p(i*l+1:-1:(i-1)*l+2))');
end

%form matrix P, vector channel matrix
P = zeros(nff*l+nbb,nff+nu);
for i=1:nff,
  P(((i-1)*l+1):(i*l),i:(i+nu)) = ptmp;
end

%precompute Rn matrix - constant for all delays
Rn  = zeros(nff*l+nbb);
Rn(1:nff*l,1:nff*l) = toeplitz(noise);

dfseSNR = -100;
P_init = P;
%loop over all possible delays
for d = delay,
    P = P_init;
    P(nff*l+1:nff*l+nbb,d+2:d+1+nbb) = eye(nbb);
    %P
    temp= zeros(1,nff+nu);
    temp(d+1)=1;
    %construct matrices
    Ry  = Ex*P*P' + Rn;
    Rxy = Ex*temp*P';
    new_w_t = Rxy*inv(Ry);
    sigma_dfse = Ex - real(new_w_t*Rxy');
    new_dfseSNR = 10*log10(Ex/sigma_dfse - 1);
    %save setting of this delay if best performance so far
    if new_dfseSNR >= dfseSNR
        w_t = new_w_t;
        dfseSNR = new_dfseSNR;
        opt_delay = d;
    end
end
```

3.7.7 Error Propagation in the DFE

To this point, this chapter has ignored the effect of decision errors in the feedback section of the DFE. At low error rates, say 10^{-5} or below, this is reasonable. There is, however, an accurate way to compute the effect of decision feedback errors, although enormous amounts of computational power may be necessary (much more than that required to simulate the DFE and measure error rate increase). At high error rates of 10^{-3} and above, error propagation can lead to several dB of loss. In coded systems (see Chapters 7 and 8), the inner channel (DFE) may have an error rate that is unacceptably high that is later reduced in a decoder for the applied code. Thus, it is common for low decision-error rates to occur in a coded DFE system. The Precoders of Section 3.8 can be used to eliminate the error propagation problem, but this requires that the channel be known in the transmitter – which is not always possible, especially in transmission systems with significant channel variation, i.e, digital mobile telephony. An analysis for the infinite-length equalizer has not yet been invented, thus the analysis here applies only to FIR DFE's with finite N_b.

By again denoting the equalized pulse response as v_k (after removal of any bias), and assuming that any error signal, e_k, in the DFE output can is uncorrelated with the symbol of interest, x_k, this error signal can be decomposed into 4 constituent signals

1. precursor ISI - $e_{pr,k} = \sum_{i=-\infty}^{-1} v_i x_{k-i}$

2. postcursor ISI - $e_{po,k} = \sum_{i=N_b+1}^{\infty} v_i x_{k-i}$

3. filtered noise - $e_{n,k} = \sum_{i=-\infty}^{\infty} w_i n_{k-i}$

4. feedback errors - $e_{f,k} = \sum_{i=1}^{N_b} v_i \left(x_{k-i} - \hat{x}_{k-i} \right)$

The sum of the first 3 signals constitute the MMSE with power $\sigma^2_{MMSE-DFE}$, which can be computed according to previous results. The last signal is often written

$$e_{f,k} = \sum_{i=1}^{N_b} v_i \cdot \epsilon_{k-i} \tag{3.425}$$

where $\epsilon_k \triangleq x_k - \hat{x}_k$. This last distortion component has a discrete distribution with $(2M-1)^{N_b}$ possible points.

The **error event vector**, $\boldsymbol{\epsilon}_k$, is

$$\boldsymbol{\epsilon}_k \triangleq \begin{bmatrix} \epsilon_{k-N_b+1} & \epsilon_{k-N_b+2} & \dots & \epsilon_k \end{bmatrix} \tag{3.426}$$

Given $\boldsymbol{\epsilon}_{k-1}$, there are only $2M-1$ possible values for $\boldsymbol{\epsilon}_k$. Equivalently, the evolution of an error event, can be described by a finite-state machine with $(2M-1)^{N_b}$ states, each corresponding to one of the $(2M-1)^{N_b}$ possible length-N_b error events. Such a finite state machine is shown in Figure 3.44. The probability that $\boldsymbol{\epsilon}_k$ takes on a specific value, or that the state transition diagram goes to the corresponding state at time k, is (denoting the corresponding new entry in $\boldsymbol{\epsilon}_k$ as ϵ_k)

$$P_{\boldsymbol{\epsilon}_k/\boldsymbol{\epsilon}_{k-1}} = Q\left[\frac{d_{\min} - |e_{f,k}(\boldsymbol{\epsilon}_{k-1})|}{2\sigma_{\text{MMSE-DFE}}} \right] \quad . \tag{3.427}$$

There are $2M-1$ such values for each of the $(2M-1)^{N_b}$ states. $\boldsymbol{\Upsilon}$ denotes a square $(2M-1)^{N_b} \times (2M-1)^{N_b}$ matrix of transition probabilities where the i,j^{th} element is the probability of entering state i, given the DFE is in state j. The column sums are thus all unity. For a matrix of non-negative entries, there is a famous "Peron-Frobenious" lemma from linear algebra that states that there is a unique eigenvector $\boldsymbol{\rho}$ of all nonnegative entries that satisfies the equation

$$\boldsymbol{\rho} = \boldsymbol{\Upsilon} \boldsymbol{\rho} \quad . \tag{3.428}$$

The solution $\boldsymbol{\rho}$ is called the **stationary state distribution** or **Markov distribution** for the state transition diagram. The ith entry, ρ_i, is the steady-state probability of being in state i. Of course,
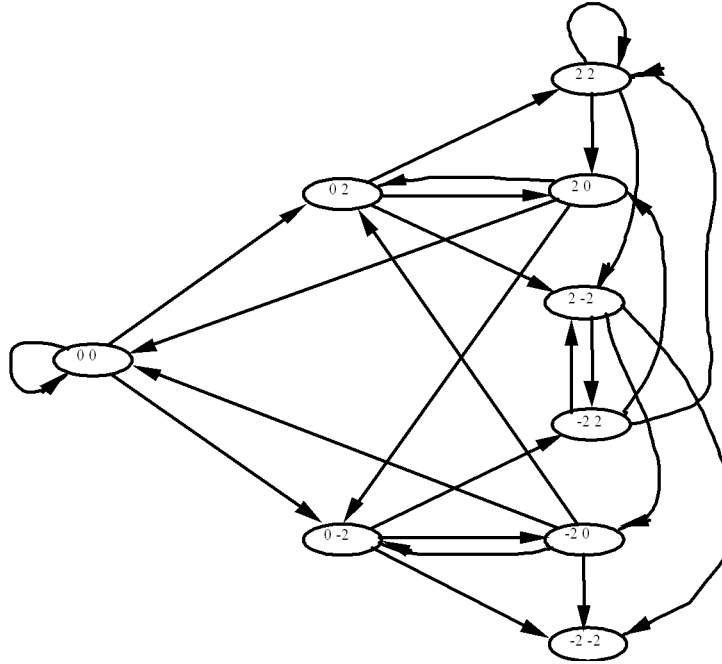
Figure 3.44: Finite State Machine for $N_b = 2$ and $M = 2$ in evaluating DFE Error Propagation

$\sum_{i=1}^{(2M-1)^{N_b}} \rho_i = 1$. By denoting the set of states for which $\epsilon_k \neq 0$ as $\mathcal{E}$, one determines the probability of error as

$$P_e = \sum_{i \in \mathcal{E}} \rho_i \quad . \tag{3.429}$$

Thus, the DFE will have an accurate estimate of the error probability in the presence of error propagation. A larger state-transition diagram, corresponding to the explicit consideration of residual ISI as a discrete probability mass function, would yield a yet more accurate estimate of the error probability for the equalized channel - however, the relatively large magnitude of the error propagation samples usually makes their explicit consideration more important than the (usually) much smaller residual ISI.

The number of states can be very large for reasonable values of M and N_b, so that the calculation of the stationary distribution $\boldsymbol{\rho}$ could exceed the computation required for a direct measurement of SNR with a DFE simulation. There are a number of methods that can be used to reduce the number of states in the finite-state machine, most of which will reduce the accuracy of the probability of error estimate.

In the usual case, the constellation for x_k is symmetric with respect to the origin, and there is essentially no difference between ϵ_k and $-\epsilon_k$, so that the analysis may merge the two corresponding states and only consider one of the error vectors. This can be done for almost half[15] the states in the state transition diagram, leading to a new state transition diagram with M^{N_b} states. Further analysis then proceeds as above, finding the stationary distribution and adding over states in $\mathcal{E}$. There is essentially no difference in this P_e estimate with respect to the one estimated using all $(2M-1)^{N_b}$ states; however, the number of states can remain unacceptably large.

At a loss in P_e accuracy, we may ignore error magnitudes and signs, and compute error statistics for binary error event vectors, which we now denote $\boldsymbol{\varepsilon} = [\varepsilon_1, ..., \varepsilon_{N_b}]$, of the type (for $N_b = 3$)

$$[\,0\,0\,0\,]\ ,\ [\,0\,1\,0\,]\ ,\ [\,1\,0\,0\,]\ ,\ [\,1\,0\,1\,]\ \ . \tag{3.430}$$

This reduces the number of states to 2^{N_b}, but unfortunately the state transition probabilities no longer depend only on the previous state. Thus, we must try to find an upper bound on these probabilities that depends only on the previous states. In so doing, the sum of the stationary probabilities corresponding

---

[15]There is no reduction for zero entries.

225

to states in $\mathcal{E}$ will also upper bound the probability of error. $\mathcal{E}$ corresponds to those states with a nonzero entry in the first position (the "odd" states, $\varepsilon_1 = 1$). To get an upperbound on each of the transition probabilities we write

$$P_{\varepsilon_{1,k}=1/\boldsymbol{\varepsilon}_{k-1}} = \sum_{\{i \mid \varepsilon_{1,k}(i)\text{is allowed transition from } \boldsymbol{\varepsilon}_{k-1}} P_{\varepsilon_{1,k}=1/\boldsymbol{\varepsilon}_{k-1},\varepsilon_{1,k}(i)}P_{\varepsilon_{1,k}(i)}\} \qquad (3.431)$$

$$\leq \sum_{i \mid \varepsilon_{1,k}(i)\text{is allowed transition from } \boldsymbol{\varepsilon}_{k-1}} \max_{\varepsilon_{1,k}(i)} P_{\varepsilon_{1,k}=1/\boldsymbol{\varepsilon}_{k-1},\varepsilon_{1,k}(i)}P_{\varepsilon_{1,k}(i)} \qquad (3.432)$$

$$= \max_{\varepsilon_{1,k}(i)} P_{\varepsilon_{1,k}=1/\boldsymbol{\varepsilon}_{k-1},\varepsilon_{1,k}(i)} \quad . \qquad (3.433)$$

Explicit computation of the maximum probability in (3.433) occurs by noting that this error probability corresponds to a worst-case signal offset of

$$\delta_{max}(\boldsymbol{\varepsilon}) = (M-1)d\sum_{i=1}^{N_b}|v_i|\varepsilon_{1,k-i} \quad , \qquad (3.434)$$

which the reader will note is analogous to peak distortion (the distortion is understood to be the worst of the two QAM dimensions, which are assumed to be rotated so that $d_{\min}$ lies along either or both of the dimensions). As long as this quantity is less than the minimum distance between constellation points, the corresponding error probability is then upper bounded as

$$P_{e_k/\boldsymbol{\varepsilon}_{k-1}} \leq Q\left[\frac{\frac{d_{\min}}{2} - \delta_{max}(\boldsymbol{\varepsilon})}{\sqrt{\sigma^2_{MMSE-DFE}}}\right] \quad . \qquad (3.435)$$

Now, with the desired state-dependent (only) transition probabilities, the upper bound for P_e with error propagation is

$$P_e \leq \sum_{\boldsymbol{\varepsilon}} Q\left[\frac{\frac{d_{\min}}{2} - \delta_{max}(\boldsymbol{\varepsilon})}{\sqrt{\sigma^2_{MMSE-DFE}}}\right] P_{\boldsymbol{\varepsilon}} \quad . \qquad (3.436)$$

Even in this case, the number of states 2^{N_b} can be too large.

A further reduction to $N_b + 1$ states is possible, by grouping the 2^{N_b} states into groups that are classified only by the number of leading in $\boldsymbol{\varepsilon}_{k-1}$; thus, state $i = 1$ corresponds to any state of the form $[0 \; \varepsilon]$, while state $i = 2$ corresponds to $[0 \; 0 \; \varepsilon \; ...]$, etc. The upperbound on probability of error for transitions into any state, i, then uses a $\delta_{max}(i)$ given by

$$\delta_{max}(i) = (M-1)d\sum_{i=i+1}^{N_b}|v_i| \quad , \qquad (3.437)$$

and $\delta_{max}(N_b) = 0$.

Finally, a trivial bound that corresponds to noting that after an error is made, we have $M^{N_b} - 1$ possible following error event vectors that can correspond to error propagation (only the all zeros error event vector corresponds to no additional errors within the time-span of the feedback path). The probability of occurrence of these error event vectors is each no greater than the initial error probability, so they can all be considered as nearest neighbors. Thus adding these to the original probability of the first error,

$$P_e(errorprop) \leq M^{N_b}P_e(first) \quad . \qquad (3.438)$$

It should be obvious that this bound gives useful results only if N_b is small (that is a probability of error bound of .5 for i.i.d. input data may be lower than this bound even for reasonable values of M and N_b). That is suppose, the first probability of error is 10^{-5}, and $M = 8$ and $N_b = 8$, then this last (easily computed) bound gives $P_e \leq 100$!
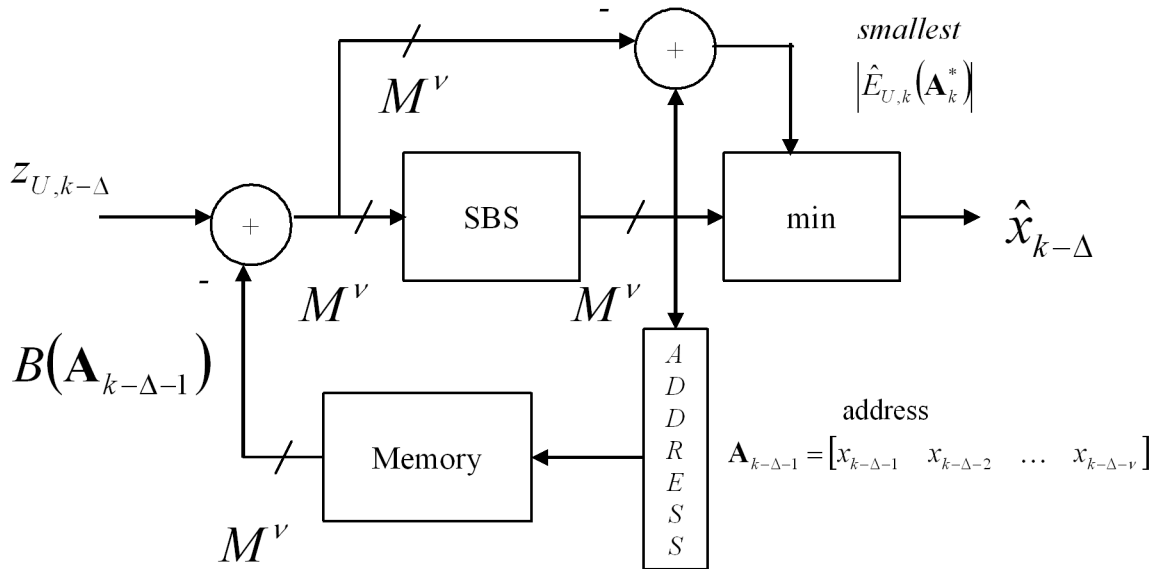
Figure 3.45: Look-Ahead mitigation of error propagation in DFEs.

3.7.8 Look-Ahead

Figure 3.45 illustrates a "look-ahead" mechanism for reducing error propagation. Instead of using the decision, M^ν possible decision vectors are retained. The vector is of dimension ν and can be viewed as an address $\boldsymbol{A}_{k-\Delta-1}$ to the memory. The possible output for each of the M^ν is computed and subtracted from $z_{U,k-\Delta}$. M^ν decisions of the symbol-by-symbol detector can then be computed and compared in terms of the distance from a potential symbol value, namely smallest $|E_{U,k-\Delta}|$. The smallest such distance is used to select the decision for $\hat{x}_{k-\Delta}$. This method is called "look-ahead" decoding basically because all possible previous decisions' ISI are precomputed and stored, in some sense looking ahead in the calculation. If M^ν calculations (or memory locations) is too complex, then the largest $\nu' < \nu$ taps can be used (or typically the most recent ν' and the rest subtracted in typical DFE fashion for whatever the decisions previous to the ν' tap interval in a linear filter. Look-ahead leads to the Maximum Likelihood Sequence detection (MLSD) methods of Chapter 9 that are no longer symbol-by-symbol based. Look-ahead methods can never exceed $\text{SNR}_{MMSE-DFE,U}$ in terms of performance, but can come very close since error propagation can be very small. (MLSD methods can exceed $\text{SNR}_{MMSE-DFE,U}$.)
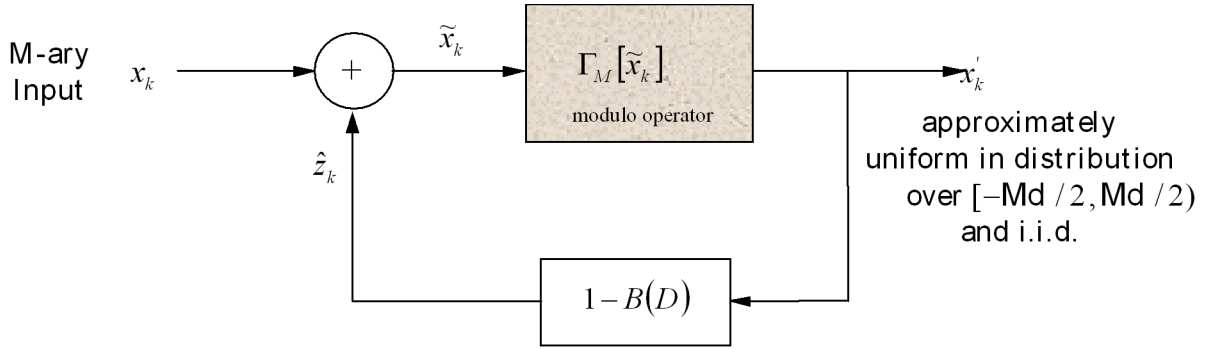
a). implementation for real baseband signals
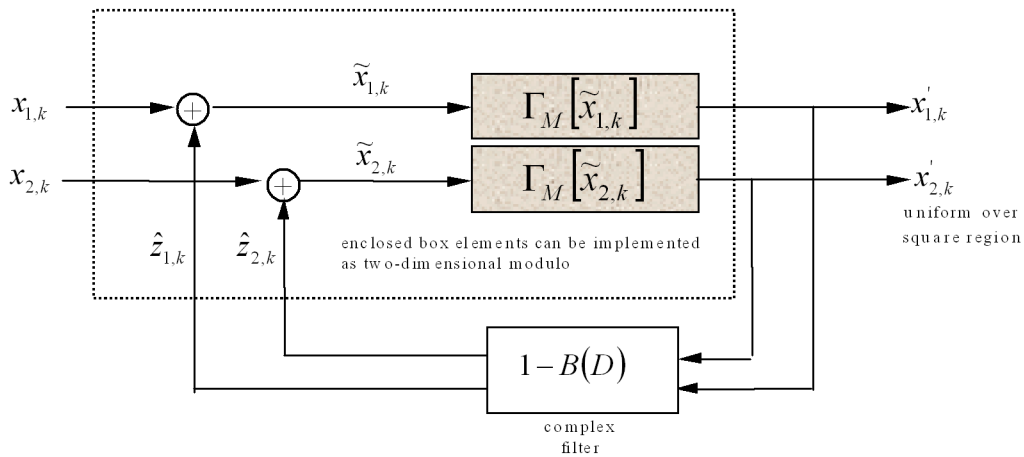
b). implementation for complex (quadrature) signals

Figure 3.46: The Tomlinson Precoder.

3.8 Precoding

This section discusses solutions to the error-propagation problem of DFE's. The first is precoding, which essentially moves the feedback section of the DFE to the transmitter with a minimal (but nonzero) transmit-power-increase penalty, but with no reduction in DFE SNR. The second approach or partial response channels (which have trivial precoders) has no transmit power penalty, but may have an SNR loss in the DFE because the feedback section is fixed to a desirable preset value for $B(D)$ rather than optimized value. This preset value (usually with all integer coefficients) leads to simplification of the ZF-DFE structure.

3.8.1 The Tomlinson Precoder

Error propagation in the DFE can be a major concern in practical application of this receiver structure, especially if constellation-expanding codes, or convolutional codes (see Chapter 10), are used in concatenation with the DFE (because the error rate on the inner DFE is lower (worse) prior to the decoder). Error propagation is the result of an incorrect decision in the feedback section of the DFE that produces additional errors that would not have occurred if that first decision had been correct.

The **Tomlinson Precoder (TPC)**, more recently known as a Tomlinson-Harashima Precoder, is a device used to eliminate error propagation and is shown in Figure 3.46. Figure 3.46(a) illustrates the case for real one-dimensional signals, while Figure 3.46(b) illustrates a generalization for complex signals. In the second complex case, the two real sums and two one-dimensional modulo operators can
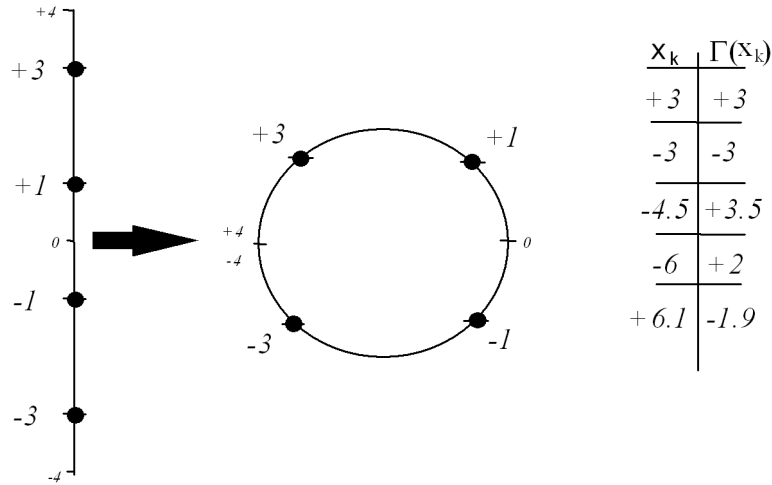
Figure 3.47: Illustration of modulo arithmetic operator.

be generalized to a two-dimensional modulo where arithmetic is modulo a two-dimensional region that tesselates two-dimensional space (for example, a hexagon, or a square).

The Tomlinson precoder appears in the transmitter as a preprocessor to the modulator. The Tomlinson Precoder maps the data symbol x_k into another data symbol x'_k, which is in turn applied to the modulator (not shown in Figure 3.46). The basic idea is to move the DFE feedback section to the transmitter where decision errors are impossible. However, straightforward moving of the filter $1/B(D)$ to the transmitter could result in significant transmit-power increase. To prevent most of this power increase, modulo arithmetic is employed to bound the value of x'_k:

Definition 3.8.1 (Modulo Operator) *The* **modulo operator** $\Gamma_M(x)$ *is a nonlinear function, defined on an M-ary (PAM or QAM square) input constellation with uniform spacing d, such that*

$$\Gamma_M(x) = x - Md\lfloor \frac{x + \frac{Md}{2}}{Md} \rfloor \tag{3.439}$$

where $\lfloor y \rfloor$ means the largest integer that is less than or equal to y. $\Gamma_M(x)$ **need not be an integer***. This text denotes modulo M addition and subtraction by $\oplus_M$ and $\ominus_M$ respectively. That is*

$$x \oplus_M y \stackrel{\Delta}{=} \Gamma_M[x + y] \tag{3.440}$$

and

$$x \ominus_M y \stackrel{\Delta}{=} \Gamma_M[x - y] \quad . \tag{3.441}$$

For complex QAM, each dimension is treated modulo $\sqrt{M}$ independently.

Figure 3.47 illustrates modulo arithmetic for $M = 4$ PAM signals with $d = 2$. The following lemma notes that the modulo operation distributes over addition:

Lemma 3.8.1 (Distribution of $\Gamma_M(x)$ over addition) *The modulo operator can be distributed over a sum in the following manner:*

$$\Gamma_M[x + y] = \Gamma_M(x) \oplus_M \Gamma_M(y) \tag{3.442}$$
$$\Gamma_M[x - y] = \Gamma_M(x) \ominus_M \Gamma_M(y) \quad . \tag{3.443}$$

The proof is trivial.

The Tomlinson Precoder generates an internal signal

$$\tilde{x}_k = x_k - \sum_{i=1}^{\infty} b_i x'_{k-i} \tag{3.444}$$

where

$$x'_k = \Gamma_M[\tilde{x}_k] = \Gamma_M \left[x_k - \sum_{i=1}^{\infty} b_i x'_{k-i} \right] \quad . \tag{3.445}$$

The scaled-by-$\text{SNR}_{MMSE-DFE}/\text{SNR}_{MMSE-DFE,U}$ output of the MS-WMF in the receiver is an optimal unbiased MMSE approximation to $X(D) \cdot G_U(D)$. That is

$$E \left[\frac{\text{SNR}_{MMSE-DFE}}{\text{SNR}_{MMSE-DFE,U}} z_k / [x_k \ x_{k-1} \ , ...,] \right] = \sum_{i=0}^{\infty} g_{U,i} x_{k-i} \quad . \tag{3.446}$$

Thus, $B(D) = G_U(D)$. From Equation (3.249) with $x'(D)$ as the new input, the scaled feedforward filter output with the Tomlinson precoder is

$$z_{U,k} = \left(x'_k + \sum_{i=1}^{\infty} g_{U,i} x'_{k-i} \right) + e_{U,k} \quad . \tag{3.447}$$

$\Gamma_M[z_{U,k}]$ is determined as

$$
\begin{aligned}
\Gamma_M[z_{U,k}] &= \Gamma_M[\Gamma_M(x_k - \sum_{i=1}^{\infty} g_{U,i} x'_{k-i}) + \sum_{i=1}^{\infty} g_{U,i} x'_{k-i} + e_{U,k}] & (3.448) \\
&= \Gamma_M[x_k - \sum_{i=1}^{\infty} g_{U,i} x'_{k-i} + \sum_{i=1}^{\infty} g_{U,i} x'_{k-i} + e_{U,k}] & (3.449) \\
&= \Gamma_M[x_k + e_{U,k}] & (3.450) \\
&= x_k \oplus_M \Gamma_M[e_{U,k}] & (3.451) \\
&= x_k + e'_{U,k} \quad . & (3.452)
\end{aligned}
$$

Since the probability that the error $e_{U,k}$ being larger than $Md/2$ in magnitude is small in a well-designed system, one can assume that the error sequence is of the same distribution and correlation properties after the modulo operation. Thus, the Tomlinson Precoder has allowed reproduction of the input sequence at the (scaled) MS-WMF output, without ISI. The original Tomlinson work was done for the ZF-DFE, which is a special case of the theory here, with $G_U(D) = P_c(D)$. The receiver corresponding to Tomlinson precoding is shown in Figure 3.48.

The noise power at the feed-forward output is thus almost exactly the same as that of the corresponding MMSE-DFE and with no error progagation because there is no longer any need for the feedback section of the DFE. As stated here without proof, there is only a small price to pay in increased transmitter power when the TPC is used.

Theorem 3.8.1 (Tomlinson Precoder Output) *The Tomlinson Precoder output, when the input is an i.i.d. sequence, is also approximately i.i.d., and futhermore the output sequence is approximately uniform in distribution over the interval $[-Md/2, Md/2)$.*

There is no explicit proof of this theorem for finite M, although it can be proved exactly as $M \to \infty$. This proof notes that the unbiased and biased receivers are identical as $M \to \infty$, because the SNR must also be infinite. Then, the modulo element is not really necessary, and the sequence x'_k can be shown to be equivalent to a prediction-error or "innovations" sequence, which is known in the estimation literature to be i.i.d. The i.i.d. part of the theorem appears to be valid for almost any M. The distribution and autocorrelation properties of the TPC, in closed form, remain an unsolved problem at present.
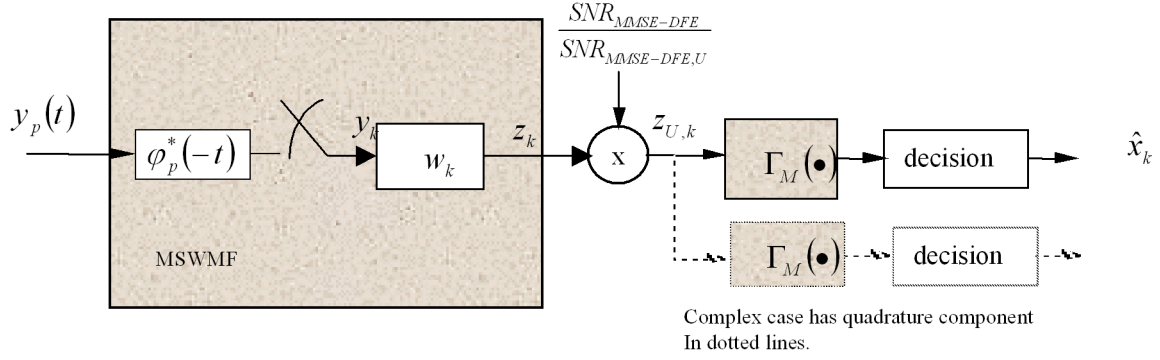
Figure 3.48: Receiver for Tomlinson precoded MMSE-DFE implementation.

Using the uniform distribution assumption, the increase in transmit power for the TPC is from the nominal value of $\frac{(M^2-1)d^2}{12}$ to the value for a continuous uniform random variable over the output interval $[-Md/2, Md/2)$, which is $\frac{M^2d^2}{12}$, leading to an input power increase of

$$\frac{M^2}{M^2 - 1} \tag{3.453}$$

for PAM and correspondingly

$$\frac{M}{M - 1} \tag{3.454}$$

for QAM. When the input is not a square constellation, the Tomlinson Precoder Power loss is usually larger, but never more than a few dB. The number of nearest neighbors also increases to $\bar{N}_e = 2$ for all constellations. These losses can be eliminated (and actually a gain is possible) using techniques called Trellis Precoding and/or shell mapping (See Section 10.6).

Laroia or Flexible Precoder

Figure 3.49 shows the Laroia precoder, which is a variation on Tomlinson precoding introduced by Rajiv Laroia, mainly to reduce the transmit-power loss of the Tomlinson precoder. The Laroia precoder largely preserves the shape of the transmitted constellation. The equivalent circuit is also shown in Figure 3.49 where the input is considered to be the difference between the actual input symbol value x_k and the "decision" output λ_k. The decision device finds the closest point in the infinite extension of the constellation[16]. The extension of the constellation is the set of points that continue to be spaced by $d_{\min}$ from the points on the edges of the original constellation and along the same dimensions as the original constellation. m_k is therefore a small error signal that is uniform in distribution over $(-d/2, d/2)$, thus having variance $d^2/12 << \mathcal{E}_x$.

Because of the combination of channel and feedforward equalizer filters, the feedforward filter output is

$$Z_U(D) = [X(D) + M(D)] \cdot G_U(D) + E_U(D) = X(D) - \lambda(D) + E_U(D) \quad . \tag{3.455}$$

Processing $Z_U(D)$ by a decision operation leaves $X(D) - \lambda(D)$, which essentially is the decision. However, to recover the input sequence $X(D)$, the receiver forms

$$Z'(D) = \frac{X(D) - \lambda(D)}{G_U(D)} = X(D) + M(D) \quad . \tag{3.456}$$

Since $M(D)$ is uniform and has magnitude always less than $d/2$, then $M(D)$ is removed by a second truncation (which is not really a decision, but operates using essentially the same logic as the first decision).

---

[16] The maximum range of such an infinite extension is actually the sum $\sum_{i=1}^{\nu} |\Re \text{ or } \Im g_{U,i}| \cdot |\bar{R}_{ee}(D) \text{ or } \Im x_{max}|$.
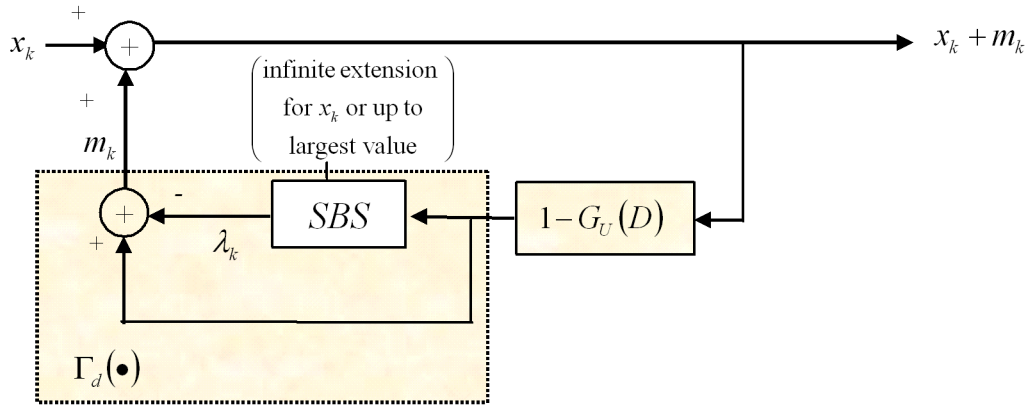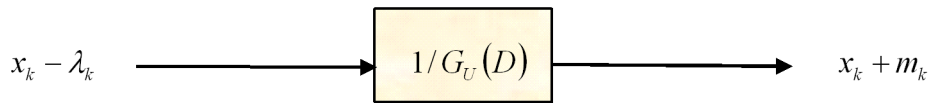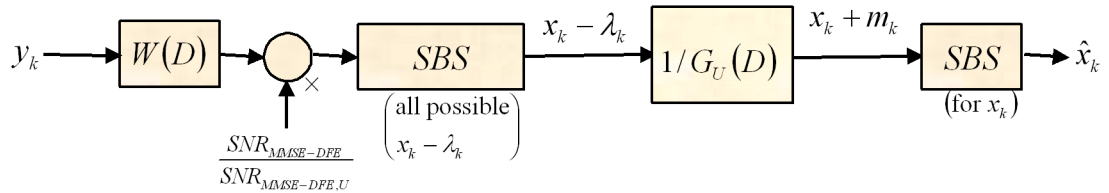
Figure 3.49: Flexible Precoding.
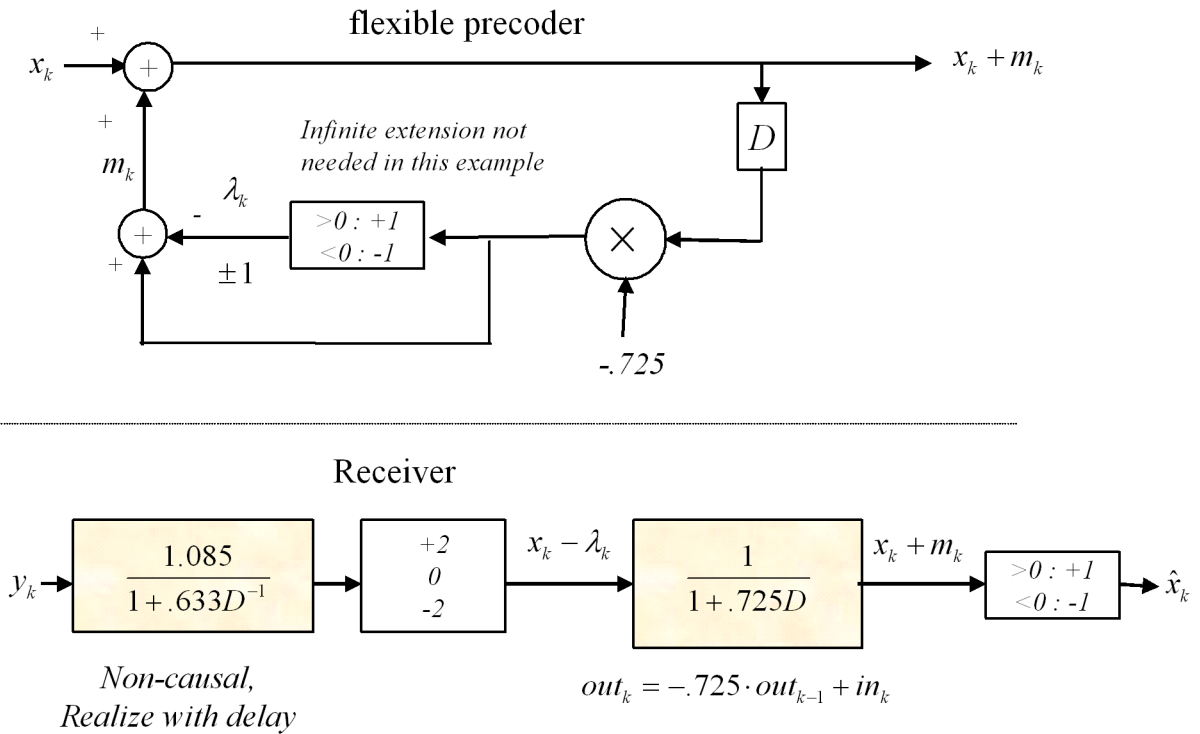
Figure 3.50: Flexible Precoding Example.

Example and error propagation in flexible precoding

EXAMPLE 3.8.1 ($1 + .9D^{-1}$ system with flexible precoding) The flexible precoder and corresponding receiver for the $1 + .9D^{-1}$ example appear in Figure 3.50. The bias removal factor has been absorbed into all filters (7.85/6.85 multiples .633 to get .725 in feedback section, and multiplies .9469 to get 1.085 in feedforward section). The decision device is binary in this case since binary antipodal transmission is used. Note the IIR filter in the receiver. If an error is made in the first SBS in the receiver, then the magnitude of the error is $2 = |+1 - (-1)| = |-1 - (+1)|$. Such an error is like an impulse of magnitude 2 added to the input of the IIR filter, which has impulse response $(-.725)^k \cdot u_k$, producing a contribution to the correct sequence of $2 \cdot (-.725)^k \cdot u_k$. This produces an additional 1 error half the time and an additional 2 errors 1/4 the time. Longer strings of errors will not occur. Thus, the bit and symbol error rate in this case increase by a factor of 1.5. (less than .1 dB loss).

A minor point is that the first decision in the receiver has an increased nearest neighbor coefficient of $N_e = 1.5$.

Generally speaking, when an error is made in the receiver for the flexible precoder,

$$(x_k - \lambda_k) - \text{decision}(x_k - \lambda_k) = \epsilon \cdot \delta_k \tag{3.457}$$

where ϵ could be complex for QAM. Then the designer needs to compute for each type of such error, its probability of occurence and then investigate the string (with $(1/b)_k$ being the impulse response of the post-first-decision filter in the receiver)

$$|\epsilon \cdot (1/b)^k| << d_{\min}/2 \quad . \tag{3.458}$$

For some k, this relation will hold and that is the maximum burst length possible for the particular type of error. Given the filter b is monic and minimum phase, this string should not be too long as long as the

roots are not too close to the unit circle. The single error may cause additional errors, but none of these additional errors in turn cause yet more errors (unlike a DFE where second and subsequent errors can lead to some small probability of infinite-length bursts), thus the probaility of an infinitely long burst is zero for the flexible precoder situation (or indeed any burst longer than the k that solves the above equation.

3.8.2 Partial Response Channel Models

Partial-response methods are a special case of precoding design where the ISI is forced to some known well-defined pattern. Receiver detectors are then designed for such partial-response channels directly, exploiting the known nature of the ISI rather than attempting to eliminate this ISI.

Classic uses of partial response abound in data transmission, some of which found very early use. For instance, the earliest use of telephone wires for data transmission inevitably found large intersymbol interference because of a transformer that was used to isolate DC currents at one end of a phone line from those at the other (see Prob 3.35). The transformer did not pass low frequencies (i.e., DC), thus inevitably leading to non-Nyquist[17] pulse shapes even if the phone line otherwise introduced no signficant intersymbol interference. Equalization may be too complex or otherwise undesirable as a solution, so a receiver can use a detector design that instead presumes the presence of a known fixed ISI. Another example is magnetic recording (see Problem 3.36) where only flux changes on a recording surface can be sensed by a read-head, and thus D.C. will not pass through the "read channel," again inevitably leading to ISI. Straightforward equalization is often too expensive at the very high speeds of magnetic-disk recording systems.

Partial-Response (PR) channels have non-Nyquist pulse responses – that is, PR channels allow intersymbol interference – over a few (and finite number of) sampling periods. A unit-valued sample of the response occurs at time zero and the remaining non-zero response samples at subsequent sampling times, thus the name "partial response." The study of PR channels is facilitated by mathematically presuming the tacit existence of a whitened matched filter, as will be described shortly. Then, a number of common PR channels can be easily addressed.

Figure 3.51(a) illustrates the whitened-matched-filter. The minimum-phase equivalent of Figure 3.51(b) exists if $Q(D) = \eta_0 \cdot H(D) \cdot H^*(D^{-*})$ is factorizable.[18] This chapter focuses on the discrete-time channel and presumes the WMF's presence without explicitly showing or considering it. The signal output of the discrete-time channel is

$$y_k = \sum_{m=-\infty}^{\infty} h_m \cdot x_{k-m} + n_k \quad , \tag{3.459}$$

or

$$Y(D) = H(D) \cdot X(D) + N(D) \quad , \tag{3.460}$$

where n_k is sampled Gaussian noise with autocorrelation $\bar{r}_{nn,k} = \|p\|^{-2} \cdot \eta_0^{-1} \cdot \frac{N_0}{2} \cdot \delta_k$ or $\bar{R}_{nn}(D) = \|p\|^{-2} \cdot \eta_0^{-1} \cdot \frac{N_0}{2}$ when the whitened-matched filter is used, and just denoted σ_{pr}^2 otherwise. In both cases, this noise is exactly AWGN with mean-square sample value σ_{pr}^2, which is conveniently abbreviated σ^2 for the duration of this chapter.

> **Definition 3.8.2 (Partial-Response Channel)** *A **partial-response** (PR) channel is any discrete-time channel with input/output relation described in (3.459) or (3.460) that also satisfies the following properties:*
>
> *1. h_k is finite-length and causal; $h_k = 0 \;\; \forall\; k < 0 \text{ or } k > \nu$, where $\nu < \infty$ and is often called the **constraint length** of the partial-response channel,*
>
> *2. h_k is monic; $h_0 = 1$,*
>
> *3. h_k is minimum phase; $H(D)$ has all ν roots on or outside the unit circle,*

---

[17]That is, they do not satisfy Nyquist's condition for nonzero ISI - See Chapter 3, Section 3.

[18]$H(D) = P_c(D)$ in Section 3.6.3 on ZF-DFE.
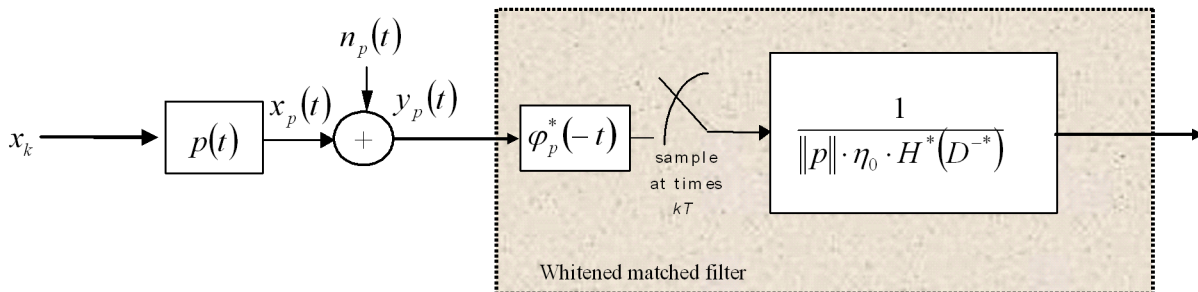
(a) ISI-Channel Model

- -
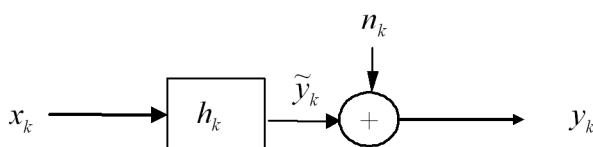
(b) Partial-Response Channel

Figure 3.51: Minimum Phase Equivalent Channel.

;'

4. h_k has all integer coefficients; $h_k \in \mathcal{Z} \; \forall \; k \neq 0$ (where $\mathcal{Z}$ denotes the set of integers).

*More generally, a discrete finite-length channel satisfying all properties above except the last restriction to all integer coefficients is known as a **controlled intersymbol-interference** channel.*

Controlled ISI and PR channels are a special subcase of all ISI channels, for which $h_k = 0 \; \forall \; k > \nu$. ν is the **constraint length** of the controlled ISI channel. Thus, effectively, the channel can be modeled as an FIR filter, and h_k is the minimum-phase equivalent of the sampled pulse response of that FIR filter. The constraint length defines the span in time νT of the non-zero samples of this FIR channel model.

The controlled ISI polynomial (D-transform)[19] for the channel simplifies to

$$ H(D) \triangleq \sum_{m=0}^{\nu} h_m D^m \quad , \tag{3.461} $$

where $H(D)$ is always monic, causal, minimum-phase, and an all-zero (FIR) polynomial. If the receiver processes the channel output of an ISI-channel with the same whitened-matched filter that occurs in the ZF-DFE of Section 3.6, and if $P_c(D)$ (the resulting discrete-time minimum-phase equivalent channel polynomial when it exists) is of finite degree ν, then the channel is a controlled intersymbol interference channel with $H(D) = P_c(D)$ and $\sigma^2 = \frac{N_0}{2} \cdot \|p\|^{-2} \cdot \eta_0^{-1}$. Any controlled intersymbol-interference channel is in the form that the Tomlinson Precoder of Section 3.8.1 could be used to implement symbol-by-symbol detection on the channel output. As noted in Section 3.8.1, a (usually small) transmit symbol energy increase occurs when the Tomlinson Precoder is used. Section 3.8.4 shows that this loss can be avoided for the special class of polynomials $H(D)$ that are partial-response channels.

---

[19]The D-Transform of FIR channels ($\nu < \infty$) is often called the "channel polynomial," rather than its "D-Transform" in partial-response theory. This text uses these two terms interchangeably.
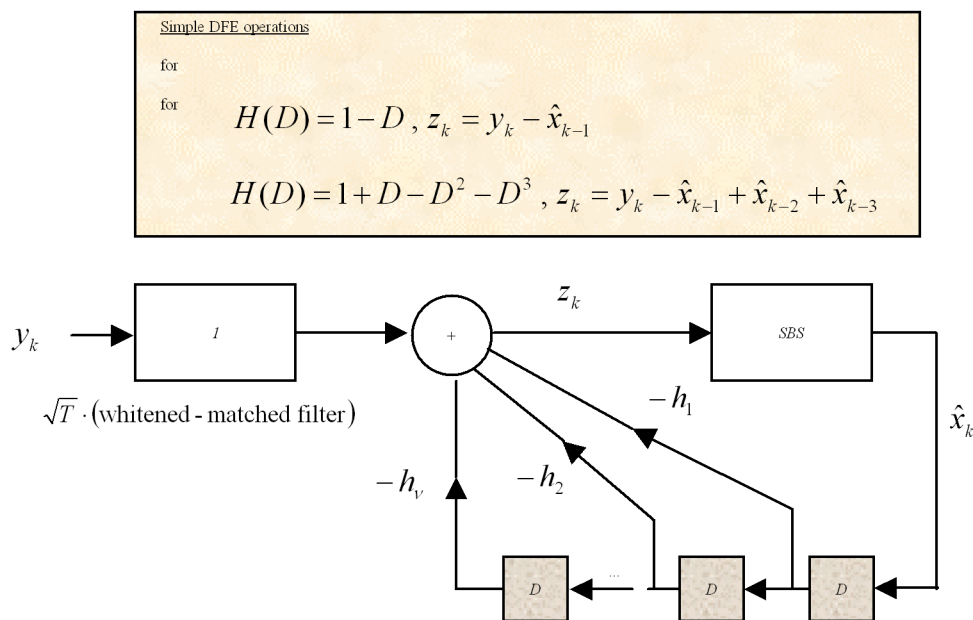
Figure 3.52: Simple DFE for some partial-response channels.

Equalizers for the Partial-response channel.

This small subsection serves to simplify and review equalization structure on the partial-response channel.

The combination of integer coefficients and minimum-phase constraints of partial-response channels allows a very simple implementation of the ZF-DFE as in Figure 3.52. Since the PR channel is already discrete time, no sampling is necessary and the minimum-phase characteristic of $H(D)$ causes the WMF of the ZF-DFE to simplify to a combined transfer function of 1 (that is, there is no feedforward section because the channel is already minimum phase). The ZF-DFE is then just the feedback section shown, which easily consists of the feedback coefficients $-h_m$ for the delayed decisions corresponding to $\hat{x}_{k-m}, m = 1, ..., \nu$. The loss with respect to the matched filter bound is trivially $1/\|H\|^2$, which is easily computed as 3 dB for $H(D) = 1 \pm D^\nu$ (any finite ν) with simple ZF-DFE operation $z_k = y_k - \hat{x}_{k-\nu}$ and 6 dB for $H(D) = 1 + D - D^2 - D^3$ with simple ZF-DFE operation $z_k = y_k - \hat{x}_{k-1} + \hat{x}_{k-2} + \hat{x}_{k-3}$.

The ZF-LE does not exist if the channel has a zero on the unit circle, which all partial-response channels do. A MMSE-LE could be expected to have signficant noise enhancement while existing. The MMSE-DFE will perform slightly better than the ZF-DFE, but is not so easy to compute as the simple DFE. Tomlinson or Flexible precoding could be applied to eliminate error propagation for a small increase in transmit power ($\frac{M^2}{M^2-1}$).

3.8.3 Classes of Partial Response

A particularly important and widely used class of partial response channels are those with $H(D)$ given by

$$H(D) = (1 + D)^l (1 - D)^n \quad , \tag{3.462}$$

where l and n are nonnegative integers.

For illustration, Let $l = 1$ and $n = 0$ in (3.462), then

$$H(D) = 1 + D \quad , \tag{3.463}$$
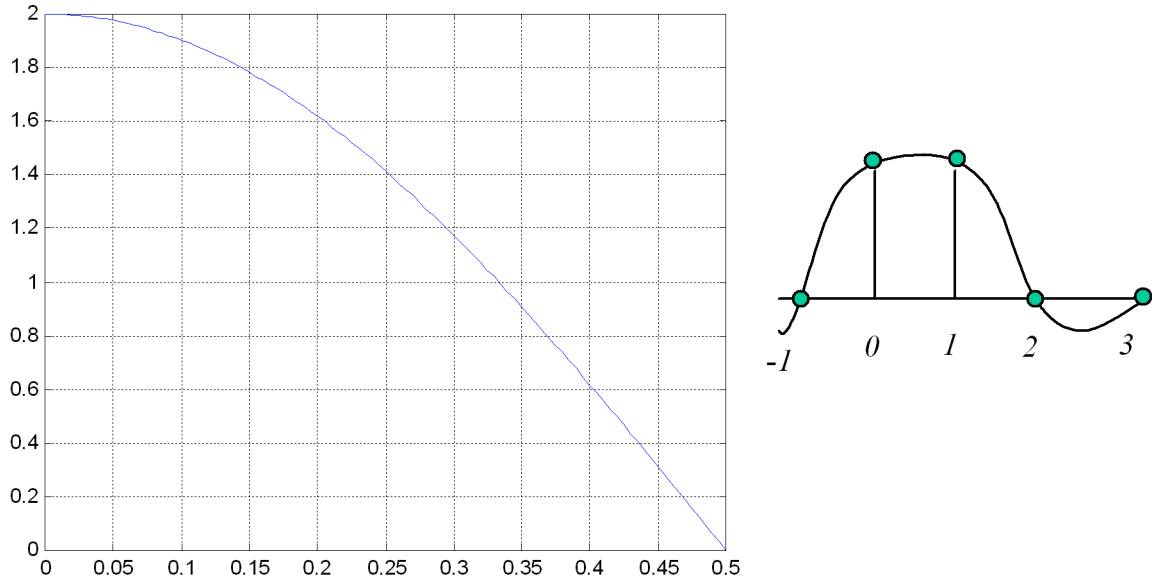
Figure 3.53: Transfer Characteristic for Duobinary signaling.

which is sometimes called a "duobinary" channel (introduced by Lender in 1960). The Fourier transform of the duobinary channel is

$$H(e^{-\jmath\omega T}) = H(D)|_{D=e^{-\jmath\omega T}} = 1 + e^{-\jmath\omega T} = 2e^{-\jmath\omega T/2} \cdot \cos\left(\frac{\omega T}{2}\right) \quad . \tag{3.464}$$

The transfer function in (3.464) has a notch at the Nyquist Frequency and is generally "lowpass" in shape, as is shown in Figure 3.53. A discrete-time ZFE operating on this channel would produce infinite noise enhancement. If $\text{SNR}_{MFB} = 16$ dB for this channel, then

$$Q(e^{-\jmath\omega T}) + \frac{1}{\text{SNR}_{MFB}} = (1 + 1/40) + \cos\omega T \quad . \tag{3.465}$$

The MMSE-LE will have performance (observe that $\frac{\mathcal{N}_0}{2} = .05$)

$$\sigma^2_{MMSE-LE} = \frac{\mathcal{N}_0}{2} \frac{T}{2\pi} \int_{-\frac{\pi}{T}}^{\frac{\pi}{T}} \frac{1}{\|p\|^2(1.025 + \cos\omega T)} d\omega = \frac{\mathcal{N}_0}{2} \frac{1/2}{\sqrt{1.025^2 - 1^2}} = 2.22 \frac{\mathcal{N}_0}{2} \quad , \tag{3.466}$$

The $\text{SNR}_{MMSE-LE,U}$ is easily computed to be 8 (9dB), so the equalizer loss is 7 dB in this case. For the MMSE-DFE, $Q(D) + \frac{1}{\text{SNR}_{MFB}} = \frac{1.025}{1.64}(1 + .8D)(1 + .8D^{-1})$, so that $\gamma_0 = 1.025/1.64 = .625$, and thus $\gamma_{\text{MMSE-DFE}} = 2.2$dB. For the ZF-DFE, $\eta_0 = \frac{1}{2}$, and thus $\gamma_{\text{ZF-DFE}} = 3$dB.

It is possible to achieve MFB performance on this channel with complexity far less than any equalizer studied earlier in this chapter, as will be shown in Chapter 9. It is also possible to use a precoder with no transmit power increase to eliminate the error-propagation-prone feedback section of the ZF-DFE.

There are several specific channels that are used in practice for partial-response detection:

EXAMPLE 3.8.2 (Duobinary $1 + D$) The duobinary channel (as we have already seen) has

$$H(D) = 1 + D \quad . \tag{3.467}$$

237

The frequency response was already plotted in Figure 3.53. This response goes to zero at the Nyquist Frequency, thus modeling a lowpass-like channel. For a binary input of $x_k = \pm 1$, the channel output (with zero noise) takes on values ± 2 with probability $1/4$ each and 0 with probability $1/2$. In general, for M-level inputs ($\pm 1 \; \pm 3 \; \pm 5 \; ... \; \pm (M-1)$), there are $2M - 1$ possible output levels, $-2M + 2$, ..., 0, ..., $2M - 2$. These output values are all possible sums of pairs of input symbols.

EXAMPLE 3.8.3 (DC Notch $1 - D$) The DC Notch channel has

$$H(D) = 1 - D \quad , \tag{3.468}$$

so that $l = 0$ and $n = 1$ in (3.462). The frequency response is

$$H(e^{-\jmath \omega T}) = 1 - e^{-\jmath \omega T} = 2\jmath e^{-\jmath \omega \frac{T}{2}} \cdot \sin \frac{\omega T}{2} \quad . \tag{3.469}$$

The response goes to zero at the DC ($\omega = 0$), thus modeling a highpass-like channel. For a binary input of $x_k = \pm 1$, the channel output (with zero noise) takes on values ± 2 with probability $1/4$ each and 0 with probability $1/2$. In general for M-level inputs ($\pm 1 \; \pm 3 \; \pm 5 \; ... \; \pm (M-1)$), there are $2M - 1$ possible output levels, $-2M + 2$, ..., 0, ..., $2M - 2$.

When the $1 - D$ shaping is imposed in the modulator itself, rather than by a channel, the corresponding modulation is known as **AMI (Alternate Mark Inversion)** if a differential encoder is also used as shown later in this section. AMI modulation prevents "charge" (DC) from accumulating and is sometimes also called "bipolar coding," although the use of the latter term is often confusing because bipolar transmission may have other meanings for some communications engineers. AMI coding, and closely related methods are used in multiplexed T1 (1.544 Mbps DS1 or "ANSI T1.403") and E1 (2.048 Mbps or "ITU-T G.703") speed digital data transmission on twisted pairs or coaxial links. These signals were once prevalent in telephone-company non-fiber central-office transmission of data between switch elements.

EXAMPLE 3.8.4 (Modified Duobinary $1 - D^2$) The modified duobinary channel has

$$H(D) = 1 - D^2 = (1 + D)(1 - D) \quad , \tag{3.470}$$

so $l = n = 1$ in (3.462). Modified Duobinary is sometimes also called "Partial Response Class IV" or PR4 or PRIV in the literature. The frequency response is

$$H(e^{-\jmath \omega T}) = 1 - e^{-\jmath \omega 2T} = 2\jmath e^{-\jmath \omega T} \cdot \sin(\omega T) \quad . \tag{3.471}$$

The response goes to zero at the DC ($\omega = 0$) and at the Nyquist frequency ($\omega = \pi/T$), thus modeling a bandpass-like channel. For a binary input of $x_k = \pm 1$, the channel output (with zero noise) takes on values ± 2 with probability $1/4$ each and 0 with probability $1/2$. In general, for M-level inputs ($\pm 1 \; \pm 3 \; \pm 5 \; ... \; \pm (M-1)$), there are $2M - 1$ possible output levels. Modified duobinary is equivalent to two interleaved $1 - D$ channels, each independently acting on the inputs corresponding to even (odd) time samples, respectively. Many commercial disk drives use PR4.

EXAMPLE 3.8.5 (Extended Partial Response 4 and 6 $(1 + D)^l(1 - D)^n$) The EPR4 channel has $l = 2$ and $n = 1$ or

$$H(D) = (1 + D)^2(1 - D) = 1 + D - D^2 - D^3 \quad . \tag{3.472}$$

This channel is called EPR4 because it has 4 non-zero samples (Thapar). The frequency response is

$$H(e^{-\jmath \omega T}) = (1 + e^{-\jmath \omega T})^2(1 - e^{-\jmath \omega T}) \quad . \tag{3.473}$$
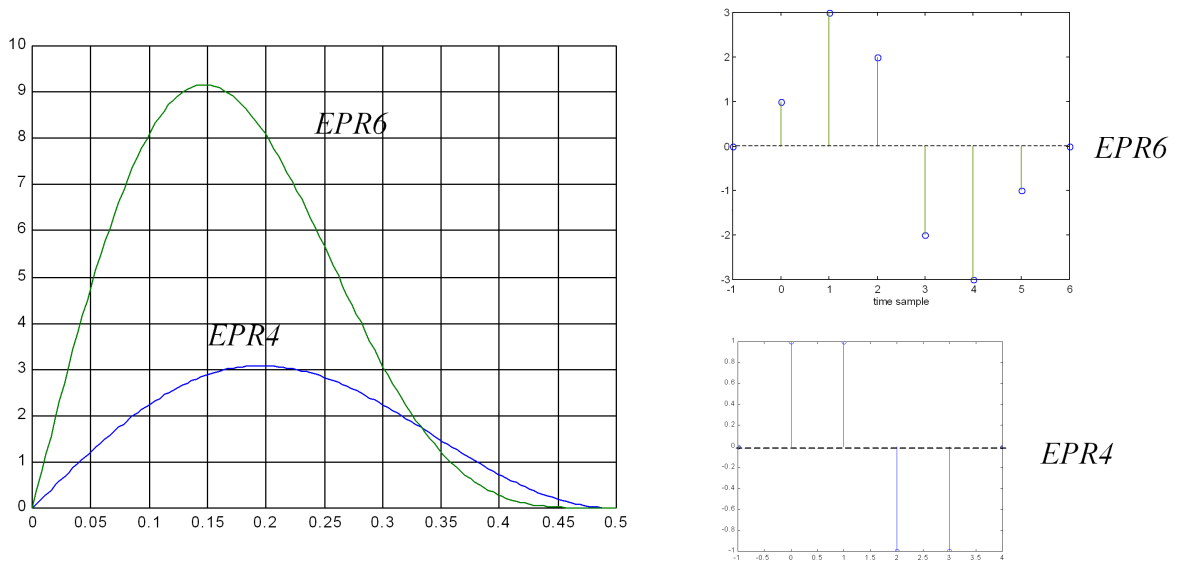
Figure 3.54: Transfer Characteristic for EPR4 and EPR6

The EPR6 channel has $l = 4$ and $n = 1$ (6 nonzero samples)

$$H(D) = (1 + D)^4(1 - D) = 1 + 3D + 2D^2 - 2D^3 - 3D^4 - D^5 \quad . \tag{3.474}$$

The frequency response is

$$H(e^{-\jmath\omega T}) = (1 + e^{-\jmath\omega T})^4(1 - e^{-\jmath\omega T}) \quad . \tag{3.475}$$

These 2 channels, along with PR4, are often used to model disk storage channels in magnetic disk or tape recording. The response goes to zero at DC ($\omega = 0$) and at the Nyquist frequency in both EPR4 and EPR6, thus modeling bandpass-like channels. The magnitude of these two frequency characteristics are shown in Figure 3.54. These are increasingly used in commercial disk storage read detectors.

The higher the l, the more "lowpass" in nature that the EPR channel becomes, and the more appropriate as bit density increases on any given disk.

For partial-response channels, the use of Tomlinson Precoding permits symbol-by-symbol detection, but also incurs an $M^2/(M^2 - 1)$ signal energy loss for PAM (and $M/(M - 1)$ for QAM). A simpler method for PR channels, that also has no transmit energy penalty, is known simply as a "precoder."

3.8.4 Simple Precoding

The simplest form of precoding for the duobinary, DC-notch, and modified duobinary partial-response channels is the so-called "**differential encoder**." The message at time k, m_k, is assumed to take on values $m = 0, 1, ..., M - 1$. The differential encoder for the case of $M = 2$ is most simply described as the device that observes the input bit stream, and changes its output if the input is 1 and repeats the last output if the input is 0. Thus, the differential encoder input, m_k, represents the difference (or sum) between adjacent differential encoder output ($\bar{m}_k$ and $\bar{m}_{k-1}$) messages[20]:

---

[20]This operation is also very useful even on channels without ISI, as an unknown inversion in the channel (for instance, an odd number of amplifiers) will cause all bits to be in error if (differential) precoding is not used.
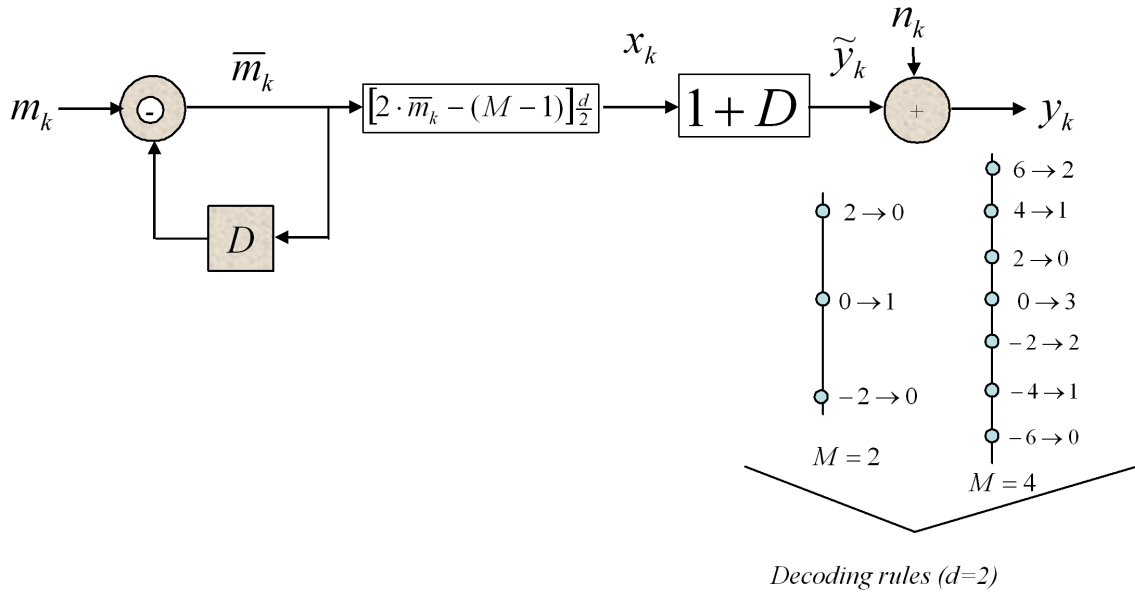
Figure 3.55: Precoded Partial Response Channel.

Definition 3.8.3 (Differential Encoder) **Differential encoders** *for PAM or QAM modulation obey one of the two following relationships:*

$$\bar{m}_k = m_k \ominus \bar{m}_{k-1} \qquad (3.476)$$

$$\bar{m}_k = m_k \oplus \bar{m}_{k-1} \quad , \qquad (3.477)$$

where $\ominus$ represents subtraction modulo M (and $\oplus$ represents addition modulo M). For SQ QAM, the modulo addition and subtraction are performed independently on each of the two dimensions, with $\sqrt{M}$ replacing M. (A differential phase encoder is also often used for QAM and is discussed later in this section.)

A differential encoder is shown on the left side of Figure 3.55. As an example if $M = 4$ the corresponding inputs and outputs are given in the following table:

m_k	-	3	1	0	2	1	0	3
$\bar{m}_k$	0	3	2	2	0	1	3	0
k	-1	0	1	2	3	4	5	6

With either PAM or QAM constellations, the dimensions of the encoder output $\bar{m}_k$ are converted into channel input symbols ($\pm\frac{d}{2}$, $\pm\frac{3d}{2}$...) according to

$$x_k = [2\bar{m}_k - (M - 1)]\frac{d}{2} \quad . \qquad (3.478)$$

Figure 3.55 illustrates the duobinary channel $H(D) = 1 + D$, augmented by the precoding operation of differential encoding as defined in (3.476). The noiseless minimum-phase-equivalent channel output $\tilde{y}_k$ is

$$\tilde{y}_k = x_k + x_{k-1} = 2(\bar{m}_k + \bar{m}_{k-1})\frac{d}{2} - 2(M - 1)\frac{d}{2} \qquad (3.479)$$

so[21]

$$\frac{\tilde{y}_k}{d} + (M - 1) = \bar{m}_k + \bar{m}_{k-1} \qquad (3.480)$$

---

[21] $(\bullet)_M$ means the quantity is computed in M-level arithmetic, for instance, $(5)_4 = 1$. Also note that $\Gamma_M(x) \neq (x)_M$, and therefore $\oplus$ is different from the $\oplus_M$ of Section 3.5. The functions $(x)_M$ and $\oplus$ have strictly integer inputs and have possible outputs $0, ..., M - 1$ only.

$$\left(\left[\frac{\tilde{y}_k}{d} + (M-1)\right]\right)_M = \bar{m}_k \oplus \bar{m}_{k-1} \tag{3.481}$$

$$\left(\left[\frac{\tilde{y}_k}{d} + (M-1)\right]\right)_M = m_k \tag{3.482}$$

where the last relation (3.482) follows from the definition in (3.476). All operations are integer mod-M. Equation (3.482) shows that a decision on $\tilde{y}_k$ about m_k can be made without concern for preceding or succeeding $\tilde{y}_k$, because of the action of the precoder. The decision boundaries are simply the obvious regions symmetrically placed around each point for a memoryless ML detector of inputs and the decoding rules for $M = 2$ and $M = 4$ are shown in Figure 3.55. In practice, the decoder observes y_k, not $\tilde{y}_k$, so that y_k must first be quantized to the closest noise-free level of y_k. That is, the decoder first quantizes $\tilde{y}_k$ to one of the values of $(-2M + 2)(d/2)$, ..., $(2M - 2)(d/2)$. Then, the minimum distance between outputs is $d_{\min} = d$, so that $\frac{d_{\min}}{2\sigma_{pr}} = \frac{d}{2\sigma_{pr}}$, which is 3 dB below the $\sqrt{MFB} = \frac{\sqrt{2}}{\sigma_{pr}}(d/2)$ for the $1 + D$ channel because $\|p\|^2 = 2$. (Again, $\sigma_{pr}^2 = \|p\|^{-2} \cdot \eta_0^{-1} \cdot \frac{N_0}{2}$ with a WMF and otherwise is just σ_{pr}^2.) This loss is identical to the loss in the ZF-DFE for this channel. One may consider the feedback section of the ZF-DFE as having been pushed through the linear channel back to the transmitter, where it becomes the precoder. With some algebra, one can show that the TPC, while also effective, would produce a 4-level output with 1.3 dB higher average transmit symbol energy for binary inputs. The output levels are assumed equally likely in determining the decision boundaries (half way between the levels) even though these levels are not equally likely.

The precoded partial-response system eliminates error propagation, and thus has lower P_e than the ZF-DFE. This elimination of error propagation can be understood by investigating the nearest neighbor coefficient for the precoded situation in general. For the $1 + D$ channel, the (noiseless) channel output levels are $-(2M - 2) - (2M - 4)... 0 ... (2M - 4) (2M - 2)$ with probabilities of occurrence $\frac{1}{M^2}$ $\frac{2}{M^2}$ ... $\frac{M}{M^2}$ ... $\frac{2}{M^2}$ $\frac{1}{M^2}$, assuming a uniform channel-input distribution. Only the two outer-most levels have one nearest neighbor, all the rest have 2 nearest neighbors. Thus,

$$\bar{N}_e = \frac{2}{M^2}(1) + \frac{M^2 - 2}{M^2}(2) = 2\left(1 - \frac{1}{M^2}\right) \quad . \tag{3.483}$$

For the ZF-DFE, the input to the decision device $\tilde{z}_k$ as

$$\tilde{z}_k = x_k + x_{k-1} + n_k - \hat{x}_{k-1} \quad , \tag{3.484}$$

which can be rewritten

$$\tilde{z}_k = x_k + (x_{k-1} - \hat{x}_{k-1}) + n_k \quad . \tag{3.485}$$

Equation 3.485 becomes $\tilde{z}_k = x_k + n_k$ if the previous decision was correct on the previous symbol. However, if the previous decision was incorrect, say $+1$ was decided (binary case) instead of the correct -1, then

$$\tilde{z}_k = x_k - 2 + n_k \quad , \tag{3.486}$$

which will lead to a next-symbol error immediately following the first almost surely if $x_k = 1$ (and no error almost surely if $x_k = -1$). The possibility of $\tilde{z}_k = x_k + 2 + n_k$ is just as likely to occur and follows an identical analysis with signs reversed. For either case, the probability of a second error propagating is $1/2$. The other half of the time, only 1 error occurs. Half the times that 2 errors occur, a third error also occurs, and so on, effectively increasing the error coefficient from $N_e = 1$ to

$$N_e = 2 = 1(\frac{1}{2}) + 2(\frac{1}{4}) + 3(\frac{1}{8}) + 4(\frac{1}{16}) + ... = \sum_{k=1}^{\infty} k \cdot (.5)^k = \frac{.5}{(1 - .5)^2} \quad . \tag{3.487}$$

(In general, the formula $\sum_{k=1}^{\infty} k \cdot r^k = \frac{r}{(1-r)^2}, r < 1$ may be useful in error propagation analysis.) The error propagation can be worse in multilevel PAM transmission, when the probability of a second error is $(M - 1)/M$, leading to

$$\frac{N_e(\text{error prop})}{N_e(\text{no error prop})} = 1 \cdot \frac{1}{M} + 2 \cdot \frac{M-1}{M} \cdot \frac{1}{M} + 3 \cdot \left(\frac{M-1}{M}\right)^2 \cdot \frac{1}{M} + ... \tag{3.488}$$

$$= \sum_{k=1}^{\infty} k \cdot \left(\frac{M-1}{M}\right)^{k-1} \cdot \frac{1}{M} \tag{3.489}$$

$$= M \quad . \tag{3.490}$$

Precoding eliminates this type of error propagation, although $\bar{N}_e$ increases by a factor[22] of $(1 + 1/M)$ with respect to the case where no error propagation occurred.

For the ZF-DFE system, $\bar{P}_e = 2(M-1)Q(\frac{d}{2\sigma_{pr}})$, while for the precoded partial-response system, $\bar{P}_e = 2\left(1 - \frac{1}{M^2}\right)Q(\frac{d}{2\sigma_{pr}})$. For $M \geq 2$, the precoded system always has the same or fewer nearest neighbors, and the advantage becomes particularly pronounced for large M. Using a rule-of-thumb that a factor of 2 increase in nearest neighbors is equivalent to an SNR loss of .2 dB (which holds at reasonable error rates in the 10^{-5} to 10^{-6} range), the advantage of precoding is almost .2 dB for $M = 4$. For $M = 8$, the advantage is about .6 dB, and for $M = 64$, almost 1.2 dB. Precoding can be simpler to implement than a ZF-DFE because the integer partial-response channel coefficients translate readily into easily realized finite-field operations in the precoder, while they represent full-precision add (and shift) operations in feedback section of the ZF-DFE.

Precoding the DC Notch or Modified Duobinary Channels

The $\bar{m}_k = m_k \ominus \bar{m}_{k-1}$ differential encoder works for the $1 + D$ channel. For the $1 - D$ channel, the equivalent precoder is

$$\bar{m}_k = m_k \oplus \bar{m}_{k-1} \quad , \tag{3.491}$$

which is sometimes also called **NRZI** (non-return-to-zero inverted) precoding, especially by storage-channel engineers. In the $1 - D$ case, the channel output is

$$\tilde{y}_k = x_k - x_{k-1} = 2(\bar{m}_k - \bar{m}_{k-1})\frac{d}{2} \tag{3.492}$$

$$\frac{\tilde{y}_k}{d} = \bar{m}_k - \bar{m}_{k-1} \tag{3.493}$$

$$\left(\frac{\tilde{y}_k}{d}\right)_M = \bar{m}_k \ominus \bar{m}_{k-1} \tag{3.494}$$

$$\left(\frac{\tilde{y}_k}{d}\right)_M = m_k \quad . \tag{3.495}$$

The minimum distance and number of nearest neighbors are otherwise identical to the $1 + D$ case just studied, as is the improvement over the ZF-DFE. The $1 - D^2$ case is identical to the $1 - D$ case, on two interleaved $1 - D$ channels at half the rate. The overall precoder for this situation is

$$\bar{m}_k = m_k \oplus \bar{m}_{k-2} \quad , \tag{3.496}$$

and the decision rule is

$$\left(\frac{\tilde{y}_k}{d}\right)_M = m_k \quad . \tag{3.497}$$

The combination of precoding with the $1 - D$ channel is often called "alternate mark inversion (AMI)" because each successive transmitted "1" bit value causes a nonzero channel output amplitude of polarity oppositie to the last nonzero channel output amplitude, while a "0" bit always produces a 0 level at the channel output.

Precoding EPR4

An example of precoding for the extended Partial Response class is EPR4, which has $l = 2$ and $n = 1$ in (3.472), or EPR4. Then,

$$\tilde{y}_k = x_k + x_{k-1} - x_{k-2} - x_{k-3} \tag{3.498}$$

---

[22]The ratio of $2(1 - 1/M^2)$ with precoding to $2(1 - 1/M)$ for M-ary PAM with no error propagation effects included

$$\tilde{y}_k = d(\bar{m}_k + \bar{m}_{k-1} - \bar{m}_{k-2} - \bar{m}_{k-3}) \tag{3.499}$$

$$\frac{\tilde{y}_k}{d} = \bar{m}_k + \bar{m}_{k-1} - \bar{m}_{k-2} - \bar{m}_{k-3} \tag{3.500}$$

$$\left(\frac{\tilde{y}_k}{d}\right)_M = \bar{m}_k \oplus \bar{m}_{k-1} \ominus \bar{m}_{k-2} \ominus \bar{m}_{k-3} \tag{3.501}$$

$$\left(\frac{\tilde{y}_k}{d}\right)_M = m_k \tag{3.502}$$

where the precoder, from (3.502) and (3.501), is

$$\bar{m}_k = m_k \ominus \bar{m}_{k-1} \oplus \bar{m}_{k-2} \oplus \bar{m}_{k-3} \quad . \tag{3.503}$$

The minimum distance at the channel output is still d in this case, so $P_e \leq N_e \cdot Q(d/2\sigma_{pr})$, but the MFB $= (\frac{d}{\sigma_{pr}})^2$, which is 6dB higher. The same 6dB loss that would occur with an error-propagation-free ZF-DFE on this channel.

For the $1 + D - D^2 - D^3$ channel, the (noiseless) channel output levels are $-(4M-4) \ -(4M-6)... 0 ... (4M-6) (4M-4)$. Only the two outer-most levels have one nearest neighbor, all the rest have 2 nearest neighbors. Thus,

$$\bar{N}_e = \frac{2}{M^4}(1) + \frac{M^4 - 2}{M^4}(2) = 2\left(1 - \frac{1}{M^4}\right) \quad . \tag{3.504}$$

Thus the probability of error for the precoded system is $\bar{P}_e = 2\left(1 - \frac{1}{M^4}\right) Q(\frac{1}{\sigma_{pr}})$. The number of nearest neighbors for the ZF-DFE, due to error propagation, is difficult to compute, but clearly will be worse.

3.8.5 General Precoding

The general partial response precoder can be extrapolated from previous results:

Definition 3.8.4 (The Partial-Response Precoder) *The* **partial-response precoder** *for a channel with partial-response polynomial $H(D)$ is defined by*

$$\bar{m}_k = m_k \bigoplus_{i=1}^{\nu} (-h_i) \cdot \bar{m}_{k-i} \quad . \tag{3.505}$$

The notation $\bigoplus$ means a mod-M summation, and the multiplication can be performed without ambiguity because the h_i and $\bar{m}_{k-i}$ are always integers.

The corresponding memoryless decision at the channel output is

$$\hat{m}_k = \left(\frac{\hat{y}_k}{d} + \sum_{i=0}^{\nu} h_i \left(\frac{M-1}{2}\right)\right)_M \quad . \tag{3.506}$$

The reader should be aware that while the relationship in (3.505) is general for partial-response channels, the relationship can often simplify in specific instances, for instance the precoder for "EPR5," $H(D) = (1+D)^3(1-D)$ simplifies to $\bar{m}_k = m_k \oplus \bar{m}_{k-4}$ when $M = 2$.

In a slight abuse of notation, engineers often simplify the representation of the precoder by simply writing it as

$$\mathcal{P}(D) = \frac{1}{H(D)} \tag{3.507}$$

where $\mathcal{P}(D)$ is a polynomial in D that is used to describe the "modulo-M" filtering in (3.505). Of course, this notation is symbolic. Furthermore, one should recognize that the D means unit delay in a finite field, and is therefore a delay operator only – one cannot compute the Fourier transform by inserting $D = e^{-\jmath\omega T}$ into $\mathcal{P}(D)$; Nevertheless, engineers commonly to refer to the NRZI precoder as a $1/(1 \oplus D)$ precoder.

Lemma 3.8.2 (Memoryless Decisions for the Partial-Response Precoder) *The partial-response precoder, often abbreviated by $\mathcal{P}(D) = 1/H(D)$, enables symbol-by-symbol decoding on the partial-response channel $H(D)$. An upper bound on the performance of such symbol-by-symbol decoding is*

$$\bar{P}_e \le 2 \left(1 - \frac{1}{M^{\nu+1}} \right) Q \left[\frac{d}{2\sigma_{pr}} \right] \quad , \tag{3.508}$$

where d is the minimum distance of the constellation that is output to the channel.

Proof: The proof follows by simply inserting (3.505) into the expression for $\tilde{y}_k$ and simplifying to cancel all terms with h_i, $i > 0$. The nearest-neighbor coefficient and $d/2\sigma_{pr}$ follow trivially from inspection of the output. Adjacent levels can be no closer than d on a partial-response channel, and if all such adjacent levels are assumed to occur for an upper bound on probability of error, then the $\bar{P}_e$ bound in (3.508) holds. **QED**.

3.8.6 Quadrature PR

Differential encoding of the type specified earlier is not often used with QAM systems, because QAM constellations usually exhibit 90° symmetry. Thus a 90° offset in carrier recovery would make the constellation appear exactly as the original constellation. To eliminate the ambiguity, the bit assignment for QAM constellations usually uses a precoder that uses the four possibilities of the most-significant bits that represent each symbol to specify a phase rotation of 0°, 90°, 180°, or 270° with respect to the last symbol transmitted. For instance, the sequence 01, 11, 10, 00 would produce (assuming an initial phase of 0°, the sequence of subsequent phases 90°, 0°, 180°, and 180°. By comparing adjacent decisions and their phase difference, these two bits can be resolved without ambiguity even in the presence of unknown phase shifts of multiples of 90°. This type of encoding is known as **differential phase encoding** and the remaining bits are assigned to points in large M QAM constellations so that they are the same for points that are just 90° rotations of one another. (Similar methods could easily be derived using 3 or more bits for constellations with even greater symmetry, like 8PSK.)

Thus the simple precoder for the $1 + D$ and $1 - D$ (or $1 - D^2$) given earlier really only is practical for PAM systems. The following type of precoder is more practical for these channels:

A Quadrature Partial Response (QPR) situation is specifically illustrated in Figure 3.56 for $M = 4$ or $\bar{b} = 1$ bit per dimension. The previous differential encoder could be applied individually to both dimensions of this channel, and it could be decoded without error. All previous analysis is correct, individually, for each dimension. There is, however, one practical problem with this approach: If the channel were to somehow rotate the phase by $\pm 90^o$ (that is, the carrier recovery system locked on the wrong phase because of the symmetry in the output), then there would be an ambiguity as to which part was real and which was imaginary. Figure 3.56 illustrates the ambiguity: the two messages $(0, 1) = 1$ and $(1, 0) = 2$ commute if the channel has an unknown phase shift of $\pm 90^o$. No ambiguity exists for either the message $(0, 0) = 0$ or the message $(1, 1) = 3$. To eliminate the ambiguity, the precoder encodes the 1 and 2 signals into a difference between the last 1 (or 2) that was transmitted. This precoder thus specifies that an input of 1 (or 2) maps to no change with respect to the last input of 1 (or 2), while an input of 2 maps to a change with respect to the last input of 1 or 2.

A precoding rule that will eliminate the ambiguity is then

Rule 3.8.1 (Complex Precoding for the 1+D Channel) if $m_k = (m_{i,k}, m_{q,k}) = (0, 0)$ or $(1, 1)$ then

$$\bar{m}_{i,k} = m_{i,k} \oplus \bar{m}_{i,k-1} \tag{3.509}$$
$$\bar{m}_{q,k} = m_{q,k} \oplus \bar{m}_{q,k-1} \tag{3.510}$$

else if $m_k = (m_{i,k}, m_{q,k}) = (0, 1)$ or $(1, 0)$, *check the last $\bar{m} = (0, 1)$ or $(1, 0)$ transmitted, call it $\bar{m}_{90}$, (that is, was $\bar{m}_{90} = 1$ or 2 ?). If $\bar{m}_{90} = 1$, the precoder leaves m_k unchanged prior to differential encoding according to (3.509) and (3.510). The operations $\oplus$ and $\ominus$ are the same in binary arithmetic.*
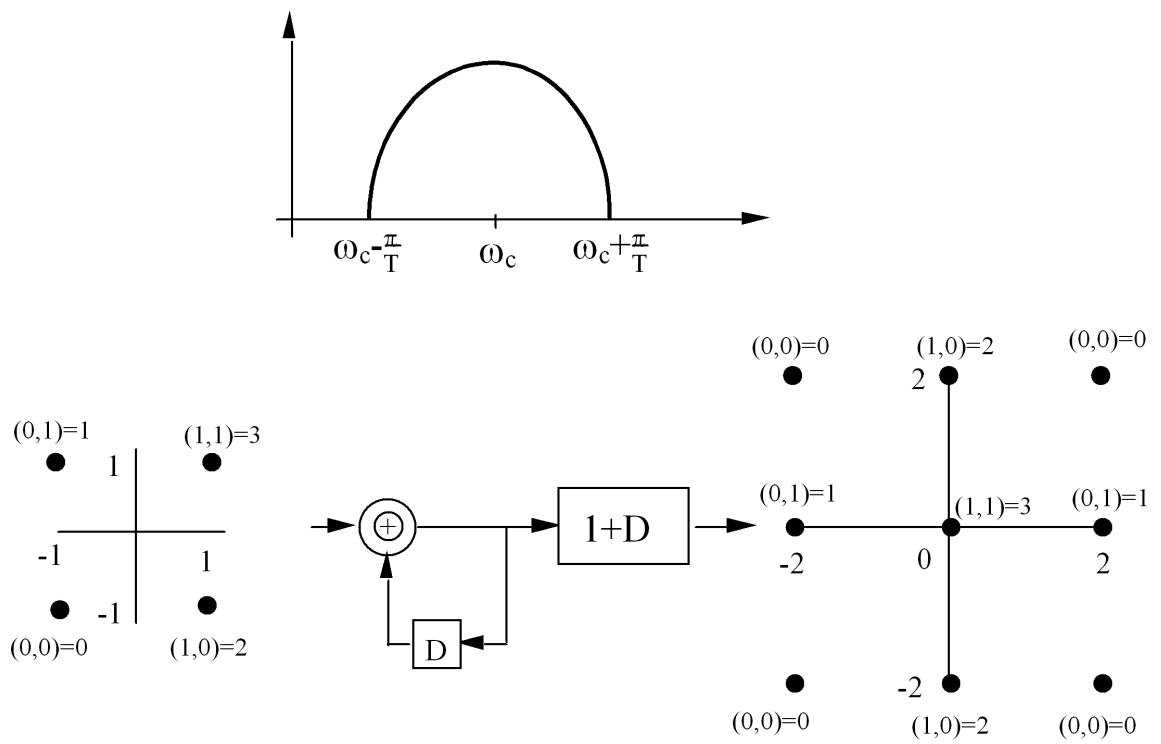
Figure 3.56: Quadrature Partial Response Example with $1 + D$.

If $\bar{m}_{90} = 2$, then the precoder changes m_k from 1 to 2 (or from 2 to 1) prior to encoding according to (3.509) and (3.510).

The corresponding decoding rule is (keeping a similar state $\hat{y}_{90} = 1, 2$ at the decoder)

$$\hat{m}_k = \begin{cases} (0,0) & \hat{y}_k = [\pm 2 \ \pm 2] \\ (1,1) & \hat{y}_k = [0 \ 0] \\ (0,1) & (\hat{y}_k = [0 \ \pm 2] \text{ or } \hat{y}_k = [\pm 2 \ 0]) \text{ and } \angle\hat{y}_k - \angle\hat{y}_{90} = 0 \\ (1,0) & (\hat{y}_k = [0 \ \pm 2] \text{ or } \hat{y}_k = [\pm 2 \ 0]) \text{ and } \angle\hat{y}_k - \angle\hat{y}_{90} \neq 0 \end{cases} . \qquad (3.511)$$

The probability of error and minimum distance are the same as was demonstrated earlier for this type of precoder, which only resolves the 90° ambiguity, but is otherwise equivalent to a differential encoder. There will however be limited error propagation in that one detection error on the 1 or 2 message points leads to two decoded symbol errors on the decoder output.
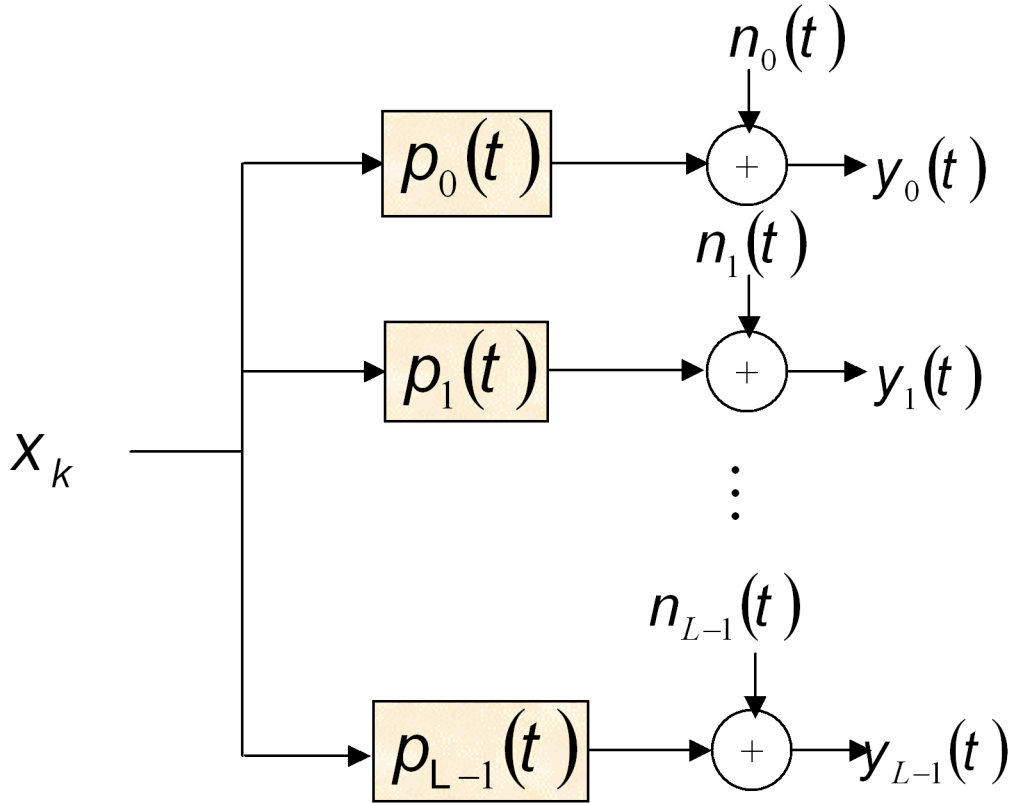
Figure 3.57: Basic diversity channel model.

3.9 Diversity Equalization

Diversity in transmission is the use of multiple channels from a single message source to several receivers, as illustrated in Figure 3.57. Optimally, the principles of Chapter 1 apply directly where the conditional probability distribution $p_{y/x}$ of the channel has a larger dimensionality on the channel output y than on the input, x, $N_y > N_x$. Often, this diversity leads to a lower probability of error for the same message, mainly because a greater channel-output minimum distance between possible (noiseless) output data symbols can be achieved with a larger number of channel output dimensions. However, intersymbol interference between successive transmissions, along with interference between the diversity dimensions, again can lead to a potentially complex optimum receiver and detector. Thus, equalization again allows productive use of suboptimal SBS detectors. The equalizers in the case of diversity become matrix equivalents of those studied in Sections 3.5 - 3.7.

3.9.1 Multiple Received Signals and the RAKE

Figure 3.57 illustrates the basic diversity channel. Channel outputs caused by the same channel input have labels $y_l(t)$, $l = 0, ..., L-1$. These channel outputs can be created intentionally by retransmission of the same data symbols at different times and/or (center) frequencies. Spatial diversity often occurs in wireless transmission where L spatially separated antennas may all receive the same transmitted signal, but possibly with different filtering and with noises that are at least partially independent.

With each channel output following the model

$$y_{p,l}(t) = \sum_k x_k p_l(t - kT) + n_l(t) \quad , \tag{3.512}$$

a corresponding $L \times 1$ vector channel description is

$$\boldsymbol{y}_p(t) = \sum_k x_k \boldsymbol{p}(t - kT) + \boldsymbol{n}_p(t) \quad , \tag{3.513}$$

where

$$\boldsymbol{y}_p(t) \triangleq \begin{bmatrix} y_0(t) \\ y_1(t) \\ \vdots \\ y_{L-1}(t) \end{bmatrix} \quad \boldsymbol{p}(t) \triangleq \begin{bmatrix} p_0(t) \\ p_1(t) \\ \vdots \\ p_{L-1}(t) \end{bmatrix} \quad \text{and} \quad \boldsymbol{n}_p(t) \triangleq \begin{bmatrix} n_0(t) \\ n_1(t) \\ \vdots \\ n_{L-1}(t) \end{bmatrix} \quad . \tag{3.514}$$

The generalization of an inner product is readily seen to be

$$< \boldsymbol{x}(t), \boldsymbol{y}(t) > = \sum_i \int_{-\infty}^{\infty} x_i(t) y_i^*(t) dt \quad . \tag{3.515}$$

Without loss of generality, the noise can be considered to be white on each of the L diversity channels, independent of the other diversity channels, and with equal power spectral densities $\frac{N_0}{2}$.[23]

A single transmission of x_0 corresponds to a vector signal

$$\boldsymbol{y}_p(t) = x_0 \cdot \boldsymbol{p}(t) + \boldsymbol{n}(t) = x_0 \cdot \|\boldsymbol{p}\| \cdot \boldsymbol{\varphi}_p(t) + \boldsymbol{n}(t) \quad . \tag{3.516}$$

This situation generalizes slightly that considered in Chapter 1, where matched-filter demodulators there combined all time instants through integration, a generalization of the inner product's usual sum of products. A matched filter in general simply combines the signal components from all dimensions that have independent noise. Here, that generalization of combination simply needs to include also the components corresponding to each of the diversity channels so that all signal contributions are summed to create maximum signal-to-noise ratio. The relative weighting of the different diversity channels is thus maintained through L unnormalized parallel matched filters each corresponding to one of the diversity channels. When several copies are combined across several diversity channels or new dimensions (whether created in frequency, long delays in time, or space), the combination is known as the **RAKE** matched filter of Figure 3.58:

> **Definition 3.9.1 (RAKE matched filter)** *A **RAKE** matched filter is a set of parallel matched filters each operating on one of the diversity channels in a diversity transmission system that is followed by a summing device as shown in Figure 3.58. Mathematically, the operation is denoted by*
>
> $$y_p(t) = \sum_{l=0}^{L-1} p_l^*(-t) * y_l(t) \quad . \tag{3.517}$$

The RAKE was originally so named by Green and Price in 1958 because of the analogy of the various matched filters being the "fingers" of a garden rake and the sum corresponding to the collection of the fingers at the rake's pole handle, nomenclature thus often being left to the discretion of the inventor, however unfortunate for posterity. The RAKE is sometimes also called a **diversity combiner**, although the latter term also applies to other lower-performance suboptimal combining methods that do not maximize overall signal to noise strength through matched filter. One structure, often called **maximal combining**, applies a matched filter only to the strongest of the L diversity paths to save complexity. The equivalent channel for this situation is then the channel corresponding to this maximum-strength individual path. The original RAKE concept was conceived in connection with a spread-spectrum transmission method that achieves diversity essentially in frequency (but more precisely in a code-division dimension to be discussed in the appendix of Chapter 5), but the matched filtering implied is

---

[23]In practice, the noises may be correlated with each other on different subchannels and not white with covariance matrix $\mathcal{R}_n(t)$ and power spectral density matrix $R_n(f) = \frac{N_0}{2} \cdot R_n^{1/2}(f) R_n^{*/2}(f)$. By prefiltering the vector channel output by the matrix filter $R_n^{-1/2}(f)$, the noise will be whitened and the noise equivalent matrix channel becomes $\boldsymbol{P}(f) \to R_n^{-1/2}(f) \boldsymbol{P}(f)$. Anaylsis with the equivalent channel can then proceed as if the noise where white, independent on the diversity channels, and of the same variance $\frac{N_0}{2}$ on all.
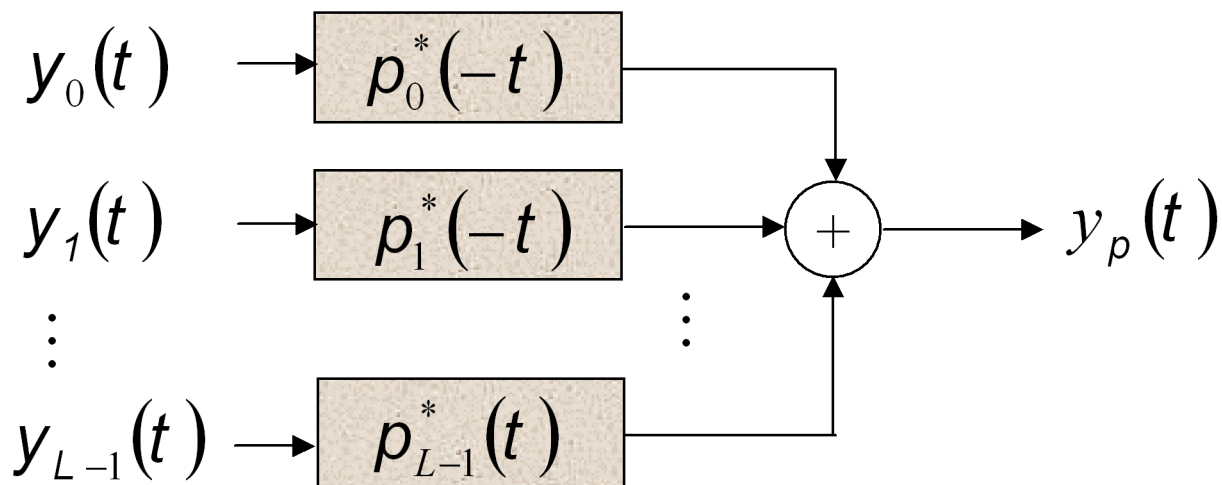
Figure 3.58: The basic RAKE matched filter combiner.

easily generalized. Some of those who later studied diversity combining were not aware of the connection to the RAKE and thus the multiple names for the same structure, although diversity combining is a more accurate name for the method.

This text also defines $r_l(t) = p_l(t) * p_l^*(-t)$ and

$$r(t) = \sum_{l=0}^{L-1} r_l(t) \tag{3.518}$$

for an equivalent RAKE-output equivalent channel and the norm

$$\|\boldsymbol{p}\|^2 = \sum_{l=0}^{L-1} \|p_l\|^2 \quad . \tag{3.519}$$

Then, the normalized equivalent channel $q(t)$ is defined through

$$r(t) = \|\boldsymbol{p}\|^2 \cdot q(t) \quad . \tag{3.520}$$

The sampled RAKE output has D-transform

$$Y(D) = X(D) \cdot \|\boldsymbol{p}\|^2 \cdot Q(D) + \boldsymbol{N}(D) \quad , \tag{3.521}$$

which is essentially the same as the early channel models used without diversity except for the additional scale factor of $\|\boldsymbol{p}\|^2$, which also occurs in the noise autcorrelation, which is

$$\bar{R}_{nn}(D) = \frac{\mathcal{N}_0}{2} \cdot \|\boldsymbol{p}\|^2 \cdot Q(D) \quad . \tag{3.522}$$

An $\text{SNR}_{MFB} = \frac{\bar{\mathcal{E}}_{\boldsymbol{x}} \|\boldsymbol{p}\|^2}{\frac{\mathcal{N}_0}{2}}$ and all other detector and receiver principles previously developed in this text now apply directly.

3.9.2 Infinite-length MMSE Equalization Structures

The sampled RAKE output can be scaled by the factor $\|\boldsymbol{p}\|^{-1}$ to obtain a model identical to that found earlier in Section 3.1 in Equation (3.26) with $Q(D)$ and $\|\boldsymbol{p}\|$ as defined in Subsection 3.9.1. Thus, the

MMSE-DFE, MMSE-LE, and ZF-LE/DFE all follow exactly as in Sections 3.5 -3.7. The matched-filter bound SNR and each of the equalization structures tend to work better with diversity because $\|\boldsymbol{p}\|^2$ is typically larger on the equivalent channel created by the RAKE. Indeed the RAKE will work better than any of the individual channels, or any subset of the diversity channels, with each of the equalizer structures.

Often while one diversity channel has severe characteristics, like an inband notch or poor transmission characteristic, a second channel is better. Thus, diversity systems tend to be more robust.

EXAMPLE 3.9.1 (Two ISI channels in parallel) Figure 3.59 illustrates two diversity channels with the same input and different intersymbol interference. The first upper channel has a sampled time equivalent of $1 + .9D^{-1}$ with noise variance per sample of .181 (and thus could be the channel consistently examined throughout this Chapter so $\bar{\mathcal{E}}_{\boldsymbol{x}} = 1$). This channel is in effect anti-causal (or in reality, the .9 comes first). A second channel has causal response $1 + .8D$ with noise variance .164 per sample and is independent of the noise in the first channel. The ISI effectively spans 3 symbol periods among the two channels at a common receiver that will decide whether $x_k = \pm 1$ has been transmitted.

The SNR_{MFB} for this channel remains $\text{SNR}_{MFB} = \frac{\bar{\mathcal{E}}_{\boldsymbol{x}} \cdot \|\boldsymbol{p}\|^2}{\frac{N_0}{2}}$, but it remains to compute this quantity correctly. First the noise needs to be whitened. While the two noises are independent, they do not have the same variance per sample, so a pre-whitening matrix is

$$\begin{bmatrix} 1 & 0 \\ 0 & \sqrt{\frac{.181}{.164}} \end{bmatrix} \tag{3.523}$$

and so then the energy quantified by $\|\boldsymbol{p}\|^2$ is

$$\|\boldsymbol{p}\|^2 = \|p_1\|^2 + \|\tilde{p}_2\|^2 = 1.81 + \left(\frac{.181}{.164}\right) 1.64 = 2(1.81) \quad . \tag{3.524}$$

Then

$$\text{SNR}_{MFB} = \frac{1 \cdot 2(1.81)}{.181} = 13 \text{ dB} . \tag{3.525}$$

Because of diversity, this channel has a higher potential performance than the single channel alone. Clearly having a second look at the input through another channel can't hurt (even if there is more ISI now). The ISI is characterized as always by $Q(D)$, which in this case is

$$\begin{aligned} Q(D) &= \frac{1}{2(1.81)} \left[(1 + .9D^{-1})(1 + .9D) + \frac{.181}{.164}(1 + .8D)(1 + .8D^{-1}) \right] \tag{3.526} \\ &= .492D + 1 + .492D^{-1} \tag{3.527} \\ &= .7082 \cdot (1 + .835D) \cdot (1 + .835D^{-1}) \tag{3.528} \\ \tilde{Q}(D) &= .492D + (1 + 1/20) + .492D^{-1} \tag{3.529} \\ &= .587 \cdot (1 + .839D) \cdot (1 + .839D^{-1}) \tag{3.530} \end{aligned}$$

Thus, the SNR of a MMSE-DFE would be

$$\text{SNR}_{MMSE-DFE,U} = .7082(20) - 1 = 13.16 \text{ (11.15 dB)} \quad . \tag{3.531}$$

The improvement of diversity with respect to a single channel is about 2.8 dB in this case. The receiver is a MMSE-DFE essentially designed for the 1+.839D ISI channel after adding the matched-filter outputs. The loss with respect to the MFB is about 1.8 dB.
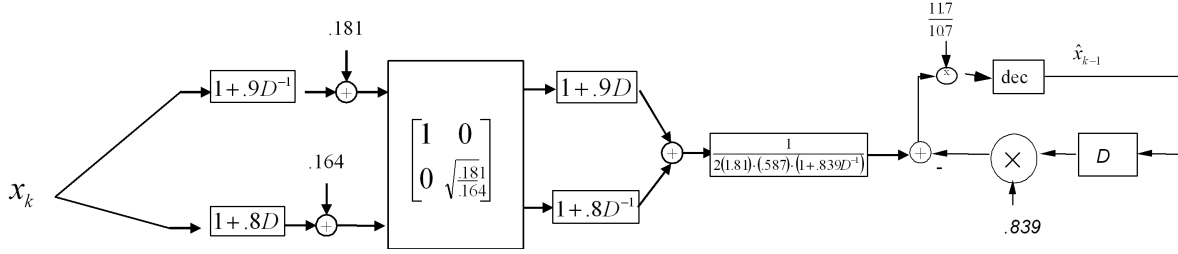
Figure 3.59: Two channel example.

3.9.3 Finite-length Multidimensional Equalizers

The case of finite-length diversity equalization becomes more complex because the matched filters are implemented within the (possibly fractionally spaced) equalizers associated with each of the diversity subchannels. There may be thus many coefficients in such a diversity equalizer.[24]

In the case of finite-length equalizers shown in figure 3.60, each of the matched filters of the RAKE is replaced by a lowpass filter of wider bandwidth (usually l times wider as in Section 3.7), a sampling device at rate l/T, and a fractionally spaced equalizer prior to the summing device. With vectors $\boldsymbol{p}_k$ in Equation (3.288) now becoming $l \cdot L$-tuples,

$$\boldsymbol{p}_k = \boldsymbol{p}(kT) \quad , \tag{3.532}$$

as do the channel output vectors $\boldsymbol{y}_k$ and the noise vector $\boldsymbol{n}_k$, the channel input/output relationship (in Eq (3.290)) again becomes

$$\boldsymbol{Y}_k \quad \triangleq \quad \begin{bmatrix} \boldsymbol{y}_k \\ \boldsymbol{y}_{k-1} \\ \vdots \\ \boldsymbol{y}_{k-N_f+1} \end{bmatrix} \tag{3.533}$$

$$= \begin{bmatrix} \boldsymbol{p}_0 & \boldsymbol{p}_1 & \cdots & \boldsymbol{p}_\nu & 0 & 0 & \cdots & 0 \\ 0 & \boldsymbol{p}_0 & \boldsymbol{p}_1 & \cdots & \cdots & \boldsymbol{p}_\nu & \cdots & 0 \\ \vdots & \vdots & \ddots & \ddots & \ddots & \ddots & \vdots \\ 0 & \cdots & 0 & 0 & \boldsymbol{p}_0 & \boldsymbol{p}_1 & \cdots & \boldsymbol{p}_\nu \end{bmatrix} \begin{bmatrix} x_k \\ x_{k-1} \\ \vdots \\ \vdots \\ x_{k-N_f-\nu+1} \end{bmatrix}$$

$$+ \begin{bmatrix} \boldsymbol{n}_k \\ \boldsymbol{n}_{k-1} \\ \vdots \\ \boldsymbol{n}_{k-N_f+1} \end{bmatrix} \quad . \tag{3.534}$$

The rest of Section 3.7 then directly applies with the matrix $\boldsymbol{P}$ changing to include the larger $l \cdot L$-tuples corresponding to L diversity channels, and the corresponding equalizer $\boldsymbol{W}$ having its $1 \times L$ coefficients corresponding to $\boldsymbol{w}_0 \ \dots \ \boldsymbol{w}_{N_f}$. Each coefficient thus contains l values for each of the L equalizers.

The astute reader will note that the diversity equalizer is the same in principle as a fractionally spaced equalizer except that the oversampling that creates diversity in the FSE generalizes to simply any type of additional dimensions per symbol in the diversity equalizer. The dfecolor program can be used where the oversampling factor is simply $l \cdot L$ and the vector of the impulse response is appropriately organized to have $l \cdot L$ phases per entry. Often, $l = 1$, so there are just L antennas or lines of samples per symbol period entry in that input vector.

---

[24]Maximal combiners that select only one (the best) of the diversity channels for equalization are popular because they reduce the equalization complexity by at least a factor of L – and perhaps more when the best subchannel needs less equalization.
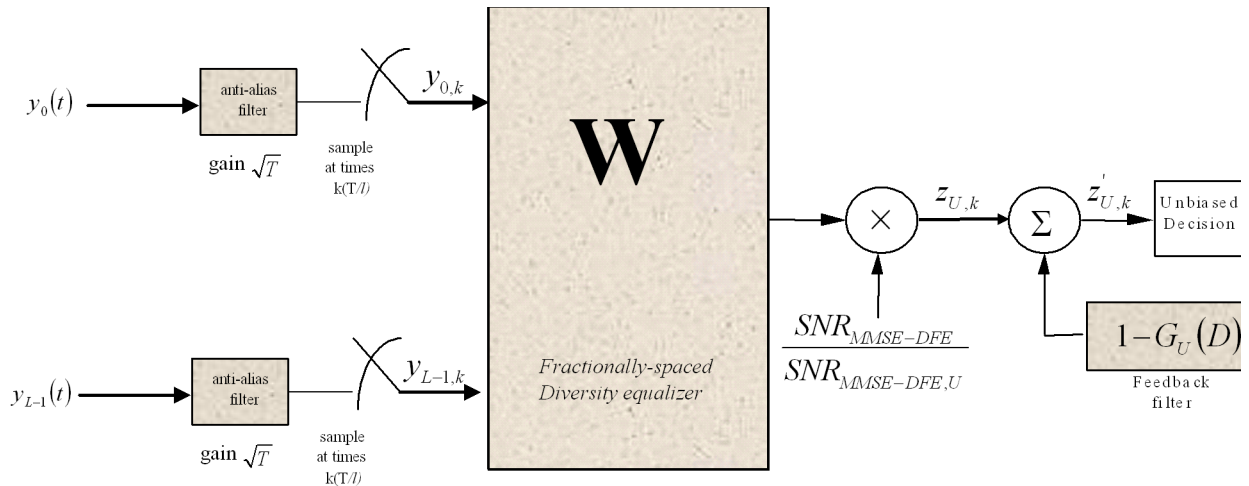
Figure 3.60: Fractionally spaced RAKE MMSE-DFE.

3.9.4 DFE RAKE Program

A DFE RAKE program similar to the DFERAKE matlab program has again been written by the students (and instructor debugging!) over the past several years. It is listed here and is somewhat self-explanatory if the reader is already using the DFECOLOR program.

```
%DFE design program for RAKE receiver
%Prepared by: Debarag Banerjee, edited by Olutsin OLATUNBOSUN
% and Yun-Hsuan Sung to add colored and spatially correlated noise
%Significant Corrections by J. Cioffi and above to get correct results --
%March 2005
%
function [dfseSNR,W,b]=dfsecolorsnr(l,p,nff,nbb,delay,Ex,noise);
% ------------------------------
%**** only computes SNR ****
% l     = oversampling factor
% L      = No. of fingers in RAKE
% p     = pulse response matrix, oversampled at l (size), each row corresponding to a diversity path
% nff   = number of feedforward taps for each RAKE finger
% nbb   = number of feedback taps
% delay = delay of system <= nff+length of p - 2 - nbb
%         if delay = -1, then choose best delay
% Ex    = average energy of signals
% noise = noise autocorrelation vector (size L x l*nff)
% NOTE: noise is assumed to be stationary, but may be spatially correlated
% outputs:
% dfseSNR = equalizer SNR, unbiased in dB
% ------------------------------

siz = size(p,2);
L=size(p,1);
nu = ceil(siz/l)-1;
p = [p zeros(L,(nu+1)*l-siz)];

% error check
if nff<=0
```

```
      error('number of feedforward taps must be > 0');
end
if delay > (nff+nu-1-nbb)
  error('delay must be <=  (nff+(length of p)-2-nbb)');
end
if delay < -1
  error('delay must be >= 0');
end


%%%%%%%%%%%%%%%%%%%%%%%%%%%%%%%%%%%%%%%%%%%%%%%%%%%%%%%%%%%%%%%%%%%%%%%
%if length(noise) ~= L*l*nff
%   error('Length of noise autocorrelation vector must be L*l*nff');
%end
if size(noise,2) ~= l*nff | size(noise,1) ~= L
   error('Size of noise autocorrelation matrix must be L x l*nff');
end
%%%%%%%%%%%%%%%%%%%%%%%%%%%%%%%%%%%%%%%%%%%%%%%%%%%%%%%%%%%%%%%%%%%%%

%form ptmp = [p_0 p_1 ... p_nu] where p_i=[p(i*l) p(i*l-1)... p((i-1)*l+1)
for m=1:L
   ptmp((m-1)*l+1:m*l,1) = [p(m,1); zeros((l-1),1)];
end
for k=1:nu
   for m=1:L
       ptmp((m-1)*l+1:m*l,k+1) = conj((p(m,k*l+1:-1:(k-1)*l+2))');
   end
end
ptmp;

% form matrix P, vector channel matrix
P = zeros(nff*l*L+nbb,nff+nu);


%First construct the P matrix as in MMSE-LE
for k=1:nff,
  P(((k-1)*l*L+1):(k*l*L),k:(k+nu)) = ptmp;
end

%Add in part needed for the feedback
P(nff*l*L+1:nff*l*L+nbb,delay+2:delay+1+nbb) = eye(nbb);
temp= zeros(1,nff+nu);
temp(delay+1)=1;

%%%%%%%%%%%%%%%%%%%%%%%%%%%%%%%%%%%%%%%%%%%%%%%%%%%%%%%%%%%%%%%%%%%%%%%%%%%%
Rn  = zeros(nff*l*L+nbb);

for i = 1:L
    n_t = toeplitz(noise(i,:));

    for j = 1:l:l*nff
        for k = 1:l:l*nff
            Rn((i-1)*l+(j-1)*L+1:i*l+(j-1)*L, (i-1)*l+(k-1)*L+1:i*l+(k-1)*L) = n_t(j:j+l-1,k:k+l-1);
        end
    end
```

```
end
%%%%%%%%%%%%%%%%%%%%%%%%%%%%%%%%%%%%%%%%%%%%%%%%%%%%%%%%%%%%%%%%%%%%%%%%%%

Ex*P*P';
Ry  = Ex*P*P' + Rn;
Rxy = Ex*temp*P';
IRy=inv(Ry);
w_t = Rxy*IRy;
%Reshape the w_t matrix into the RAKE filter bank and feedback matrices
ww=reshape(w_t(1:nff*l*L),l*L,nff);
for m=1:L
   W(m,:)=reshape(ww((m-1)*l+1:m*l,1:nff),1,l*nff);
end
b=-w_t(nff*l*L+1:nff*l*L+nbb);
sigma_dfse = Ex - w_t*Rxy';
dfseSNR = 10*log10(Ex/sigma_dfse - 1);
```

For the previous example, some command strings that work are (with whitened-noise equivalent channel first):

```
>> p
p =    0.9000    1.0000         0
            0    1.0500    0.8400
>> [snr,W,b] = dfeRAKE(1,p,6,1,5,1,[.181 zeros(1,5) ; .181 zeros(1,5)])

snr =  11.1465
W = 0.0213   -0.0439    0.0668   -0.0984    0.1430    0.3546
   -0.0027    0.0124   -0.0237    0.0382    0.4137   -0.0000
b = 0.7022
```

or with colored noise directly inserted

```
>> p1
p1 =    0.9000    1.0000         0
             0    1.0000    0.8000

>> [snr,W,b] = dfeRAKE(1,p1,6,1,5,1,[.181 zeros(1,5) ; .164 zeros(1,5)])

snr = 11.1486

W = 0.0213   -0.0439    0.0667   -0.0984    0.1430    0.3545
   -0.0028    0.0130   -0.0249    0.0401    0.4347    0.0000

b = 0.7022
```

Two outputs are not quite the same because of the finite number of taps.

3.9.5   Multichannel Transmission

Multichannel transmission in Chapters 4 and 5 is the logical extension of diversity when many inputs may share a transmission channel. In the multichannel case, each of many inputs may affect each of many outputs, logically extending the concept of intersymbol interference to other types of overlap than simple ISI. Interference from other transmissions is more generally called **crosstalk**. Different inputs may for instance occupy different frequency bands that may or may not overlap, or they may be transmitted from different antennas in a wireless system and so thus have different channels to some common receiver or set of receivers. Code division systems (See Chapter 5 Appendix) use different codes for the different

sources. A diversity equalizer can be designed for some set of channel outputs for each and every of the input sequences, leading to **multichannel transmission**. In effect the set of equalizers attempts to "diagonalize" the channels so that no input symbol from any source interferes with any other source at the output of each of the equalizers. From an equalizer perspective, the situation is simply multiple instances of the diversity equalizer already discussed in this section. However, when the transmit signals can be optimized also, there can be considerable improvement in the performance of the set of equalizers. Chapters 4 and 5 (EE379C) develop these concepts.

However, the reader may note that a system that divides the transmission band into several different frequency bands may indeed benefit from a reduced need for equalization within each band. Ideally, if each band is sufficiently narrow to be viewed as a "flat" channel, no equalizer is necessary. The SNR of each of these "sub-channels" relates (via the "gap" approximation) how many bits can be transferred with QAM on each. By allocating energy intelligently, such a system can be simpler (avoiding equalization complexity) and actually perform better than equalized wider-band QAM systems. While this chapter has developed in depth the concept of equalization because there are many wide-band QAM and PAM systems that are in use and thus benefit from equalization, an intuition that for the longest time transmission engineers might have been better off never needing the equalizer and simply transmitting in separate disjoint bands is well-founded. Chapters 4 and 5 support this intuition. Progress of understanding in the field of transmission should ultimately make equalization methods obsolete. As in many technical fields, this has become a line of confrontation between those resisting change and those with vision who see a better way.

Exercises - Chapter 3

3.1 *Quadrature Modulation.*
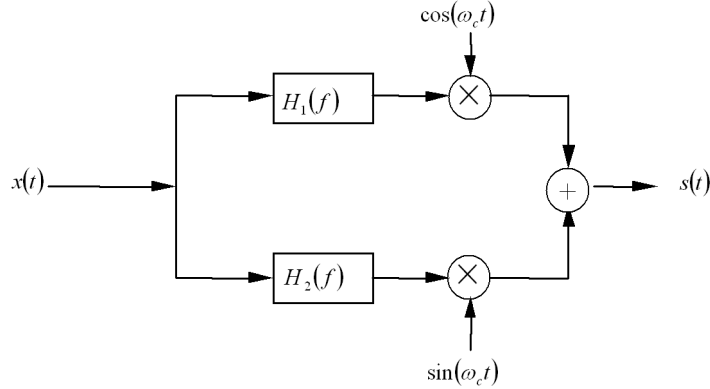Consider the quadrature modulator shown below,

Figure 3.61: Quadrature modulator.

a. What conditions must be imposed on $H_1(f)$ and $H_2(f)$ if the output signal s(t) is to have no spectral components between $-f_c$ and f_c? Assume that f_c is larger than the bandwidth of $H_1(f)$ and $H_2(f)$. (2 pts.)

b. Let the input signal be of the form,

$$x(t) = \sum_{n=-\infty}^{\infty} a_n \phi(t - nT)$$

What conditions must be imposed on $H_1(f)$ and $H_2(f)$ if the real part of the demodulated signal is to have no ISI. (3 pts.)

c. Find the impulse responses $h_1(t)$ and $h_2(t)$ corresponding to the minimum bandwidth $H_1(f)$ and $H_2(f)$ which simultaneously satisfy (a) and (b). You can express your answer in terms of $\phi(t)$. (3 pts.)

3.2 *Sampling time and Eye Patterns.*
The received signal for a binary transmission system is,

$$y(t) = \sum_{n=-\infty}^{\infty} a_n q(t - nT) + n(t)$$

where $a_n \in \{-1, +1\}$ and $Q(f)$ is a triangular, i.e. $q(t) = sinc^2(\frac{t}{T})$. The received signal is sampled at $t = kT + t_0$, where k is an integer and t_0 is the sampling phase, $|t_0| < \frac{1}{2}T$.

a. Neglecting the noise for the moment, find the peak distortion as a function of t_0. *Hint:* use Parseval's relation. (3 pts.)

b. Consider the following four binary sequences $\{u_n\}_{-\infty}^{\infty}, \{v_n\}_{-\infty}^{\infty}, \{w_n\}_{-\infty}^{\infty}, \{x_n\}_{-\infty}^{\infty}$:

$$
\begin{aligned}
u_n &= -1 & \forall n \\
v_n &= +1 & \forall n
\end{aligned}
$$

256

$$w_n = \begin{cases} +1, & \text{for } n = 0 \\ -1, & \text{otherwise} \end{cases}$$

$$x_n = \begin{cases} -1, & \text{for } n = 0 \\ +1, & \text{otherwise} \end{cases}$$

Using the result of (a), find expressions for the 4 outlines of the binary eye pattern. Sketch the eye pattern for these four sequences over two symbol periods $-T \le t \le T$. (2 pts.)

c. Find the width (horizontal) of the eye pattern at its widest opening. (2 pts.)

d. If the noise variance is σ^2, find a worst case bound (using peak distortion) on the probability of error as a function of t_0. (2 pts.)

3.3 *The 379 channel model.*

Consider the ISI-model shown in Figure 3.2 with PAM and symbol period T. Let $\varphi(t) = \frac{1}{\sqrt{T}}\text{sinc}(\frac{t}{T})$ and $h(t) = \delta(t) - \frac{1}{2}\delta(t - T)$.

a. Determine $p(t)$, the pulse response. (1 pt)

b. Find $\|p\|$ and $\varphi_p(t)$. (2 pts.)

c. (2 pts.) Find $q(t)$, the function that characterizes how one symbol interferes with other symbols. Confirm that $q(0) = 1$ and that $q(t)$ is hermitian (conjugate symmetric). You may find it useful to note that

$$\text{sinc}\left(\frac{t + mT}{T}\right) * \text{sinc}\left(\frac{t + nT}{T}\right) = T\text{sinc}\left(\frac{t + (m + n)T}{T}\right).$$

d. Use Matlab to plot $q(t)$. For this plot you may assume that $T = 10$ and plot $q(t)$ for integer values of t. Assuming that we sample $y(t)$ at the perfect instants (i.e. when $t = kT$ for some integer k), how many symbols are distorted by a given symbol? Assume that the given symbol was positive, how will the distorted symbols be affected? Specifically, will they be increased or decreased? (2 pts.)

e. For the rest of the problem consider 8 PAM with d=1. Determine the peak distortion, $\mathcal{D}_p$. (2 pts.)

f. Determine the MSE distortion, $\mathcal{D}_{mse}$. Compare with the peak distortion. (2 pts.)

g. Find an approximation to the probability of error (using the MSE distortion). You may express your answer in terms of σ.(1 pt.)

3.4 *Bias and SNR.*

Continuing the setup of the previous problem with 8 PAM and $d = 1$, let

$$\frac{1}{2}\mathcal{N}_0 = \sigma^2 = 0.1.$$

Assume that a detector first scales the sampled output y_k by α and chooses the closest x to $y_k \cdot \alpha$ as illustrated in Figure 3.13. **Please express your SNR's below both as a ratio of powers and in dB.**

a. For which value of α is the receiver unbiased? (1 pt.)

b. For the value of α found in (a), find the receiver signal-to-noise ratio, SNR_R. (2 pts.)

c. Find the value of α that maximizes SNR_R and the corresponding SNR_R. (2 pts.)

d. Show that the receiver found in the previous part is biased. (1 pt.)

e. Find the matched filter bound on signal-to-noise ratio, SNR_{MFB}. (1 pt.)

f. Discuss the ordering of the three SNR's you have found in this problem. Which inequalities will always be true? (1 pt.)

3.5 *Raised cosine pulses with Matlab.*

For this problem you will need to get all the .m files from /usr/class/ee379a/hw5/ on leland. If you are logon to leland, you could do a *cd* and copy the files to your directory. Alternatively, you could do an anonymous ftp to ftp.stanford.edu, and *cd* to class/ee379a/hw5 and copy the files.

a. Consider the formula for the raised cosine pulse (Eq. 3.79 of chapter 3):

$$q(t) = sinc\left(\frac{t}{T}\right) \cdot \left[\frac{\cos\left(\frac{\alpha\pi t}{T}\right)}{1 - \left(\frac{2\alpha t}{T}\right)^2}\right]$$

There are three values of t that would cause a program, such as Matlab, difficulty because of a division by zero. Identify these trouble spots and evaluate what $q(t)$ should be for these values. (2 pts)

b. Once you have identified those three trouble spots, a function to generate raised cosine pulses is a straightforward implementation of Eq. 3.75. We have implemented this for you in **mk_rcpulse.m**. Executing **q = mk_rcpulse(a)** will generate a raised cosine pulse with $\alpha = $ **a**. The pulses generated by **mk_rcpulse** assume $T = 10$ and are truncated to 751 points. (2 pts)

Use **mk_rcpulse** to generate raised cosine pulses with 0%, 50%, and 100% excess bandwith and plot them with **plt_pls_lin**. The syntax is **plt_pls_lin(q_50, 'title')** where **q_50** is the vector of pulse samples generated by **mk_rcpulse(0.5)** (50% excess bandwidth). Turn in your three plots and discuss any deviations from the ideal expected frequency domain behavior.

c. Use **plt_pls_dB(q, 'title')** to plot the same three raised cosine pulses as in part (b). Turn in your plots. Which of these three pulses would you choose if you wanted the one which had the smallest band of frequencies with energy above -40dB? Explain this unexpected result. (3 pts)

d. The function **plt_qk (q, 'title')** plots $q(k)$ for sampling at the optimal time and for sampling that is off by 4 samples (i.e., $q(kT)$ and $q(kT + 4)$ where $T = 10$). Use **plt_qk** to plot **q_k** for 0%, 50%, and 100% excess bandwidth raised cosine pulses. Discuss how excess bandwidth affects sensitivity of ISI performance to sampling at the correct instant. (3 pts)

3.6 *Noise enhancement: MMSE-LE vs ZFE.*

Consider the channel with

$$\|p\|^2 = 1 + aa^*$$
$$Q(D) = \frac{a^* D^{-1} + \|p\|^2 + aD}{\|p\|^2}$$
$$0 \le |a| < 1.$$

a. (2 pts) Find the zero forcing and minimum mean square error linear equalizers $W_{ZFE}(D)$ and $W_{MMSE-LE}(D)$. Use the variable $b = \|p\|^2 \left(1 + \frac{1}{SNR_{MFB}}\right)$ in your expression for $W_{MMSE-LE}(D)$.

b. (6 pts) By substituting $e^{-jwT} = D$ (with $T = 1$) and taking $SNR_{MFB} = 10\|p\|^2$, use Matlab to plot (lots of samples of) $W(e^{jw})$ for both ZFE and MMSE-LE for $a = .5$ and $a = .9$. Discuss the differences between the plots.

c. (3 pts) Find the roots r_1, r_2 of the polynomial

$$aD^2 + bD + a^*.$$

Show that $b^2 - 4aa^*$ is always a real positive number (for $|a| \ne 1$). *Hint:* Consider the case where $\frac{1}{SNR_{MFB}} = 0$. Let r_2 be the root for which $|r_2| < |r_1|$. Show that $r_1 r_2^* = 1$.

d. (2 pts) Use the previous results to show that for the MMSE-LE

$$W(D) = \frac{\|p\|}{a} \frac{D}{(D - r_1)(D - r_2)} = \frac{\|p\|}{a(r_1 - r_2)} \left(\frac{r_1}{D - r_1} - \frac{r_2}{D - r_2} \right). \qquad (3.535)$$

e. (2 pts) Show that for the MMSE-LE, $w_0 = \frac{\|p\|}{\sqrt{b^2 - 4aa^*}}$. By taking $\frac{1}{SNR_{MFB}} = 0$, show that for the ZFE $w_0 = \frac{\|p\|}{1 - aa^*}$.

f. (4 pts) For $\bar{\mathcal{E}}_x = 1$ and $\sigma^2 = 0.1$ find expressions for σ^2_{ZFE}, $\sigma^2_{MMSE-LE}$, γ_{ZFE}, and $\gamma_{MMSE-LE}$.

g. (4 pts) Find γ_{ZFE} and $\gamma_{MMSE-LE}$ in terms of the paramter a and calculate for $a = 0, 0.5, 1$. Sketch γ_{ZFE} and $\gamma_{MMSE-LE}$ for $0 \le a < 1$.

3.7 *DFE is even better.*

a. (2 pts) For the channel of problem 3.6, show that the canonical factorization is

$$Q(D) + \frac{1}{SNR_{MFB}} = \gamma_0(1 - r_2 D^{-1})(1 - r_2^* D).$$

What is γ_0 in terms of a and b? *Please* don't do this from scratch. You have done much of the work for this in problem 3.6.

b. (2 pts) Find $B(D)$ and $W(D)$ for the MMSE DFE.

c. (4 pts) Give an expression for $\gamma_{MMSE-DFE}$. Compute its values for $a = 0, .5, 1$ for the $\bar{\mathcal{E}}_x$ and σ^2 of problem 3.6. Sketch $\gamma_{MMSE-DFE}$ as in problem 3.6. Compare with your sketches from Problem 3.6.

3.8 *Noise predictive DFE.*
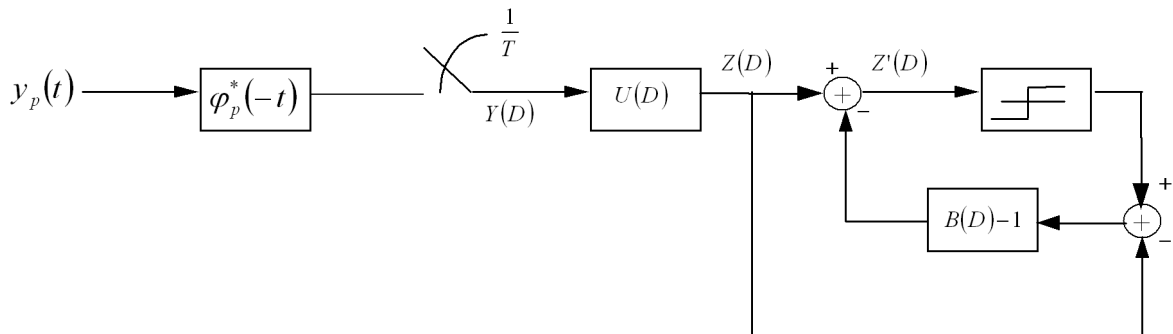
Figure 3.62: Noise-Predictive DFE

Consider the equalizer shown above with B(D) restricted to be causal and monic. Assume all decisions are correct. We use a MMSE criterion to choose $U(D)$ and $B(D)$ to minimize $E[|x_k - z'_k|^2]$. (x_k is the channel input.)

a. (5 pts) Show this equalizer is equivalent to a MMSE-DFE and find $U(D)$ and $B(D)$ in terms of $G(D)$, $Q(D)$, $\|p\|$, $\bar{\mathcal{E}}_x$, SNR_{MFB} and γ_0.

b. (2 pts) Relate $U_{\text{NPDFE}}(D)$ to $W_{\text{MMSE-LE}}(D)$ and to $W_{\text{MMSE-DFE}}(D)$.

c. (1 pt) If we remove feedback $(B(D) = 1)$, what does this equalizer become?

d. (1 pt) Interpret the name "noise-predictive" DFE by explaining what the feedback section is doing.

e. (2 pts) Is the NPDFE biased? If so, show how to remove the bias.

3.9 *Receiver SNR relationships.*

a. (3 pts) Recall that:

$$Q(D) + \frac{1}{\text{SNR}_{\text{MFB}}} = \gamma_0 G(D) G^*(D^{-*})$$

Show that:

$$1 + \frac{1}{\text{SNR}_{\text{MFB}}} = \gamma_0 \|g\|^2$$

b. (3 pts) Show that:

$$\|g\| \geq 1$$

with equality if and only if $Q(D) = 1$ (i.e. if the channel is flat) and therefore:

$$\gamma_0 \leq 1 + \frac{1}{\text{SNR}_{\text{MFB}}}$$

c. (3 pts) Let x_0 denote the time-zero value of the sequence X. Show that:

$$\left[\frac{1}{Q(D) + \frac{1}{\text{SNR}_{\text{MFB}}}} \right]_0 \geq \frac{1}{\gamma_0}$$

and therefore:

$$\text{SNR}_{\text{MMSE-LE,U}} \leq \text{SNR}_{\text{MMSE-DFE,U}}$$

(with equality if and only if $Q(D) = 1$, that is $Q(\omega)$ has vestigial symmetry.)

d. (2 pts) Use the results of parts b) and c) to show:

$$\text{SNR}_{\text{MMSE-LE,U}} \leq \text{SNR}_{\text{DFE,U}} \leq \text{SNR}_{\text{MFB}}$$

3.10 *Bias and probability of error.*

We have used the fact that the best unbiased receiver has a lower P_e than the (biased) MMSE receiver. Here is a simple illustration of this fact.
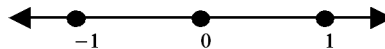

Figure 3.63: A three point PAM constellation.

Consider the constellation above with additive white noise n_k having

$$\frac{\mathcal{N}_0}{2} = \sigma^2 = 0.1.$$

Assume that the inputs are independent and identically distributed uniformly over the three possible values. Assume also that n_k is zero mean and independent of x_k.

a. (1 pt) Find the mean square error between $y_k = x_k + n_k$ and x_k. (easy)

b. (1 pt) Find P_e exactly for the ML detector on the unbiased values y_k.

c. (2 pts) Find the scale factor α that will minimize the mean square error

$$E[e_k^2] = E[(x_k - \alpha y_k)^2].$$

Prove that your α does in fact provide a minimum by taking the appropriate second derivative.

d. (2 pts) Find $E[e_k^2]$ and P_e for the scaled output αy_k. When you compute P_e, use the decision regions for the unbiased ML detector you found in (b). You should find that the biased receiver of part c has a P_e which is higher than the (unbiased) ML detector of part b, even though it has a smaller squared error.

e. (1 pt) Where are the optimal decision boundaries for detecting x_k from αy_k (for the MMSE α) in part c? What is the probability of error for these decision boundaries?

3.11 *Bias and the DFE.*
Consider the DFE you designed in Problem 3.7. Recall that you (hopefully) found

$$\gamma_0 = \frac{b + \sqrt{b^2 - 4aa^*}}{2(1 + aa^*)}.$$

a. (2 pts) Find G_u in terms of a, b, and r_2. Assume the same SNR_{MFB} as in Prob 3.7.

b. (1 pt) Give a block diagram of the DFE with scaling after the feedback summation.

c. (1 pt) Give a block diagram of the DFE with scaling before the feedback summation.

3.12 *Zero forcing DFE.*
Consider once again the general channel model of Problems 3.6 and 3.7 with $\bar{\mathcal{E}}_x = 1$ and $\sigma^2 = 0.1$.

a. (2 pts) Find η_0 and $P_c(D)$ so that

$$Q(D) = \eta_0 P_c(D) P_c^*(D^{-*}).$$

b. (2 pts) Find $B(D)$ and $W(D)$ for the ZF-DFE.

c. (1 pt) Find σ^2_{ZF-DFE}

d. (2 pts) Find the loss with respect to SNR_{MFB} for $a = 0, .5, 1$. Sketch the loss for $0 \le a < 1$.

3.13 *Complex baseband channel.*
The pulse response of a channel is band-limited to $\frac{\pi}{T}$ and has

$$p_0 = \frac{1}{\sqrt{T}}(1 + 1.1j)$$

$$p_1 = \frac{1}{\sqrt{T}}(0.95 + 0.5j)$$

$$p_k = 0 \quad \text{for } k \neq 0, 1$$

where $p_k = p(kT)$ and $SNR_{MFB} = 15$ dB.

a. (2 pts) Find $\|p\|^2$ and find a so that

$$Q(D) = \frac{a^* D^{-1} + \|p\|^2 + aD}{\|p\|^2}$$

b. (2 pts) Find $SNR_{MMSE-LE,U}$ and $SNR_{MMSE-DFE,U}$ for this channel. Use the results of Problems 3.6 and 3.7 wherever appropriate. Note $\|p\|^2 \neq 1 + aa^*$ so some care should be exercised in using the results of Problems 3.6 and 3.7.

c. (2 pts) Use the SNR's from (b) to compute the NNUB on P_e for 4-QAM with the MMSE-LE and the MMSE-DFE.

3.14 *Tomlinson Precoding.*

We will be working with the $1 + 0.9D$ channel (i.e. the $1 + aD$ channel that we have been exploring at length with $a = 0.9$). For this problem, we will assume that $\sigma^2 = 0$. Furthermore, assume a 4-PAM constellation with $x_k \in \{-3, -1, 1, 3\}$.

a. (5 pts) Design a Tomlinson precoder and its associated receiver for this system. Your system will be fairly simple. How would your design change if noise were present in the system?

b. (5 points) Implement the precoder and its associated receiver using any computer method you would like (or you can do the following computations by hand if you prefer). Turn in a hard copy of whatever code you write, and assume no noise.

For the following input sequence compute the output of the precoder, the output of the channel, and the output of your receiver. Assume that the symbol $x' = -3$ was sent just prior to the input sequence below.

$$\{3, -3, 1, -1, 3, -3, -1\}$$

c. (3 pts) Now, again with zero noise, remove the modulo operations from your precoder and your receiver. For this modified system, compute the output of the precoder, the output of the channel, and the output of your receiver for the same inputs as in the previous part. Turn in hard copies of whatever code you write.

Did the system still work? What changed? What purpose do the modulo operators serve?

3.15 *Flexible Precoding.*

This problem considers the $1 + 0.9D$ channel (i.e. the $1 + aD$ channel that we have been exploring at length with $a = 0.9$). For this problem, we will assume that $\sigma^2 = 0$. Furthermore, assume a 4-PAM constellation with $x_k \in \{-3, -1, 1, 3\}$.

a. (5 pts) Design a Flexible precoder and its associated receiver for this system. Your system will be fairly simple. How would your design change if noise were present in the system?

b. (5 points) Implement the precoder and its associated receiver using any computer method you would like (or you can do the following computations by hand if you prefer). Turn in a hard copy of whatever code you write, and assume no noise.

For the following input sequence compute the output of the precoder, the output of the channel, and the output of your receiver. Assume that the symbol $x' = -3$ was sent just prior to the input sequence below.

$$\{3, -3, 1, -1, 3, -3, -1\}$$

c. (3 pts) Now, again with zero noise, remove the modulo operations from your precoder and your receiver. For this modified system, compute the output of the precoder, the output of the channel, and the output of your receiver for the same inputs as in the previous part. Turn in hard copies of whatever code you write.

Did the system still work? What changed? What purpose do the modulo operators serve?

3.16 *Finite length equalization and matched filtering.*

We design the optimal FIR MMSE-LE without assuming a matched filter. However, it turns out that we get a "matched filter" anyway. Consider a system whose pulse response is band limited to $|w| < \frac{\pi}{T}$ that is sampled at the symbol rate T after pass through an anti-alias filter with gain $\sqrt{T}$.

  a. (3 pts)

  Show that

$$w = R_{xY}R_{YY}^{-1} = (0, \ldots, 0, 1, 0, \ldots, 0)\Phi_p{}^* \left(\|p\| \left(\hat{Q} + l\frac{1}{SNR_{MFB}}\mathbf{I} \right) \right)^{-1}.$$

  where

$$\hat{Q} = \frac{PP^*}{\|p\|^2}$$

  b. (2 pts) Which terms correspond to the matched filter? Which terms correspond to the infinite length $W_{MMSE-LE}$?

3.17 *Finite Length equalization and MATLAB.*

Consider the $1 + 0.25D$ channel with $\sigma^2 = .1$ and $\bar{\mathcal{E}}_x = 1$.

  a. (1 pt) Find $SNR_{MMSE-LE,U}$ for the infinite length filter.

  b. (2 pts) In this problem we will use the MATLAB program **mmsele**. This program is interactive, so just type **mmsele** and answer the questions. When it asks for the pulse response, you can type **[1 0.25]** or **p** if you have defined **p** = **[1 0.25]**.

  Use **mmsele** to find the best Δ and the associated $SNR_{MMSE-LE,U}$ for a 5 tap linear equalizer . Compare with your value from part (a). How sensitive is performance to Δ for this system?

  c. (2 pts) Plot $|P(e^{(jwT)}|$ and $|P(e^{(jwT)})W(e^{(jwT)}|$ for $w \in [0, \frac{\pi}{T}]$. Discuss the plots briefly.

3.18 *Computing finite-length equalizers.*

Consider the following system description.

$$\bar{\mathcal{E}}_x = 1 \qquad \frac{\mathcal{N}_0}{2} = \frac{1}{8} \qquad \phi(t) = \frac{1}{\sqrt{T}}\mathrm{sinc}(\frac{t}{T}) \qquad h(t) = \delta(t) - 0.5\delta(t - T) \qquad l = 1$$

Feel free to use matlab for any matrix manipulations as you complete the parts below. You may wish to check your answers with **dfecolor.m**. However, for this problem, you should go through the calculations yourself. (You may use matlab for matrix inversion.)

  a. (2 pts) We assume perfect anti-alias filtering with gain $\sqrt{T}$. Find $\tilde{p}(t) = (\phi(t) * h(t))$ and $\|\tilde{p}\|^2$, corresponding to the discrete-time channel

$$y_k = x_k - .5 \cdot x_{k-1} + n_k \qquad . \tag{3.536}$$

  Also, find $\|\tilde{P}(D)\|^2 = \sum_k |\tilde{p}_k|^2$.

  b. (1 pt) Compute SNR_{MFB} for this channel.

  c. (2 pts) Design a 3 tap FIR MMSE-LE for $\Delta = 0$.

  d. (1 pt) Find the $\sigma^2_{MMSE-LE}$ for the equalizer of the previous part.

  e. (2 pts) Design a 3 tap FIR ZF-LE for $\Delta = 0$.

  f. (1 pt) Find the associated σ^2_{ZF-LE}.

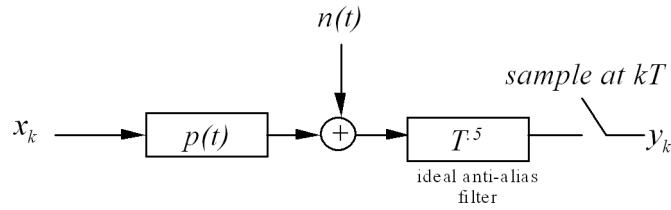 g. (2 pts) Design an MMSE-DFE which has 2 feedforward taps and 1 feedback tap. Again, assume that $\Delta = 0$.

Figure 3.64: Channel for Problem 3.19.

h. (2 pts) Compute the unbiased SNR's for the MMSE-LE and MMSE-DFE. Compare these two SNR's with each other and the SNR_{MFB}.

3.19 *Equalizer Design - Final 1996*

An AWGN channel has pulse response $p(t) = \frac{1}{\sqrt{T}}\left[\text{sinc}\left(\frac{t}{T}\right) - \text{sinc}\left(\frac{t-4T}{T}\right)\right]$. The receiver anti-alias filter has gain $\sqrt{T}$ over the entire Nyquist frequency band, $-1/2T < f < 1/2T$, and zero outside this band. The filter is followed by a $1/T$ rate sampler so that the sampled output has D-Transform

$$y(D) = (1 - D^4)x(D) + n(D) \quad . \tag{3.537}$$

$x(D)$ is the D-Transform of the sequence of M-ary PAM input symbols, and $n(D)$ is the D-Transform of the Gaussian noise sample sequence. The noise autocorrelation function is $R_{nn}(D) = \frac{N_0}{2}$. Further equalization of $y(D)$ is in discrete time where (in this case) the matched filter and equalizer discrete responses (i.e., D-Transforms) can be combined into a single discrete-time response. The target P_e is 10^{-3}.

Let $\frac{N_0}{2}$ = -100 dBm/Hz (0 dBm = 1 milliwatt = .001 Watt) and let $1/T = 2$ MHz.

a. Sketch $|P(e^{-\jmath\omega T})|^2$. (2 pts)

b. In your engineering judgement, what kind of equalizer should be used on this channel?

c. For a ZF-DFE, find the transmit symbol mean-square value (i.e., the transmit energy) necessary to achieve a data rate of 6 Mbps using PAM and assuming a probability of symbol error equal to 10^{-3}. (4 pts)

d. For your transmit energy in part c, how would a MMSE-DFE perform on this channel? (2pts)

3.20 *FIR Equalizer Design - Final 1996*

A symbol-spaced FIR equalizer $(l = 1)$ is applied to a stationary sequence y_k at the sampled output of an anti-alias filter, which produces a discrete-time IIR channel with response given by

$$y_k = a \cdot y_{k-1} + b \cdot x_k + n_k \quad , \tag{3.538}$$

where n_k is white Gaussian noise.

The SNR (ratio of mean square x to mean square n) is $\frac{\bar{\mathcal{E}}_x}{\frac{N_0}{2}} = 20$ dB. $|a| < 1$ and both a and b are real. For all parts of this question, choose the best Δ where appropriate.

a. Design a 2-tap FIR ZFE. (3 pts)

b. Compute the SNR_{zfe} for part a. (2 pts)

c. Compute your answer in part b with that of the infinite-length ZFE. (1 pt)

d. Let $a = .9$ and $b = 1$. Find the 2-tap FIR MMSE-LE. (4 pts)

264

e. Find the $\text{SNR}_{mmse-le,u}$ for part d.

f. Find the SNR_{zf-dfe} for an infinite-length ZF-DFE. How does the SNR compare to the matched-filter bound if we assume there is no information loss incurred in the symbol-spaced anti-alias filter? Use $a = .9$ and $b = 1$. (2 pts)

3.21 *ISI quantification - Midterm 1996*
For the channel $P(\omega) = \sqrt{T}(1 + .9e^{\jmath\omega T}) \; \forall |\omega| < \pi/T$ studied repeatedly in this chapter, use binary PAM with $\bar{\mathcal{E}}_x = 1$ and $\text{SNR}_{MFB} = 10$ dB. Remember that $q_0 = 1$.

a. Find the peak distortion, $\mathcal{D}_p$. (1 pt)

b. Find the peak-distortion bound on P_e. (2 pts)

c. Find the mean-square distortion, $\mathcal{D}_{MS}$. (1 pt)

d. Approximate P_e using the $\mathcal{D}_{MS}$ of part c. (2 pts)

e. ZFE: Compare P_e in part d with the P_e for the ZFE. Compute SNR difference in dB between the SNR based on mean-square distortion implied in parts c and d and SNR_{ZFE}. (hint, see example in this chapter for SNR_{ZFE}) (2 pts)

3.22 *Precoding - Final 1995*
For an ISI channel with

$$Q(D) + \frac{1}{\text{SNR}_{MFB}} = .82 \left[\frac{\jmath}{2} D^{-1} + 1.25 - \frac{\jmath}{2} D \right] \tag{3.539}$$

a. Find SNR_{MFB} and $\text{SNR}_{MMSE-DFE}$. (2 pts)

b. Find $G(D)$ and $G_U(D)$ for the MMSE-DFE. (1 pt)

c. Design (show/draw) a Tomlinson-Harashima precoder, showing from x_k through the decision device in the receiver in your diagram (any M). (2 pts)

d. Let $M = 4$ for your precoder in part c. Find P_e.

e. Design (show/draw) a Flexible precoder, showing from x_k through the decision device in the receiver in your diagram (any M). (2 pts)

f. Let $M = 4$ for your precoder in part e. Find P_e.

3.23 *Finite-delay tree search*
A channel with multipath fading has one reflecting path with gain (voltage) 90% of the main path. The relative delay on this path is approximately T seconds, but the carrier sees a phase-shift of -60° that is constant on the second path. Assume binary transmission throught this problem.
Use the model
$$P(\omega) = \begin{cases} \sqrt{T}\left(1 + ae^{-\jmath\omega T}\right) & |\omega| < \pi/T \\ 0 & \text{elsewhere} \end{cases}$$
to approximate this channel. $\frac{N_0}{2} = .0181$ and $\bar{\mathcal{E}}_x = 1$.

a. Find a. (1 pt)

b. Find SNR_{MFB}. (1 pt)

c. Find $W(D)$ and SNR_U for the MMSE-LE. (3 pts)

d. Find $W(D)$, $B(D)$, and SNR_U for the MMSE-DFE. (3 pts)

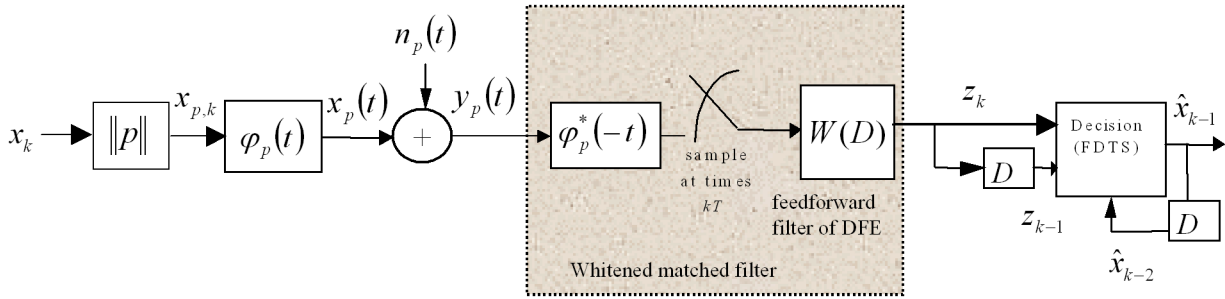e. Show a simple method and compute SNR_{zf-dfe}.

Figure 3.65: Finite-delay tree search.

f. A finite-delay tree search detector at time k decides $\hat{x}_{k-1}$ by choosing that $\hat{x}_{k-1}$ value that minimizes

$$\min_{\hat{x}_k, \hat{x}_{k-1}} |z_k - \hat{x}_k - a\hat{x}_{k-1}|^2 + |z_{k-1} - \hat{x}_{k-1} - a\hat{x}_{k-2}|^2 \quad,$$

where $\hat{x}_{k-2} = x_{k-2}$ by assumption. How does this compare with the ZF-DFE (better or worse)? (1 pt)

g. Find an SNR_{fdts} for this channel. (bonus)

h. Could you generalize SNR in part g for FIR channels with ν taps? (bonus)

3.24 *Peak Distortion -(5 pts)*
Peak Distortion can be generalized to channels without reciever matched filtering (that is $\varphi_p(-t)$ is a lowpass anti-alias filter). Let us suppose

$$y(D) = x(D) \cdot (1 - .5D) + N(D) \tag{3.540}$$

after sampling on such a channel, where $N(D)$ is discrete AWGN. $P(D) = 1 - .5D$.

a. write y_k in terms of x_k, x_{k-1} and n_k. (hint, this is easy. 1 pt)

b. We define peak distortion for such a channel as $\mathcal{D}_p \overset{\Delta}{=} |x_{max}| \sum_{m \neq 0} |p_m|$. Find this new $\mathcal{D}_p$ for this channel if $|x_{max}| = 1$. (2 pts)

c. Suppose $\frac{N_0}{2}$, the mean-square of the sample noise, is .05 and $\bar{\mathcal{E}}_x = 1$. What is P_e for symbol-by-symbol detection with PAM and $M = 2$. (2 pts)

3.25 *More Equalization - Final 1994*
Given an ISI channel with $p(t) = 1/\sqrt{T}\,[\mathrm{sinc}(t/T) - \jmath\mathrm{sinc}[(t - T)/T]]$, $\bar{\mathcal{E}}_x = 1$, and $\frac{N_0}{2} = .05$. for each equalizer, find the filter transforms $W(D)$ (and $B(D)$), the unbiased detection SNR, and the loss with respect to the MFB.

a. What is SNR_{MFB}?

b. Find the ZFE.

c. Find the MMSE-LE.

d. Find the ZF-DFE.

e. Find the MMSE-DFE.

f. Draw a diagram illustrating the MMSE-DFE implementation with Tomlinson precoding.

g. For $P_e < 10^{-6}$ and using square or cross QAM, choose a design and find the largest data rate you can transmit using one of the equalizers above.

3.26 *Raised Cosine pulses*

Show through inverse Fourier transforming that the raised cosine and square-root raised cosine time-domain responses given in Section 3.3 are correct.

3.27 *Expert Understanding - Final 1998*
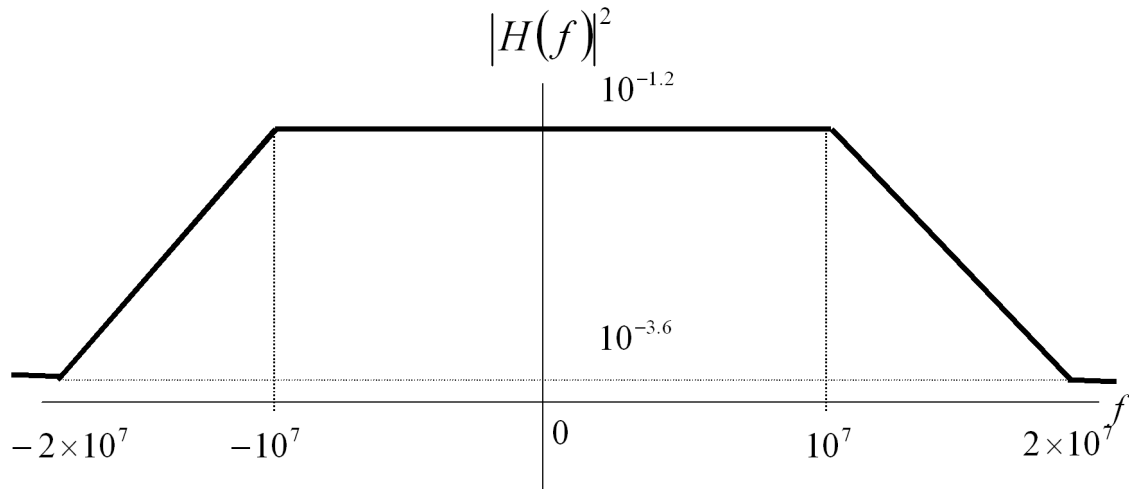
Figure 3.66: Channel for Problem 3.27.

A channel baseband transfer function for PAM transmission is shown in Figure 3.66. PAM transmission with sinc basis function is used on this channel with a transmit power level of 10 mW $=\mathcal{E}_x/T$. The one-sided AWGN psd is -100 dBm/Hz.

a. Let the symbol rate be 20 MHz - find SNR_{MFB}.(1 pt)

b. For the same symbol rate as part a, what is $\text{SNR}_{MMSE-LE}$? (1 pt)

c. For the equalizer in part b, what is the data rate for PAM if $P_e \leq 10^{-6}$? (1 pt)

d. Let the symbol rate be 40 MHz - find the new SNR_{MFB}.(2 pts)

e. Draw a the combined shape of the matched-filter and feedforward filter for a ZF-DFE corresponding to the new symbol rate of part d. (1 pt)

f. Estimate $\text{SNR}_{MMSE-DFE,U}$ for the new symbol rate, assuming a MMSE-DFE receiver is used. (2 pts) (Hint: you may note the relationship of this transfer function to the channel often used as an example in EE379A).

g. What is the new data rate for this system at the same probability of error as part c - compare with the data rate of part c. (1 pt)

h. What can you conclude about incurring ISI if the transmitter is allowed to vary its bandwidth?

3.28 *Infinite-Length EQ - 10 pts, Final 1998*

An ISI channel with PAM transmission has channel correlation function given by

$$Q(D) = \frac{.19}{(1 + .9D)(1 + .9D^{-1})} \quad , \tag{3.541}$$

with $\text{SNR}_{MFB} =$10 dB, $\mathcal{E}_x = 1$, and $\|p\|^2 = \frac{1}{.19}$.

a. (3 pts) Find $W_{ZFE}(D)$, σ^2_{ZFE}, and SNR_{ZFE}.

b. (1 pt) Find $W_{MMSE-LE}(D)$

c. (3 pts) Find $W_{ZF-DFE}(D)$, $B_{ZF-DFE}(D)$, and SNR_{ZF-DFE}.

d. (3 pts) Find $W_{MMSE-DFE}(D)$, $B_{MMSE-DFE}(D)$, and $\text{SNR}_{MMSE-DFE,U}$.

3.29 *Finite-Length EQ - 9 pts, Final 1998*
A baseband channel is given by

$$P(f) = \begin{cases} \sqrt{T} \cdot \left(1 - .7e^{j2\pi fT}\right) & |f| < \frac{.5}{T} \\ 0 & |f| \geq \frac{.5}{T} \end{cases} \tag{3.542}$$

and finite-length equalization is used with anti-alias perfect LPR with gain $\sqrt{T}$ followed by symbol-rate sampling. After the sampling, a maximum complexity of 3 taps TOTAL over a feedforward filter and a feedback filter can be tolerated. $\mathcal{E}_{\boldsymbol{x}} = 2$ and $\frac{N_0}{2} = .01$ for a symbol rate of $1/T = 100\text{kHz}$ is used with PAM transmission. Given the complexity constraint, find the highest data rate achievable with PAM transmission when the corresponding probability of symbol error must be less than 10^{-5}.

3.30 *Equalizers - Miterm 2000 - 10 pts*
PAM transmission on a filtered AWGN channel uses basic function $\varphi(t) = \frac{1}{\sqrt{T}} \cdot \text{sinc}\left(\frac{t}{T}\right)$ with $T = 1$ and undergoes channel impulse response with Fourier transform ($|a| < 1$)

$$H(\omega) = \begin{cases} \frac{1}{1+a \cdot e^{j\omega}} & |\omega| \leq \pi \\ 0 & |\omega| > \pi \end{cases} \tag{3.543}$$

and $\text{SNR} = \frac{\bar{\mathcal{E}}_{\boldsymbol{x}}}{\sigma^2} = 15$ dB.

a. Find the Fourier Transform of the pulse response, $P(\omega)$? (1 pt)

b. Find $\|p\|^2$. (2 pts)

c. Find $Q(D)$, the function characterizing ISI. (3 pts)

d. Find the $W(D)$ for the zero-forcing and MMSE linear equalizers on this channel. (3 pts)

e. If $a = 0$, what data rate is achievable on this channel according to the gap approximation at $P_e = 10^{-6}$? (1 pt)

3.31 *Diversity Channel - Final 2000 - 6 pts*
We would like to evaluate the channel studied throughout this course and in the text with the same input energy and noise PSD versus almost the same channel except that two receivers independently receive:

- an undistorted delayed-by-T signal (that is $P(D) = D$), and

- a signal that is not delayed, but reduced to 90% of its amplitude (that is $P(D) = .9$).

a. Find $Q(D)$, $\|\boldsymbol{p}\|$, and SNR_{MFB} for the later diversity channel. (3 pts)

b. Find the performance of the MMSE-LE, MMSE-DFE for the later diversity channel and compare to that on the original one-receiver channel and with respect to the matched filter bound. (2 pts)

c. Find the probability of bit error on the diversity channel for the case of 1 bit/dimension transmission. (1 pt)

3.32 *Do we understand basic detection - Final 2000 - 9 pts*
A filtered AWGN channel with $T = 1$ has pulse response $p(t) = \text{sinc}(t) + \text{sinc}(t-1)$ with $\text{SNR}_{MFB} = 14.2$ dB.

a. Find the probability of error for a ZF-DFE if a binary symbol is transmitted (2 pts).

b. The Tomlinson precoder in this special case of a monic pulse response with all unity coefficients can be replaced by a simpler precoder whose output is

$$x'_k = \begin{cases} x'_{k-1} & \text{if } x_k = 1 \\ -x'_{k-1} & \text{if } x_k = -1 \end{cases} \tag{3.544}$$

Find the possible channel outputs and determine an SBS decoder rule. What is the performance (probability of error) for this decoder? (2 pts)

c. Suppose this channel is used one time for the transmission of one of the 8 4-dimensional messages that are defined by $[+ \pm \pm \pm]$, which produce 8 possible 5-dimensional outputs. ML detection is now used for this multidimensional 1-shot channel. What are the new minimum distance and number of nearest neighbors and how do they relate to those for the system in part a? What is the new number of bits per output dimension? (3 pts)

d. Does the probability of error change significantly if the input is extended to arbitrarily long block length N with only the first sample fixed at $+$, and all other inputs being equally likely $+$ or $-$? What happens to the number of bits per output dimension in this case? (2 pts).

3.33 *Equalization - Final 2000 - 10 pts*

PAM transmission is used on a filtered AWGN channel with $\frac{N_0}{2} = .01$, $T = 1$, and pulse repsonse $p(t) = \mathrm{sinc}(t) + 1.8\mathrm{sinc}(t-1) + .81\mathrm{sinc}(t-1)$. The desired probability of symbol error is 10^{-6}.

a. Find $\|p\|^2$, SNR_{MFB}, AND $Q(D)$ for this channel. (2 pts)

b. Find the MMSE-LE and corresponding unbiased SNR for this channel. (2 pts)

c. Find the ZF-DFE detection SNR and loss with respect to SNR_{MFB}. (1 pt)

d. Find the MMSE-DFE. Also compute the MMSE-DFE SNR and maximum data rate in bits/dimension using the gap approximation. (3 pts)

e. Draw the flexible (Laroia) precoder for the MMSE-DFE and draw the system from transmit symbol to detector in the receiver using this precoder. Implement this precoder for the largest number of integer bits that can be transmitted according to your answer in part (d). (2 pts)

3.34 *Finite-Length Equalizer Design - Final 2000 - 15 pts*

A filtered AWGN channel has impulse response $h(t) = \frac{1}{T} \cdot \frac{1}{1 + \left(\frac{10^7 t}{3}\right)^2}$ and is used in the transmission system of Figure 3.67. QAM transmission with $1/T = 1$ MHz and carrier frequency $f_c = 600$kHz are used on this channel. The AWGN psd is $\frac{N_0}{2} = -86.5$ dBm/Hz. The transmit power is $\frac{\mathcal{E}_x}{T} = 1$ mW. The oversampling factor for the equalizer design is chosen as $l = 2$. Square-root raised cosine filtering with 10% excess bandwidth is applied as a transmit filter, and an ideal filter is used for anti-alias filtering at the receiver. A matlab subroutine at the course web site may be useful in computing responses in the frequency domain.

a. Find ν so that an FIR pulse response approximates this pulse response so that less than 5% error in $\|p\|^2$.

b. Calculate SNR_{MFB}. Determine a reasonable set of parameters and settings for an FIR MMSE-LE and the corresponding data rate at $P_e = 10^{-7}$. Calculate the data rate using both an integer and a possibly non-integer number of bits/symbol. (4 pts)

c. Repeat part b for an FIR MMSE-DFE design and draw receiver. Calculate the data rate using both an integer and a possibly non-integer number of bits/symbol. (3 pts)
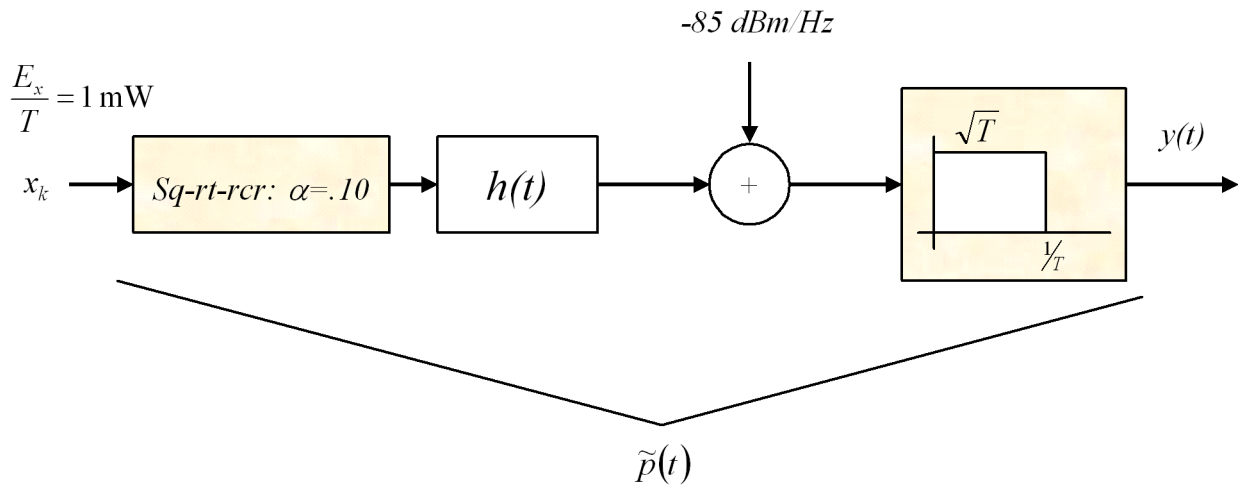
-85 dBm/Hz

$\frac{E_x}{T} = 1\,\text{mW}$

x_k → Sq-rt-rcr: α=.10 → $h(t)$ → + → $\sqrt{T}$ ... $\frac{1}{T}$ → $y(t)$

$\tilde{p}(t)$

Figure 3.67: Transmission system for Problem 3.34.

d. Can you find a way to improve the data rate on this channel by changing the symbol rate and or carrier frequency? (2 pts)

3.35 *Telephone-Line Transmission with "T1"*

Digital transmission on telephone lines necessarily must pass through two "isolation transformers" as illustrated in Figure 3.68. These transformers prevent large D.C. voltages accidentally placed on the line from unintentionally harming the telephone line or equipment attached to it, and they provide immunity to earth currents, noises, and ground loops. These transformers also introduce ISI.

modem — xformer — phone line — xformer — modem
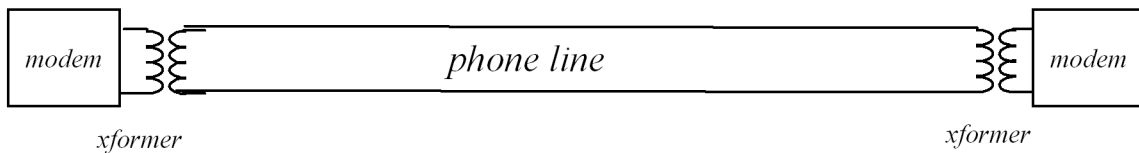
Figure 3.68: Illustration of a telephone-line data transmission for Problem 3.35.

a. The "derivative taking" combined characteristic of the transformers can be approximately modeled at a sampling rate of $1/T = 1.544$ MHz as successive differences between channel input symbols. For sufficiently short transmission lines, the rest of the line can be modeled as distortionless. What is a reasonable partial-response model for the channel $H(D)$? Sketch the channel transfer function. Is there ISI?

b. How would a zero-forcing decision-feedback equalizer generally perform on this channel with respect to the case where channel output energy was the same but there are no transformers?

c. What are some of the drawbacks of a ZF-DFE on this channel?

d. Suppose a Tomlinson precoder were used on the channel with $M = 2$, how much is transmit energy increased generally? Can you reduce this increase by good choice of initial condition for the Tomlinson Precoder?

270

e. Show how a binary precoder and corresponding decoder can significantly simplify the implementation of a detector. What is the loss with respect to optimum MFB performance on this channel with your precoder and detector?

f. Suppose the channel were not exactly a PR channel as in part a, but were relatively close. Characterize the loss in performance that you would expect to see for your detector.

3.36 *Magnetic Recording Channel*

Digital magnetic information storage (i.e., disks) and retrieval makes use of the storage of magnetic fluexes on a magnetic disk. The disk spins under a "read head" and by Maxwell's laws the read-head wire senses flus changes in the moving magnetic field, thus generating a read current that is translated into a voltage through amplifiers succeeding the read head. Change in flux is often encoded to mean a "1" was stored and no change means a "0" was stored. The read head has finite band limitations also.

a. Pick a partial-resonse channel with $\nu = 2$ that models the read-back channel. Sketch the magnitude characteristic (versus frequency) for your channel and justify its use.

b. How would a zero-forcing decision-feedback equalizer generally perform on this channel with respect to the best case where all read-head channel output energy convenyed either a positive or negative polarity for each pulse?

c. What are some of the drawbacks of a ZF-DFE on this channel?

d. Suppose a Tomlinson precoder were used on the channel with $M = 2$, how much is transmit energy increased generally? Can you reduce this increase by good choice of initial condition for the Tomlinson Precoder?

e. Show how a binary precoder and corresponding decoder can significantly simplify the implementation of a detector. What is the loss with respect to optimum MFB performance on this channel with your precoder and detector?

f. Suppose the channel were not exactly a PR channel as in part a, but were relatively close. Characterize the loss in performance that you would expect to see for your detector.

g. Suppose the density (bits per linear inch) of a disk is to be increased so one can store more files on it. What new partial response might apply with the same read-channel electronics, but with a correspondingly faster symbol rate?

3.37 *Tomlinson preocoding and simple precoding*

In Section 3.8, the simple precoder for $H(D) = 1 + D$ is derived.

a. Design the Tomlinson precoder corresponding to a ZF-DFE for this channel with the possible binary inputs to the precoder being ± 1. (4 pts)

b. How many distinct outputs are produced by the Tomlinson Precoder assuming an initial state (feedback D element contents) of zero for the precoder. (1 pt)

c. Compute the average energy of the Tomlinson precoder output. (1 pt)

d. How many possible outputs are produced by the simple precoder with binary inputs? (1 pt)

e. Compute the average energy of the channel input for the simple precoder with the input constellation of part (a). (1 pt)

3.38 *Flexible precoding and simple precoding*

In Section 3.8, the simple precoder for $H(D) = 1 + D$ is derived.

a. Design the Flexible precoder corresponding to a ZF-DFE for this channel with the possible binary inputs to the precoder being ± 1. (4 pts)

b. How many distinct outputs are produced by the Flexible Precoder assuming an initial state (feedback D element contents) of zero for the precoder. (1 pt)

c. Compute the average energy of the Flexible precoder output. (1 pt)

d. How many possible outputs are produced by the simple precoder with binary inputs? (1 pt)

e. Compute the average energy of the channel input for the simple precoder with the input constellation of part (a). (1 pt)

3.39 *Partial Response Precoding and the ZF-DFE*
  Consider an AWGN with $H(D) = (1 - D)^2$ with noise variance σ^2 and one-dimensional real input $x_k = \pm 1$.

a. Determine a partial-response (PR) precoder for the channel, as well as the decoding rule for the noiseless channel output. (2 pts)

b. What are the possible noiseless outputs and their probabilities? From these, determine the P_e for the precoded channel. (4 pts)

c. If the partial-response precoder is used with symbol-by-symbol detection, what is the loss with respect to the MFB? Ignore nearest neighbor terms for this calculation since the MFB concerns only the argument of the Q-function. (1 pt)

d. If a ZF-DFE is used instead of a precoder for this channel, so that $P_c(D) = 1 - 2D + D^2$, what is η_0? Determine also the SNR loss with respect to the SNR_{MFB} (2 pts)

e. Compare this with the performance of the precoder, ignoring nearest neighbor calculations. (1 pt)

3.40 *Error propagation and nearest neighbors*
  Consider the $H(D) = 1 - D^2$ channel with AWGN noise variance σ^2 and $d = 2$ and 4-level PAM transmission.

a. State the precoding rule and the noiseless decoding rule. (1 pts)

b. Find the possible noiseless outputs and their probabilities. Find also N_e and P_e with the use of precoding. (4 pts)

c. Suppose a ZF-DFE is used on this system and that at time $k = 0$ an incorrect decision $x_0 - \hat{x}_0 = 2$ occurs. This incorrect decision affects z_k at time $k = 2$. Find the N_e (taking the error at $k = 0$ into account) for the ZF-DFE. From this, determine the P_e with the effect of error propagation included. (4 pts)

d. Compare the P_e in part (c) with that of the use of the precoder in part (a). (1 pt)

3.41 *Forcing Partial Response*
  Consider a $H(D) = 1 + .9D$ channel with AWGN noise variance σ^2. We would like to convert this to a $1 + D$ channel

a. Design an equalizer that will convert the channel to a $1 + D$ channel. (2 pts)

b. The received signal is $y_k = x_k + .9x_{k-1} + n_k$ where n_k is the AWGN. Find the autocorrelation of the noise after going through the receiver designed in part (a). Evaluate r_0, $r_{\pm 1}$, and $r_{\pm 2}$. Is the noise white? (3 pts)

c. Do you think that the noise terms would be more or less correlated if we were to convert a $1 + .1D$ channel to a $1 + D$ channel? You need only discuss briefly. (1 pt)

3.42 *Final 2001 - Equalizers - 11 pts*

PAM transmission on a filtered AWGN channel uses basis function $\varphi(t) = \frac{1}{\sqrt{T}}\mathrm{sinc}\left(\frac{t}{T}\right)$ with $T = 1$ and undergoes channel impulse response with Fourier transform $(|\alpha| < 1)$

$$H(\omega) = \begin{cases} \frac{1}{1+a\cdot e^{j\omega}} & |\omega| \leq \pi \\ 0 & |\omega| > \pi \end{cases} \tag{3.545}$$

and SNR $= \frac{\bar{\mathcal{E}}_x}{\sigma^2} = 28$ dB.

a. Find the Fourier Transform of the pulse response, $P(\omega) =?$ (1 pt)

b. Find $\|p\|^2$. (1 pt)

c. Find $Q(D)$, the function characterizing ISI. (2 pts)

d. Find the filters and sketch the block diagram of receiver for the MMSE-DFE on this channel for $a = .9$. (3 pts)

e. Estimate the data rate for uncoded PAM transmission and $P_e < 10^{-6}$ that is achievable with your answer in part d. (2 pts)

f. Draw a diagram of the better precoder's (Tomlinson or Laroia), xmit and rcvr, implementations with $d = 2$ in the transmitted constellation. (2 pts)

3.43 *Final 2001 - Finite-Length Equalizer Design - 16 pts*

Transmission lines can sometimes have their transfer function described by the function

$$H(f) = k \cdot e^{-\alpha \cdot |f|} \tag{3.546}$$

where α and k are some positive real constants, here assigned the values $\alpha = 6\pi \cdot 10^{-7}$ and $k = 3\pi/10$. Our task in this problem is to design a transmission system for such a transmission line. Initially we begin with $1/T = 800$ kHz and carrier frequency $f_c = 600$ kHz on this channel. The AWGN psd is $\frac{N_0}{2} = -92$ dBm/Hz. The transmit power is $\mathcal{E}_x/T = 1$ mW. The oversampling factor for the equalizer design is chosen as $l = 2$. Square-root raised cosine filtering with 10% excess bandwidth is applied as a transmit filter and an ideal lowpass filter is used for anti-alias filtering at the receiver.

a. Find ν so that an FIR pulse response approximates this pulse response so that less than .25 dB error in $\|p\|^2$ (that is, the norm square of the difference between the actual $p(t)$ and the truncated p_k is less than $(10^{.025} - 1) \cdot \|p\|^2$. (4 pts)

b. Determine a reasonable set of parameters and settings for an FIR MMSE-LE and the corresponding data rate at $P_e \leq 10^{-7}$. Please print $\boldsymbol{w}$ filter coefficients. (2 pts)

c. Repeat part b for an FIR MMSE-DFE design and print coefficients. (2 pts)

d. Can you find a way to improve the data rate on this channel by changing the symbol rate and or carrier frequency? Try to maximize the data rate with QAM transmission by a suitable choice of carrier frequency and symbol rate, and provide that data rate - you may maintain the assumption of oversampling by a factor of 2 and 10% excess bandwidth. (6 pts)

e. Suppose a narrowband Gaussian noise with PSD -62 dBm/Hz were injected over a bandwith of 1 kHz - hereustically, would you expect this to change the performance much? What would you expect to happen in the filters of the DFE? (2 pts).

3.44 *Final 2001 - Diversity Concept - 7 pts*

An additive white Gaussian noise channel supports QAM transmission with a symbol rate of $1/T = 100$ kHz (with 0 % excess bandwidth) anywhere in a total baseband-equivalent bandwidth of 10 MHz transmission. Each 100 kHz wide QAM signal can be nominally received with an SNR of 14.5 dB without equalization. However, this 10 MHz wide channel has a 100 kHz wide band that is attenuated by 20 dB with respect to the rest of the band, but the location of the frequency of this notch is not known in advance to the designer. The transmitters are collocated.

a. What is the data rate sustainable at probability of bit error $\bar{P}_b \leq 10^{-7}$ in the nominal condition? (1 pt)

b. What is the maximum number of simultaneous QAM users can share this channel at the performance level of part a if the notch does not exist? (1 pt)

c. What is the worst-case probability of error for the number of users in part b if the notch does exist? (1 pt)

d. Suppose now (unlike part b) that the notch does exist, and the designer decides to send each QAM signal in two distinct frequency bands. What is the worst-case probability of error for a diversity-equalization system applied to this channel? (1 pt)

e. For the same system as part c, what is the best SNR that a diversity equalizer system can achieve? (1 pt)

f. For the system of part c, how many users can now share the band all with probability of bit error less than 10^{-7}? Can you think of a way to improve this number closer to the level of the part b? (2 pts)

3.45 *Final 2002 - Diversity Viewpoint - 12 pts*

A time-varying wireless channel is used to send long packets of information that are decoded by a receiver that uses a symbol-by-symbol decision device. The channel has pulse response in the familiar form:

$$P(\omega) = \begin{cases} \sqrt{T} \cdot \left(1 + a_i \cdot e^{-\jmath\omega T}\right) & |\omega| \leq \frac{\pi}{T} \\ 0 & |\omega| > \frac{\pi}{T} \end{cases} \tag{3.547}$$

where a_i may vary from packet to packet (but not within a packet). There is also AWGN with constant power spectral density $\frac{N_0}{2} = .1$. QPSK (4QAM) is sent on this channel with symbol energy 2.

a. Find the best DFE SNR and corresponding probability of symbol error for the two cases when $a_1 = .9$ and $a_2 = .5$. (2 pts)

Now, suppose the transmitter can resend the same packet of symbols to the receiver, which can delay the channel output packet from the first transmission until the symbols from the new packet arrive. However, the same symbol-by-symbol detector is still to be used by the receiver.

b. Explain why this is a diversity situation. (1 pt)

c. Find a new SNR_{MFB} for this situation. (1 pt)

d. Find the new function $Q(D)$ for this diversity situation. (2 pts)

e. Determine the performance of the best DFE this time (SNR and P_e). (2 pts)

f. Compare the P_e of part e with the product of the two P_e's found in part a. Comment. (2 pts)

g. Draw the receiver with RAKE illustrated as well as DFE, unbiasing, and decision device. (phase splitter can be ignored in diagram and all quantities can be assumed complex.) (2 pts).

3.46 *Precoder Diversity - Final 2003 - 7 pts*

A system with 4PAM transmits over two discrete-time channels shown with the two independent AWGN shown. ($\bar{\mathcal{E}}_x = 1$)

a. Find the RAKE matched filter(s) for this system ? (1 pt)

b. Find the single feedforward filter for a ZF-DFE? (1 pt)

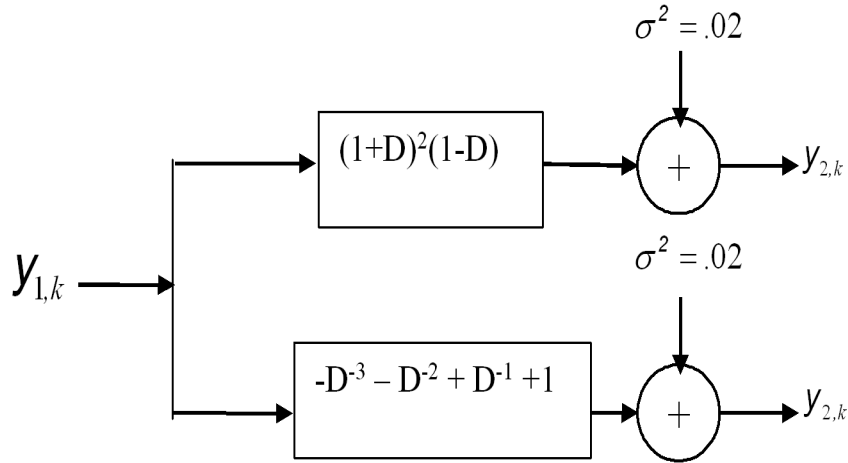c. Show the best precoder for the system created in part b. (1 pt)

Figure 3.69: Transmission system for Problem 3.47.

d. Find the SNR at the detector for this precoded system? (1 pt)

e. Find the loss in SNR with respect to the of either single channel. (1 pt)

f. Find the P_e for this precoded diversity system. (1 pt)

g. Find the probability that a packet of 1540 bytes contains one or more errors. (1 pt)

3.47 *Equalizer Performance and Means*

Recall that arithmetic mean, geometric mean, and harmonic mean are of the form $\frac{1}{n} \sum_{i=1}^{n} x_i$, $\left(\prod_{i=1}^{n} x_i \right)^{\frac{1}{n}}$, $\left(\frac{1}{n} \sum_{i=1}^{n} \frac{1}{x_i} \right)^{-1}$, respectively. Furthermore, they satisfy the following inequalities:

$$\frac{1}{n} \sum_{i=1}^{n} x_i \quad \geq \quad \left(\prod_{i=1}^{n} x_i \right)^{\frac{1}{n}} \quad \geq \quad \left(\frac{1}{n} \sum_{i=1}^{n} \frac{1}{x_i} \right)^{-1},$$

with equality when $x_1 = x_2 = \cdots = x_n$

a. **(4 pts)** Express SNR_{ZFE}, SNR_{ZF-DFE}, SNR_{MFB} in terms of SNR_{MFB} and frequency response of the autocorrelation function q_k. Prove that $SNR_{ZFE} \leq SNR_{ZF-DFE} \leq SNR_{MFB}$ using above inequalities. When does equality hold? *hint*: use $\int_a^b x(t)dt = \lim_{n \to \infty} \sum_{k=1}^{n} x(\frac{b-a}{n}k + a) \cdot \frac{b-a}{n}$

b. **(4 pts)** Similarly, prove that $SNR_{MMSE-LE,U} \leq SNR_{MMSE-DFE,U} \leq SNR_{MFB}$ using above inequalities. When does equality hold?

c. **(4 pts)** Compare SNR_{ZF-DFE} and $SNR_{MMSE-LE}$. Can you say which scheme has better performance?

3.48 *Unequal Channels (Moshe Malkin- instructor, Midterm 2007)*

Please assume the gap approximation works in all SNR ranges for this problem.

a. A sequence of 16-QAM symbols with in-phase component a_k and quadrature component b_k at time k is transmitted on a passband channel by the modulated signal

$$x(t) = \sqrt{2} \left\{ \left[\sum_k a_k \cdot \phi(t - kT) \right] \cdot cos(\omega_c t) - \left[\sum_k b_k \cdot \phi(t - kT) \right] \cdot sin(\omega_c t) \right\}, \qquad (3.548)$$

where $T = 40$ ns, $f_c = 2.4$ GHz, and the transmit power is 700 μW.

The waveform $\phi(t)$ is given by

$$\phi(t) = \frac{1}{\sqrt{T}} sinc\left(\frac{t}{T}\right) \qquad (3.549)$$

and the channel response is given by $H(f) = e^{-j5\pi fT}$ and so the received signal is given by

$$y(t) = h(t) * x(t) + n(t) \qquad (3.550)$$

where $n(t)$ is an additive white Gaussian noise random process with two-sided PSD of -100 dBm/Hz.

(i) (1 pts) What is the data rate for this system?

(ii) (2 pts) What are $\mathcal{E}_x$, $\bar{\mathcal{E}}_x$ and d_{min} for this constellation?

(iii) (1.5 pts) What is $\tilde{x}_{bb}(t)$?

(iv) (1.5 pts) What is the ISI characterizing function $q(t)$? what is q_k?

(v) (2 pts) What are P_e and $\bar{P}_e$ for an optimal ML detector?

(vi) (2 pts) Draw a block diagram of the receiver and label major components.

Unfortunately, the implementation of the baseband demodulator is faulty and the additive Gaussian noise power in the quadrature component is $\alpha = 4$ times what it should be. That is, the noise variance of the quadrature component is $\alpha\frac{N_0}{2} = 2N_0$ while the noise variance in the in-phase dimension is $\frac{N_0}{2}$. Answer the following questions for this situation.

(vii) (2.5 pts) What is the receiver SNR?

(viii) (3 pts) What are P_e and $\bar{P}_e$?

(ix) (1.5 pts) Instead of using QAM modulation as above, two independent 4-PAM constellations (with half the total energy allocated for each constellation) are now transmitted on the in-phase and quadrature channels, respectively. What is P_e averaged over both of the PAM constellations?

(x) (3 pts) The transmitter realizes that if he allocates different energies for the in-phase and quadrature channels (**BUT still using QAM modulation with an equal number of bits for the in-phase and quadrature channels and original power constraint of 700 μW**) he could improve the $\bar{P}_e$ performance from (aviii). What is the optimal energy allocation between the in-phase and quadrature channels? Given that we need $\bar{P}_e = 10^{-6}$, what is $\bar{b}$ and the achievable data rate?

(xi) (2.5 pts) Using the results from part (ax) find the minimal increase in transmit power needed to guarantee $\bar{P}_e = 10^{-6}$ for 16-QAM transmission?

The transmitter now decides to reduce losses. Given this increased noise in the quadrature dimension, the transmitter decides to use only the in-phase dimension for transmission (but subject to the original transmit power constraint of 700 μW).

(xii) (1.5 pts) What data rate can be then supported that gives $\bar{P}_e = 10^{-6}$?

(xiii) (3 pts) Using a fair comparison, compare the QAM transmission system from part (ax) to the single-dimensional scheme ($N = 1$) from part (axii). Which scheme is better?

(xiv) (3 pts) Can you derive a new transmission scheme that uses both the in-phase and quadrature channels to get a higher data rate than part (ax)? (subject to the same $\bar{P}_e = 10^{-6}$, and original symbol rate and power constraint of 700 μW)

3.49 *Equalizer Design (9 pts, Moshe Malkin- instructor, Final 2007)*

A transmission system uses the basis function $\phi(t) = sinc(t)$ with $\frac{1}{T} = 1$ Hz. The Fourier transform of the channel impulse response is:

$$H(f) = \begin{cases} \frac{1}{1-0.5j \cdot e^{-j2\pi f}}, & \text{for} |f| \leq \frac{1}{2} \\ 0, & \text{for} |f| > \frac{1}{2} . \end{cases} \qquad (3.551)$$

and $SNR = \frac{\bar{\mathcal{E}}_x}{\sigma^2} = 10dB$.

a. (1 pt) Find $||p||^2$ and Q(D).

b. (1 pt) Find $W_{ZFE}(D)$ and $W_{MMSE-LE}(D)$.

c. (1 pt) Find $W(D)$ and $B(D)$ for ZF-DFE.

d. (2 pts) Find $W(D)$ and $B(D)$ for MMSE-DFE (Hint: the roots of the numerator of $Q(D) + 1/SNR_{MFB}$ are $22.4555j$ and $0.0445j$).

e. (0.5 pts) What is SNR_{ZF-DFE}?

f. (1.5 pts) Design a Tomlinson-Harashima precoder based on the ZF-DFE. Show both the precoder and the corresponding receiver (For any M).

g. (2 pts) Design a Laroia precoder based on the ZF-DFE. Assume you are using 4-QAM modulation. Show both the precoder and the corresponding receiver. Make sure to mention which kind of constellation is used at each SBS detector in your drawing.

3.50 *Diversity (7 pts Moshe Malkin- instructor, Final 2007)*

A receiver has access to an infinite number of diversity channels where the output of channel i at time k is

$$y_{k,i} = x_k + 0.9 \cdot x_{k+1} + n_{k,i}, \qquad i = 0, 1, 2, \ldots$$

where $n_{k,i}$ is a Gaussian noise process independent across time and across all the channels, and with variance $\sigma_i^2 = 1.2^i \cdot 0.181$. Also, $\bar{\mathcal{E}}_x = 1$.

a. (1 pts) Find $SNR_{MFB,i}$, the SNR_{MFB} for channel i.

b. (2 pts) What is the matched filter for each diversity channel?

c. (1.5 pts) What is the resulting $Q(D)$ for this diversity system?

d. (2.5 pts) What is the detector SNR for this system for a ZF-DFE receiver?

3.51 *DFE with Finite Length Feedback Filter (9 pts Moshe Malkin- instructor, Final 2007)*

A symbol-rate sampled MMSE-DFE structure, where the received signal is filtered by a continuous time matched filter, uses an *infinite length feedforward filter*. However, the MMSE-DFE *feedback filter* to be of finite length N_b.

a. (2 pts) Formulate the optimization problem you would have to solve to find the optimal feedforward and feedback coefficients to minimize the mean squared error (Hint: Don't approach this as a finite-length equalization problem as in section 3.7).

Assume that $\frac{N_0}{2} = .181$, $\mathcal{E}_x = 1$, and $P(D) = 1 + .9 \cdot D^{-1}$. (and $SNR_{MFB} = 10$ dB).

b. (2 pts) Using only 1 feedback tap ($N_b = 1$), determine the optimal feedforward and feedback filters (Hint: This is easy - you have already seen the solution before).

c. (2 pts) Now consider the ZF-DFE version of this problem. State the optimization problem for this situation (analogous to part a).

Now, assume that we have $P(D) = \frac{1}{1+0.9D^{-1}}$ (and $\|p\|^2 = \frac{1}{1-0.9^2} = \frac{1}{0.19}$).

d. (3 pts) Determine the optimal feedforward and feedback filters for the ZF-DFE formulation using only 1 feedback tap ($N_b = 1$).

3.52 *Packet Processing (10 pts Moshe Malkin- instructor, Final 2007)*
Suppose that in a packet-based transmission system, a receiver makes a decision from the set of transmit symbols x_1, x_2, x_3 based on the channel outputs y_1, y_2, y_3, where

$$
\begin{bmatrix} y_3 \\ y_2 \\ y_1 \end{bmatrix} = \begin{bmatrix} p_{11} & p_{12} & p_{13} \\ 0 & p_{22} & p_{23} \\ 0 & 0 & p_{33} \end{bmatrix} \begin{bmatrix} x_3 \\ x_2 \\ x_1 \end{bmatrix} + \begin{bmatrix} n_3 \\ n_2 \\ n_1 \end{bmatrix} = \begin{bmatrix} 0.6 & 1.9 & -3.86 \\ 0 & 1.8 & 3.3 \\ 0 & 0 & 1.2 \end{bmatrix} \begin{bmatrix} x_3 \\ x_2 \\ x_1 \end{bmatrix} + \begin{bmatrix} n_3 \\ n_2 \\ n_1 \end{bmatrix} \quad (3.552)
$$

and where the noise autocorrelation matrix is given by

$$
R_n = E\left(\begin{bmatrix} n_3 \\ n_2 \\ n_1 \end{bmatrix} \begin{bmatrix} n_3^* & n_2^* & n_1^* \end{bmatrix} \right) = \begin{bmatrix} 0.3 & 0 & 0 \\ 0 & 0.5 & 0 \\ 0 & 0 & 0.1 \end{bmatrix}. \quad (3.553)
$$

The inverse of the channel matrix is given by

$$
\begin{bmatrix} 0.6 & 1.9 & -3.86 \\ 0 & 1.8 & 3.3 \\ 0 & 0 & 1.2 \end{bmatrix}^{-1} = \begin{bmatrix} 1.67 & -1.76 & 10.19 \\ 0 & 0.56 & -1.52 \\ 0 & 0 & 0.83 \end{bmatrix}. \quad (3.554)
$$

The transmit symbols are i.i.d with $\mathcal{E}_{\S_\infty} = \mathcal{E}_{\S_\in} = \mathcal{E}_{\S_\ni} = \in I$.

a. (1.5 pts) What is the 3-tap zero-forcing equalizer for x_1 based on the observation y_1, y_2, y_3? Repeat for x_2 and x_3.

b. (1 pts) What is the matrix ZFE for detecting x_1, x_2, and x_3? (Hint: This is easy - all the work occurred in the previous part)

c. (1.5 pts) What is the detection SNR for x_1 using a ZFE? Answer the same for x_2 and x_3.

d. (1 pts) An engineer now realizes that the performance could be improved through use previous decisions when detecting the current symbol. If the receiver starts by detecting x_1, then x_2, and finally x_3, describe how this modified ZF detector would work?

e. (1.5 pts) Assuming previous decisions are correct, what is now the detection SNR for each symbol?

f. (1 pts) The approach above does not necessarily minimize the MMSE. How would a packet MMSE-DFE work? How would you describe the feedback structure? (Don't solve for the optimal matrices - just describe the signal processing that would take place).

g. (1 pts) Can the THP also be implemented for this packet based system? Describe how this would be done (again, don't solve - just describe how this would work).

Appendix A

Useful Results in Linear Minimum Mean-Square Estimation

This appendix derives and/or lists some key results from linear Minimum Mean-Square-Error estimation.

A linear MMSE estimate of some random variable x, given observations of some other random sequences $\{y_k\}$, chooses a set of parameters w_k (with the index k having one distinct value for each observation of y_k that is used) to minimize

$$E\left[|e|^2\right] \tag{A.1}$$

where

$$e \triangleq x - \sum_{k=0}^{N-1} w_k \cdot y_k \quad . \tag{A.2}$$

One can let $N \to \infty$ without difficulty. The term linear MMSE estimate is derived from the linear combination of the random variables y_k in (A.2). More generally, it can be shown that the MMSE estimate is $E\left[x/\{y_k\}\right]$, the conditional expectation of x, given y_0, ..., y_{N-1}. which will be linear for jointly Gaussian x and $\{y_k\}$. This text is interested only in linear MMSE estimates. In this text's developments, y_i will usually be successive samples of some channel output sequence, and x will be the current channel-input symbol that the receiver attempts to estimate.

A.1 The Orthogonality Principle

While (A.1) can be minimized directly by differentiation in each case or problem of interest, it is often far more convenient to use a well-known principle of linear MMSE estimates - that is that the error signal e must always be uncorrelated with all the observed random variables in order for the MSE to be minimized.

Theorem A.1.1 (Orthogonality Principle) *The MSE is minimized if and only if the following condition is met*

$$E\left[e \cdot y_k^*\right] = 0 \quad \forall\, k = 0, ..., N-1 \tag{A.3}$$

Proof: By writing $|e|^2 = [\Re(e)]^2 + [\Im(e)]^2$, we may differentiate the MSE with respect to both the real and imaginary parts of w_k for each k of interest. The pertinent parts of the real and imaginary errors are (realizing that all other w_i, $i \neq k$, will drop from the corresponding derivatives)

$$
\begin{aligned}
e_r &= x_r - w_{r,k} \cdot y_{r,k} + w_{i,k} \cdot y_{i,k} \tag{A.4} \\
e_i &= x_i - w_{i,k} \cdot y_{r,k} - w_{r,k} \cdot y_{i,k} \quad , \tag{A.5}
\end{aligned}
$$

where subscripts of r and i denote real and imaginary part in the obvious manner. Then, to optimize over $w_{r,k}$ and $w_{i,k}$,

$$\frac{\partial |e|^2}{\partial w_{r,k}} = 2e_r \frac{\partial e_r}{\partial w_{r,k}} + 2e_i \frac{\partial e_i}{\partial w_{r,k}} = -2\left(e_r y_{r,k} + e_i y_{i,k}\right) = 0 \qquad (A.6)$$

$$\frac{\partial |e|^2}{\partial w_{i,k}} = 2e_r \frac{\partial e_r}{\partial w_{i,k}} + 2e_i \frac{\partial e_i}{\partial w_{i,k}} = 2\left(e_r y_{i,k} - e_i y_{r,k}\right) = 0 \quad . \qquad (A.7)$$

The desired result is found by taking expectations and rewriting the series of results above in vector form. Since the MSE is positive-semi-definite quadratic in the parameters $w_{r,k}$ and $w_{i,k}$, this setting must be a global minimum. If the MSE is strictly positive-definite, then this minimum is unique. **QED**.

A.2   Spectral Factorization

This section uses D-transform notation for sequences:

Definition A.2.1 (D- Transforms) *A sequence $\{x_k\}$ has D-Transform $X(D) = \sum_k x_k D^k$.*

In this chapter, all sequences can be complex. The sequence $\{x^*_{-k}\}$ has a D-Transform $X^*(D^{-*}) \triangleq \sum_k x_k^* D^{-k}$.

Definition A.2.2 (Autocorrelation and Power Spectrum) *If $\{x_k\}$ is any stationary complex sequence, its **autocorrelation function** is defined as the sequence $R_{xx}(D)$ whose terms are $r_{xx,j} = E[x_k x^*_{k-j}]$; symbolically[1]*

$$R_{xx}(D) \triangleq E\left[X(D) \cdot X^*(D^{-*})\right] \quad . \qquad (A.8)$$

*By stationarity, $r_{xx,j} = r^*_{xx,-j}$ and $R_{xx}(D) = R^*_{xx}(D^{-*})$. The **power spectrum** of a stationary sequence is the Fourier transform of its autocorrelation function, which is written as*

$$R_{xx}(e^{-\jmath\omega T}) = R_{xx}(D)|_{D=e^{-\jmath\omega T}} \quad , \quad -\frac{\pi}{T} < \omega \leq \frac{\pi}{T} \quad , \qquad (A.9)$$

which is real and nonnegative for all ω. Conversely, we say that any complex sequence $R(D)$ for which $R(D) = R^*(D^{-*})$ is an autocorrelation function, and any function $R(e^{-\jmath\omega T})$ that is real and nonnegative over the interval $\{-\frac{\pi}{T} < \omega \leq \frac{\pi}{T}\}$ is a power spectrum.

The quantity $E\left[|x_k|^2\right]$ is $\mathcal{E}_{\boldsymbol{x}}$, or $\bar{\mathcal{E}}_{\boldsymbol{x}}$ per dimension, and is determined by either the autocorrelation function or the power spectrum as follows:

$$\mathcal{E}_{\boldsymbol{x}} = E\left[|x_k|^2\right] = r_{xx,0} = \frac{T}{2\pi} \int_{-\frac{\pi}{T}}^{\frac{\pi}{T}} R(e^{-\jmath\omega T}) d\omega \quad . \qquad (A.10)$$

The spectral factorization of an autocorrelation function is:

Definition A.2.3 (Factorizability) *An autocorrelation function $R(D)$ will be called **factorizable** if it can be written in the form*

$$R(D) = S_0 \cdot F(D) \cdot F^*(D^{-*}), \qquad (A.11)$$

*where S_0 is a positive real number and $F(D)$ is a canonical filter response. A filter response $F(D)$ is called **canonical** if it is **causal** ($f_k = 0$ for $k < 0$), **monic** ($f_0 = 1$), and **minimum-phase** (all of its poles are outside the unit circle, and all of its zeroes are on or outside the unit circle). If $F(D)$ is canonical, then $F^*(D^{-*})$ is **anticanonical**; i.e., anticausal, monic, and maximum-phase.*

---

[1]The expression $R_{xx}(D) \triangleq E\left[X(D)X^*(D^{-1})\right]$ is used in a symbolic sense, since the terms of $X(D)X^*(D^{-1})$ are of the form $\sum_k x_k x^*_{k-j}$, implying the additional operation $\lim_{N\to\infty}[1/(2N+1)]\sum_{-N \leq k \leq N}$ on the sum in such terms.

If $F(D)$ is a canonical response, then $\|f\|^2 \triangleq \sum_j |f_j|^2 \geq 1$, with equality if and only if $F(D) = 1$, since $F(D)$ is monic. This simple inequality has many uses, see Exercises for Chapter 3.

The following lemma from discrete-time spectral factorization theory describes when an autocorrelation function is factorizable, and also gives the value of S_0.

> **Lemma A.2.1 (Spectral Factorization)** *If $R(e^{-\jmath\omega T})$ is any power spectrum such that both $R(e^{-\jmath\omega T})$ and $\log R(e^{-\jmath\omega T})$ are integrable over $-\frac{\pi}{T} < \omega \leq \frac{\pi}{T}$, and $R(D)$ is the corresponding autocorrelation function, then there is a canonical discrete-time response $F(D)$ that satisfies the equation*
>
> $$R(D) = S_0 \cdot F(D) \cdot F^*(D^{-*}), \tag{A.12}$$
>
> *where the finite constant S_0 is given by*
>
> $$\log S_0 = \frac{1}{2\pi} \int_{-\frac{\pi}{T}}^{\frac{\pi}{T}} \log R(e^{-\jmath\omega T}) d\omega \tag{A.13}$$
>
> *(where the logarithms can have any common base). For S_0 to be finite, $R(e^{-\jmath\omega T})$ satisfies the **discrete-time Paley-Wiener criterion***
>
> $$\frac{1}{2\pi} \int_{-\frac{\pi}{T}}^{\frac{\pi}{T}} |\log R(e^{-\jmath\omega T})| d\omega < \infty \quad . \tag{A.14}$$

Linear Prediction

The inverse of $R(D)$ is also an autocorrelation function and can be factored when $R(D)$ also satisfies the PW criterion with finite γ_0. In this case, as with the MMSE-DFE in Section 3.6, the inverse autocorrelation factors as

$$R_{xx}^{-1}(D) = \gamma_0 \cdot G(D) \cdot G^*(D^{-*}) \quad . \tag{A.15}$$

If $x(D)$ is a discrete-time sequence with factorizable inverse autocorrelation function $R_{xx}^{-1}(D) = \gamma_0 G(D) G^*(D^{-*})$, and $A(D)$ is any causal and monic sequence, then $1 - A(D)$ is a strictly causal sequence that may be used as a prediction filter, and the prediction error sequence $E(D)$ is given by

$$E(D) = X(D) - X(D)[1 - A(D)] = X(D)A(D) \quad . \tag{A.16}$$

The autocorrelation function of the prediction error sequence is

$$R_{ee}(D) = R_{xx}(D) \cdot A(D) \cdot A^*(D^{-*}) = \frac{A(D) \cdot A^*(D^{-*})}{\gamma_0 \cdot G(D) \cdot G^*(D^{-*})} \quad , \tag{A.17}$$

so its average energy satisfies $\mathcal{E}_e = S_0 \|1/g * a\|^2 \geq S_0$ (since $A(D)/G(D)$ is monic), with equality if and only if $A(D)$ is chosen as the **whitening filter** $A(D) = G(D)$. The process $X(D) \cdot G(D)$ is often called the **innovations** of the process $X(D)$, which has mean square value $S_0 = 1/\gamma_0$. Thus, S_0 of the direct spectral factorization is the mean-square value of the innovations process or equivalent of the MMSE in linear prediction. $X(D)$ can be viewed as being generated by inputting a white innovations process $U(D) = G(D)X(D)$ with mean square value S_0 into a filter $F(D)$ so that $X(D) = F(D)U(D)$.

The factorization of the inverse and resultant interpretation of the factor $G(D)$ as a linear-prediction filter helps develop an interest interpretation of the MMSE-DFE in Section 3.6.

A.2.1 Cholesky Factorization

Cholesky factorization is the finite-length equivalent of spectral factorization. In this finite-length case, there are really two factorizations, both of which converge to the infinite-length spectral factorization.

Cholesky Form 1 - Forward Prediction

Cholesky factorization of a positive semidefinite $N \times N$ matrix R_N produces a unique upper triangular monic (ones along the diagonal) matrix $\boldsymbol{F}_N$ and a unique diagonal positive-semidefinite matrix $\boldsymbol{S}_N$ such that

$$\boldsymbol{R}_N = \boldsymbol{F}_N \boldsymbol{S}_N \boldsymbol{F}_N^* \quad . \tag{A.18}$$

It is convenient in transmission theory to think of the matrix $\boldsymbol{R}_N$ as an autocorrelation matrix for N samples of some random vector process x_k with ordering

$$\boldsymbol{X}_N = \begin{bmatrix} x_{N-1} \\ \vdots \\ x_0 \end{bmatrix} \quad . \tag{A.19}$$

A corresponding order of $\boldsymbol{F}_N$ and $\boldsymbol{S}_N$ is then

$$\boldsymbol{F}_N = \begin{bmatrix} \boldsymbol{f}_{N-1} \\ \boldsymbol{f}_{N-2} \\ \vdots \\ \boldsymbol{f}_0 \end{bmatrix} \quad \text{and} \quad \boldsymbol{S}_N = \begin{bmatrix} s_{N-1} & 0 & \dots & 0 \\ 0 & s_{N-2} & \dots & 0 \\ 0 & \vdots & \ddots & 0 \\ 0 & 0 & \dots & s_0 \end{bmatrix} \quad . \tag{A.20}$$

Since $\boldsymbol{F}_N$ is monic, it is convenient to write

$$\boldsymbol{f}_i = \begin{bmatrix} 1 & \tilde{\boldsymbol{f}}_i \end{bmatrix} \quad . \tag{A.21}$$

The determinant of $\boldsymbol{R}_N$ is easily found as

$$\gamma_0^2 = |\boldsymbol{R}_N| = \prod_{n=0}^{N-1} s_n \quad . \tag{A.22}$$

(or $\ln \gamma_0^2 = \ln |\boldsymbol{R}_N|$ for readers taking limits as $N \to \infty$). A convenient description of $\boldsymbol{R}_N$'s components is then

$$\boldsymbol{R}_N = \begin{bmatrix} r_N & \boldsymbol{r}_1^* \\ \boldsymbol{r}_1 & \boldsymbol{R}_{N-1} \end{bmatrix} \quad . \tag{A.23}$$

The submatrix $\boldsymbol{R}_{N-1}$ has Cholesky Decomposition

$$\boldsymbol{R}_{N-1} = \boldsymbol{F}_{N-1} \boldsymbol{S}_{N-1} \boldsymbol{F}_{N-1} \quad , \tag{A.24}$$

which because of the 0 entries in the triangular and diagonal matrices shows the recursion inherent in Cholesky decomposition (that is the $\boldsymbol{F}_{N-1}$ matrix is the lower right $(N-1) \times (N-1)$ submatrix of $\boldsymbol{F}_N$, which is also upper triangular). The inverse of $\boldsymbol{R}_N$ (pseudoinverse when singular) has a Cholesky factorization

$$\boldsymbol{R}_N^{-1} = \boldsymbol{G}_N^* \boldsymbol{S}_N^{-1} \boldsymbol{G}_N \tag{A.25}$$

where $\boldsymbol{F}_N = \boldsymbol{G}_N^{-1}$ is also upper triangular and monic with ordering

$$\boldsymbol{G}_N = \begin{bmatrix} \boldsymbol{g}_{N-1} \\ \boldsymbol{g}_{N-2} \\ \vdots \\ \boldsymbol{g}_0 \end{bmatrix} \quad . \tag{A.26}$$

Also,

$$\boldsymbol{g}_i = \begin{bmatrix} 1 & \tilde{\boldsymbol{g}}_i \end{bmatrix} \quad . \tag{A.27}$$

linear prediction A straightforward algorithm for computing Cholesky factorization derives from a linear prediction interpretation. The **innovations**, $\boldsymbol{U}_N$, of the N samples of X_N are defined by

$$\boldsymbol{X}_N = \boldsymbol{F}\boldsymbol{U}_N \tag{A.28}$$

where $E\left[\boldsymbol{U}_N\boldsymbol{U}_N^*\right] = \boldsymbol{S}_N$, and

$$\boldsymbol{U}_N = \begin{bmatrix} u_{N-1} \\ \vdots \\ u_0 \end{bmatrix} \quad . \tag{A.29}$$

Also, $\boldsymbol{U}_N = \boldsymbol{G}\boldsymbol{X}_N$. The cross-correlation between $\boldsymbol{X}_N$ and $\boldsymbol{U}_N$ is

$$\bar{R}\boldsymbol{ux} = \boldsymbol{S}_N\boldsymbol{G}_N^* \quad , \tag{A.30}$$

which is lower triangular. Thus,

$$E\left[u_k x_{k-i}^*\right] = 0 \ \ \forall \, i \geq 1 \ . \tag{A.31}$$

Since $\boldsymbol{X}_{N-1} = \boldsymbol{F}_{N-1}\boldsymbol{U}_{N-1}$ shows a reversible mapping from $\boldsymbol{U}_{N-1}$ to $\boldsymbol{X}_{N-1}$, then (A.31) relates that the sequence u_k is a set of MMSE prediction errors for x_k in terms of $x_{k-1} \dots x_0$ (i.e., (A.31) is the orthogonality principle for linear prediction). Thus,

$$u_N = x_N - \boldsymbol{r}_1^* R_{N-1}^{-1}\boldsymbol{X}_{N-1} \tag{A.32}$$

since $\boldsymbol{r}_1$ is the cross-correlation between x_N and $\boldsymbol{X}_{N-1}$. Equation (A.32) rewrites as

$$\begin{aligned} x_N &= u_N + \boldsymbol{r}_1^* R_{N-1}^{-1}\boldsymbol{X}_{N-1} & \tag{A.33} \\ &= U_N + \underbrace{\boldsymbol{r}_1^*\boldsymbol{G}_{N-1}^*\boldsymbol{S}_{N-1}^{-1}}_{\tilde{\boldsymbol{f}}_N}\underbrace{\boldsymbol{G}_{N-1}\boldsymbol{X}_{N-1}}_{\boldsymbol{U}_{N-1}} & \tag{A.34} \\ &= \boldsymbol{f}_N\boldsymbol{U}_N \quad , & \tag{A.35} \end{aligned}$$

so

$$\boldsymbol{f}_N = \begin{bmatrix} 1 & \boldsymbol{r}_1^*\boldsymbol{G}_{N-1}^*\boldsymbol{S}_{N-1}^{-1} \end{bmatrix} \quad . \tag{A.36}$$

Then, from (A.32) and (A.34),

$$\boldsymbol{g}_N = \begin{bmatrix} 1 & -\tilde{\boldsymbol{f}}_N\boldsymbol{G}_{N-1} \end{bmatrix} \quad . \tag{A.37}$$

Finally,

$$s_N = r_N - \tilde{\boldsymbol{f}}_N\boldsymbol{S}_{N-1}\tilde{\boldsymbol{f}}_N^* \quad . \tag{A.38}$$

Forward Cholesky Algorithm Summary: For nonsingular R_N:
Set $\boldsymbol{f}_0 = \boldsymbol{F}_0 = \boldsymbol{g}_0 = \boldsymbol{G}_0 = 1$, $\boldsymbol{S}_0 = s_0 = E|x_0|^2$
For $n = 1 \dots N$:

a. $\tilde{\boldsymbol{f}}_n = \boldsymbol{r}_1^*\boldsymbol{G}_{n-1}^* S_{n-1}^{-1}$.

b. $\boldsymbol{F}_n = \begin{bmatrix} 1 & \tilde{\boldsymbol{f}}_n \\ 0 & \boldsymbol{F}_{n-1} \end{bmatrix} \quad .$

c. $\boldsymbol{G}_n = \begin{bmatrix} 1 & -\tilde{\boldsymbol{f}}_n\boldsymbol{G}_{n-1} \\ 0 & \boldsymbol{G}_{N-1} \end{bmatrix} \quad .$

d. $s_n = r_n - \tilde{\boldsymbol{f}}_N\boldsymbol{S}_{N-1}\tilde{\boldsymbol{f}}_{N-1}^* \quad .$

A singular R_N means that $s_n = 0$ for at least one index $n = i$, which is equivalent to $u_i = 0$, meaning that x_i can be exactly predicted from the samples $x_{i-1} \ldots x_0$ or equivalently can be exactly constructed from $u_{i-1} \ldots u_0$. In this case, Cholesky factorization is not unique. One factorization is to save $\boldsymbol{F}_i$ and $\boldsymbol{G}_i$ and "restart" the algorithm for $n > i$ realizing that x_i is equivalent to knowing all lower-index samples. The new $\boldsymbol{F}_{n>i}$ and $\boldsymbol{G}_{n>i}$ created will have smaller dimension, but when the algorithm is complete, zeros can be added to all the "right-most" positions of $\boldsymbol{F}$ and $\boldsymbol{G}$, and maintaining the previous $\boldsymbol{F}_i$ and $\boldsymbol{G}_i$ for the lower rightmost positions.

That is,

$$\boldsymbol{F}_N = \begin{bmatrix} \boldsymbol{F}_{n>i} & 0 \\ 0 & \boldsymbol{F}_i \end{bmatrix} \ and \ \boldsymbol{G}_N = \begin{bmatrix} \boldsymbol{G}_{n>i} & 0 \\ 0 & \boldsymbol{G}_i \end{bmatrix} \tag{A.39}$$

and

$$\boldsymbol{S}_N = \begin{bmatrix} \boldsymbol{S}_{n>i} & 0 & 0 \\ 0 & 0 & 0 \\ 0 & 0 & \boldsymbol{S}_{i-1} \end{bmatrix} \quad . \tag{A.40}$$

The forward Cholesky factorization can also be written

$$\boldsymbol{R}_N = \boldsymbol{G}_N^{-1} \boldsymbol{S}_N \boldsymbol{G}_N^{-*} \quad , \tag{A.41}$$

which is convenient for the alternative finite-length MMSE-DFE interpretations in Section 3.7.

Cholesky Form 2 - Backward Prediction

The backward Cholesky factorization is into a lower-diagonal-upper (instead of the upper-diagonal-lower in forward prediction). This involves extension of $\boldsymbol{R}_N$ on the lower right corner instead of at the upper-left corner. Rather than repeat the development of forward prediction, this section notes that the reverse backward prediction problem is inherent in the algorithm already given, except that this algorithm is performed on the inverse (which, granted, might be harder to compute than just repeating the steps above with the appropriate transpositions).

The inverse matrix $\boldsymbol{Q}_N = \boldsymbol{R}_N^{-1} = \boldsymbol{G}_N^* \boldsymbol{S}_N^{-1} \boldsymbol{G}_N$ is also an autocorrelation matrix for some process $\boldsymbol{Y}_N$ with innovations $\boldsymbol{V}_N$ where $\boldsymbol{Y}_N = \boldsymbol{G}_N^* \boldsymbol{V}_N$ such that $E[\boldsymbol{V}_N \boldsymbol{V}_N^*] = S_N^{-1}$. If $\boldsymbol{Q}$ is singular, then its pseudoinverse is used by definition here. Thus,

$$\boldsymbol{V}_N = \boldsymbol{F}_N^* \boldsymbol{Y} \quad , \tag{A.42}$$

illustrating the backward prediction error $v_{1-N} = \bar{\boldsymbol{f}}_N^* \boldsymbol{Y}_{N-1}$ where $\bar{\boldsymbol{f}}_N^*$ is the Nth row of $\boldsymbol{F}_N^*$ or equivalently $\bar{\boldsymbol{f}}_N$ is the last column of $\boldsymbol{F}_N$.

This factorization of $\boldsymbol{Q}$ is lower-diagonal-upper and the filters $\bar{\boldsymbol{f}}_n$ are backward prediction filters for $\boldsymbol{y}_{1-n}$ in terms of $\boldsymbol{y}_{2-n} \ldots \boldsymbol{y}_0$. So to perform backward-prediction Cholesky, first invert the given $\boldsymbol{Q}$ autocorrelation matrix to get $\boldsymbol{R}$ and then do forward Cholesky on the inverse ($\boldsymbol{R}_N = \boldsymbol{F}_N \boldsymbol{S}_N \boldsymbol{F}_N^* = \boldsymbol{G}_N^{-1} \boldsymbol{S} \boldsymbol{G}_N^{-*}$. Then, the backward Cholesky factorization uses the $\boldsymbol{G}$ of forward Cholesky (for $R = Q^{-1}$) in

$$\boldsymbol{Q} = \boldsymbol{G}_N^* \boldsymbol{S}_N^{-1} \boldsymbol{G}_N \quad . \tag{A.43}$$

Infinite-length convergence

For infinite-length stationary sequences, one takes the limit as $N \to \infty$ in either forward or backward Cholesky factorization. In this case, the matrix $\boldsymbol{R}$ (and therefore $\boldsymbol{Q}$) must be nonsingular to satsify the Paley-Weiner Criterion. The equivalence to spectral factorization is evident from the two linear-prediction interpretations for finite-length and infinite length series of samples from random processes.

For the stationary case, the concepts of forward and backward prediction are the same so that the forward predictor is just the time reverse of the coeffcients in the backward predictor.

Thus, the inverse autocorrelation function factors as

$$R^{-1}(D) = \gamma_0 G(D) G^*(D^{-*}) \quad , \tag{A.44}$$

where $G(D)$ is the forward prediction polynomial (and its time reverse specified by $G^*(D^{-*})$ is the backward prediction polynomial). The series of matrices $\{R_n\}_{n=1:\infty}$ formed from the coefficients of $R(D)$ creates a series of linear predictors $\{g_n\}_{n=1:\infty}$ with D-transforms $G_n(D)$. In the limit as $N \to \infty$ for a stationary nonsingular series,

$$\lim_{n\to\infty} G_n(D) = G(D) \quad . \tag{A.45}$$

Similarly,

$$\lim_{n\to\infty} G_n^*(D) = G^*(D^{-*}) \quad . \tag{A.46}$$

As $N \to \infty$, the prediction error varianc,es S_{N-1}, should tend to a constant. Finally, defining the geometric-average determinants as $S_{0,n} = |R|^{1/N}$ and $\gamma_{0,N} = |R^{-1}|^{1/N}$

$$\lim_{n\to\infty} S_{0,n} = S_0 = e^{\left\{ \frac{T}{2\pi} \int_{-\pi/T}^{\pi/T} \ln(R(e^{-j\omega T}))d\omega \right\}} \tag{A.47}$$

$$\lim_{n\to\infty} \gamma_{0,n}(D) = \gamma_0 = e^{-\left\{ \frac{T}{2\pi} \int_{-\pi/T}^{\pi/T} \ln(R(e^{-j\omega T}))d\omega \right\}} \quad . \tag{A.48}$$

The convergence to these limits implies that the series of filters converges or that the bottom row (last column) of the Cholesky factors tends to a constant repeated row.

Interestingly, a Cholesky factorization of a singular process exists only for finite lengths. Using the modifications to Cholesky factorization suggested above with "restarting," it becomes obvious why such a process cannot converge to a constant limit and so only nonsingular processes are considered in spectral factorization. Factorization of a singular process at infinite-length involves separating that process into a sum of subprocesses, each of which is resampled at a new sampling rate so that the PW criterion (nonsingular needs PW) is satisfied over each of the subbands associated with these processes. This is equivalent to the "restarting" of Cholesky at infinite length. For more, see Chapter 5.

Appendix B

Equalization for Partial Response

Just as practical channels are often not free of intersymbol interference, such channels are rarely equal to some desirable partial-response (or even controlled-ISI) polynomial. Thus, an equalizer may be used to adjust the channel's shape to that of the desired partial-response polynomial. This equalizer then enables the use of a partial-response sequence detector or a symbol-by-symbol detector at its output (with partial-response precoder). The performance of either of these types of detectors is particularly sensitive to errors in estimating the channel, and so the equalizer can be crucial to achieving the highest levels of performance in the partial-response communication channel. There are a variety of ways in which equalization can be used in conjunction with either sequence detection and/or symbol-by-symbol detection. This section introduces some equalization methods for partial-response signaling.

Chapter 9 studies sequence detection so terms related to it like MLSD (maximum likelihood sequence detection) and Viterbi detectors/algorithm are pertinent to readers already familiar with Chapter 9 contents and can be ignored by other readers otherwise in this Appendix.

B.1 Controlled ISI with the DFE

Section 3.8.2 showed that a minimum-phase channel polynomial $H(D)$ can be derived from the feedback section of a DFE. This polynomial is often a good controlled intersymbol interference model of the channel when $H(D)$ has finite degree ν. When $H(D)$ is of larger degree or infinite degree, the first ν coefficients of $H(D)$ form a controlled intersymbol interference channel. Thus, sequence detection on the output of the feedforward filter of a DFE can be designed using the controlled ISI polynomial $H(D)$ or approximations to it.

B.1.1 ZF-DFE and the Optimum Sequence Detector

Section 3.1 showed that the sampled outputs, y_k, of the receiver matched filter form a sufficient statistic for the underlying symbol sequence. Thus a maximum likelihood (or MAP) detector can be designed that uses the sequence y_k to estimate the input symbol sequence x_k without performance loss. The feedforward filter $1/(\eta_0 \|p\| H^*(D^{-*}))$ of the ZF-DFE is invertible when $Q(D)$ is factorizable. The reversibility theorem of Chapter 1 then states that a maximum likelihood detector that observes the output of this invertible ZF-DFE-feedforward filter to estimate x_k also has no performance loss with respect to optimum. The feedforward filter output has D-transform

$$Z(D) = X(D)H(D) + N'(D) \quad . \tag{B.1}$$

The noise sequence n'_k is exactly white Gaussian for the ZF-DFE, so the ZF-DFE produces an equivalent channel $H(D)$. If $H(D)$ is of finite degree ν, then a sequence detector can be designed based on the controlled-ISI polynomial $H(D)$ and this detector has minimum probability of error. Figure B.1 shows such an optimum receiver. When $H(D)$ has larger degree than some desired ν determined by complexity constraints, then the first ν feedback taps of $H(D)$ determine

$$H'(D) = 1 + h_1 D^1 + ... + h_\nu D^\nu \quad , \tag{B.2}$$
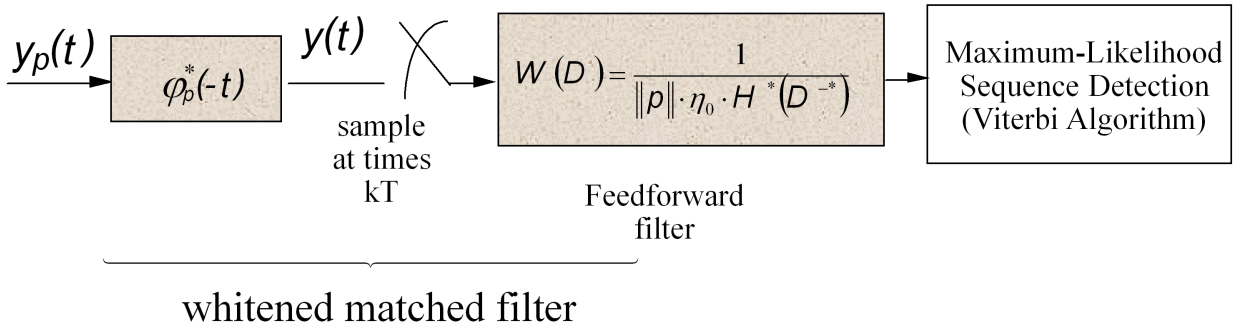
Figure B.1: The optimum maximum-likelihood detector, implemented with the assistance of the WMF, the feedforward section of the ZF-DFE
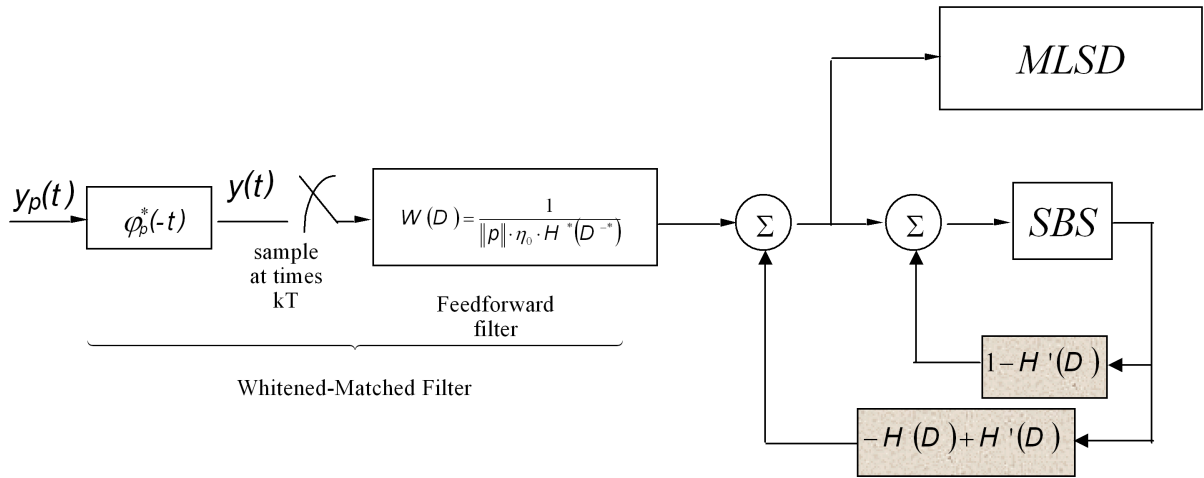

Figure B.2: Limiting the number of states with ZF-DFE and MLSD.

a controlled-ISI channel. Figure B.2 illustrates the use of the ZF-DFE and a sequence detector. The second feedback section contains all the channel coefficients that are not used by the sequence detector. These coefficients have delay greater than ν. When this second feedback section has zero coefficients, then the configuration shown in Figure B.2 is an optimum detector. When the additional feedback section is not zero, then this structure is intermediate in performance between optimum and the ZF-DFE with symbol-by-symbol detection. The inside feedback section is replaced by a modulo symbol-by-symbol detector when precoding is used.

Increase of ν causes the minimum distance to increase, or at worst, remain the same (which is proved simply by examining a trellis with more states and realizing that the smaller degree $H'(D)$ is a sub trellis for which distance cannot be greater. Thus, the ZF-DFE with sequence detector in Figure B.2 defines a series of increasingly complex receivers whose performance approach optimum as $\nu \to \infty$. A property of a minimum-phase $H(D)$ is that

$$\sum_{i=0}^{\nu'} |h_i|^2 = \|h'\|^2 \tag{B.3}$$

is maximum for all $\nu' \geq 0$. No other polynomial (that also preserves the AWGN at the feedforward filter output) can have greater energy. Thus the SNR of the signal entering the Viterbi Detector in Figure B.2, $\frac{\bar{\mathcal{E}}_{\boldsymbol{x}}\|h'\|^2}{\frac{N_0}{2}}$, also increases (nondecreasing) with ν. This SNR must be less than or equal to SNR_{MFB}.
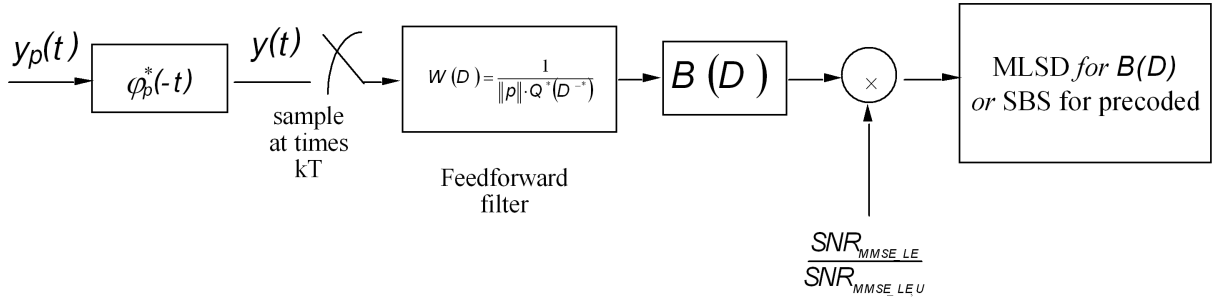
Figure B.3: Partial-response linear equalization.

B.1.2 MMSE-DFE and sequence detection

Symbol-by-symbol detection's objective is to maximize SNR in an unbiased detector, and so SNR maximization was applied in Chapter 3 to the DFE to obtain the MMSE-DFE. A bias in symbol-by-symbol detector was removed to minimize probability of error. The monic, causal, minimum-phase, and unbiased feedback polynomial was denoted $G_U(D)$ in Section 3.6. A sequence detector can use the same structures as shown in Figure B.1 and B.2 with $H(D)$ replaced by $G_u(D)$. For instance, Figure B.4 is the same as Figure B.2, with an unbiased MMSE-DFE's MS-WMF replacing the WMF of the ZF-DFE. A truncated version of $G_U(D)$ corresponding to $H'(D)$ is denoted $G'_U(D)$. The error sequence associated with the unbiased MMSE-DFE is not quite white, nor is it Gaussian. So, a sequence detector based on squared distance is not quite optimum, but it is nevertheless commonly used because the exact optimum detector could be much more complex. As ν increases, the probability of error decreases from the level of the unbiased MMSE-DFE, $\text{SNR}_{MMSE-DFE,U}$ when $\nu = 0$, to that of the optimum detector when $\nu \to \infty$. The matched filter bound, as always, remains unchanged and is not necessarily obtained. However, minimum distance does increase with ν in the sequence detectors based on a increasing-degree series of $G_U(D)$.

B.2 Equalization with Fixed Partial Response $B(D)$

The derivations of Section 3.6 on the MMSE-DFE included the case where $B(D) \neq G'(D)$, which this section reuses.

B.2.1 The Partial Response Linear Equalization Case

In the linear equalizer case, the equalization error sequence becomes

$$E_{pr}(D) = B(D)X(D) - W(D)Y(D) \quad . \tag{B.4}$$

Section 3.6 minimized MSE for any $B(D)$ over the coefficients in $W(D)$. The solution was found by setting $E\left[E_{pr}(D)y^*(D^{-1})\right] = 0$, to obtain

$$W(D) = B(D)\frac{\bar{R}_{xy}(D)}{\bar{R}_{yy}(D)} = \frac{B(D)}{\|p\|\left(Q(D) + 1/\text{SNR}_{MFB}\right)} \quad , \tag{B.5}$$

which is just the MMSE-LE cascaded with $B(D)$. Figure B.3, shows the MMSE-PREQ (MMSE - "Partial Response Equalizer"). The designer need only realize the MMSE-LE of Section 3.4 and follow it by a filter of the desired partial-response (or controlled-ISI) polynomial $B(D)$.[1] For this choice of $W(D)$, the error sequence is

$$E_{pr}(D) = B(D)X(D) - B(D)Z(D) = B(D)\left[E(D)\right] \tag{B.6}$$

---

[1]This also follows from the linearity of the MMSE estimator.

where $E(D)$ is the error sequence associated with the MMSE-LE. From (B.6),

$$\bar{R}_{e_{pr},e_{pr}}(D) = B(D)\bar{R}_{ee}(D)B^*(D^{-1}) = \frac{B(D)\frac{N_0}{2}B^*(D^{-1})}{\|p\|^2\left(Q(D) + 1/\text{SNR}_{MFB}\right)} \quad . \tag{B.7}$$

Thus, the MMSE for the PREQ can be computed as

$$\sigma^2_{\text{MMSE-PREQ}} = \frac{T}{2\pi}\int_{-\frac{\pi}{T}}^{\frac{\pi}{T}}\frac{|B(e^{-\jmath\omega T})|^2\frac{N_0}{2}}{\|p\|^2\left(Q(e^{-\jmath\omega T}) + 1/\text{SNR}_{MFB}\right)}d\omega \quad . \tag{B.8}$$

The symbol-by-symbol detector is equivalent to subtracting $(B(D) - 1)X(D)$ before detection based on decision regions determined by x_k. The $\text{SNR}_{\text{MMSE-PREQ}}$ becomes

$$\text{SNR}_{\text{MMSE-PREQ}} = \frac{\bar{\mathcal{E}}\boldsymbol{x}}{\sigma^2_{\text{MMSE-PREQ}}} \quad . \tag{B.9}$$

This performance can be better or worse than the MMSE-LE, depending on the choice of $B(D)$; the designer usually selects $B(D)$ so that $\text{SNR}_{\text{MMSE-PREQ}} > \text{SNR}_{MMSE-LE}$. This receiver also has a bias, but it is usually ignored because of the integer coefficients in $B(D)$ – any bias removal could cause the coefficients to be noninteger.

While the MMSE-PREQ should be used for the case where symbol-by-symbol and precoding are being used, the error sequence $E_{pr} = B(D)E(D)$ is not a white noise sequence (nor is $E(D)$ for the MMSE-LE), so that a Viterbi Detector designed for AWGN on the channel $B(D)$ would not be the optimum detector for our MMSE-PREQ (with scaling to remove bias). In this case, the ZF-PREQ, obtained by setting $\text{SNR}_{MFB} \to \infty$ in the above formulae, would also not have a white error sequence. Thus a linear equalizer for a partial response channel $B(D)$ that is followed by a Viterbi Detector designed for AWGN may not be very close to an optimum detection combination, unless the channel pulse response were already very close to $B(D)$, so that equalization was not initially necessary. While this is a seemingly simple observation made here, there are a number of systems proposed for use in disk-storage detection that overlook this basic observation, and do equalize to partial response, "color" the noise spectrum, and then use a WGN Viterbi Detector. The means by which to correct this situation is the PR-DFE of the next subsection.

B.2.2   The Partial-Response Decision Feedback Equalizer

If $B(D) \neq G(D)$ and the design of the detector mandates a partial-response channel with polynomial $B(D)$, then the optimal MMSE-PRDFE is shown in Figure B.4.

Again, using our earlier result that for any feedback section $G_U(D) = B(D) + \tilde{B}(D)$. The error sequence is the same as that for the MMSE-DFE, and is therefore a white sequence. The signal between the the two feedback sections in Figure B.4 is input to the sequence or symbol-by-symbol detector. This signal can be processed on a symbol-by-symbol basis if precoding is used (and also scaling is used to remove the bias - the scaling is again the same scaling as used in the MMSE-DFE), and $\tilde{B}_U(D) = G_U(D) - B_U(D)$, where

$$B_U(D) = \frac{\text{SNR}_{MMSE-DFE}}{\text{SNR}_{MMSE-DFE,U}}\left[B(D) - \frac{1}{\text{SNR}_{MMSE-DFE}}\right] \quad . \tag{B.10}$$

However, since the MMSE-PRDFE error sequence is white, and because the bias is usually small so that the error sequence in the unbiased case is also almost white, the designer can reasonably use a Viterbi Detector designed for $B(D)$ with white noise.

If the bias is not negligible, then a ZF-PRDFE should be used, which is illustrated in Figure B.2, and the filter settings are obtained by setting $\text{SNR}_{MFB} \to \infty$ in the above formula.
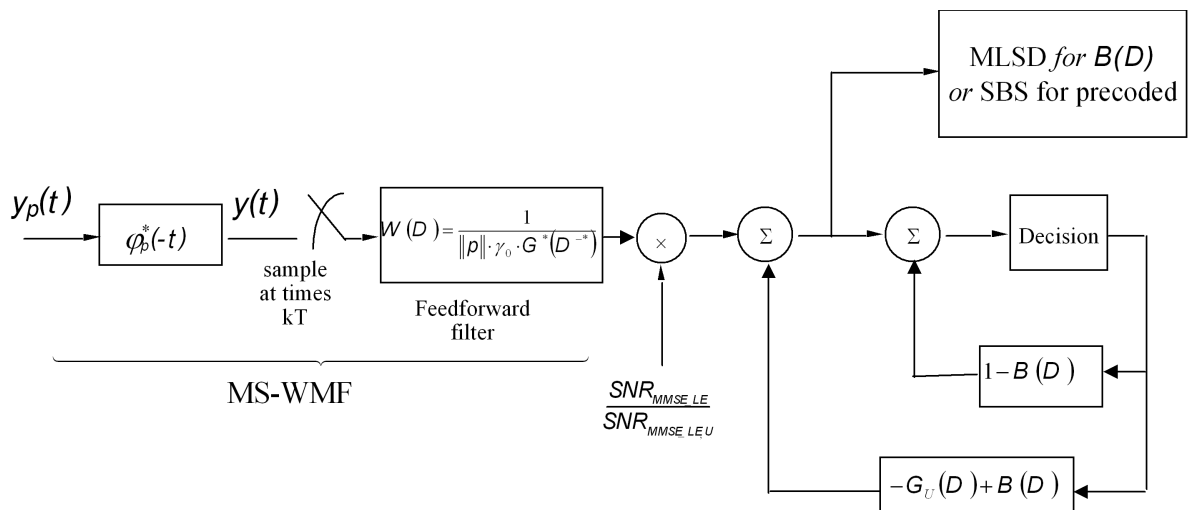
Figure B.4: Partial-response DFE with $B(D)$

Appendix C

The Matrix Inversion Lemma:

The matrix inversion lemma:

$$[A + BCD]^{-1} = A^{-1} - A^{-1}B\left[C^{-1} + DA^{-1}B\right]^{-1}DA^{-1} \quad . \tag{C.1}$$